FORCED, NONLINEAR, PLANAR AND NONPLANAR OSCILLATIONS OF A CANTILEVERED BEAM INCLUDING STATIC DEFLECTION

by

In-Ming Kevin Shyu

Dissertation submitted to the Faculty of the
Virginia Polytechnic Institute and State University
in partial fulfillment of the requirements for the degree of
DOCTOR OF PHILOSOPHY
in
Engineering Mechanics

APPROVED:

Dean T. Mook, Co-Chairman

Raymond H. Plaut, Co-Chairman

Scott L. Hendricks

John W. Grant

Martin Klaus

August, 1991

Blacksburg, Virginia

FORCED, NONLINEAR, PLANAR AND NONPLANAR OSCILLATIONS OF A CANTILEVERED BEAM INCLUDING STATIC DEFLECTION

by

In-Ming Kevin Shyu

Dean T. Mook, Co-Chairman

Raymond H. Plaut, Co-Chairman

Engineering Mechanics

(ABSTRACT)

In this dissertation, the response of a slender, elastic, cantilevered beam to a simple harmonic excitation is investigated. The effects of nonlinear curvature, nonlinear inertia, viscous damping and static load are included.

The nonlinear equations governing the motion of the beam are derived by the Lagrangian approach. The deflections are expressed as expansions in terms of the linear free-vibration modes. Galerkin's method is used to eliminate the spatial functions from the governing equations. Three modes are used in this procedure. Approximate solutions of the temporal equations are determined by the method of multiple scales. Four first-order ordinary differential equations govern the amplitudes and phases, and predict a whirling motion under certain situations. The solutions of the modulation equations can be fixed points, limit cycles or chaotic motions.

Previous studies considered whirling produced by a primary resonance. In this dissertation, secondary resonances are considered in addition to primary resonance. Previous derivations of equations of motion contain only the linear and cubic terms without consideration of the static displacement produced by the weight of the beam. As a result of this static deflection, there are quadratic terms in the governing equations which introduce the possibility of a superharmonic resonance of order two and a subharmonic resonance of order two.

It is shown that out-of-plane motion is possible in every resonance when the principal moments of inertia of the beam cross-section are approximately equal. The longer the beam is, the more prominent the whirling motion becomes. If the excitation frequency is increased or decreased

through a resonance, for most cases, the non-stationary response from the method of multiple scales shows good agreement with that from the original differential equations.

Acknowledgements

I would like to express my sincere appreciation to my advisors, Dr. Dean T. Mook and Dr. Raymond H. Plaut, for their counsel and guidance throughout the development of this dissertation. Their expertise, patience, and encouragement made the completion of this dissertation possible. Also, I would like to thank Dr. Scott L. Hendricks, Dr. John W. Grant and Dr. Martin Klaus for serving as dissertation committee members. Thanks are also due to the U.S. Army Research Office for supporting this research under Grant No. DAAL03-87-K-0040.

Special thanks are due to Sally G. Shrader for all of her assistance. Also, thanks are due to Perng-Jin F. Pai for his help on understanding some previous work in this field.

Finally, I am most indebted to my family, especially to my father, for their support, love and understanding throughout my graduate studies. I dedicate this work to my father and to the memory of my mother.

Table of Contents

List of Figures

two, bound of the disturbance = 0.0001, f = 5W, $\delta = 0.002$, $\hat{\varepsilon}a_0 = 0.0001$, $\hat{\varepsilon}b_0 = \gamma_0 = \psi_0 = 0$; (a) in-plane component, (b) out-of-plane component, (c) total amplitude.

Figure 5.99 Comparison of the amplitudes from the integration of the original differential equations and the MMS. First mode, primary resonance, f = 0.0005W, $\delta = 0.0002$, $\hat{\varepsilon}a_0 = 0.0001$, $\hat{\varepsilon}b_0 = \gamma_0 = \psi_0 = 0$, $\lambda = 1\times10^{-6}$; (a) amplitude from the integration of the original differential equations, (b) stationary amplitude, non-stationary amplitude from the MMS and the outline from (a).

Figure 5.100 Comparison of the amplitudes from the integration of the original differential equations and the MMS. First mode, primary resonance, f = 0.0005W, $\delta = 0.0002$, $\hat{\varepsilon}a_0 = 0.0001$, $\hat{\varepsilon}b_0 = \gamma_0 = \psi_0 = 0$, $\lambda = 1\times10^{-7}$; (a) amplitude from the integration of the original differential equations, (b) stationary amplitude, non-stationary amplitude from the MMS and the outline from (a).

Figure 5.101 Comparison of the amplitudes from the integration of the original differential equations and the MMS. First mode, primary resonance, f = 0.0005W, $\delta = 0.0002$, $\hat{\varepsilon}a_0 = 0.0001$, $\hat{\varepsilon}b_0 = \gamma_0 = \psi_0 = 0$, $\lambda = -1\times10^{-6}$; (a) amplitude from the integration of the original differential equations, (b) stationary amplitude, non-stationary amplitude from the MMS and the outline from (a).

Figure 5.102 Comparison of the amplitudes from the integration of the original differential equations and the MMS. First mode, primary resonance, f = 0.0005W, $\delta = 0.0002$, $\hat{\varepsilon}a_0 = 0.0001$, $\hat{\varepsilon}b_0 = \gamma_0 = \psi_0 = 0$, $\lambda = -1\times10^{-7}$; (a) amplitude from the integration of the original differential equations, (b) stationary amplitude, non-stationary amplitude from the MMS and the outline from (a).

Figure 5.103 Comparison of the amplitudes from the integration of the original differential equations and the MMS. First mode, primary resonance, f = 0.0005W, $\delta = 0.0002$, $\hat{\varepsilon}a_0 = \hat{\varepsilon}b_0 = 0.0001$, $\gamma_0 = \psi_0 = 0$, $\lambda = 1\times10^{-6}$; (a) in-plane component, (b) out-of-plane component of the amplitude from the integration of the original differential equations; (c) in-plane component, (d) out-of-plane component of stationary and non-stationary amplitudes from the MMS.

Figure 5.104 Comparison of the amplitudes from the integration of the original differential equations and the MMS. First mode, primary resonance, f = 0.0005W, $\delta = 0.0002$, $\hat{\varepsilon}a_0 = \hat{\varepsilon}b_0 = 0.0001$, $\gamma_0 = \psi_0 = 0$, $\lambda = 1\times10^{-7}$; (a) in-plane component, (b) out-of-plane component of the amplitude from the integration of the original differential equations; (c) in-plane component, (d) out-of-plane component of stationary and non-stationary amplitudes from the MMS.

Figure 5.105 Amplitudes from the integration of the original differential equations. First mode, primary resonance, f = 0.0005W, $\delta = 0.0002$, $\hat{\varepsilon}a_0 = 0.0001$, $\hat{\varepsilon}b_0 = \gamma_0 = \psi_0 = 0$, $\lambda = 1\times10^{-6}$, bound of the persistent random disturbance = 0.0001; (a) in-plane component, (b) out-of-plane component.

Figure 5.106 Amplitudes from the integration of the original differential equations. First mode, primary resonance, f = 0.0005W, $\delta = 0.0002$, $\hat{\varepsilon}a_0 = 0.0001$, $\hat{\varepsilon}b_0 = \gamma_0 = \psi_0 = 0$, $\lambda = -1\times10^{-6}$, bound of the persistent random disturbance = 0.0001; (a) in-plane component, (b) out-of-plane component.

Figure 5.107 Comparison of the amplitudes from the integration of the original differential equations and the MMS. First mode, superharmonic resonance of order two, f = 0.5W, $\delta = 0.0002$, $\hat{\varepsilon}a_0 = 0.0001$, $\hat{\varepsilon}b_0 = \gamma_0 = \psi_0 = 0$, $\lambda = 1\times10^{-6}$; (a) amplitude from the integration of the original differential equations, (b) reconstructed amplitude from the result of MMS.

Figure 5.108 Comparison of the amplitudes from the integration of the original differential equations and the MMS. First mode, superharmonic resonance of order two, f = 0.5W,

1 Introduction

1.1 Motivation

In many engineering systems, beam-like structures play an important role. A slender beam will undergo moderately large deformations under some circumstances. Many phenomena cannot be described by linear theory and must be explained by nonlinear theory. Nonlinear analyses are important in helicopter blades, robot arms, some space structures and other systems which experience large deformations.

It was found in previous nonlinear studies of beam vibrations that the coupling between motions in the principal directions can become significant. Nonlinear terms must be used to model this coupling. In general, nonlinear inertia, nonlinear curvature, shear forces and midplane stretching are to be considered. In some earlier studies nonlinear longitudinal inertia was used, but curvature was linearized to simplify the calculations. However, for moderately large deformations or motions involving torsion, linearized curvature may not be a good assumption and the results may not be accurate. Hence, a nonlinear curvature is used in some studies to improve the beam model. The effect of static deflection could become important under some circumstances. For example, static deflection could change the natural frequencies and affect the stability. In some studies, static deflection is taken into account. Due to the effects of nonlinear factors, whirling

motion is possible and, sometimes, it is undesirable for structures. Therefore, a study of whirling motion is an important topic in nonlinear analysis.

Because primary resonance is the most threatening to structures, primary resonance is always the first consideration. Sometimes secondary resonance can be important because it also can produce a large deformation.

Sometimes, the forcing frequency is not a constant. This is the case when a motor attached to the base of a cantilevered beam is started up, shut down, or varied from one operating frequency to another. It is possible that the forcing frequency will pass through one or more resonance regions during this variation. The amplitude of vibration will tend to increase during the passage through a resonance. Furthermore, the magnitude and position of the maximum amplitude are shifted from those for the stationary resonance. A problem of interest in this passage through resonance is the dependence of the magnitude and position of the maximum amplitude on the sweep rate of the forcing frequency, the initial conditions, and the system parameters. Non-stationary phenomena are important in rotors, turbines, and structures with motors attached to their bases. Therefore, a study of passage through resonance is important.

1.2 Literature Review

The behavior of beams has been studied for centuries. At first linear (classical) theory was used to describe the motion of a beam. The linear theory models the motions in principal directions independently and is only valid for small deflections. It failed to describe the instability of a planar motion due to out-of-plane disturbances, and thus the motion subjected to a planar force is always an in-plane motion in the forcing direction if predicted by linear theory. But near resonance the displacements could be large. The coupling between motions in the principal directions can become significant and whirling motion can occur. The linear theory is not adequate to describe such a situation. Also, linear theory fails to predict some phenomena, such as the jumps, secondary

resonances, and chaotic motions. Hence, nonlinear theory must be used to model the dynamics of beams near resonances.

Nonlinear vibration could be caused by a variety of factors. For example, nonlinear elasticity terms could arise from moderately large curvatures, and nonlinear inertia terms could be produced from longitudinal and rotatory inertia of the beam. In addition, shear forces and midplane stretching could cause nonlinear terms. Under different assumptions, different nonlinearities have been used to investigate nonlinear vibration. Wagner [1965] used a simplified curvature, which is the source of the nonlinear terms, but ignored other nonlinearities. Atluri [1973] considered a pinned-pinned-sliding beam utilizing the effects of large curvature, longitudinal inertia and rotatory inertia. As most people did, he also ignored the effects of midplane stretching as well as transverse shear deformation. Haight and King [1972] and Hyer [1978a,b,c] used a linearized curvature and nonlinear axial inertia to form the nonlinear equations of motion. The latter term causes the nonlinearity in their derivations. Instead of using curvatures, Ho, Scott and Eisley [1975, 1976] used Green's shear measure to include nonlinearities. Crespo da Silva and Glynn [1978a,b] and Rosen and Friedmann [1979] used both nonlinear curvatures and nonlinear inertia to obtain the nonlinearities. All of them obtained cubic nonlinear terms in their governing equations, and their governing equations are of the Duffing type. The beam dynamics thus preserves the nonlinear phenomena of the Duffing equation. For example, a jump phenomenon is commonly seen in the nonlinear systems as a result of hardening or softening effects. Superharmonic and subharmonic resonances might occur in the beam dynamics. In addition, whirling motion as well as chaotic motion could occur in this multiple-degree-of-freedom Duffing system.

The nonlinearities were used to discover the nonlinear phenomena which were not revealed from the linear theory. A change of frequencies can arise from nonlinear effects. Wagner [1965] studied a free-free and a clamped-free inextensional beam with a simplified curvature undergoing very large dynamic deflections. He derived an approximate formula for the nonlinear frequency for the first mode, which is a function of deflections. Atluri [1973] used the method of multiple scales to obtain the frequency-response relations and the formula for frequency. He concluded that the

frequency will change depending on the relative magnitudes of the nonlinear elasticity and the nonlinear inertia coefficients, and the coupling between the modes.

Nonlinearities can be either of the hardening or softening type, depending on many factors, such as curvatures, inertia, and mode number. The bending of the amplitude-frequency curve produces a jump phenomenon. It can be verified theoretically by the investigation of the instability due to the in-plane perturbations of the in-plane motion, or experimentally by sweeping the forcing frequency carefully across the resonance region. As a result of calculations, it is found that, for a fixed-free beam, the nonlinear curvatures tend to harden the system while the nonlinear inertias tend to soften the system. Many researchers have reached the same conclusion. Haight and King [1972], Crespo da Silva and Glynn [1978b], Hyer [1980a], Nayfeh and Pai [1989], Pai and Nayfeh [1990], and others found that in the first mode, the nonlinear curvature dominates the nonlinearities, and hence the response is of the hardening type, while in the higher modes, the dominant term is the nonlinear inertia which is of the softening type. Atluri [1973] found that the nonlinear longitudinal inertia, which is of the softening type, dominated the nonlinearity of each mode in his study of a pinned-pinned-sliding beam. For a hinged-clamped beam, Nayfeh and Mook [1979] found the first two modes to be of the hardening type.

When a planar motion under planar forcing becomes unstable to out-of-plane perturbations, a nonplanar motion occurs. Haight and King [1972] reported this whirling phenomenon. They studied the whirling motion of a cantilever beam, with nearly equal principal moments of inertia of the cross-section, excited at its base by a known harmonic displacement in the direction of one of the principal axes. They predicted the excitation frequencies and amplitudes at which whirling motions are possible. In addition to theoretical results, they also verified the instability zone experimentally. The frequencies are accurately predicted, but not the amplitudes. They concluded that the whirling motion is a result of the coupling between motions in the two principal directions through the nonlinear axial inertia. In addition, they concluded that the whirling motion is not possible for an axially driven rod when the principal moments of inertia are equal.

In a similar way, Ho, Scott and Eisley [1975,[1976] studied the large-amplitude whirling of a simply supported beam under a transverse harmonic excitation. They predicted both the in-plane

and out-of-plane instabilities. They obtained regions where the out-of-plane motions are stable, which confirms the existence of nonplanar motion.

Hyer [1978a,b] extended the equations derived by Haight and King [1972] to obtain the out-of-plane motion. He used the method of harmonic balance and the method of multiple scales to obtain four simultaneous, nonlinear, algebraic equations governing the responses. In addition, Hyer found that damping will not only change the shape of the ellipse described by the tip of the beam as it whirls, but also has the effect of shifting some of the energy provided by the base excitation from the out-of-plane displacement to the in-plane displacement. Also, he found that the frequency range where the whirling motion occurs increases with the level of excitation. In his report [1978a], Hyer found that all the whirling motions are stable. But in a later paper [1980b], he found unstable whirling motions in both the first and the second mode under some circumstances. In some of the unstable regions, neither the out-of-plane nor the in-plane motion is stable. This indicates that either limit cycles or chaotic motions might exist in the beam dynamics.

In general, for a slender beam, the frequencies of torsional modes are considerally larger than the bending frequencies. It is usual to assume torsional motions are small and to neglect them. In other words, torsion is not modeled in most of the studies. Hence, the system is always assumed to contain only three degrees of freedom (axial-flexural-flexural) or two degrees of freedom (flexural-flexural). Consequently, bending and torsion are uncoupled.

In all the works mentioned above, the authors followed these assumptions except Crespo da Silva and Glynn [1978a] and Rosen and Friedmann [1979]. Crespo da Silva and Glynn found that the generally neglected nonlinear curvature is the same order as the nonlinear inertia. Because the nonlinear curvature involves the utilization of the Euler angles (for example, Love [1944]), one of the Euler angles, the roll angle ϕ, was used to model the torsion. They derived a set of nonlinear equations of motion containing four degrees of freedom, which describes axial-flexural-flexural-torsional motion. After introducing the inextensionality assumption, the axial equation of motion is used to solve for the constraint force. By ignoring the rotatory inertia and knowing that the Euler angle ϕ does not represent the actual twisted angle (also see Rosen, Loewy and Mathew [1987b] and Pai [1990]), they used one of the curvature components to define a twist angle with

physical meaning. They ended up with a two-degree-of-freedom system which is symmetric, unique and independent of the sequence of Euler-angle rotation, with the relationship of the lateral displacements and torsion included in it. A variety of cases are examined by using these equations, including combinations of clamped, clamped/sliding (Crespo da Silva and Glynn [1979b]), pinned/sliding (Crespo da Silva and Zaretzky [1990]), and spring-like support (Crespo da Silva and Glynn [1979a]) boundaries, and combinations of distributed forces (Crespo da Silva [1978a,b]), end forces (Crespo da Silva [1980]) or free vibrations (Crespo da Silva and Glynn [1979a]). Whirling motion was found in the first three modes for primary resonance in every case. Later, Crespo da Silva [1988a, b] used the same nonlinearities, as used by Crespo da Silva and Glynn [1978a], to derive the equations of motion of an extensional beam. Only linear response was presented.

Rosen and Friedmann [1979] also used nonlinear curvatures to derive the equilibrium equations for a cantilevered beam undergoing moderate rotations and deflections. Their theoretical results are in very good agreement with the experimental results from Dowell, Traybar and Hodges [1977] for both deflections and rotation angle. Recently, Rosen, Loewy and Mathew [1987a, b] used a principal curvature transformation combined with the technique of generalized coordinates to derive the governing equations for a pretwisted rod. In these papers, they described in detail the difference between a physical twist angle and a mathematical rotation angle (the roll angle ϕ). They concluded that the presence of ϕ does not necessarily indicate the existence of a twisting moment. But they did not use this result to form a symmetric system, as Crespo da Silva and Glynn [1978a,b] did.

The static displacement caused by the weight or pre-load could have an important influence on a slender beam. For example, the static deflection could change the natural frequencies and some characteristics of a slender beam. Saito, Sato and Yutani [1976] and Sato, Saito and Otomi [1978] considered a simply supported horizontal beam carrying a movable concentrated mass under a transverse excitation and a parametric excitation, respectively. They found that the change of the lowest natural frequency is proportional to the deflection caused by the concentrated mass. Also, they found that the static deflection has a softening effect which depends on both the weight and the position of the concentrated mass. Hughes and Bert [1990] also found that the softening effects

produced by static deflections could overcome the hardening terms if the static deflections are large enough or the beam is slender enough. Shih, Chen and Garba [1986] studied the effects of weight on a system. By using this information, ground tests for simulating a zero-gravity environment to verify the dynamic characteristics in space are possible.

The governing equations obtained by the above researchers who studied the static deflection contain only one degree of freedom, and are only valid for planar motions. Rosen, Loewy and Mathew [1987c] extended the static analysis in Rosen, Loewy and Mathew [1987a,b] to include the dynamic case. Their equations are suitable for flexural-flexural-torsional motions with the consideration of static deflections. But they did not solve for whirling motion from these equations. Crespo da Silva and Zaretzky [1991] studied the equilibrium deflections and natural frequencies of a cantilevered beam produced by a tip mass. They found that the effect of the tip mass on the approximation of the deflection is significant when the tip mass is heavy.

All the governing equations contain both cubic and quadratic nonlinearities if the static deflection is included. The quadratic term is a contribution from the static displacements. One consequence that could arise from the quadratic term, and thus from the static displacement, is superharmonic resonance of order two and subharmonic resonance of order two. Tseng and Dugundji [1970,1971] studied a fixed-fixed beam under a transverse harmonic excitation. They obtained a governing equation of the Duffing type. The method of harmonic balance was used to find the responses. Primary resonance, subharmonic resonance and superharmonic resonance, including the second order, were found analytically and experimentally. Saito, Sato and Yutani [1976] also found that a planar superharmonic resonance of order two is possible if static displacement is included. Minguet [1989] and Kim and Dugundji [1991] investigated the nonlinear large amplitude free-vibration of composite helicopter blades under large static deflection analytically and experimentally. Linearized model without consideration of rotatory inertia is used in their studies. They found that both large static deflection and large amplitude can affect torsional modes significantly, but bending modes are not influenced much by the geometrical nonlinearities.

In the current study, the governing equations derived by Crespo da Silva and Glynn [1978a] were extended to include static deflection. These equations not only include nonlinear curvature,

nonlinear inertia, inextensionality and static deflection, but also include torsional displacement. In all cases, the torsional displacement was written in terms of lateral displacements and eliminated from the governing equations. This symmetric two-degree-of-freedom system, which is suitable for flexural-flexural motion, is used to re-examine primary resonance, and to develop secondary resonances. Because quadratic terms show up in the governing equations, whirling motions of both superharmonic resonance of order two and subharmonic resonance of order two were found in this study. Both stable and unstable whirling motions were found in every resonance. For some circumstances, both planar and nonplanar motions are unstable which indicates a limit cycle or chaotic motion might exist.

Many types of machinery, for example, rotors, turbines, and structures with motors mounted to their base, are normally operated above their first few natural frequencies. Similarly, the base of a very flexible beam may be subjected to harmonic oscillations at frequencies that are higher than fundamental natural frequency. During the start-up and shut-down periods, such systems must pass through resonance regions. These non-stationary vibrations can be seen often and are important in practical problems. One of the earliest studies on this type of non-stationary vibration was presented by Lewis [1932]. He studied the response of a single-mass elastic system with linear damping under a force with a uniform acceleration in frequency. He found that the maximum amplitude will be smaller than that for a constant frequency. Furthermore, the frequency at which the maximum amplitude occurs is shifted when the frequency is accelerating or decelerating. Kevorkian [1971] investigated a linear one-dimensional oscillator with slowly varying natural frequency under a constant forcing frequency. The results show that the amplitude increases and then decreases when the natural frequency is passing through the forcing frequency. Schumacher [1970] studied the vibrations of a linear elastic beam passing through the resonance region under an excitation with a constant amplitude and varying frequency. Evan-Iwanowski [1976] studied the combination additive resonance of a beam on forked end supports excited by a non-stationary in-plane end moment. Collinge and Ockendon [1979] examined the transition through resonance of a Duffing oscillator with a forcing frequency varying very slowly in the neighborhood of the natural frequency. Nayfeh and Mook [1979] studied the motion of an unbalanced motor mounted

on a cantilevered beam. They found the jump phenomenon in the planar motion when passing through the fundamental mode. Ishida, Ikeda and Yamamoto [1987] examined the transient vibration of a rotating shaft with nonlinear spring characteristics during acceleration through a fundamental resonance. Later, Ishida, Ikeda, Yamamoto and Murakami [1989], and Ishida, Yamamoto, Ikeda and Murakami [1990] investigated non-stationary vibration of the same system during acceleration through a second order subharmonic oscillation and a summed-and-differential harmonic oscillation, respectively. They found that the maximum amplitude depends on both the sweep rate and initial conditions. They concluded that resonance in the non-linear system is hard to pass when compared with the linear system. Nayfeh and Asfar [1988] and Neal and Nayfeh [1990] investigated the response of a single-degree-of-freedom system with cubic non-linearity to a non-stationary principal parametric excitation. They found that the non-stationary response penetrates the instability regions and that the higher the sweeping rate, the deeper the penetration. The penetration depends on the initial conditions and the system parameters.

Although non-stationary resonances have received considerable attention, only a few studies have dealt with a nonlinear beam and the interaction between multiple degrees of freedom. Schumacher [1970] studied a linear beam with the consideration of one degree of freedom. Evan-Iwanowski [1976] studied a non-linear beam with bending and twisting coupled. In the same book, Evan-Iwanowski also investigated the internal resonances of a double pendulum, cylindrical shell and spherical shell. The non-stationary response of the interaction between two lateral displacements, in-plane and out-of-plane, has not been investigated. In this dissertation, the non-stationary resonances of both in-plane and out-of-plane components, when the forcing frequency is passing through primary and secondary resonances, are investigated. The effects of the sweep rate, initial conditions, force amplitude and damping on the magnitude and position of the maximum response amplitude are examined.

1.3 Outline of Dissertation

In Chapter 2, a derivation of the nonlinear equations governing the motion of a beam, by the extended Hamilton's principle, is presented. Taylor series expansions are applied to obtain order-three approximate equations. Later, the governing equations are nondimensionalized. By introducing the inextensionality and torsional rigidity assumptions, the system is reduced to contain only two displacement functions (flexural-flexural), but still includes the bending-torsion coupling effect.

In Chapter 3, Galerkin's procedure is used to eliminate the spatial functions from the governing equations. Three modes are included. The static deflection is determined and is used to obtain new governing equations, which contain both quadratic and cubic terms.

In Chapter 4, the method of multiple scales is used to find an approximate solution. Superharmonic resonances of order two and three, subharmonic resonances of order two and three, and primary resonance are studied. Four nonlinear autonomous modulation equations, describing the amplitudes and phases, are produced by eliminating the secular terms in the second-order equations. The steady-state solution is then found by algebraic calculations.

In Chapter 5, a variety of stationary results are shown, including the effects of damping and the level of forces. Also, non-stationary results are shown including the effects of the sweep rate of the forcing frequency, the initial conditions, and system parameters on the magnitude and position of the maximum amplitude. Furthermore, the non-stationary result from the integration of the modulation equations is compared with that from the integration of the original differential equations.

In Chapter 6, conclusions and suggestions for future work are given.

2 Formulation of Governing Equations

2.1 Statement of Problem

The response of a slender horizontal fixed-free beam excited by a harmonic force, as shown in Figure 2.1, is investigated in this dissertation. The notation needed in the derivation of the governing equations is defined as follows: x denotes the coordinate in the longitudinal direction; y denotes the coordinate in the vertical direction; z therefore is defined following the right-hand rule; s is the undeformed arc length; t is the time; η, ξ, and ζ are the principal axes of the cross section at position s; u, v, and w are the components of the displacement of the centroid at an arbitrary position s along the axes x, y, and z, respectively; and ϕ, θ, and ψ are three Euler angles that perform the sequence of rotations.

Next, the extended Hamilton's principle will be applied to formulate the equations of motion of a beam. Few assumptions will be used and a sequence of rotations, which relates two coordinate systems, will be defined first.

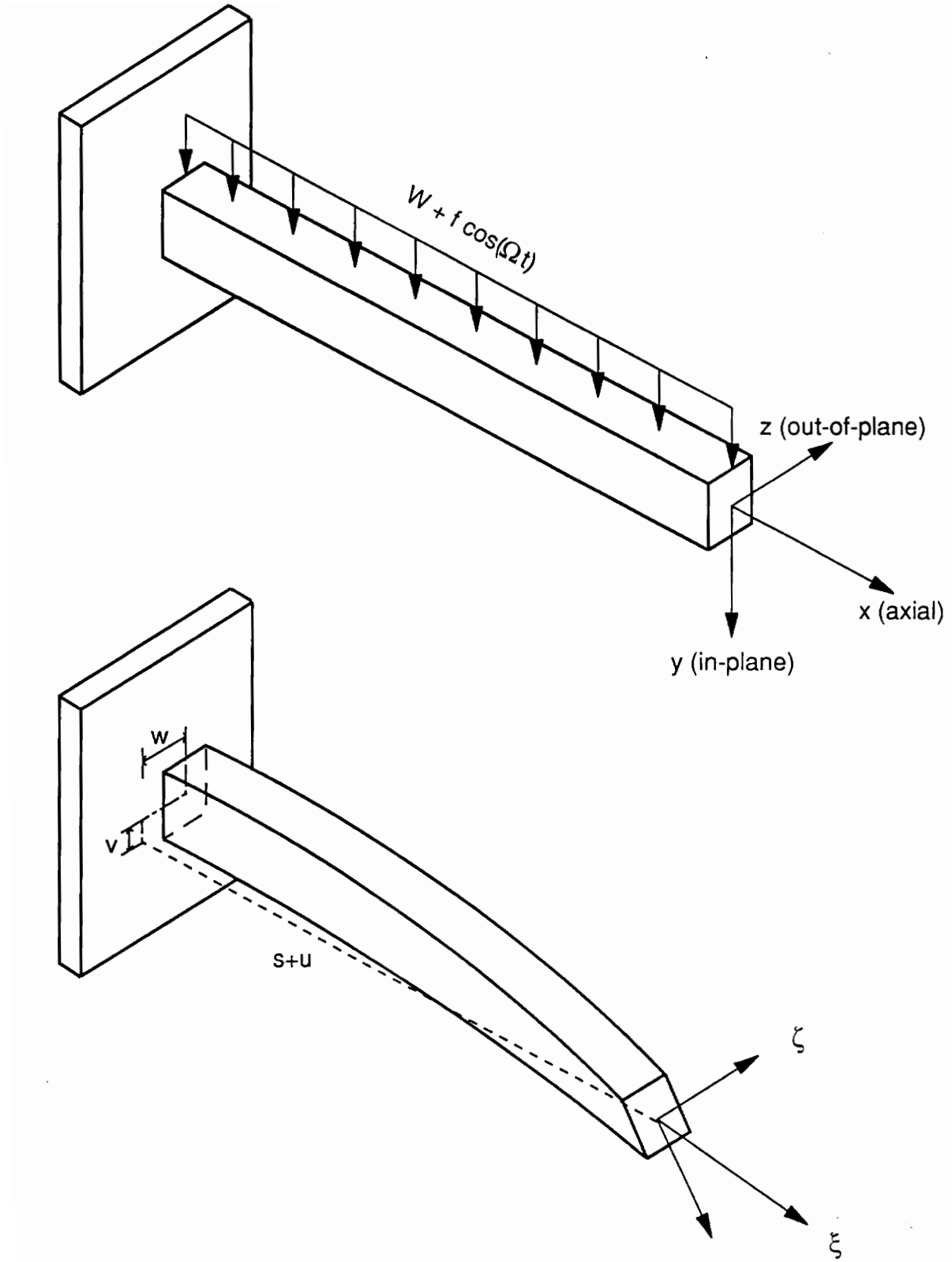

Figure 2.1 Fixed-free beam excited by distributed force.

2.2 Extended Hamilton's Principle

In this section, the equations of motion of a beam are formulated. The equations of motion can be derived by Newton's second law or variational methods. Newton's second law contains more physical information, while the variational methods are more systematic. In this dissertation, the extended Hamilton's principle is used to derive the equations of motion. Basically, we follow Crespo da Silva and Glynn [1978a]. The assumptions used in their derivation are as follows:

1. The beam is inextensional.

2. The material properties are assumed to be constant, i.e., the beam is assumed to be uniform and homogeneous.

The normal strain in the axial direction is:

$$e_0 = \sqrt{(1+u')^2 + v'^2 + w'^2} - 1 \tag{2.2.1}$$

where

$$(\ )' = \frac{\partial(\ )}{\partial s}$$

Because the beam is assumed to be inextensional, the normal strain in the axial direction must be equal to zero. Hence the following equation must be true for an inextensional beam:

$$(1+u')^2 + v'^2 + w'^2 = 1 \tag{2.2.2}$$

To calculate the kinetic energy and strain energy, two coordinate systems are introduced to describe the beam dynamics (see Figure 2.2). The axes (x, y, z) denote the inertial axes, while (ξ, η, ζ) denote the principal axes attached to the beam's cross section at an arbitrary position s. The components of the angular velocity $(\omega_\xi, \omega_\eta, \omega_\zeta)$ are defined with respect to the axes (ξ, η, ζ).

The orientation of the principal axes is obtained by aligning axes (ξ, η, ζ) with inertial axes (x, y, z) and then carrying out three consecutive Euler angle rotations. First, we rotate an angle ψ about the z-axis to give (x_2, y_2, z_2) axes. Then the second rotation about the y_2-axis with an angle θ is carried out to give (x_3, y_3, z_3) axes. The third rotation is about the x_3-axis, or ξ-axis, with an angle ϕ to give (ξ, η, ζ) axes. The relationship between the inertial axes and the rotating axes is thus:

$$\begin{bmatrix} \vec{x} \\ \vec{y} \\ \vec{z} \end{bmatrix} = \begin{bmatrix} \cos\psi & -\sin\psi & 0 \\ \sin\psi & \cos\psi & 0 \\ 0 & 0 & 1 \end{bmatrix} \begin{bmatrix} \cos\theta & 0 & \sin\theta \\ 0 & 1 & 0 \\ -\sin\theta & 0 & \cos\theta \end{bmatrix} \begin{bmatrix} 1 & 0 & 0 \\ 0 & \cos\phi & -\sin\phi \\ 0 & \sin\phi & \cos\phi \end{bmatrix} \begin{bmatrix} \vec{\xi} \\ \vec{\eta} \\ \vec{\zeta} \end{bmatrix} \tag{2.2.3a}$$

$$= \begin{bmatrix} \cos\psi\cos\theta & -\sin\psi\cos\phi + \cos\psi\sin\theta\sin\phi & \sin\psi\sin\phi + \cos\psi\sin\theta\cos\phi \\ \sin\psi\cos\theta & \cos\psi\cos\phi + \sin\psi\sin\theta\sin\phi & -\cos\psi\sin\phi + \sin\psi\sin\theta\cos\phi \\ -\sin\theta & \cos\theta\sin\phi & \cos\theta\cos\phi \end{bmatrix} \begin{bmatrix} \vec{\xi} \\ \vec{\eta} \\ \vec{\zeta} \end{bmatrix} \tag{2.2.3b}$$

$$= \begin{bmatrix} l_1 & l_2 & l_3 \\ m_1 & m_2 & m_3 \\ n_1 & n_2 & n_3 \end{bmatrix} \begin{bmatrix} \vec{\xi} \\ \vec{\eta} \\ \vec{\zeta} \end{bmatrix} \tag{2.2.3c}$$

where

ϕ, θ, ψ: Euler angles

The kinematic equations describe the relationship between Euler angles (ϕ, θ, ψ) and angular velocities $(\omega_\xi, \omega_\eta, \omega_\zeta)$. The derivation of the kinematic equations is based on the time rate of change of Euler angles from inertial axes into rotating axes. The Euler angles, ψ, θ and ϕ, are measured in the inertial axes, the (x_2, y_2, z_2) axes and the (x_3, y_3, z_3) axes, respectively, while the angular velocities are measured in the rotating axes. Hence, it is obvious that the changes of the Euler angles $\dot{\phi}, \dot{\theta}$ and $\dot{\psi}$ are not equal to the angular velocities ω_ξ, ω_η and ω_ζ.

The procedure for expressing the angular velocity in terms of the derivatives of the Euler angles ϕ, θ and ψ is as follows. First, the angular velocity vector $\vec{\omega}$ can be expressed in the rotating system:

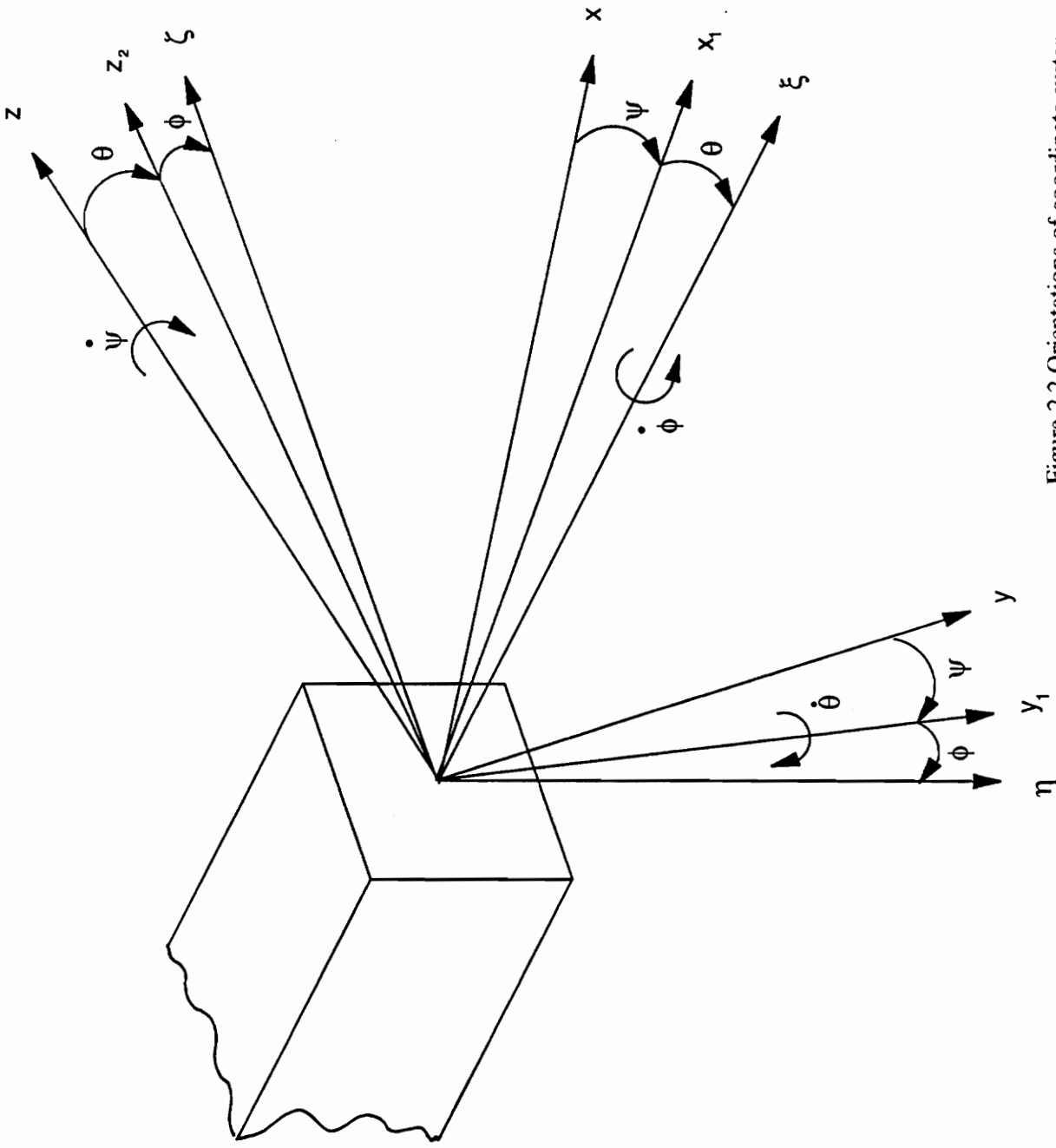

Figure 2.2 Orientations of coordinate systems

$$\vec{\omega} = \omega_\xi \vec{\xi} + \omega_\eta \vec{\eta} + \omega_\zeta \vec{\zeta} \tag{2.2.4}$$

Second, $\dot{\phi}, \dot{\theta}$ and $\dot{\psi}$ are associated with the rotations about the $\vec{x_3}, \vec{y_2}$ and $\vec{z}$ axes, respectively (see Figure 2.2). Hence the angular velocity $\vec{\omega}$ can be expressed as:

$$\vec{\omega} = \dot{\phi}\vec{x_3} + \dot{\theta}\vec{y_2} + \dot{\psi}\vec{z} \tag{2.2.5}$$

where

$$\dot{(\ )} = \frac{\partial(\ )}{\partial t}$$

Similar to the transformation of eq (2.2.3a), the relationships between $\vec{x_3}, \vec{y_2}, \vec{z}$ and the rotating axes are:

$$\vec{x_3} = \vec{\xi} \tag{2.2.6}$$

$$\vec{y_2} = \cos\phi\vec{\eta} - \sin\phi\vec{\zeta} \tag{2.2.7}$$

$$\vec{z} = -\sin\theta\vec{\xi} + \sin\phi\cos\theta\vec{\eta} + \cos\phi\cos\theta\vec{\zeta} \tag{2.2.8}$$

By substituting eqs (2.2.6)-(2.2.8) into eq (2.2.5) and rearranging, eq (2.2.5) becomes:

$$\begin{aligned}\vec{\omega} = \vec{\omega}(s, t) &= \omega_\xi \vec{\xi} + \omega_\eta \vec{\eta} + \omega_\zeta \vec{\zeta} \\ &= (\dot{\phi} - \dot{\psi}\sin\theta)\vec{\xi} + (\dot{\theta}\cos\phi + \dot{\psi}\sin\phi\cos\theta)\vec{\eta} + (-\dot{\theta}\sin\phi + \dot{\psi}\cos\phi\cos\theta)\vec{\zeta}\end{aligned} \tag{2.2.9}$$

Because the Euler angles describing the orientation of the principal axes at an arbitrary position along the x-axis are functions of time and only one spatial variable s along the x-axis, the angular velocities of the principal axes are also functions of t and s only. They are not functions of y and z. The displacement vector of the centroid of the cross section at an arbitrary position s is denoted as:

$$\vec{u}(s,t) = u(s,t)\vec{x} + v(s,t)\vec{y} + w(s,t)\vec{z} \tag{2.2.10}$$

Because the displacements are described in the inertial axes, the velocity is simply:

$$\vec{V} = \dot{u}\vec{x} + \dot{v}\vec{y} + \dot{w}\vec{z} \tag{2.2.11}$$

The kinetic energy per unit length is:

$$T = \frac{1}{2} m(\dot{u}^2 + \dot{v}^2 + \dot{w}^2) + \frac{1}{2}(j_\xi \omega_\xi^2 + j_\eta \omega_\eta^2 + j_\zeta \omega_\zeta^2) \tag{2.2.12}$$

where

m: mass per unit length,
u, v, w: displacements,
$\omega_\xi, \omega_\eta, \omega_\zeta$: angular velocities,
j_ξ, j_η, j_ζ: principal mass moments of inertia.

The derivation of the strain energy is based on the following assumptions: (1) the Poisson effect, shear deformation, and warping are neglected; (2) the bending and twisting moments are proportional to the curvatures. The components of the curvature vector $\vec{\rho} = \tilde{\rho}_\xi \vec{\xi} + \tilde{\rho}_\eta \vec{\eta} + \tilde{\rho}_\zeta \vec{\zeta}$ are defined as (Love [1944]):

$$\tilde{\rho}_\xi \equiv \frac{\partial \vec{\eta}}{\partial \tilde{s}} \cdot \vec{\zeta} \tag{2.2.13a}$$

$$\tilde{\rho}_\eta \equiv \frac{\partial \vec{\zeta}}{\partial \tilde{s}} \cdot \vec{\xi} \tag{2.2.13b}$$

$$\tilde{\rho}_\zeta \equiv \frac{\partial \vec{\xi}}{\partial \tilde{s}} \cdot \vec{\eta} \tag{2.2.13c}$$

where dot stands for the inner product of two vectors, and $\tilde{s}$ is the position along the deformed curve through the centroids of the cross sections. By using eq (2.2.3c), the above equations can be expressed as follows:

$$\tilde{\rho}_\xi \equiv l_3 \frac{\partial l_2}{\partial \tilde{s}} + m_3 \frac{\partial m_2}{\partial \tilde{s}} + n_3 \frac{\partial n_2}{\partial \tilde{s}} \tag{2.2.14a}$$

$$\tilde{\rho}_\eta \equiv l_1 \frac{\partial l_3}{\partial \tilde{s}} + m_1 \frac{\partial m_3}{\partial \tilde{s}} + n_1 \frac{\partial n_3}{\partial \tilde{s}} \tag{2.2.14b}$$

$$\tilde{\rho}_\zeta \equiv l_2 \frac{\partial l_1}{\partial \tilde{s}} + m_2 \frac{\partial m_1}{\partial \tilde{s}} + n_2 \frac{\partial n_1}{\partial \tilde{s}} \tag{2.2.14c}$$

where l_i, m_i and n_i, $i = 1,2,3$, are the elements of the transformation matrix defined in eq (2.2.3c). Due to the small strain assumption, the distinctions between $\tilde{s}$ and s, and $\tilde{\rho}_i$ and ρ_i, $i = \xi, \eta, \zeta$, can be ignored. After carrying out the calculations, the curvatures can be expressed as functions of the Euler angles:

$$\rho_\xi = \phi' - \psi' \sin\theta \tag{2.2.15a}$$

$$\rho_\eta = \psi' \cos\theta \sin\phi + \theta' \cos\phi \tag{2.2.15b}$$

$$\rho_\zeta = \psi' \cos\theta \cos\phi + \theta' \sin\phi \tag{2.2.15c}$$

The curvatures then can also be obtained using Love's kinetic analogy by replacing the time derivatives by spatial derivatives in the expressions for the angular velocities. The results are the same as those shown in eqs (2.2.15a)-(2.2.15c). The strain energy thus is:

$$V = \frac{1}{2}(D_\xi \rho_\xi^2 + D_\eta \rho_\eta^2 + D_\zeta \rho_\zeta^2) \tag{2.2.16}$$

where

D_ξ, D_η, D_ζ: principal stiffnesses,
$\rho_\xi, \rho_\eta, \rho_\zeta$: curvatures.

The extended Hamilton's principle is defined as:

$$\int_{t_1}^{t_2} (\delta T + \delta W) dt = 0 \tag{2.2.17}$$

where T is the kinetic energy, W is the work done by the forces. It can be expressed in detail as follows:

$$\begin{aligned} \delta I \equiv \delta \int_{t_1}^{t_2} \{ \int_0^l [L + \frac{1}{2} \lambda (1 - (1 + u')^2 - v'^2 - w'^2) ds] dt \\ + \int_{t_1}^{t_2} [\delta W_B + \int_0^l (Q^u \delta u + Q^v \delta v + Q^w \delta w + Q^\phi \delta \phi)] ds \} dt = 0 \end{aligned} \tag{2.2.18}$$

$$\begin{aligned} L = Lagrangian\ per\ unit\ length = (T - V)/l = [(Kinetic\ \ energy) - (Strain\ \ energy)]/Length \\ = \frac{1}{2} m(\dot{u}^2 + \dot{v}^2 + \dot{w}^2) + \frac{1}{2} (j_\xi \omega_\xi^2 + j_\eta \omega_\eta^2 + j_\zeta \omega_\zeta^2) - \frac{1}{2} (D_\xi \rho_\xi^2 + D_\eta \rho_\eta^2 + D_\zeta \rho_\zeta^2) \end{aligned} \tag{2.2.19}$$

where

λ: Lagrange multiplier,
δW_B: virtual work associated with boundary force,
Q^u, Q^v, Q^w, Q^ϕ: generalized forces per unit length.

The first variation δI is a function of the following variables:

$$\delta I = \delta I(u, v, w, \phi, \theta, \psi, \dot{u}, \dot{v}, \dot{w}, \dot{\phi}, \dot{\theta}, \dot{\psi}, u', v', w', \phi', \theta', \psi')$$

$$
\begin{aligned}
= 0 = & \frac{\partial I}{\partial u}\delta u + \frac{\partial I}{\partial v}\delta v + \frac{\partial I}{\partial w}\delta w + \frac{\partial I}{\partial \phi}\delta\phi + \frac{\partial I}{\partial \theta}\delta\theta + \frac{\partial I}{\partial \psi}\delta\psi \\
& + \frac{\partial I}{\partial \dot{u}}\delta\dot{u} + \frac{\partial I}{\partial \dot{v}}\delta\dot{v} + \frac{\partial I}{\partial \dot{w}}\delta\dot{w} + \frac{\partial I}{\partial \dot{\phi}}\delta\dot{\phi} + \frac{\partial I}{\partial \dot{\theta}}\delta\dot{\theta} + \frac{\partial I}{\partial \dot{\psi}}\delta\dot{\psi} \\
& + \frac{\partial I}{\partial u'}\delta u' + \frac{\partial I}{\partial v'}\delta v' + \frac{\partial I}{\partial w'}\delta w' + \frac{\partial I}{\partial \phi'}\delta\phi' + \frac{\partial I}{\partial \theta'}\delta\theta' + \frac{\partial I}{\partial \psi'}\delta\psi'
\end{aligned} \tag{2.2.20}
$$

A total of six variables (u, v, w, ϕ, θ and ψ) is involved in the last equation, but only three of them are independent. In other words, three more equations are needed. From the inextensional assumption, one can express u' in terms of v' and w':

$$
u' = \sqrt{1 - v'^2 - w'^2} - 1 \tag{2.2.21}
$$

Moreover, the angles θ and ψ can be expressed in terms of u', v' and w' by the following calculations. We select an arbitrary point, p, on the x-axis and let $\vec{s}$ denotes its position vector. After deformation, the point, p, moves to a new position, p', and we let $\vec{s'}$ denotes the corresponding position vector (see Figure 2.3). The relationship between $\vec{s}$ and $\vec{s'}$ is written as:

$$
\vec{s'} = \vec{s} + \vec{u} \tag{2.2.22}
$$

where $\vec{u}$ is the displacement vector from point p to p'. The above equation can also be expressed as:

$$
s'\vec{\xi} = s\vec{x} + u\vec{x} + v\vec{y} + w\vec{z} \tag{2.2.23}
$$

After differentiating both sides of eq (2.2.23), we obtain:

$$
ds'\vec{\xi} = ds\vec{x} + du\vec{x} + dv\vec{y} + dw\vec{z} \tag{2.2.24}
$$

From the transformation matrix, eq (2.2.3b), we can find the expression for the base vector $\vec{\xi}$ in terms of $\vec{x}, \vec{y}$ and $\vec{z}$, and substitute it in eq (2.2.24), giving:

$$
ds'(\cos\theta\cos\psi\vec{x} + \cos\theta\sin\psi\vec{y} - \sin\theta\vec{z}) = ds\vec{x} + du\vec{x} + dv\vec{y} + dw\vec{z} \tag{2.2.25}
$$

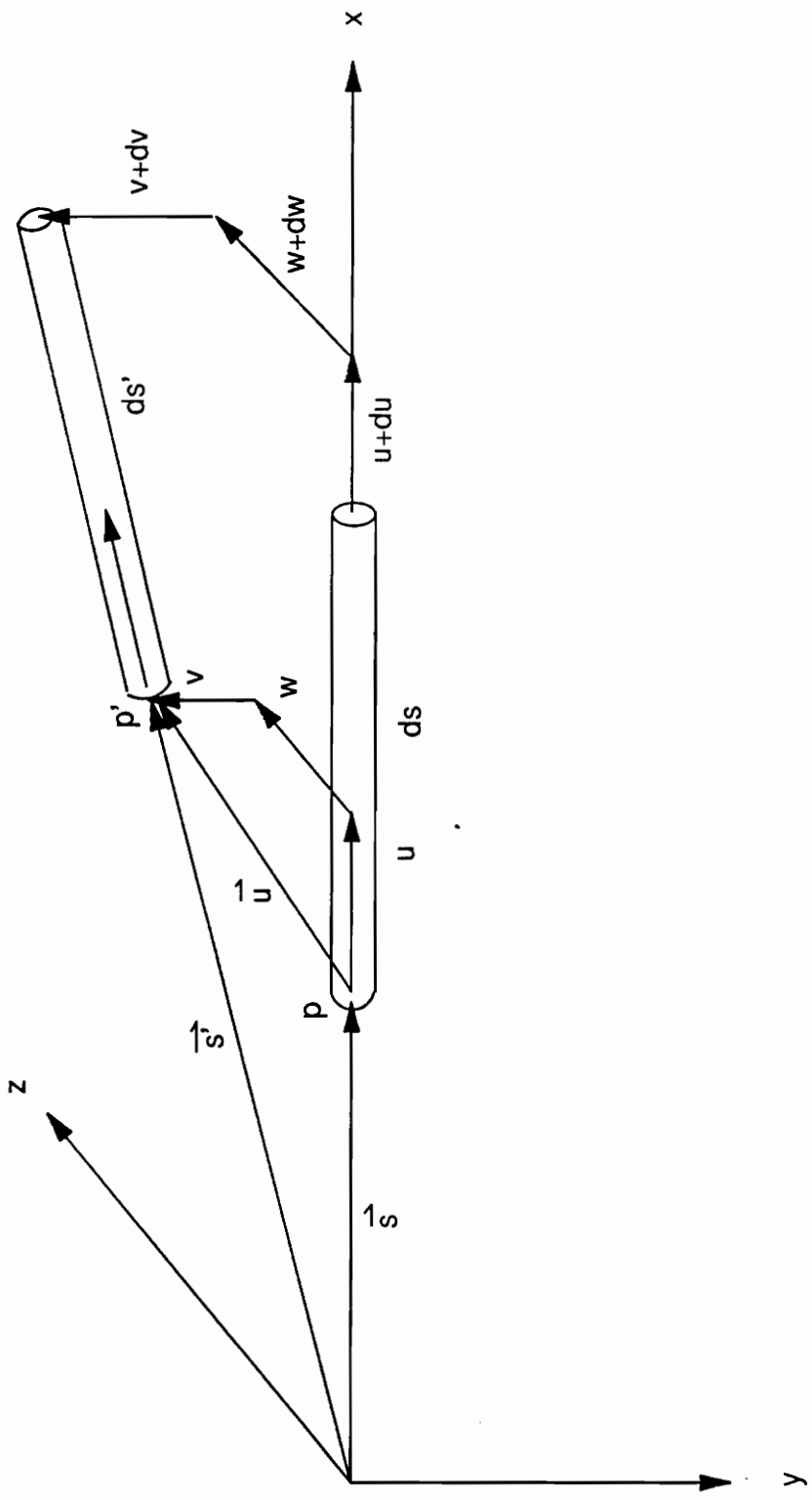

Figure 2.3 Transformation geometry

We can obtain the following equations by equating the components on both sides and taking derivatives with respect to s:

$$\frac{ds'}{ds}\cos\theta\cos\psi = 1 + u' \tag{2.2.26a}$$

$$\frac{ds'}{ds}\cos\theta\sin\psi = v' \tag{2.2.26b}$$

$$-\frac{ds'}{ds}\sin\theta = w' \tag{2.2.26c}$$

If we divide eq (2.2.26b) by eq (2.2.26a), the expression for ψ in terms of u' and v' can be found as:

$$\tan\psi = \frac{v'}{1+u'} \tag{2.2.27}$$

The expression for θ in terms of u', v' and w' can be found by the following calculations. First we square eqs (2.2.26a) and (2.2.26b), and add them together; then we divide eq (2.2.26c) by the square root of the previous result to find:

$$\tan\theta = \frac{-w'}{\sqrt{(1+u')^2 + v'^2}} \tag{2.2.28}$$

From the above two equations, one can derive the following expressions, which can be used to eliminate $\delta\theta$ and $\delta\psi$ after integrating by parts:

$$\delta\theta = \frac{\partial\theta}{\partial u'}\delta u' + \frac{\partial\theta}{\partial v'}\delta v' + \frac{\partial\theta}{\partial w'}\delta w' \tag{2.2.29}$$

$$\delta\psi = \frac{\partial\psi}{\partial u'}\delta u' + \frac{\partial\psi}{\partial v'}\delta v' \tag{2.2.30}$$

Thus only δu, δv, δw and $\delta\phi$ will be used to form the Euler-Lagrange equations:

$$\delta u: \quad Q^u - m\ddot{u} + \frac{\partial}{\partial s}\left[A_\theta \frac{\partial \theta}{\partial u'} + A_\psi \frac{\partial \psi}{\partial u'} + \lambda(1 + u')\right] \equiv Q^u - m\ddot{u} + G_u{}' = 0 \tag{2.2.31a}$$

$$\delta v: \quad Q^v - m\ddot{v} + \frac{\partial}{\partial s}\left[A_\theta \frac{\partial \theta}{\partial v'} + A_\psi \frac{\partial \psi}{\partial v'} + \lambda v'\right] \equiv Q^v - m\ddot{v} + G_v{}' = 0 \tag{2.2.31b}$$

$$\delta w: \quad Q^w - m\ddot{w} + \frac{\partial}{\partial s}\left[A_\theta \frac{\partial \theta}{\partial w'} + \lambda w'\right] \equiv Q^w - m\ddot{w} + G_w{}' = 0 \tag{2.2.31c}$$

$$\delta \phi: \quad Q^\phi - A_\phi = 0 \tag{2.2.31d}$$

where

$$A_\theta = -\frac{\partial L}{\partial \theta} + \frac{\partial^2 L}{\partial t \partial \dot{\theta}} + \frac{\partial^2 L}{\partial s \partial \theta'} \tag{2.2.32a}$$

$$A_\psi = -\frac{\partial L}{\partial \psi} + \frac{\partial^2 L}{\partial t \partial \dot{\psi}} + \frac{\partial^2 L}{\partial s \partial \psi'} \tag{2.2.32b}$$

$$A_\phi = -\frac{\partial L}{\partial \phi} + \frac{\partial^2 L}{\partial t \partial \dot{\phi}} + \frac{\partial^2 L}{\partial s \partial \phi'} \tag{2.2.32c}$$

At this point we have four equations of motion plus the constraint, and five unknowns, u, v, w, ϕ and λ. The constraint will be used to solve for u, and the equation for u, eq (2.2.31a), will be used to obtain the constraint force, λ. The twist angle ϕ will be obtained from the equation for ϕ, eq (2.2.31d), after some simplifications are made.

The boundary conditions can be grouped into seven terms from δu, δv, δw, $\delta \phi$, $\delta u'$, $\delta v'$ and $\delta w'$. But from eq (2.2.21) the following equation can be obtained to eliminate $\delta u'$:

$$\delta u' = -(1 + u')^{-1} v' \delta v' - (1 + u')^{-1} w' \delta w' \tag{2.2.33}$$

The boundary conditions are listed as follows:

$$\delta u: \qquad \int_{t_1}^{t_2} [- G_u \delta u \Big|_0^l] dt = 0 \tag{2.2.34a}$$

$$\delta v: \qquad \int_{t_1}^{t_2} [- G_v \delta v \Big|_0^l] dt = 0 \tag{2.2.34b}$$

$$\delta w: \qquad \int_{t_1}^{t_2} [- G_w \delta w \Big|_0^l] dt = 0 \tag{2.2.34c}$$

$$\delta \phi: \qquad \int_{t_1}^{t_2} [\frac{\partial L}{\partial \phi'} \delta \phi \Big|_0^l] dt = 0 \tag{2.2.34d}$$

$$\delta v': \qquad \int_{t_1}^{t_2} [(- H_u (1 + u')^{-1} v' + H_v) \delta v' \Big|_0^l] dt = 0 \tag{2.2.34e}$$

$$\delta w': \qquad \int_{t_1}^{t_2} [(- H_u (1 + u')^{-1} w' + H_w) \delta v' \Big|_0^l] dt = 0 \tag{2.2.34f}$$

where

$$H_u = \frac{\partial L}{\partial \theta'} \frac{\partial \theta}{\partial u'} + \frac{\partial L}{\partial \psi'} \frac{\partial \psi}{\partial u'} \tag{2.2.35a}$$

$$H_v = \frac{\partial L}{\partial \theta'}\frac{\partial \theta}{\partial v'} + \frac{\partial L}{\partial \psi'}\frac{\partial \psi}{\partial v'} \tag{2.2.35b}$$

$$H_w = \frac{\partial L}{\partial \theta'}\frac{\partial \theta}{\partial w'} + \frac{\partial L}{\partial \psi'}\frac{\partial \psi}{\partial w'} \tag{2.2.35c}$$

Because the exact solution of the above nonlinear equations is not possible to find, Taylor-series expansions will be used to find the approximate solution. Terms will be kept up to $O(\hat{\varepsilon}^3)$ only.

2.3 Order-Three Taylor-Series Expansion

The equations of motion derived from the extended Hamilton's principle are nonlinear and involve transcendental functions. It is not possible to find the exact solution; hence an approximate solution is determined by a perturbation method. To determine approximate solutions, the equations of motion are first expanded in Taylor-series.

For small but finite oscillations, the displacements u, v, w and ϕ are first assumed to be of order $\hat{\varepsilon}$, where $\hat{\varepsilon}$ is a small parameter for bookkeeping purposes. Because the equations of motion have been reduced to involve only u, v, w and ϕ, the expansions must be expressed in terms of these four variables. Furthermore, from eq (2.2.21), one can replace u' as a function of v' and w', and then the expansions can be expressed in terms of only three variables, v, w and ϕ. From eqs (2.2.27) and (2.2.28), the corresponding expressions for cos and sin can be obtained. Then one can find the following expansions:

$$\tan\theta = \frac{-w'}{\sqrt{(1+u')^2 + v'^2}} \tag{2.3.1a}$$

$$\sin\theta = \frac{-w'}{\sqrt{(1+u')^2+v'^2+w'^2}} \left(= -w'\right) \tag{2.3.1b}$$

$$\cos\theta = \frac{\sqrt{(1+u')^2+v'^2}}{\sqrt{(1+u')^2+v'^2+w'^2}} \left(= \sqrt{(1+u')^2+v'^2} = \sqrt{1-w'^2} \simeq 1 - \frac{w'^2}{2}\right) \tag{2.3.1c}$$

$$\tan\psi = \frac{v'}{1+u'} \tag{2.3.1d}$$

$$\sin\psi = \frac{v'}{\sqrt{(1+u')^2+v'^2}} \left(= \frac{v'}{\sqrt{1-w'^2}} \simeq v' + \frac{v'w'^2}{2} + \ldots\right) \tag{2.3.1e}$$

$$\cos\psi = \frac{1+u'}{\sqrt{(1+u')^2+v'^2}} \left(= \frac{\sqrt{1-v'^2-w'^2}}{\sqrt{1-w'^2}} \simeq 1 - \frac{v'^2}{2} + \ldots\right) \tag{2.3.1f}$$

$$\sin\phi \simeq \phi - \frac{\phi^3}{6} + \ldots \tag{2.3.1g}$$

$$\cos\phi \simeq 1 - \frac{\phi^2}{2} + \ldots \tag{2.3.1h}$$

$$\theta = \tan^{-1}\frac{-w'}{\sqrt{(1+u')^2+v'^2}} \left(\simeq -w'\left(1+\frac{w'^2}{6}\right)\right) \tag{2.3.1i}$$

$$\psi = \tan^{-1}\frac{v'}{1+u'} \left(\simeq v'\left(1+\frac{v'^2}{6}+\frac{w'^2}{2}\right)\right) \tag{2.3.1j}$$

Substituting the above expansions eqs (2.3.1a)-(2.3.1j) into eqs (2.2.31a)-(2.2.35c), and keeping terms up to order $O(\hat{\varepsilon}^3)$, one obtains the following equations:

The order-three equations of motion are:

$$\begin{aligned} m\ddot{u} - Q_u = {} & [(j_\eta - j_\zeta)(\dot{v}'\dot{\phi})w' - j_\eta\ddot{w}'w' + (j_\eta - j_\zeta)(\dot{w}'\dot{\phi})v' - j_\zeta\ddot{v}'v' + j_\xi(\dot{\phi}\dot{v}')w' - j_\xi(\dot{\phi}\dot{w}')v' \\ & - (D_\eta - D_\zeta)(v''\phi)'w' + D_\eta w'''w' - (D_\eta - D_\zeta)(w''\phi)'v' + D_\zeta v'''v' - D_\xi(\phi'v'')w' \\ & + D_\xi(\phi'w'')v' - v'w'Q_\phi + \lambda(1+u')]' \end{aligned} \tag{2.3.2a}$$

$$m\ddot{v} - Q_v = [j_\xi(\dot{\phi} + \dot{v}'w')\dot{w}' + j_\eta(\phi^2\dot{v}' - \phi\dot{w}' - v'\dot{w}'w')\dot{} - j_\zeta(\phi^2\dot{v}' - \phi\dot{w}' - v'w'\dot{w}' - \dot{v}')\dot{}$$
$$+ (j_\zeta\dot{v}'^2 + j_\eta\dot{w}'^2)v' - D_\xi(\phi' + v''w')w'' - D_\eta(\phi^2v'' - \phi w'' - v'w'w'')'$$
$$+ D_\zeta(\phi^2v'' - \phi w'' - v'w'w'' - v'')' - (D_\zeta v''^2 + D_\eta w''^2)v' + w'Q_\phi + \lambda v']' \tag{2.3.2b}$$

$$m\ddot{w} - Q_w = [-(j_\eta - j_\zeta)(\phi\dot{v}' + \phi^2\dot{w}')\dot{} - j_\eta(-\ddot{w}' - w'\dot{w}'^2) + j_\zeta\dot{v}'^2w' - j_\xi(\dot{\phi} + \dot{v}'w')\dot{v}'$$
$$+ (D_\eta - D_\zeta)(\phi v'' + \phi^2w'')' + D_\eta(-w''' - w'w''^2) - D_\zeta v''^2w' + D_\xi(\phi' + v''w')v'' + \lambda w']' \tag{2.3.2c}$$

$$Q_\phi = j_\xi(\dot{\phi} + \dot{v}'w')\dot{} - (j_\eta - j_\zeta)(\dot{v}'^2\phi - \dot{w}'^2\phi - \dot{v}'\dot{w}')$$
$$- D_\xi(\phi' + v''w')' + (D_\eta - D_\zeta)(v''^2\phi - w''^2\phi - v''w'') \tag{2.3.2d}$$

The order-three boundary conditions are:

$$\frac{\partial L}{\partial \phi'}\delta\phi\Big|_0^l \simeq [-D_\xi(\phi' + v''w')]\delta\phi\Big|_0^l = 0 \tag{2.3.3a}$$

$$[H_v - H_u(1+u')^{-1}v']\delta v\Big|_0^l \simeq \{-D_\xi(\phi' + v''w')w' - D_\eta(v''\phi^2 - w''\phi) + D_\zeta(v''\phi^2 - w''\phi)$$
$$- D_\zeta[v'' + v'(w'w'' + v'v'')]\}\delta v\Big|_0^l = 0 \tag{2.3.3b}$$

$$[H_w - H_u(1+u')^{-1}w']\delta w\Big|_0^l \simeq [(D_\eta - D_\zeta)(w''\phi^2 + v''\phi) - D_\eta w'' - D_\eta w''w'^2$$
$$- D_\zeta v'v''w']\delta w\Big|_0^l = 0 \tag{2.3.3c}$$

The equations of motion involve the Euler angles. The angles are not unique and depend on the order of the sequence, i.e., the $\psi - \theta - \phi$ rotation does not lead to the same equations as the $\phi - \theta - \psi$ rotation with the same magnitudes of the angles. In other words, the equations of motion in eqs (2.3.2a)-(2.3.2d) are not symmetric in v and w; the displacements v and w are not interchangeable. Due to the fact that the ψ and θ rotations will create an extra twist angle around the ξ axis, the angle ϕ around the ξ axis in the $\psi - \theta - \phi$ rotation is not the actual twist angle of the beam. The actual twist angle of the beam is the accumulated angle of the twist curvature ρ_ξ from

0 to s. This is discussed by Rosen [1987b] and Pai [1990]. They proved the existence of symmetry by rotating the reference coordinate by 90° for a beam with a square or circular cross section, i.e., replacing w by v and v by $-w$. They concluded that the equations expressed in v, w and γ are symmetric, unique and independent of the sequence of Euler angle rotations. The twist curvature ρ_ξ is defined in eq (2.2.15a) as:

$$\rho_\xi = \phi' - \psi' \sin\theta \tag{2.3.4}$$

After using eqs (2.3.1b) and (2.3.1j), it becomes:

$$\rho_\xi = \phi' + v''w' \tag{2.3.5}$$

According to the above equation, a twist angle γ can be defined as:

$$\gamma = \phi + \int_0^s v''w'ds \tag{2.3.6}$$

Substituting γ into eqs (2.3.2a)-(2.3.2d), one obtains the symmetric order-three equations of motion as follows:

$$\begin{aligned} m\ddot{u} - Q_u = {} & [(j_\eta - j_\zeta)(\ddot{v}'w'\gamma + v'\ddot{w}'\gamma + \dot{v}'w'\dot{\gamma} + v'\dot{w}'\dot{\gamma}) - j_\eta\ddot{v}'v' - j_\eta\ddot{w}'w' + j_\xi(\dot{v}'w'\dot{\gamma} - v'\dot{w}'\dot{\gamma}) \\ & - (D_\eta - D_\zeta)(v'''w'\gamma + v'w'''\gamma + v''w'\gamma' + v'w''\gamma') + D_\eta v'''v' + D_\eta w'''w' \\ & - D_\xi(v''w'\gamma' - v'w''\gamma') + \lambda(1+u')]' \end{aligned} \tag{2.3.7a}$$

$$\begin{aligned} m\ddot{v} - Q_v = {} & [j_\xi(\dot{w}'\dot{\gamma} - \dot{w}'[\int_0^s v''w'ds]^{\cdot} + \dot{v}'\dot{w}'w') + j_\eta(\dot{v}'\gamma^2 - \dot{w}'\gamma + \dot{w}'\int_0^s v''w'ds - v'\dot{w}'w')^{\cdot} \\ & - j_\zeta(\dot{v}'\gamma^2 - \dot{w}'\gamma + \dot{w}'\int_0^s v''w'ds - v'\dot{w}'w' - \dot{v}')^{\cdot} + j_\zeta\dot{v}'^2v' + j_\eta v'\dot{w}'^2 \\ & - D_\xi w''\gamma' - D_\eta(v''\gamma^2 - w''\gamma + w''\int_0^s v''w'ds - v'w'w'')' \\ & + D_\zeta(v''\gamma^2 - w''\gamma + w''\int_0^s v''w'ds - v'w'w'' - v'')' - D_\zeta v''^2v' - D_\eta v'w''^2 + \lambda v']' \end{aligned} \tag{2.3.7b}$$

$$
\begin{aligned}
m\ddot{w} - Q_w = [& -(j_\eta - j_\zeta)(\dot{v}'\gamma - \dot{v}'\int_0^s v''w'ds + \dot{w}'\gamma^2)^{\cdot} - j_\eta(-\ddot{w}' - w'\dot{w}'^2) + j_\zeta\dot{v}'^2w' \\
& - j_\xi(\dot{v}'\dot{\gamma} - \dot{v}'[\int_0^s v''w'ds]^{\cdot} + \dot{v}'^2w') \\
& + (D_\eta - D_\zeta)(v''\gamma - v''\int_0^s v''w'ds + w''\gamma^2)' + D_\eta(-w''' - w'w''^2) - D_\zeta v''^2w' \\
& + D_\xi v''\gamma' + \lambda w']'
\end{aligned}
\tag{2.3.7c}
$$

$$
\begin{aligned}
Q_\phi = & j_\xi(\dot{\gamma} - [\int_0^s v''w'ds]^{\cdot} + \dot{v}'w')^{\cdot} - (j_\eta - j_\zeta)(\dot{v}'^2\gamma - \dot{w}'^2\gamma - \dot{v}'\dot{w}') \\
& - D_\xi\gamma'' + (D_\eta - D_\zeta)(v''^2\gamma - w''^2\gamma - v''w'')
\end{aligned}
\tag{2.3.7d}
$$

In order to find the dominant terms in the expansions, it is necessary to use a dimensionless form to analyze the governing equations. Hence, the governing equations will be nondimensionalized in the next section.

2.4 Dimensionless Form of the Governing Equations and Boundary Conditions

One important step in finding the approximate solution is the process of keeping dominant terms and dropping trivial ones. To accomplish this process, the orders of the parameters need to be decided by comparing them with each other. One way to do this is to select the characteristic parameters used to nondimensionalize the variables. The dimensionless equations contain important information on the behavior of the system.

As the first step to write the equations of motion in dimensionless form, we define:

$$u^* = \frac{u}{l};\ v^* = \frac{v}{l};\ w^* = \frac{w}{l};\ \gamma^* = \gamma;\ t^* = t\sqrt{\frac{D_\eta}{ml^4}};\ \lambda^* = \lambda\frac{l^2}{D_\eta};\ C^* = C\frac{l^2}{\sqrt{mD_\eta}};$$
$$Q^* = Q\frac{l^3}{D_\eta};\ \Omega^* = \Omega l^2\sqrt{\frac{m}{D_\eta}};\ j_i{}^* = \frac{j_i}{ml^2},\ i = \xi, \eta, \zeta;\ G_i{}^* = G_i\frac{l^2}{D_\eta},\ i = u, v, w \tag{2.4.1}$$

Also, we define

$$\beta_\gamma = \frac{D_\xi}{D_\eta} \tag{2.4.2a}$$

$$\beta_y = \frac{D_\zeta}{D_\eta} \tag{2.4.2b}$$

Then, the equations of motion and boundary conditions can be expressed in dimensionless form (where script *, which denotes the dimensionless form, is dropped for convenience after the substitutions are made):

$$\begin{aligned}\ddot{u} - Q_u = [&(\frac{j_\eta - j_\zeta}{D_\eta})(\ddot{v}'w'\gamma + v'\ddot{w}'\gamma + \dot{v}'w'\dot{\gamma} + v'\dot{w}'\dot{\gamma}) - \frac{j_\eta}{D_\eta}\ddot{v}'v' - \frac{j_\eta}{D_\eta}\ddot{w}'w' + \frac{j_\xi}{D_\eta}(\dot{v}'w'\dot{\gamma} - v'\dot{w}'\dot{\gamma}) \\ &- (1-\beta_y)(v'''w'\gamma + v'w'''\gamma + v''w'\gamma' + v'w''\gamma') + v'''v' + w'''w' \\ &- \beta_\gamma(v''w'\gamma' - v'w''\gamma') + \lambda(1+u')]'\end{aligned} \tag{2.4.3a}$$

$$\begin{aligned}\ddot{v} - Q_v = [&\frac{j_\xi}{D_\eta}(\dot{w}'\dot{\gamma} - \dot{w}'[\int_0^s v''w'ds]^{\cdot} + \dot{v}'\dot{w}'w') + \frac{j_\eta}{D_\eta}(\dot{v}'\gamma^2 - \dot{w}'\gamma + \dot{w}'\int_0^s v''w'ds - v'\dot{w}'w')^{\cdot} \\ &- \frac{j_\zeta}{D_\eta}(\dot{v}'\gamma^2 - \dot{w}'\gamma + \dot{w}'\int_0^s v''w'ds - v'\dot{w}'w' - \dot{v}')^{\cdot} + \frac{j_\zeta}{D_\eta}\dot{v}'^2v' + \frac{j_\eta}{D_\eta}v'\dot{w}'^2 \\ &- \beta_\gamma w''\gamma' - (v''\gamma^2 - w''\gamma + w''\int_0^s v''w'ds - v'w'w'')' \\ &+ \beta_y(v''\gamma^2 - w''\gamma + w''\int_0^s v''w'ds - v'w'w'' - v'')' - \beta_y v''^2v' - v'w''^2 + \lambda v']'\end{aligned} \tag{2.4.3b}$$

$$\ddot{w} - Q_w = [-(\frac{j_\eta - j_\zeta}{D_\eta})(\dot{v}'\gamma - \dot{v}'\int_0^s v''w'ds + \dot{w}'\gamma^2)\dot{} - \frac{j_\eta}{D_\eta}(-\ddot{w}' - w'\dot{w}'^2) + j_\zeta\dot{v}'^2w'$$
$$- \frac{j_\xi}{D_\eta}(\dot{v}'\dot{\gamma} - \dot{v}'[\int_0^s v''w'ds]\dot{} + \dot{v}'^2w') \qquad (2.4.3c)$$
$$+ (1-\beta_y)(v''\gamma - v''\int_0^s v''w'ds + w''\gamma^2)' + (-w''' - w'w''^2) - \beta_y v''^2 w' + \beta_y v''\gamma' + \lambda w']'$$

$$Q_\phi = \frac{j_\xi}{D_\eta}(\dot{\gamma} - [\int_0^s v''w'ds]\dot{} + \dot{v}'w')\dot{} - (\frac{j_\eta - j_\zeta}{D_\eta})(\dot{v}'^2\gamma - \dot{w}'^2\gamma - \dot{v}'\dot{w}') \qquad (2.4.3d)$$
$$- \beta_y\dot{\gamma}'' + (1-\beta_y)(v''^2\gamma - w''^2\gamma - v''w'')$$

The boundary conditions at $s = 0$:

$$u(0,t) = 0,\ \gamma(0,t) = 0,\ v(0,t) = v'(0,t) = 0,\ w(0,t) = w'(0,t) = 0 \qquad (2.4.4a)$$

The boundary conditions at $s = 1$:

$$(w'w''' + \beta_y v'v''' + \lambda)\Big|_{s=1} = 0,\ \gamma'(1,t) = 0,\ v''(1,t) = v'''(1,t) = 0,\ w''(1,t) = w'''(1,t) = 0 \qquad (2.4.4b)$$

Next, the above four equations of motion and boundary conditions can be used to solve for the displacement u, the torsion γ and the constraint λ by introducing the inextensional assumption. Then the equations of motion can be simplified to contain only two displacement functions, v and w.

2.5 Solution for u, γ and λ

From the inextensional assumption in eq (2.2.2), it is obvious that the displacement u is not an independent variable. It is a function of v' and w' as follows:

$$u' = -\frac{v'^2 + w'^2}{2} \tag{2.5.1}$$

Integrating the above equation with respect to s from 0 to s, we obtain the following:

$$u(s,t) = \int_0^s u' ds = -\frac{1}{2}\int_0^s (v'^2 + w'^2) ds + c_1(t) \tag{2.5.2}$$

Substituting the boundary condition $u(0,t) = 0$ into the above equation, we find that $c_1(t)$ is 0. The displacement u in terms of v' and w' is:

$$u(s,t) = -\int_0^s \frac{v'^2 + w'^2}{2} ds \tag{2.5.3}$$

Due to the fact that the twist motion cannot be excited by relatively low flexural frequencies, the effects of the mass moments of inertia on the motion can be ignored. If a torque is not applied and the mass moments of inertia are neglected, then the twist will be produced only by the coupling of the two bending deflections, v and w. The twist angle γ can be obtained from eq (2.4.3d) by setting the torque Q_ϕ and the time derivatives equal to zero:

$$-\beta_\gamma \gamma'' + (1 - \beta_y)(v''^2 \gamma - w''^2 \gamma - v'' w'') = 0 \tag{2.5.4}$$

By ignoring high-order terms, eq (2.5.4) can be simplified to:

$$\gamma'' = -\frac{1 - \beta_y}{\beta_\gamma} v'' w'' \tag{2.5.5}$$

Integrating eq (2.5.5) twice with respect to s, one obtains the following equation:

$$\gamma(s,t) = -\frac{1 - \beta_y}{\beta_\gamma}\int_0^s [\int_0^s v''(s,t) w''(s,t) ds] ds + \int_0^s c_1(t) ds + c_2(t) \tag{2.5.6}$$

Substituting boundary conditions eqs (2.4.4a) and (2.4.4b) into eq (2.5.6), we obtain the twist angle produced by bending:

$$\gamma(s,t) = -\frac{1-\beta_y}{\beta_y}\int_0^s [\int_1^s v''(s,t)w''(s,t)ds]ds \tag{2.5.7}$$

Because u is a function of v' and w', eq (2.4.3a) can be used to obtain the constraint force λ. The effects of the mass moments of inertia can be ignored as discussed earlier, and from eq (2.5.7), we conclude that γ is of second order. After substituting eq (2.5.3) for u into eq (2.4.3a) and eliminating high-order terms, and assuming the force in the u direction, Q_u, is zero, one can simplify eq (2.4.3a) to:

$$(w'''w' + \beta_y v'''v' + \lambda)' = -\frac{1}{2}[\int_0^s (v'^2 + w'^2)ds]^{\cdot\cdot} \tag{2.5.8}$$

Integrating eq (2.5.8) with respect to s and using the boundary condition, eq (2.4.4b), the constraint force λ is given by:

$$\lambda(s,t) = -w'w''' - \beta_y v'v''' - \frac{1}{2}\int_1^s [\int_0^s (v'^2 + w'^2)ds]^{\cdot\cdot} ds \tag{2.5.9}$$

From eqs (2.5.3), (2.5.7) and (2.5.9), it is obvious that u, γ and λ are of second order. After substituting them into eqs (2.4.3b) and (2.4.3c), and keeping terms to order $\hat{\varepsilon}^3$, we obtain the equations of motion for in-plane and out-of-plane components as follows:

$$\begin{aligned}\ddot{v} + C_v\dot{v} + \beta_y v'''' - Q_v = (1-\beta_y)[w'''\int_1^s v''w''ds + v''w''w'' - w''''\int_0^s v''w'ds - v''w'w''' \\ - \beta_x w''''\int_0^s\int_1^s v''w''dsds - 2\beta_x w'''\int_1^s v''w''ds - \beta_x v''w''w''] \qquad (2.5.10a) \\ - \beta_y(v'v''v'' + v'v'v''' + v'w''w'' + v'w'w''')' - \frac{1}{2}\{v'\int_1^s [\int_0^s (v'^2 + w'^2)ds]^{\cdot\cdot} ds\}'\end{aligned}$$

$$\ddot{w} + C_w\dot{w} + w'''' - Q_w = -(1-\beta_y)[v'''\int_1^s v''w''ds + v''v''w'' - v''''\int_0^s v'w''ds - v'v'''w''$$
$$+ \beta_x v''''\int_0^s\int_1^s v''w''dsds + 2\beta_x v'''\int_1^s v''w''ds + \beta_x v''v''w''] \qquad (2.5.10b)$$
$$- (v''v''w' + v'v'''w' + w'w''w'' + w'w'w''')' - \frac{1}{2}\{w'\int_1^s [\int_0^s (v'^2 + w'^2)ds]\ddot{}\, ds\}'$$

The above two symmetric equations of motion will be used to find static displacement and dynamic displacement in the next two chapters.

3 Static Displacement

For a slender horizontal beam, a static displacement in the in-plane direction (v direction) due to gravity is obvious. The influence of this static displacement on the beam vibration can be important. Hence, the static displacement is taken into account. In this chapter, static displacement due to gravity will be determined by setting all the dynamic terms to zero. Galerkin's method, with consideration of three modes, will be used to eliminate the spatial functions.

3.1 Governing Equation of Static Displacement

The in-plane displacement is separated into a dynamic displacement v_d and a static displacement v_s, i.e.,

$$v(s,t) = \hat{\varepsilon}[v_d(s,t) + v_s(s)] \tag{3.1.1}$$

where v_d is a function of t and s while v_s is a function of s only. Here we assume v_s is of the same order as v_d because the small displacement assumption had to be made when applying Taylor-series expansions. The governing equations, for both static and dynamic behavior, are only good for

small displacements. The static displacement will add quadratic terms and contribute more resonances. In the same way, the distributed force in the in-plane direction can be divided into a static part, i.e., the weight of the beam which is a function of s only, and a dynamic part which is a function of t and s:

$$Q_v(s,t) = \hat{\varepsilon}[Q_{v_s}(s) + Q_{v_d}(s,t)] \tag{3.1.2}$$

The equation for the static displacement v_s is obtained by substituting eqs (3.1.1) and (3.1.2) into eq (2.5.10a) and letting all the dynamic components be equal to zero, i.e., $v_d = w = Q_{v_d} = 0$. Then eq (2.5.10a) becomes:

$$-Q_{v_s} + \beta_y {v_s}'''' = \hat{\varepsilon}^2[-\beta_y({v_s}'{v_s}''{v_s}'' + {v_s}'{v_s}'{v_s}''')'] \tag{3.1.3}$$

Galerkin's method will be used to eliminate the spatial functions. Both the static and dynamic displacements are written as expansions in terms of free-vibration modes. The free-vibration modes are assumed to be the products of a time function and a spatial function as follows :

$$v_d(s,t) = \sum_{i=1}^{n} v_i(t) F_{v_i}(s) \tag{3.1.4a}$$

$$v_s(s) = \sum_{i=1}^{n} v_{s_i} F_{v_i}(s) \tag{3.1.4b}$$

$$w(s,t) = \sum_{i=1}^{n} w_i(t) F_{w_i}(s) \tag{3.1.4c}$$

where $F_{v_i}(s)$ and $F_{w_i}(s)$ are the so-called linear free-vibration mode functions found from the linear solution of undamped and free vibration. Next, the modes are determined.

3.2 Linear Solution of Undamped and Free Vibration

The equations of motion of a beam are simplified from eqs (2.5.10a) and (2.5.10b) by eliminating the damping and forcing terms, and high-order terms, to give:

$$\ddot{v} + \beta_y v'''' = 0 \tag{3.2.1}$$

$$\ddot{w} + w'''' = 0 \tag{3.2.2}$$

The corresponding boundary conditions, from eqs (2.4.4a) and (2.4.4b), are:

$$\begin{aligned} &v(0, t) = v'(0, t) = w(0, t) = w'(0, t) = 0 \\ &v''(1, t) = v'''(1, t) = w''(1, t) = w'''(1, t) = 0 \end{aligned} \tag{3.2.3}$$

Eqs (3.2.1) and (3.2.2) can be solved by the method of separation of variables. We assume v and w can be written as:

$$v(s, t) = G_v(t)F_v(s) \tag{3.2.4a}$$

$$w(s, t) = G_w(t)F_w(s) \tag{3.2.4b}$$

After subsituting eqs (3.2.4a) and (3.2.4b) into eqs (3.2.1)-(3.2.3), the problems are transformed into the following initial-boundary value problems:

$$\begin{aligned} &F_v''''(s) - \lambda^2 F_v(s) = 0, \quad F_v(0) = 0, F_v'(0) = 0, F_v''(1) = 0, F_v'''(1) = 0. \\ &\ddot{G}_v(t) + \beta\lambda^2 G_v(t) = 0, \qquad G_v(0) = f(0), \dot{G}_v(0) = \dot{f}(0) \end{aligned} \tag{3.2.5}$$

$$\begin{aligned} &F_w''''(s) - \lambda^2 F_w(s) = 0, \quad F_w(0) = 0, F_w'(0) = 0, F_w''(1) = 0, F_w'''(1) = 0. \\ &\ddot{G}_w(t) + \lambda^2 G_w(t) = 0, \qquad G_w(0) = g(0), \dot{G}_w(0) = \dot{g}(0) \end{aligned} \tag{3.2.6}$$

where $f(0), g(0), \dot{f}(0)$ and $\dot{g}(0)$ are initial conditions. But v and w share the same eigenvalues and eigenfunctions in this fixed-free case, because they have the same boundary conditions. Hence, $F_v = F_w = F$. The eigenvalues and eigenfunctions are thus:

$$F_i(s) = \cosh(\sqrt{\lambda_i}\, s) - \cos(\sqrt{\lambda_i}\, s) - G_i[\, \sinh(\sqrt{\lambda_i}\, s) - \sin(\sqrt{\lambda_i}\, s)] \ , \quad i = 1, 2, 3... \tag{3.2.7}$$

$$G_i = \frac{\cos\sqrt{\lambda_i} + \cosh\sqrt{\lambda_i}}{\sin\sqrt{\lambda_i} + \sinh\sqrt{\lambda_i}} \ , \quad i = 1, 2, 3... \tag{3.2.8}$$

where λ_i is a root of the characteristic equation:

$$\cosh\sqrt{\lambda} = -\sec\sqrt{\lambda} \tag{3.2.9}$$

The first three roots of eq (3.2.9) are:

$$\lambda_1 = 3.516, \quad \lambda_2 = 22.034, \quad \lambda_3 = 61.697$$

The natural frequencies are obtained from eqs (3.2.5) and (3.2.6) as:

$$\omega_{v_i} = \sqrt{\beta_y}\, \lambda_i \tag{3.2.10}$$

$$\omega_{w_i} = \lambda_i \tag{3.2.11}$$

The natural frequency ω_{v_i} for the v direction is not equal to the natural frequency ω_{w_i} for the w direction unless $\beta_y = 1$, e.g., the cross section of the beam is square or circular.

3.3 Galerkin's Method

Galerkin's method is used to eliminate the spatial functions. After substituting eq (3.1.4b)

$$v_s(s) = \sum_{i=1}^{n} v_{s_i} F_i(s) \tag{3.1.4b}$$

into the governing equation for the static displacement, eq (3.1.3), the equation is multiplied by an eigenfunction and the result is integrated from 0 to 1 to eliminate the spatial variable:

$$-\int_0^1 F_i Q_{v_s} ds + \beta_y \sum_{j=1}^{n} v_{s_j} \int_0^1 F_i F_j'''' ds = \hat{\varepsilon}^2 \{ -\beta_y \sum_{j=1}^{n} \sum_{k=1}^{n} \sum_{l=1}^{n} v_{s_j} v_{s_k} v_{s_l} [\int_0^1 F_i (F_j' F_k'' F_l'')' ds + \int_0^1 F_i (F_j' F_k' F_l''')' ds]\} \tag{3.3.1}$$

The result is a set of nonlinear, coupled algebraic equations for the coefficients v_{s_i}. The order-$\hat{\varepsilon}$ equation governing the static displacement is:

$$-Q_{v_{s_i}} + \beta_y \omega_{v_i}^2 v_{s_i} = 0 \tag{3.3.2}$$

where $Q_{v_{s_i}}$ is:

$$Q_{v_{s_i}} = \int_0^1 F_i Q_{v_s} ds \tag{3.3.3}$$

From the above equation, the first-order approximation for v_{s_i} is thus:

$$v_{s_i} = \frac{Q_{v_{s_i}}}{\beta_y \omega_{v_i}^2} \tag{3.3.4}$$

The high-order terms are neglected because they are small compared with the first-order terms due to the appearance of the small parameter $\hat{\varepsilon}^2$. After substituting eqs (3.1.4a)-(3.1.4c) and the static displacement eq (3.3.4) into eqs (2.5.10a) and (2.5.10b), the equations are multiplied by the eigenfunction and are integrated from 0 to 1 to eliminate the spatial function. The equations are then grouped into linear, quadratic and cubic terms. The equations of motion, which contain the effect of the static displacement, describe the motion of the tip of the beam and are as follows:

$$
\begin{aligned}
&\ddot{v}_i + C_v\dot{v}_i - Q_{v_i} + \beta_y\omega_{v_i}^2 v_i \\
&\quad + \hat{\varepsilon}^2[\sum_{j=1}^{n}(T_{ij}{}^{v}v_j + X_{ij}{}^{v}\ddot{v}_j) \\
&\quad + \sum_{j=1}^{n}\sum_{k=1}^{n}(\Lambda_{ijk}{}^{v1}w_jw_k + \Lambda_{ijk}{}^{v2}v_jv_k + Y_{ijk}{}^{v1}\dot{v}_j\dot{v}_k + Y_{ijk}{}^{v2}\dot{w}_j\dot{v}_k + Z_{ijk}{}^{v1}v_j\ddot{v}_k + Z_{ijk}{}^{v2}w_j\ddot{w}_k) \\
&\quad + \sum_{j=1}^{n}\sum_{k=1}^{n}\sum_{l=1}^{n}(\Gamma_{ijkl}{}^{v1}w_jv_kw_l + \Gamma_{ijkl}{}^{v2}v_jw_kw_l + \Gamma_{ijkl}{}^{v3}v_jv_kv_l + V_{ijkl}{}^{v1}v_j\dot{v}_k\dot{v}_l + V_{ijkl}{}^{v2}v_j\dot{w}_k\dot{w}_l \\
&\qquad\qquad + W_{ijkl}{}^{v1}v_jv_k\ddot{v}_l + W_{ijkl}{}^{v2}v_jw_k\ddot{w}_l)] = 0
\end{aligned}
\tag{3.3.5}
$$

$$
\begin{aligned}
&\ddot{w}_i + C_w\dot{w}_i - Q_{w_i} + \omega_{w_i}^2 w_i \\
&\quad + \hat{\varepsilon}^2[\sum_{j=1}^{n}(T_{ij}{}^{w}w_j) \\
&\quad + \sum_{j=1}^{n}\sum_{k=1}^{n}(\Lambda_{ijk}{}^{w}v_jw_k + Z_{ijk}{}^{w}w_j\ddot{v}_k) \\
&\quad + \sum_{j=1}^{n}\sum_{k=1}^{n}\sum_{l=1}^{n}(\Gamma_{ijkl}{}^{w1}v_jv_kw_l + \Gamma_{ijkl}{}^{w2}w_jw_kw_l + V_{ijkl}{}^{w1}w_j\dot{v}_k\dot{v}_l + V_{ijkl}{}^{w2}w_j\dot{w}_k\dot{w}_l \\
&\qquad\qquad + W_{ijkl}{}^{w1}w_jv_k\ddot{v}_l + W_{ijkl}{}^{w2}w_jw_k\ddot{w}_l)] = 0
\end{aligned}
\tag{3.3.6}
$$

where the coefficients and parameters are listed in Appendix A.

4 Dynamic Displacement

The dynamic displacements under soft excitation and hard excitation are determined by using the method of multiple scales in this chapter. The static displacement obtained in the previous chapter not only influences the coefficients of the governing equations but also adds quadratic terms to these equations. Four nonlinear autonomous modulation equations are produced. These first-order ordinary differential equations govern the amplitudes and phases, and predict a whirling motion under certain situations.

4.1 Asymptotic Analysis

To analyze the weakly nonlinear equations of motion, the method of multiple scales is used (for example, Nayfeh [1980]). The linear parts characterize the fast change of the motion; they describe the constant amplitude and phase of the motion. The nonlinear parts characterize the slow change of the motion; they describe the changes of the amplitude and phase. It takes a long time to observe the changes of the amplitude and phase, and hence we need different time scales to describe the fast change and slow change parts of the motion. Two time scales are introduced. The

fast time scale $T_0 = t$ describes the fast change, while the slow time scale $T_1 = \varepsilon t$ describes the slow change. The small parameter ε is equal to $\hat{\varepsilon}^2$ defined earlier in previous chapter. It is found convenient to make this change when using the method of multiple scales. Thus, instead of expressing the parameters as functions of t, we express those parameters as functions of T_0 and T_1, and expand uniformly in terms of ε as:

$$v_n(t;\varepsilon) = v_{n0}(T_0, T_1) + \varepsilon v_{n1}(T_0, T_1) + \ldots \tag{4.1.1}$$

$$w_n(t;\varepsilon) = w_{n0}(T_0, T_1) + \varepsilon w_{n1}(T_0, T_1) + \ldots \tag{4.1.2}$$

The time derivatives are changed by the chain rule:

$$\frac{d}{dt} = D_0 + \varepsilon D_1 + \ldots \tag{4.1.3a}$$

$$\frac{d^2}{dt^2} = D_0{}^2 + 2\varepsilon D_0 D_1 + \ldots \tag{4.1.3b}$$

where

$$D_n = \frac{\partial}{\partial T_n}, \quad T_n = \varepsilon^n t \tag{4.1.4}$$

Because we are seeking an asymptotic solution, the appropriate ordering will ensure an asymptotic expansion as will be discussed in the next section. The damping coefficients and forces are expanded in power series of ε as:

$$C_v(\varepsilon) = \varepsilon C_{v_1} + \varepsilon^2 C_{v_2} + \ldots \tag{4.1.5a}$$

$$C_w(\varepsilon) = \varepsilon C_{w_1} + \varepsilon^2 C_{w_2} + \ldots \tag{4.1.5b}$$

$$Q_{v_n}(t;\varepsilon) = g_{n0}(T_0, T_1) + \varepsilon g_{n1}(T_0, T_1) + \ldots \tag{4.1.5c}$$

$$Q_{w_n}(t;\varepsilon) = f_{n0}(T_0, T_1) + \varepsilon f_{n1}(T_0, T_1) + \ldots \tag{4.1.5d}$$

Substituting eqs (4.1.1)-(4.1.5d) into eqs (3.3.5) and (3.3.6), and equating the coefficients of the same power of ε to zero, we obtain the order- ε^0 equations:

$$D_0{}^2 v_{n0} + \omega_{v_n}^2 v_{n0} = g_{n0} \tag{4.1.6}$$

$$D_0{}^2 w_{n0} + \omega_{w_n}^2 w_{n0} = f_{no} \tag{4.1.7}$$

The order- ε equations are:

$$\begin{aligned} D_0{}^2 v_{n1} + \omega_{v_n}^2 v_{n1} = {} & g_{n1} - 2(D_0 D_1 + C_{v_1} D_0) v_{n0} \\ & - \sum_{j=1}^{m} (T_{jn}{}^{v} v_{j0} + X_{jn}{}^{v} D_0{}^2 v_{j0}) \\ & - \sum_{j=1}^{m} \sum_{k=1}^{m} (\Lambda_{jkn}{}^{v1} w_{j0} w_{k0} + \Lambda_{jkn}{}^{v2} v_{j0} v_{k0} + Y_{jkn}{}^{v1} D_0 v_{j0} D_0 v_{k0} + Y_{jkn}{}^{v2} D_0 w_{j0} D_0 w_{k0} \\ & \qquad + Z_{jkn}{}^{v1} v_{j0} D_0{}^2 v_{k0} + Z_{jkn}{}^{v2} w_{j0} D_0{}^2 w_{k0}) \\ & - \sum_{j=1}^{m} \sum_{k=1}^{m} \sum_{l=1}^{m} (\Gamma_{jkln}{}^{v1} w_{j0} v_{k0} w_{l0} + \Gamma_{jkln}{}^{v2} v_{j0} w_{k0} w_{l0} + \Gamma_{jkln}{}^{v3} v_{j0} v_{k0} v_{l0} \\ & \qquad + V_{jkln}{}^{v1} v_{j0} D_0 v_{k0} D_0 v_{l0} + V_{jkln}{}^{v2} v_{j0} D_0 w_{k0} D_0 w_{l0} \\ & \qquad + W_{jkln}{}^{v1} v_{j0} v_{k0} D_0{}^2 v_{l0} + W_{jkln}{}^{v2} v_{j0} w_{k0} D_0{}^2 w_{l0}) \end{aligned} \tag{4.1.8}$$

$$\begin{aligned} D_0{}^2 w_{n1} + \omega_{w_n}^2 w_{n1} = {} & f_{n1} - 2(D_0 D_1 + C_{w_1} D_0) w_{n0} \\ & - \sum_{j=1}^{m} (T_{jn}{}^{w} w_{j0}) \\ & - \sum_{j=1}^{m} \sum_{k=1}^{m} (\Lambda_{jkn}{}^{w} v_{j0} w_{k0} + Z_{jkn}{}^{w} w_{j0} D_0{}^2 v_{k0}) \\ & - \sum_{j=1}^{m} \sum_{k=1}^{m} \sum_{l=1}^{m} (\Gamma_{jkln}{}^{w1} v_{j0} v_{k0} w_{l0} + \Gamma_{jkln}{}^{w2} w_{j0} w_{k0} w_{l0} \\ & \qquad + V_{jkln}{}^{w1} w_{j0} D_0 v_{k0} D_0 v_{l0} + V_{jkln}{}^{w2} w_{j0} D_0 w_{k0} D_0 w_{l0} \\ & \qquad + W_{jkln}{}^{w1} w_{j0} v_{k0} D_0{}^2 v_{l0} + W_{jkln}{}^{w2} w_{j0} w_{k0} D_0{}^2 w_{l0}) \end{aligned} \tag{4.1.9}$$

Because a uniform expansion is sought, anything that breaks the uniformity must be ruled out. If the force is put in the first order, the particular solution of the first order will be large due to the appearance of a small divisor, $\frac{1}{\omega_{v_n}^2 - \Omega^2}$ or $\frac{1}{\omega_{w_n}^2 - \tilde{\Omega}^2}$, when the forcing frequency is close to one of the natural frequencies, ω_{v_n} or ω_{w_n}. This implies the order of the force is not appropriate; the force should appear at the second order. In such a case, the external force is of order ε, i.e., the force is small, and it is known as soft excitation. For other cases, when Ω is not near one of the ω_{v_n} or ω_{w_n}, the external force is of order $O(1)$, and it is known as hard excitation.

4.2 *Soft Excitation*

For a soft excitation, the external forces are set to the second order:

$$g_{n0} = 0, \quad g_{n1} = 2K_n \cos \Omega T_0, \quad f_{n0} = 0, \quad f_{n1} = 2\tilde{K}_n \cos \tilde{\Omega} T_0 \tag{4.2.1}$$

To ensure that damping acts at the same order as the external force and nonlinearity, the damping coefficients C_{v_1} and C_{w_1} are taken to be positive, and we write:

$$C_{v_1} = \mu_{v_n}, \quad C_{w_1} = \mu_{w_n} \tag{4.2.2}$$

After substituting eqs (4.2.1) and (4.2.2) into eqs (4.1.6) and (4.1.7), the order- ε^0 equations become :

$$D_0^2 v_{n0} + \omega_{v_n}^2 v_{n0} = 0 \tag{4.2.3}$$

$$D_0^2 w_{n0} + \omega_{w_n}^2 w_{n0} = 0 \tag{4.2.4}$$

The solutions of the first order equations are then obtained:

$$v_{n0} = a_n(T_1)\cos[\omega_{v_n}T_0 + \alpha_n(T_1)] = \frac{1}{2}a_n e^{i\alpha_n}e^{i\omega_{v_n}T_0} + cc = A_n(T_1)e^{i\omega_{v_n}T_0} + cc \tag{4.2.5}$$

$$w_{n0} = b_n(T_1)\cos[\omega_{w_n}T_0 + \beta_n(T_1)] = \frac{1}{2}b_n e^{i\beta_n}e^{i\omega_{w_n}T_0} + cc = B_n(T_1)e^{i\omega_{w_n}T_0} + cc \tag{4.2.6}$$

where

$$cc : \text{complex conjugate;}$$
$$A_n = \frac{1}{2}a_n e^{i\alpha_n}, \quad B_n = \frac{1}{2}b_n e^{i\beta_n} \tag{4.2.7}$$

The amplitudes and phases of the first-order solutions are not constants. They are only constants with respect to T_0, but are functions of T_1, i.e.,

$$a_n = a_n(T_1), \quad \alpha_n = \alpha_n(T_1), \quad b_n = b_n(T_1) \text{ and } \beta_n = \beta_n(T_1) \tag{4.2.8}$$

The amplitudes and phases are obtained from the second-order equations by using the solvability condition. In this case, it is equivalent to eliminating the secular terms. The explicit expressions for the second-order equations are obtained by substituting the first-order solutions, eqs (4.2.5) and (4.2.6), into eqs (4.1.8) and (4.1.9) and carrying out the expansions:

$$
\begin{aligned}
D_0^2 v_{n1} + \omega_{v_n}^2 v_{n1} &= K_n e^{i\Omega T_0} - 2i\omega_{v_n}(D_1 A_n + \mu_{v_n} A_n) e^{i\omega_{v_n} T_0} \\
&- \sum_{j=1}^{m} T_{jn}{}^{v} A_j e^{i\omega_{v_j} T_0} - X_{jn}{}^{v} \omega_{v_j}^2 A_j e^{i\omega_{v_j} T_0} \\
&- \sum_{j=1}^{m}\sum_{k=1}^{m} \Lambda_{jkn}{}^{v1}[B_j B_k e^{i(\omega_{w_j} + \omega_{w_k})T_0} + B_j \overline{B}_k e^{i(\omega_{w_j} - \omega_{w_k})T_0}] \\
&- \sum_{j=1}^{m}\sum_{k=1}^{m} \Lambda_{jkn}{}^{v2}[A_j A_k e^{i(\omega_{v_j} + \omega_{v_k})T_0} + A_j \overline{A}_k e^{i(\omega_{v_j} - \omega_{v_k})T_0}] \\
&- \sum_{j=1}^{m}\sum_{k=1}^{m} Y_{jkn}{}^{v1}[-\omega_{v_j}\omega_{v_k} A_j A_k e^{i(\omega_{v_j} + \omega_{v_k})T_0} + \omega_{v_j}\omega_{v_k} A_j \overline{A}_k e^{i(\omega_{v_j} - \omega_{v_k})T_0}] \\
&- \sum_{j=1}^{m}\sum_{k=1}^{m} Y_{jkn}{}^{v2}[-\omega_{w_j}\omega_{w_k} B_j B_k e^{i(\omega_{w_j} + \omega_{w_k})T_0} + \omega_{w_j}\omega_{w_k} B_j \overline{B}_k e^{i(\omega_{w_j} - \omega_{w_k})T_0}] \\
&- \sum_{j=1}^{m}\sum_{k=1}^{m} Z_{jkn}{}^{v1}[-\omega_{v_k}^2 A_j A_k e^{i(\omega_{v_j} + \omega_{v_k})T_0} - \omega_{v_k}^2 A_j \overline{A}_k e^{i(\omega_{v_j} - \omega_{v_k})T_0}] \\
&- \sum_{j=1}^{m}\sum_{k=1}^{m} Z_{jkn}{}^{v2}[-\omega_{w_k}^2 B_j B_k e^{i(\omega_{w_j} + \omega_{w_k})T_0} - \omega_{w_k}^2 B_j \overline{B}_k e^{i(\omega_{w_j} - \omega_{w_k})T_0}] \\
&- \sum_{j=1}^{m}\sum_{k=1}^{m}\sum_{l=1}^{m} \Gamma_{jkln}{}^{v1}[B_j A_k B_l e^{i(\omega_{w_j} + \omega_{v_k} + \omega_{w_l})T_0} + B_j A_k \overline{B}_l e^{i(\omega_{w_j} + \omega_{v_k} - \omega_{w_l})T_0} \\
&\qquad + B_j \overline{A}_k B_l e^{i(\omega_{w_j} - \omega_{v_k} + \omega_{w_l})T_0} + B_j \overline{A}_k \overline{B}_l e^{i(\omega_{w_j} - \omega_{v_k} - \omega_{w_l})T_0}] \\
&- \sum_{j=1}^{m}\sum_{k=1}^{m}\sum_{l=1}^{m} \Gamma_{jkln}{}^{v2}[A_j B_k B_l e^{i(\omega_{v_j} + \omega_{w_k} + \omega_{w_l})T_0} + A_j B_k \overline{B}_l e^{i(\omega_{v_j} + \omega_{w_k} - \omega_{w_l})T_0} \\
&\qquad + A_j \overline{B}_k B_l e^{i(\omega_{v_j} - \omega_{w_k} + \omega_{w_l})T_0} + A_j \overline{B}_k \overline{B}_l e^{i(\omega_{v_j} - \omega_{w_k} - \omega_{w_l})T_0}] \\
&- \sum_{j=1}^{m}\sum_{k=1}^{m}\sum_{l=1}^{m} \Gamma_{jkln}{}^{v3}[A_j A_k A_l e^{i(\omega_{v_j} + \omega_{v_k} + \omega_{v_l})T_0} + A_j A_k \overline{A}_l e^{i(\omega_{v_j} + \omega_{v_k} - \omega_{v_l})T_0} \\
&\qquad + A_j \overline{A}_k A_l e^{i(\omega_{v_j} - \omega_{v_k} + \omega_{v_l})T_0} + A_j \overline{A}_k \overline{A}_l e^{i(\omega_{v_j} - \omega_{v_k} - \omega_{v_l})T_0}] \\
&- \sum_{j=1}^{m}\sum_{k=1}^{m}\sum_{l=1}^{m} V_{jkln}{}^{v1}[-\omega_{v_k}\omega_{v_l} A_j A_k A_l e^{i(\omega_{v_j} + \omega_{v_k} + \omega_{v_l})T_0} + \omega_{v_k}\omega_{v_l} A_j A_k \overline{A}_l e^{i(\omega_{v_j} + \omega_{v_k} - \omega_{v_l})T_0} \\
&\qquad + \omega_{v_k}\omega_{v_l} A_j \overline{A}_k A_l e^{i(\omega_{v_j} - \omega_{v_k} + \omega_{v_l})T_0} - \omega_{v_k}\omega_{v_l} A_j \overline{A}_k \overline{A}_l e^{i(\omega_{v_j} - \omega_{v_k} - \omega_{v_l})T_0}]
\end{aligned}
$$

$$
\begin{aligned}
&- \sum_{j=1}^{m}\sum_{k=1}^{m}\sum_{l=1}^{m} V_{jkln}{}^{v2}[- \omega_{w_k}\omega_{w_l}A_jB_kB_le^{i(\omega_{v_j}+\omega_{w_k}+\omega_{w_l})T_0} + \omega_{w_k}\omega_{w_l}A_jB_k\overline{B}_le^{i(\omega_{v_j}+\omega_{w_k}-\omega_{w_l})T_0} \\
&\qquad + \omega_{w_k}\omega_{w_l}A_j\overline{B}_kB_le^{i(\omega_{v_j}-\omega_{w_k}+\omega_{w_l})T_0} - \omega_{w_k}\omega_{w_l}A_j\overline{B}_k\overline{B}_le^{i(\omega_{v_j}-\omega_{w_k}-\omega_{w_l})T_0}] \\
&- \sum_{j=1}^{m}\sum_{k=1}^{m}\sum_{l=1}^{m} W_{jkln}{}^{v1}[- \omega_{v_l}^2A_jA_kA_le^{i(\omega_{v_j}+\omega_{v_k}+\omega_{v_l})T_0} - \omega_{v_l}^2A_jA_k\overline{A}_le^{i(\omega_{v_j}+\omega_{v_k}-\omega_{v_l})T_0} \\
&\qquad - \omega_{v_l}^2A_j\overline{A}_kA_le^{i(\omega_{v_j}-\omega_{v_k}+\omega_{v_l})T_0} - \omega_{v_l}^2A_j\overline{A}_k\overline{A}_le^{i(\omega_{v_j}-\omega_{v_k}-\omega_{v_l})T_0}] \\
&- \sum_{j=1}^{m}\sum_{k=1}^{m}\sum_{l=1}^{m} W_{jkln}{}^{v2}[- \omega_{w_l}^2A_jB_kB_le^{i(\omega_{v_j}+\omega_{w_k}+\omega_{w_l})T_0} - \omega_{w_l}^2A_jB_k\overline{B}_le^{i(\omega_{v_j}+\omega_{w_k}-\omega_{w_l})T_0} \\
&\qquad - \omega_{w_l}^2A_j\overline{B}_kB_le^{i(\omega_{v_j}-\omega_{w_k}+\omega_{w_l})T_0} - \omega_{w_l}^2A_j\overline{B}_k\overline{B}_le^{i(\omega_{v_j}-\omega_{w_k}-\omega_{w_l})T_0}] \\
&+ cc
\end{aligned}
\tag{4.2.9}
$$

$$
\begin{aligned}
D_0{}^2 w_{n1} + \omega_{w_n}^2 w_{n1} &= \tilde{K}_n e^{i\tilde{\Omega}T_0} - 2i\omega_{w_n}(D_1 B_n + \mu_{w_n} B_n) e^{i\omega_{w_n}T_0} \\
&\quad - \sum_{j=1}^{m} T_{jn}{}^{w} B_j e^{i\omega_{w_j}T_0} \\
&\quad - \sum_{j=1}^{m}\sum_{k=1}^{m} \Lambda_{jkn}{}^{w}[A_j B_k e^{i(\omega_{v_j}+\omega_{w_k})T_0} + A_j \bar{B}_k e^{i(\omega_{v_j}-\omega_{w_k})T_0}] \\
&\quad - \sum_{j=1}^{m}\sum_{k=1}^{m} Z_{jkn}{}^{w}[-\omega_{v_k}^2 B_j A_k e^{i(\omega_{w_j}+\omega_{v_k})T_0} - \omega_{v_k}^2 B_j \bar{A}_k e^{i(\omega_{w_j}-\omega_{v_k})T_0}] \\
&\quad - \sum_{j=1}^{m}\sum_{k=1}^{m}\sum_{l=1}^{m} \Gamma_{jkln}{}^{w1}[A_j A_k B_l e^{i(\omega_{v_j}+\omega_{v_k}+\omega_{w_l})T_0} + A_j A_k \bar{B}_l e^{i(\omega_{v_j}+\omega_{v_k}-\omega_{w_l})T_0} \\
&\qquad + A_j \bar{A}_k B_l e^{i(\omega_{v_j}-\omega_{v_k}+\omega_{w_l})T_0} + A_j \bar{A}_k \bar{B}_l e^{i(\omega_{v_j}-\omega_{v_k}-\omega_{w_l})T_0}] \\
&\quad - \sum_{j=1}^{m}\sum_{k=1}^{m}\sum_{l=1}^{m} \Gamma_{jkln}{}^{w2}[B_j B_k B_l e^{i(\omega_{w_j}+\omega_{w_k}+\omega_{w_l})T_0} + B_j B_k \bar{B}_l e^{i(\omega_{w_j}+\omega_{w_k}-\omega_{w_l})T_0} \\
&\qquad + B_j \bar{B}_k B_l e^{i(\omega_{w_j}-\omega_{w_k}+\omega_{w_l})T_0} + B_j \bar{B}_k \bar{B}_l e^{i(\omega_{w_j}-\omega_{w_k}-\omega_{w_l})T_0}] \\
&\quad - \sum_{j=1}^{m}\sum_{k=1}^{m}\sum_{l=1}^{m} V_{jkln}{}^{w1}[-\omega_{v_k}\omega_{v_l} B_j A_k A_l e^{i(\omega_{w_j}+\omega_{v_k}+\omega_{v_l})T_0} + \omega_{v_k}\omega_{v_l} B_j A_k \bar{A}_l e^{i(\omega_{w_j}+\omega_{v_k}-\omega_{v_l})T_0} \\
&\qquad + \omega_{v_k}\omega_{v_l} B_j \bar{A}_k A_l e^{i(\omega_{w_j}-\omega_{v_k}+\omega_{v_l})T_0} - \omega_{v_k}\omega_{v_l} B_j \bar{A}_k \bar{A}_l e^{i(\omega_{w_j}-\omega_{v_k}-\omega_{v_l})T_0}] \\
&\quad - \sum_{j=1}^{m}\sum_{k=1}^{m}\sum_{l=1}^{m} V_{jkln}{}^{w2}[-\omega_{w_k}\omega_{w_l} B_j B_k B_l e^{i(\omega_{w_j}+\omega_{w_k}+\omega_{w_l})T_0} + \omega_{w_k}\omega_{w_l} B_j B_k \bar{B}_l e^{i(\omega_{w_j}+\omega_{w_k}-\omega_{w_l})T_0} \\
&\qquad + \omega_{w_k}\omega_{w_l} B_j \bar{B}_k B_l e^{i(\omega_{w_j}-\omega_{w_k}+\omega_{w_l})T_0} - \omega_{w_k}\omega_{w_l} B_j \bar{B}_k \bar{B}_l e^{i(\omega_{w_j}-\omega_{w_k}-\omega_{w_l})T_0}] \\
&\quad - \sum_{j=1}^{m}\sum_{k=1}^{m}\sum_{l=1}^{m} W_{jkln}{}^{w1}[-\omega_{v_l}^2 B_j A_k A_l e^{i(\omega_{w_j}+\omega_{v_k}+\omega_{v_l})T_0} - \omega_{v_l}^2 B_j A_k \bar{A}_l e^{i(\omega_{w_j}+\omega_{v_k}-\omega_{v_l})T_0} \\
&\qquad - \omega_{v_l}^2 B_j \bar{A}_k A_l e^{i(\omega_{w_j}-\omega_{v_k}+\omega_{v_l})T_0} - \omega_{v_l}^2 B_j \bar{A}_k \bar{A}_l e^{i(\omega_{w_j}-\omega_{v_k}-\omega_{v_l})T_0}] \\
&\quad - \sum_{j=1}^{m}\sum_{k=1}^{m}\sum_{l=1}^{m} W_{jkln}{}^{w2}[-\omega_{w_l}^2 B_j B_k B_l e^{i(\omega_{w_j}+\omega_{w_k}+\omega_{w_l})T_0} - \omega_{w_l}^2 B_j B_k \bar{B}_l e^{i(\omega_{w_j}+\omega_{w_k}-\omega_{w_l})T_0} \\
&\qquad - \omega_{w_l}^2 B_j \bar{B}_k B_l e^{i(\omega_{w_j}-\omega_{w_k}+\omega_{w_l})T_0} - \omega_{w_l}^2 B_j \bar{B}_k \bar{B}_l e^{i(\omega_{w_j}-\omega_{w_k}-\omega_{w_l})T_0}] \\
&\quad + cc
\end{aligned}
\tag{4.2.10}
$$

Small divisors in the solutions occur under the following conditions:

1. $\Omega \simeq \omega_{v_n}$
2. $\tilde{\Omega} \simeq \omega_{w_n}$
3. $\omega_{v_n} \simeq \omega_{w_j} \pm \omega_{w_k}$
4. $\omega_{v_n} \simeq \omega_{v_j} \pm \omega_{v_k}$
5. $\omega_{w_n} \simeq \omega_{v_j} \pm \omega_{w_k}$
6. $\omega_{w_n} \simeq \omega_{w_j} \pm \omega_{v_k}$
7. $\omega_{v_n} \simeq \omega_{w_j} \pm \omega_{v_k} \pm \omega_{w_l}$
8. $\omega_{v_n} \simeq \omega_{v_j} \pm \omega_{w_k} \pm \omega_{w_l}$
9. $\omega_{v_n} \simeq \omega_{v_j} \pm \omega_{v_k} \pm \omega_{v_l}$
10. $\omega_{w_n} \simeq \omega_{v_j} \pm \omega_{v_k} \pm \omega_{w_l}$
11. $\omega_{w_n} \simeq \omega_{w_j} \pm \omega_{w_k} \pm \omega_{w_l}$
12. $\omega_{w_n} \simeq \omega_{w_j} \pm \omega_{v_k} \pm \omega_{v_l}$

(4.2.11)

Conditions 1 and 2 involve the frequency of the external forcing and are known as external resonances. The rest involve only the natural (internal) frequencies and are known as internal resonances. When the forcing frequency is close to one of the natural frequencies, we call it primary resonance. When the forcing frequency is close to a combination of the natural frequencies (a case not considered here), we speak of secondary resonance, tertiary resonance, etc.

4.2.1 Primary Resonance with a Square Cross Section

A detuning parameter σ is introduced as a quantitative measurement of the difference between the natural frequency and forcing frequency:

$$\Omega = \omega_{v_q} + \varepsilon\sigma \tag{4.2.12}$$

$$\tilde{\Omega} = \omega_{w_q} + \varepsilon\tilde{\sigma} \tag{4.2.13}$$

If the cross section of the beam is assumed to be square, the natural frequency in the v direction, ω_{v_i}, is equal to the natural frequency in the w direction, ω_{w_i}. For a beam with a square cross section, small divisors can occur in conditions 7 to 12. After carrying out the permutation of the indices to extract the small divisors, the secular terms of the order- ε equations are given by:

$$\begin{aligned} &-2i\omega_{v_n}(D_1A_n + \mu_{v_n}A_n) - 2\omega_{v_n}f_{v_n}A_n + 8\omega_{v_n}A_n\sum_{j=1}^{m}(\alpha_{v_{jn}}A_j\bar{A}_j + \alpha_{v_{jn}}{}^{*}B_j\bar{B}_j) \\ &+ \underline{8\omega_{v_n}B_n\sum_{j=1}^{m}(\beta_{v_{jn}}A_j\bar{B}_j + \beta_{v_{jn}}{}^{*}\bar{A}_jB_j)} + \delta_{nq}K_qe^{i\sigma T_1} = 0 \end{aligned} \tag{4.2.14}$$

$$\begin{aligned} &-2i\omega_{w_n}(D_1B_n + \mu_{w_n}B_n) - 2\omega_{w_n}f_{w_n}B_n + 8\omega_{w_n}B_n\sum_{j=1}^{m}(\alpha_{w_{jn}}B_j\bar{B}_j + \alpha_{w_{jn}}{}^{*}A_j\bar{A}_j) \\ &+ \underline{8\omega_{w_n}A_n\sum_{j=1}^{m}(\beta_{w_{jn}}A_j\bar{B}_j + \beta_{w_{jn}}{}^{*}\bar{A}_jB_j)} + \delta_{nq}\tilde{K}_qe^{i\tilde{\sigma}T_1} = 0 \end{aligned} \tag{4.2.15}$$

where

$$\omega_{v_n} = \omega_{w_n} = \omega_n \tag{4.2.16a}$$

$$f_{v_n} = \frac{1}{2\omega_{v_n}}(T_{nn}{}^{v} - \omega_{v_n}^2X_{nn}{}^{v}) \tag{4.2.16b}$$

$$\alpha_{v_{jn}} = \frac{-1}{8(1+\delta_{jn})\omega_{v_n}}(\Gamma_{jjnn}{}^{v3^{*}} + 2V_{njjn}{}^{v1}\omega_{v_j}^2 - W_{jjnn}{}^{v1^{*}}) \tag{4.2.16c}$$

$$\alpha_{v_{jn}}{}^{*} = \frac{-2}{8(1+\delta_{jn})\omega_{v_n}}(\Gamma_{jnjn}{}^{v1} + \Gamma_{njjn}{}^{v2} + V_{njjn}{}^{v2}\omega_{w_j}^2 - W_{njjn}{}^{v2}\omega_{w_j}^2) \tag{4.2.16d}$$

$$\beta_{v_{jn}} = \frac{-1}{8(1+\delta_{jn})\omega_{v_n}} [\Gamma_{njjn}{}^{v1} + \Gamma_{jjnn}{}^{v1} + \Gamma_{jnjn}{}^{v2} + \Gamma_{jjnn}{}^{v2} + \omega_{w_n}\omega_{w_j}(V_{jnjn}{}^{v2} + V_{jjnn}{}^{v2}) - W_{jnjn}{}^{v2}\omega_{w_j}^2 - W_{jjnn}{}^{v2}\omega_{w_n}^2] \tag{4.2.16e}$$

$$\beta_{v_{jn}}{}^{*} = \frac{-1}{8(1+\delta_{jn})\omega_{v_n}} [\Gamma_{njjn}{}^{v1} + \Gamma_{jjnn}{}^{v1} + \Gamma_{jnjn}{}^{v2} + \Gamma_{jjnn}{}^{v2} - \omega_{w_n}\omega_{w_j}(V_{jnjn}{}^{v2} + V_{jjnn}{}^{v2}) - W_{jnjn}{}^{v2}\omega_{w_j}^2 - W_{jjnn}{}^{v2}\omega_{w_n}^2] \tag{4.2.16f}$$

$$f_{w_n} = \frac{T_{nn}{}^{w}}{2\omega_{w_n}} \tag{4.2.17a}$$

$$\alpha_{w_{jn}} = \frac{-1}{8(1+\delta_{jn})\omega_{w_n}} (\Gamma_{jjnn}{}^{w2^{\bullet}} + 2V_{njjn}{}^{w2}\omega_{w_j}^2 - W_{jjnn}{}^{w2^{\bullet}}) \tag{4.2.17b}$$

$$\alpha_{w_{jn}}{}^{*} = \frac{-2}{8(1+\delta_{jn})\omega_{w_n}} (\Gamma_{jjnn}{}^{w1} + V_{njjn}{}^{w1}\omega_{v_j}^2 - W_{njjn}{}^{w1}\omega_{v_j}^2) \tag{4.2.17c}$$

$$\beta_{w_{jn}} = \frac{-1}{8(1+\delta_{jn})\omega_{w_n}} [\Gamma_{njjn}{}^{w1} + \Gamma_{jnjn}{}^{w1} - \omega_{v_n}\omega_{v_j}(V_{jnjn}{}^{w1} + V_{jjnn}{}^{w1}) - W_{jnjn}{}^{w1}\omega_{v_j}^2 - W_{jjnn}{}^{w1}\omega_{v_n}^2] \tag{4.2.17d}$$

$$\beta_{w_{jn}}{}^{*} = \frac{-1}{8(1+\delta_{jn})\omega_{w_n}} [\Gamma_{njjn}{}^{w1} + \Gamma_{jnjn}{}^{w1} + \omega_{v_n}\omega_{v_j}(V_{jnjn}{}^{w1} + V_{jjnn}{}^{w1}) - W_{jnjn}{}^{w1}\omega_{v_j}^2 - W_{jjnn}{}^{w1}\omega_{v_n}^2] \tag{4.2.17e}$$

Those terms with underline are for beams with square cross section only. For a beam with a rectangular cross section, the natural frequencies in the v direction, ω_{v_i}, is not equal to the natural frequencies in the w direction, ω_{w_i}. Then, if there is no internal resonance, there is no coupling between the v and w directions. Consequently, the motion in the w direction will no longer be excited by the force in the v direction. The secular terms of the order- ε equation are obtained from eqs (4.2.14) and (4.2.15) by dropping those terms with underline. In other words, the coefficients

$\beta_{v_{jn}}$, $\beta_{v_{jn}}^*$, $\beta_{w_{jn}}$, $\beta_{w_{jn}}^*$, associating with the coupling of the v and w directions disappear. The remaining coefficients have the same forms as those for a square cross section but have different values.

4.3 Hard Excitation

For hard excitation, the external forces are set to the first order as:

$$g_{n0} = 2K_n \cos \Omega T_0, \quad f_{n0} = 2\tilde{K}_n \cos \tilde{\Omega} T_0, \quad g_{n1} = 0, \quad f_{n1} = 0 \tag{4.3.1}$$

To ensure that the nonlinearity, external force and damping all interact at the same order, the damping coefficients C_{v_1} and C_{w_1} are taken to be positive and are written as:

$$C_{v_1} = \mu_{v_n}, \quad C_{w_1} = \mu_{w_n} \tag{4.3.2}$$

After the above orderings are substituted into eqs (4.1.6) and (4.1.7), the order- ε^0 equations become :

$$D_0{}^2 v_{n0} + \omega_{v_n}^2 v_{n0} = 2K_n \cos \Omega T_0 \tag{4.3.3}$$

$$D_0{}^2 w_{n0} + \omega_{w_n}^2 w_{n0} = 2\tilde{K}_n \cos \tilde{\Omega} T_0 \tag{4.3.4}$$

The general solutions including the homogeneous part and the particular part are:

$$\begin{aligned} v_{n0} &= a_n \cos(\omega_{v_n} T_0 + \alpha_n) + \frac{2K_n}{\omega_{v_n}^2 - \Omega^2} \cos \Omega T_0 = \frac{1}{2} a_n e^{i\alpha_n} e^{i\omega_{v_n} T_0} + \frac{K_n}{\omega_{v_n}^2 - \Omega^2} e^{i\Omega T_0} + cc \\ &= A_n e^{i\omega_{v_n} T_0} + E_n e^{i\Omega T_0} + cc \end{aligned} \tag{4.3.5}$$

$$w_{n0} = b_n \cos(\omega_{w_n} T_0 + \beta_n) + \frac{2\tilde{K}_n}{\omega_{w_n}^2 - \tilde{\Omega}^2} \cos \tilde{\Omega} T_0 = \frac{1}{2} b_n e^{i\beta_n} e^{i\omega_{w_n} T_0} + \frac{\tilde{K}_n}{\omega_{w_n}^2 - \tilde{\Omega}^2} e^{i\tilde{\Omega} T_0} + cc \tag{4.3.6}$$

$$= B_n e^{i\omega_{w_n} T_0} + \tilde{E}_n e^{i\tilde{\Omega} T_0} + cc$$

The amplitudes and phases are functions of T_1 and are obtained by eliminating the secular terms from the second-order equations. The second-order equations are obtained by substituting the linear solutions, eqs (4.3.5) and (4.3.6), into eqs (4.1.8) and (4.1.9). Since these equations are lengthy, they are presented in eqs (C.1) and (C.2) of Appendix C.

Small divisors in the solutions occur under the following conditions:

1. $2\Omega \simeq \omega_{v_n}$
2. $2\tilde{\Omega} \simeq \omega_{w_n}$
3. $3\Omega \simeq \omega_{v_n}$
4. $3\tilde{\Omega} \simeq \omega_{w_n}$
5. $\frac{\Omega}{2} \simeq \omega_{v_n}$
6. $\frac{\tilde{\Omega}}{2} \simeq \omega_{w_n}$
7. $\frac{\Omega}{3} \simeq \omega_{v_n}$
8. $\frac{\tilde{\Omega}}{3} \simeq \omega_{w_n}$
9. $\Omega \simeq \omega_{v_j} \pm \omega_{v_k}$
10. $\Omega \simeq \omega_{v_j} \pm \omega_{w_k}$
11. $\tilde{\Omega} \simeq \omega_{w_j} \pm \omega_{w_k}$ (4.3.7)
12. $\tilde{\Omega} \simeq \omega_{v_j} \pm \omega_{w_k}$
13. $\omega_{v_n} \simeq \omega_{w_j} \pm \omega_{w_k}$
14. $\omega_{v_n} \simeq \omega_{v_j} \pm \omega_{v_k}$
15. $\omega_{w_n} \simeq \omega_{v_j} \pm \omega_{w_k}$
16. $\omega_{w_n} \simeq \omega_{w_j} \pm \omega_{v_k}$
17. $\omega_{v_n} \simeq \omega_{w_j} \pm \omega_{v_k} \pm \omega_{w_l}$
18. $\omega_{v_n} \simeq \omega_{v_j} \pm \omega_{w_k} \pm \omega_{w_l}$
19. $\omega_{v_n} \simeq \omega_{v_j} \pm \omega_{v_k} \pm \omega_{v_l}$
20. $\omega_{w_n} \simeq \omega_{v_j} \pm \omega_{v_k} \pm \omega_{w_l}$
21. $\omega_{w_n} \simeq \omega_{w_j} \pm \omega_{w_k} \pm \omega_{w_l}$
22. $\omega_{w_n} \simeq \omega_{w_j} \pm \omega_{v_k} \pm \omega_{v_l}$

Conditions 1 to 12 involve the frequency of the external forcing and are known as secondary external resonances. The rest only involve the natural (internal) frequencies and are known as internal resonances. For a hard excitation, we only consider the case when the forcing frequency is away from all of the natural frequencies, since the primary resonance must be ruled out to have a solution with uniform expansion. When the forcing frequency is close to one-half of a natural frequency as in conditions 1 and 2, we speak of a superharmonic resonance of order 2. If the forcing

frequency is close to one-third of a natural frequency, as in conditions 3 and 4, we speak of a superharmonic resonance of order three. For conditions 5 and 6, the forcing frequency is close to twice a natural frequency. This case is known as a subharmonic resonance of order two. Similarly, the forcing frequency in conditions 7 and 8 is close to three times a natural frequency, and this case is known as a subharmonic resonance of order three.

4.3.1 Superharmonic Resonance of Order Two with a Square Cross Section

In this dissertation, the force is assumed to act only in the v direction. Hence, the force in the w direction is set to zero at this point:

$$\widetilde{K} = \widetilde{E_n} = \widetilde{\Omega} = 0 \tag{4.3.8}$$

To study the resonance when the forcing frequency is close to one-half of one of the natural frequencies in the v direction, a detuning parameter σ is introduced as:

$$2\Omega = \omega_{v_q} + \varepsilon\sigma \tag{4.3.9}$$

If the cross section of the beam is assumed to be square or circular, the natural frequencies in the v direction, ω_{v_i}, are equal to those in the w direction, ω_{w_i}, i.e.,

$$\omega_{v_i} = \omega_{w_i} = \omega_i \tag{4.3.10}$$

For a beam with a square cross section, the small divisors can occur in conditions 17 to 22. To extract the small divisors, the secular terms of the order- ε equations are set equal to zero, giving:

$$-2i\omega_{v_n}(D_1A_n+\mu_{v_n}A_n)-2\omega_{v_n}f_{v_n}A_n+8\omega_{v_n}A_n\sum_{j=1}^{m}(\alpha_{v_{jn}}A_j\bar{A}_j+\alpha_{v_{jn}}{}^{*}B_j\bar{B}_j)$$
$$+8\omega_{v_n}B_n\sum_{j=1}^{m}(\beta_{v_{jn}}A_j\bar{B}_j+\beta_{v_{jn}}{}^{*}\bar{A}_jB_j)+\delta_{nq}K_qe^{i\sigma T_1}=0 \tag{4.3.11}$$

$$-2i\omega_{w_n}(D_1B_n+\mu_{w_n}B_n)-2\omega_{w_n}f_{w_n}B_n+8\omega_{w_n}B_n\sum_{j=1}^{m}(\alpha_{w_{jn}}B_j\bar{B}_j+\alpha_{w_{jn}}{}^{*}A_j\bar{A}_j)$$
$$+8\omega_{w_n}A_n\sum_{j=1}^{m}(\beta_{w_{jn}}A_j\bar{B}_j+\beta_{w_{jn}}{}^{*}\bar{A}_jB_j)=0 \tag{4.3.12}$$

The form is the same as that for the primary resonance with only forcing in the v direction. The coefficients $\alpha_{v_{jn}}$, $\alpha_{v_{jn}}{}^{*}$, $\alpha_{w_{jn}}$, $\alpha_{w_{jn}}{}^{*}$, $\beta_{v_{jn}}$, $\beta_{v_{jn}}{}^{*}$, $\beta_{w_{jn}}$, $\beta_{w_{jn}}{}^{*}$ are the same as those for the primary resonance except for the following three:

$$f_{v_n}=\frac{1}{2\omega_{v_n}}[T_{nn}{}^{v}-\omega_{v_n}^2X_{nn}{}^{v}+\sum_{j=1}^{m}\sum_{k=1}^{m}(\Gamma_{jknn}{}^{v3^{*}}+2\Omega^2V_{nkjn}{}^{v1}-W_{jknn}{}^{v1^{**}})E_jE_k] \tag{4.3.13a}$$

$$f_{w_n}=\frac{1}{2\omega_{w_n}}[T_{nn}{}^{w}+\sum_{j=1}^{m}\sum_{k=1}^{m}2(\Gamma_{jknn}{}^{w1}+V_{nkjn}{}^{w1}\Omega^2-W_{nkjn}{}^{w1}\Omega^2)E_jE_k] \tag{4.3.13b}$$

$$K_q=\sum_{j=1}^{m}\sum_{k=1}^{m}(-\Lambda_{jkq}{}^{v2}+\Omega^2Y_{jkq}{}^{v1}+\Omega^2Z_{jkq}{}^{v1})E_jE_k \tag{4.3.13c}$$

The definitions of the coefficients are listed in Appendix A and Appendix B.

4.3.2 Superharmonic Resonance of Order Three with Square Cross Section

For the superharmonic resonance of order three, a detuning parameter σ is introduced as:

$$3\Omega = \omega_{v_q} + \varepsilon\sigma \tag{4.3.14}$$

The natural frequency in the v direction is the same as that in the w direction because a beam with a square cross section is considered in this section. After substituting ω_n for ω_{v_n} and ω_{w_n}, and considering all the possibilities of the small divisor terms, one can obtain the following:

$$\begin{aligned} &-2i\omega_{v_n}(D_1A_n + \mu_{v_n}A_n) - 2\omega_{v_n}f_{v_n}A_n + 8\omega_{v_n}A_n\sum_{j=1}^{m}(\alpha_{v_{jn}}A_j\bar{A}_j + \alpha_{v_{jn}}{}^{*}B_j\bar{B}_j) \\ &\underline{+ 8\omega_{v_n}B_n\sum_{j=1}^{m}(\beta_{v_{jn}}A_j\bar{B}_j + \beta_{v_{jn}}{}^{*}\bar{A}_jB_j)} + \delta_{nq}K_qe^{i\sigma T_1} = 0 \end{aligned} \tag{4.3.15}$$

$$\begin{aligned} &-2i\omega_{w_n}(D_1B_n + \mu_{w_n}B_n) - 2\omega_{w_n}f_{w_n}B_n + 8\omega_{w_n}B_n\sum_{j=1}^{m}(\alpha_{w_{jn}}B_j\bar{B}_j + \alpha_{w_{jn}}{}^{*}A_j\bar{A}_j) \\ &\underline{+ 8\omega_{w_n}A_n\sum_{j=1}^{m}(\beta_{w_{jn}}A_j\bar{B}_j + \beta_{w_{jn}}{}^{*}\bar{A}_jB_j)} = 0 \end{aligned} \tag{4.3.16}$$

The form is the same as that for the primary resonance in eqs (4.2.12) and (4.2.13) with only forcing in the v direction. The coefficients $\alpha_{v_{jn}}$, $\alpha_{v_{jn}}{}^{*}$, $\alpha_{w_{jn}}$, $\alpha_{w_{jn}}{}^{*}$, $\beta_{v_{jn}}$, $\beta_{v_{jn}}{}^{*}$, $\beta_{w_{jn}}$, $\beta_{w_{jn}}{}^{*}$ are the same as those for the primary resonance. The coefficients f_{v_n} and f_{w_n} have the same form as those for the superharmonic resonance of order two, but with different values. Because the forcing frequencies are different, only the forcing term is new:

$$K_q = \sum_{j=1}^{m}\sum_{k=1}^{m}\sum_{l=1}^{m}(-\Gamma_{jkiq}{}^{v3} + \Omega^2V_{jklq}{}^{v1} + \Omega^2W_{jklq}{}^{v1})E_jE_kE_l \tag{4.3.17}$$

The definitions of the coefficients are given in Appendix A and Appendix B.

4.3.3 Subharmonic Resonance of Order Two with a Square Cross Section

In the case when the forcing frequency is close to twice a natural frequency, the detuning parameter σ is introduced as:

$$\Omega = 2\omega_{v_q} + \varepsilon\sigma \tag{4.3.18}$$

After substituting ω_n for ω_{v_n} and ω_{w_n} under the square cross section assumption, and considering all the possibilities of the small divisor terms, one can obtain:

$$\begin{aligned} &-2i\omega_{v_n}(D_1A_n + \mu_{v_n}A_n) - 2\omega_{v_n}f_{v_n}A_n + 8\omega_{v_n}A_n\sum_{j=1}^{m}(\alpha_{v_{jn}}A_j\overline{A}_j + \alpha_{v_{jn}}{}^{*}B_j\overline{B}_j) \\ &+ \underline{8\omega_{v_n}B_n\sum_{j=1}^{m}(\beta_{v_{jn}}A_j\overline{B}_j + \beta_{v_{jn}}{}^{*}\overline{A}_jB_j)} + \delta_{nq}\overline{A}_qH_q{}^{v}e^{i\sigma T_1} = 0 \end{aligned} \tag{4.3.19}$$

$$\begin{aligned} &-2i\omega_{w_n}(D_1B_n + \mu_{w_n}B_n) - 2\omega_{w_n}f_{w_n}B_n + 8\omega_{w_n}B_n\sum_{j=1}^{m}(\alpha_{w_{jn}}B_j\overline{B}_j + \alpha_{w_{jn}}{}^{*}A_j\overline{A}_j) \\ &+ \underline{8\omega_{w_n}A_n\sum_{j=1}^{m}(\beta_{w_{jn}}A_j\overline{B}_j + \beta_{w_{jn}}{}^{*}\overline{A}_jB_j)} + \underline{\delta_{nq}\overline{B}_qH_q{}^{w}e^{i\sigma T_1}} = 0 \end{aligned} \tag{4.3.20}$$

The form is the same as that for the primary resonance except for the force terms. In the primary resonance, the force term appears in the w equation only if a force acts in the w direction, while in the subharmonic resonance of order 2, there is a force term in the w equation even if the force is in the v direction only. Furthermore, the force terms are connected with the unknown variables $\overline{A}$ and $\overline{B}$. Special treatment is required to find the steady-state solution, as will be discussed in the

next section. The coefficients $\alpha_{v_{jn}}$, $\alpha_{v_{jn}}^{\bullet}$, $\alpha_{w_{jn}}$, $\alpha_{w_{jn}}^{\bullet}$, $\beta_{v_{jn}}$, $\beta_{v_{jn}}^{\bullet}$, $\beta_{w_{jn}}$, $\beta_{w_{jn}}^{\bullet}$ are the same as those for the primary resonance. The coefficients f_{v_n} and f_{w_n} have the same form as those for the superharmonic resonance of order two, but with different values. Only the forcing terms are new, as:

$$H_q^{\,v} = \sum_{j=1}^{m} \sum_{k=1}^{m} (-\Lambda_{jqq}^{\,v2^{\bullet}} - \Omega\omega_{v_q} Y_{jqq}^{\,v1^{\bullet}} + Z_{jqq}^{\,v1^{\bullet}}) E_j \tag{4.3.21a}$$

$$H_q^{\,w} = \sum_{j=1}^{m} \sum_{k=1}^{m} (-\Lambda_{jqq}^{\,w} + \Omega^2 Z_{qjq}^{\,w}) E_j \tag{4.3.21b}$$

The definitions of the coefficients are listed in Appendix A and Appendix B.

4.3.4 Subharmonic Resonance of Order Three with a Square Cross Section

Similarly, a detuning parameter σ is introduced for the subharmonic resonance of order 3 as:

$$\Omega = 3\omega_{v_q} + \varepsilon\sigma \tag{4.3.22}$$

After proceeding as for the secondary resonances in the previous sections, the secular terms are found:

$$-2i\omega_{v_n}(D_1A_n+\mu_{v_n}A_n)-2\omega_{v_n}f_{v_n}A_n+8\omega_{v_n}A_n\sum_{j=1}^{m}(\alpha_{v_{jn}}A_j\bar{A}_j+\alpha_{v_{jn}}{}^{*}B_j\bar{B}_j)$$
$$+\underline{8\omega_{v_n}B_n\sum_{j=1}^{m}(\beta_{v_{jn}}A_j\bar{B}_j+\beta_{v_{jn}}{}^{*}\bar{A}_jB_j)}+\delta_{nq}\bar{A}_q^2\Upsilon_q{}^{v1}e^{i\sigma T_1}+\underline{\delta_{nq}\bar{B}_q^2\Upsilon_q{}^{v2}e^{i\sigma T_1}}=0 \tag{4.3.23}$$

$$-2i\omega_{w_n}(D_1B_n+\mu_{w_n}B_n)-2\omega_{w_n}f_{w_n}B_n+8\omega_{w_n}B_n\sum_{j=1}^{m}(\alpha_{w_{jn}}B_j\bar{B}_j+\alpha_{w_{jn}}{}^{*}A_j\bar{A}_j)$$
$$+\underline{8\omega_{w_n}A_n\sum_{j=1}^{m}(\beta_{w_{jn}}A_j\bar{B}_j+\beta_{w_{jn}}{}^{*}\bar{A}_jB_j)}+\underline{\delta_{nq}\bar{A}_q\bar{B}_q\Upsilon_q{}^{w}e^{i\sigma T_1}}=0 \tag{4.3.24}$$

The form is the same as that for the primary resonance except for the force terms. In this case, two force terms show up in the v equation, while there is only one such term in the v equation of the subharmonic resonance of order 2. There is also one force term in the w equation, the same as that in the w equation of the subharmonic resonance of order 2, even if the force is only in the v direction. These force terms are also connected with the unknown variables $\bar{A}$ and $\bar{B}$; hence, to find a steady-state solution, special treatment is needed. The coefficients $\alpha_{v_{jn}}$, $\alpha_{v_{jn}}{}^{*}$, $\alpha_{w_{jn}}$, $\alpha_{w_{jn}}{}^{*}$, $\beta_{v_{jn}}$, $\beta_{v_{jn}}{}^{*}$, $\beta_{w_{jn}}$, $\beta_{w_{jn}}{}^{*}$ are the same as those for the primary resonance. The coefficients f_{v_n} and f_{w_n} have the same form as those for the superharmonic resonance of order two, but with different values. Only the forcing terms are new, as:

$$\Upsilon_q{}^{v1}=\sum_{j=1}^{m}\sum_{k=1}^{m}(-\Gamma_{jqqq}{}^{v3^{*}}-V_{jqqq}{}^{v1^{*}}+W_{jqqq}{}^{v1^{***}})\frac{E_j}{2} \tag{4.3.25a}$$

$$\Upsilon_q{}^{v2}=\sum_{j=1}^{m}\sum_{k=1}^{m}(-\Gamma_{qjqq}{}^{v1}-\Gamma_{jqqq}{}^{v2}+\omega_{w_q}^2V_{jqqq}{}^{v2}+\omega_{w_q}^2W_{jqqq}{}^{v2})E_j \tag{4.3.25b}$$

$$\Upsilon_q^w = \sum_{j=1}^{m}\sum_{k=1}^{m}(-\Gamma_{qjqq}{}^{w1^*} - V_{qjqq}{}^{w1^*} + W_{qjqq}{}^{w1^*})E_j \tag{4.3.25c}$$

The definitions of the coefficients are listed in Appendix A and Appendix B.

4.4 Steady-State Solutions

4.4.1 Steady-State Solutions for Primary and Superharmonic Resonances with a Square Cross Section

To find the steady-state solution of the amplitudes, a_n and b_n, in the first-order equations, eqs (4.2.5) and (4.2.6), and (or) eqs (4.3.5) and (4.3.6), we express A and B in polar form:

$$A_n = \frac{1}{2} a_n e^{i\alpha_n} \tag{4.4.1}$$

$$B_n = \frac{1}{2} b_n e^{i\beta_n} \tag{4.4.2}$$

where a_n, b_n, α_n and β_n are functions of T_1. After separating real and imaginary parts, eqs (4.2.14) and (4.2.15) become:

$$-\omega_n \dot{a_n} - \omega_n \mu_n a_n + \underline{\omega_n \sum_{j=1}^{m} \beta_{v_{jn}} b_n a_j b_j \sin(\beta_n - \alpha_n + \alpha_j - \beta_j)}$$
$$\underline{+ \omega_n \sum_{j=1}^{m} \beta_{v_{jn}}{}^{*} b_n a_j b_j \sin(\beta_n - \alpha_n - \alpha_j + \beta_j)} + \delta_{nq} K_q \sin(\sigma T_1 - \alpha_q) = 0 \tag{4.4.3}$$

$$\omega_n a_n \dot{\alpha_n} - \omega_n f_{v_n} a_n + \omega_n a_n \sum_{j=1}^{m} (\alpha_{v_{jn}} a_j{}^2 + \alpha_{v_{jn}}{}^{*} b_j{}^2) + \underline{\omega_n \sum_{j=1}^{m} \beta_{v_{jn}} b_n a_j b_j \cos(\beta_n - \alpha_n + \alpha_j - \beta_j)}$$
$$\underline{+ \omega_n \sum_{j=1}^{m} \beta_{v_{jn}}{}^{*} b_n a_j b_j \cos(\beta_n - \alpha_n - \alpha_j + \beta_j)} + \delta_{nq} K_q \cos(\sigma T_1 - \alpha_q) = 0 \tag{4.4.4}$$

$$-\omega_n \dot{b_n} - \omega_n \mu_n b_n + \underline{\omega_n \sum_{j=1}^{m} \beta_{w_{jn}} a_n a_j b_j \sin(-\beta_n + \alpha_n + \alpha_j - \beta_j)}$$
$$\underline{+ \omega_n \sum_{j=1}^{m} \beta_{w_{jn}}{}^{*} a_n a_j b_j \sin(-\beta_n + \alpha_n - \alpha_j + \beta_j)} = 0 \tag{4.4.5}$$

$$\omega_n b_n \dot{\beta_n} - \omega_n f_{w_n} b_n + \omega_n b_n \sum_{j=1}^{m} (\alpha_{w_{jn}} b_j{}^2 + \alpha_{w_{jn}}{}^{*} a_j{}^2) + \underline{\omega_n \sum_{j=1}^{m} \beta_{w_{jn}} a_n a_j b_j \cos(-\beta_n + \alpha_n + \alpha_j - \beta_j)}$$
$$\underline{+ \omega_n \sum_{j=1}^{m} \beta_{w_{jn}}{}^{*} a_n a_j b_j \cos(-\beta_n + \alpha_n - \alpha_j + \beta_j)} = 0 \tag{4.4.6}$$

The above ordinary differential equations govern the amplitudes and phases of the n-th mode of the first-order solution, v_{n0} and w_{n0}. The steady-state solutions are obtained by setting the time derivatives equal to zero and introducing a new variable to transform the equations to an autonomous system. Two cases are studied. The first one is when the index n is not equal to q, i.e.,

when the mode being studied is not the mode being excited. The second is when the index n is equal to q, i.e., the mode being studied is the mode being excited. For the first case, the following equation is obtained by multiplying eq (4.4.3) by a_n, multiplying eq (4.4.5) by b_n, and then adding the results together:

$$-\omega_n\mu_n(a_n{}^2+b_n{}^2)+\omega_n\sum_{j=1}^{m}[(\beta_{v_{jn}}-\beta_{w_{jn}}{}^*)\sin(\beta_n-\alpha_n+\alpha_j-\beta_j) + (\beta_{v_{jn}}{}^*-\beta_{w_{jn}})\sin(\beta_n-\alpha_n-\alpha_j+\beta_j)]a_nb_na_jb_j=0 \tag{4.4.7}$$

Because the coefficient $\beta_{v_{jn}}$ is equal to $\beta_{w_{jn}}{}^*$, and $\beta_{v_{jn}}{}^*$ is equal to $\beta_{w_{jn}}$ (see Appendix A), the above equation can be simplified to:

$$a_n{}^2+b_n{}^2=0 \tag{4.4.8}$$

There is only one solution for the above equation:

$$a_n=b_n=0 \tag{4.4.9}$$

Hence, for n not equal to q, the n-th mode decays to zero. The only steady-state solution is the trivial solution. For the second case, when n is equal to q, only the q-th mode exists since all other modes decay to zero. Then the sums can be replaced by single terms. The only remaining index is q, and we can drop it for simplicity (e.g., α_q can be replaced by α). Because the equations are explicit functions of T_1, to find a steady-state solution it is convenient to introduce new variables γ and ψ given by:

$$\gamma=\sigma T_1-\alpha \tag{4.4.10}$$

$$\psi=\beta+\gamma-\sigma T_1 \tag{4.4.11}$$

Then the autonomous equations are given by eqs (4.4.12)-(4.4.15). The steady-state solution is obtained by setting the time derivatives $\dot{a}$, $\dot{\gamma}$, $\dot{b}$ and $\dot{\psi}$ to zero:

$$\dot{a} = -\mu a + \underline{\beta_v^* a b^2 \sin(2\psi)} + \frac{K}{\omega}\sin\gamma = 0 \tag{4.4.12}$$

$$\dot{\gamma} = \sigma - f_v + \alpha_v a^2 + \alpha_v^* b^2 + \underline{\beta_v b^2 + \beta_v^* b^2 \cos(2\psi)} + \frac{K}{\omega a}\cos\gamma = 0 \tag{4.4.13}$$

$$\dot{b} = -\mu b + \underline{\beta_w a^2 b \sin(-2\psi)} = 0 \tag{4.4.14}$$

$$b\dot{\psi} = b[f_w - f_v + (\alpha_v - \alpha_w^*)a^2 + (\alpha_v^* - \alpha_w)b^2 - \underline{\beta_w^* a^2 + \beta_v b^2 + (\beta_v^* b^2 - \beta_w a^2)\cos(2\psi)} + \frac{K}{\omega a}\cos\gamma] = 0 \tag{4.4.15}$$

To find the steady-state responses, a and b as functions of σ, we start from the above four equations but with five unknown variables. We can vary any one of the five variables and find the rest as functions of this specified variable. Trigonometric identities can be used to eliminate the phase angles γ and ψ:

$$\sin^2\gamma + \cos^2\gamma = 1, \quad \sin^2\psi + \cos^2\psi = 1 \tag{4.4.16}$$

Then b can be expressed as a function of a, and the following relationship between σ and a can be obtained:

$$\sigma = -X_1 + \frac{\beta_v^* b^2 Y_1}{Y_2} \pm \left(-1 + \frac{\beta_v^* b^2}{Y_2}\right)\frac{1}{\omega a^2}\sqrt{K^2 a^2 - \omega^2\mu^2(a^2 + b^2)^2} \tag{4.4.17}$$

where

$$X_1 = -f_v + \alpha_v a^2 + \alpha_v^* b^2 + \beta_v b^2 \tag{4.4.18a}$$

$$Y_1 = f_w - f_v + (\alpha_v - \alpha_w^* - \beta_w^*)a^2 + (\alpha_v^* - \alpha_w + \beta_v)b^2 \tag{4.4.18b}$$

$$Y_2 = \beta_v^* b^2 - \beta_w a^2 \tag{4.4.18c}$$

By varying a, we can find the corresponding σ value and the remaining three variables. The planar responses can be obtained by setting b and ψ in eq (4.4.17) to zero, as:

$$\sigma = f_v - \alpha_v a^2 \pm \sqrt{\frac{K^2}{\omega^2 a^2} - \mu^2} \tag{4.4.19}$$

Some numerical results, including planar and nonplanar responses, are presented in Chapter 5.

4.4.2 Steady-State Solutions for Subharmonic Resonance of Order Two with a Square Cross Section

To transform the nonautonomous system to an autonomous system in this case, new variables are introduced as:

$$\gamma = \sigma T_1 - 2\alpha \tag{4.4.20}$$

$$\psi = \sigma T_1 - 2\beta \tag{4.4.21}$$

After substituting the polar forms for A_n and B_n into eqs (4.3.19) and (4.3.20), the real and imaginary parts are then separated to give:

$$\begin{aligned} &-\omega_n \dot{a}_n - \omega_n \mu_n a_n + \omega_n \sum_{j=1}^{m} \beta_{v_{jn}} b_n a_j b_j \sin[\frac{1}{2}(-\psi_n + \psi_j + \gamma_n - \gamma_j)] \\ &+ \omega_n \sum_{j=1}^{m} \beta_{v_{jn}}{}^{*} b_n a_j b_j \sin[\frac{1}{2}(-\psi_n - \psi_j + \gamma_n + \gamma_j)] + \delta_{nq} \frac{1}{2} a_q H_q{}^{v} \sin \gamma_q = 0 \end{aligned} \tag{4.4.22}$$

$$\omega_n a_n \dot{\alpha}_n - \omega_n f_{v_n} a_n + \omega_n a_n \sum_{j=1}^{m} (\alpha_{v_{jn}} a_j^2 + \alpha_{v_{jn}}^* b_j^2) + \underline{\omega_n \sum_{j=1}^{m} \beta_{v_{jn}} b_n a_j b_j \cos[\frac{1}{2}(-\psi_n + \psi_j + \gamma_n - \gamma_j)]}$$

$$+ \underline{\omega_n \sum_{j=1}^{m} \beta_{v_{jn}}^* b_n a_j b_j \cos[\frac{1}{2}(-\psi_n - \psi_j + \gamma_n + \gamma_j)] + \delta_{nq} \frac{1}{2} a_q H_q^v \cos\gamma_q = 0} \tag{4.4.23}$$

$$-\omega_n \dot{b_n} - \omega_n \mu_n b_n + \underline{\omega_n \sum_{j=1}^{m} \beta_{w_{jn}} a_n a_j b_j \sin[\frac{1}{2}(\psi_n + \psi_j - \gamma_n - \gamma_j)]}$$

$$+ \underline{\omega_n \sum_{j=1}^{m} \beta_{w_{jn}}^* a_n a_j b_j \sin[\frac{1}{2}(\psi_n - \psi_j - \gamma_n + \gamma_j)] + \delta_{nq} \frac{1}{2} b_q H_q^w \sin\psi_q = 0} \tag{4.4.24}$$

$$\omega_n b_n \dot{\beta}_n - \omega_n f_{w_n} b_n + \omega_n b_n \sum_{j=1}^{m} (\alpha_{w_{jn}} b_j^2 + \alpha_{w_{jn}}^* a_j^2) + \underline{\omega_n \sum_{j=1}^{m} \beta_{w_{jn}} a_n a_j b_j \cos[\frac{1}{2}(\psi_n + \psi_j - \gamma_n - \gamma_j)]}$$

$$+ \underline{\omega_n \sum_{j=1}^{m} \beta_{w_{jn}}^* a_n a_j b_j \cos[\frac{1}{2}(\psi_n - \psi_j - \gamma_n + \gamma_j)] + \delta_{nq} \frac{1}{2} b_q H_q^w \cos\psi_q = 0} \tag{4.4.25}$$

Similar to primary and superharmonic resonances, a mode decays to zero when it is not excited. Only the one excited by the external force does not always decay, The differential equations for this mode are given by:

$$\dot{a} = a[-\mu + \underline{\beta_v^* b^2 \sin(\gamma - \psi)} + \frac{H^v}{2\omega} \sin\gamma] = 0 \tag{4.4.26}$$

$$a\dot{\gamma} = a[\sigma - 2f_v + 2\alpha_v a^2 + 2\alpha_v^* b^2 + \underline{2\beta_v b^2 + 2\beta_v^* b^2 \cos(\gamma - \psi)} + \frac{H^v}{\omega} \cos\gamma] = 0 \tag{4.4.27}$$

$$\dot{b} = b[-\mu + \underline{\beta_w a^2 \sin(\psi - \gamma)} + \frac{H^w}{2\omega} \sin\psi] = 0 \tag{4.4.28}$$

$$b\dot{\psi} = b[\sigma - 2f_w + 2\alpha_w b^2 + 2\alpha_w{}^* a^2 + \underline{2\beta_w{}^* a^2 + 2\beta_w a^2 \cos(\psi - \gamma) + \frac{H^w}{\omega}\cos\psi}] = 0 \tag{4.4.29}$$

After a careful examination of the above equations, it is observed that four kinds of steady-state solutions may exist. They are as follows: (1) $a = 0, b = 0$; (2) $a \neq 0, b = 0$; (3) $a = 0, b \neq 0$; (4) $a \neq 0, b \neq 0$. The second and third ones can be obtained simply by setting $b = \psi = 0$ and $a = \gamma = 0$, respectively, as:

$$\sigma = 2f_v - 2\alpha_v a^2 \pm \frac{1}{\omega}\sqrt{H^{v2} - 4\mu^2\omega^2} \tag{4.4.30a}$$

$$\sigma = 2f_w - 2\alpha_w b^2 \pm \frac{1}{\omega}\sqrt{H^{w2} - 4\mu^2\omega^2} \tag{4.4.30b}$$

For the last one, instead of varying a to find the remaining variables as in the primary and superharmonic resonances, we vary a phase angle to find the corresponding values of the rest of the variables in the subharmonic resonance of order two. First, eqs (4.4.26) and (4.4.27) are used to express γ as a function of a, b and ψ. Next, eqs (4.4.27) and (4.4.29) are used to eliminate σ from this equation; then a can be expressed as a function of b and ψ. Because the equations involve transcendental functions, the trigonometric identities will give another equation which expresses the relationship between b and ψ. We use

$$\sin^2(\psi - \gamma) + \cos^2(\psi - \gamma) = 1 \tag{4.4.31}$$

to find b as a function of ψ. We end up with an eighth- order polynomial of b with ψ in its coefficients. Once a value of ψ is specified, the corresponding solution of b can be obtained. The value of ψ is varied from 0 to 2π to cover all the possible solutions. The range 2π to 4π, for example, does not furnish additional solutions. In turn, the rest of the variables can also be obtained. Some numerical results are presented in Chapter 5.

4.4.3 Steady-State Solutions for Subharmonic Resonance of Order Three with a Square Cross Section

As before, two new variables are defined to transform the nonautonomous system into an autonomous system:

$$\gamma = \sigma T_1 - 3\alpha \tag{4.4.32}$$

$$\psi = \sigma T_1 - \alpha - 2\beta \tag{4.4.33}$$

The real and imaginary parts are given in eqs (4.3.23)-(4.3.24) after substituting the polar forms for A_n and B_n:

$$\begin{aligned} &-\omega_n \dot{a}_n - \omega_n \mu_n a_n + \underline{\omega_n \sum_{j=1}^{m} \beta_{v_{jn}} b_n a_j b_j \sin[\tfrac{1}{2}(-\psi_n + \psi_j + \gamma_n - \gamma_j)]} \\ &\quad + \underline{\omega_n \sum_{j=1}^{m} \beta_{v_{jn}}{}^{*} b_n a_j b_j \sin[\tfrac{1}{2}(-\psi_n - \psi_j + \gamma_n + \gamma_j)]} \\ &\quad + \delta_{nq} \frac{1}{4} [a^2 \Upsilon_q{}^{v1} \sin\gamma + \underline{b^2 \Upsilon_q{}^{v2} \sin\psi}] = 0 \end{aligned} \tag{4.4.34}$$

$$\begin{aligned} &\omega_n a_n \dot{\alpha}_n - \omega_n f_{v_n} a_n + \omega_n a_n \sum_{j=1}^{m} (\alpha_{v_{jn}} a_j{}^2 + \alpha_{v_{jn}}{}^{*} b_j{}^2) + \underline{\omega_n \sum_{j=1}^{m} \beta_{v_{jn}} b_n a_j b_j \cos[\tfrac{1}{2}(-\psi_n + \psi_j + \gamma_n - \gamma_j)]} \\ &\quad + \underline{\omega_n \sum_{j=1}^{m} \beta_{v_{jn}}{}^{*} b_n a_j b_j \cos[\tfrac{1}{2}(-\psi_n - \psi_j + \gamma_n + \gamma_j)]} + \delta_{nq} \frac{1}{4} [a^2 \Upsilon_q{}^{v1} \sin\gamma + \underline{b^2 \Upsilon_q{}^{v2} \sin\psi}] = 0 \end{aligned} \tag{4.4.35}$$

$$-\omega_n \dot{b_n} - \omega_n \mu_n b_n + \omega_n \sum_{j=1}^{m} \beta_{w_{jn}} a_n a_j b_j \sin[\frac{1}{2}(\psi_n + \psi_j - \gamma_n - \gamma_j)] + \omega_n \sum_{j=1}^{m} \beta_{w_{jn}}{}^* a_n a_j b_j \sin[\frac{1}{2}(\psi_n - \psi_j - \gamma_n + \gamma_j)] + \delta_{nq} \frac{1}{4} a b_q \Upsilon_q{}^w \sin \psi_q = 0 \tag{4.4.36}$$

$$\omega_n b_n \dot{\beta}_n - \omega_n f_{w_n} b_n + \omega_n b_n \sum_{j=1}^{m} (\alpha_{w_{jn}} b_j{}^2 + \alpha_{w_{jn}}{}^* a_j{}^2) + \omega_n \sum_{j=1}^{m} \beta_{w_{jn}} a_n a_j b_j \cos[\frac{1}{2}(\psi_n + \psi_j - \gamma_n - \gamma_j)] + \omega_n \sum_{j=1}^{m} \beta_{w_{jn}}{}^* a_n a_j b_j \cos[\frac{1}{2}(\psi_n - \psi_j - \gamma_n + \gamma_j)] + \delta_{nq} \frac{1}{4} a b_q \Upsilon_q{}^w \sin \psi_q = 0 \tag{4.4.37}$$

The autonomous differential equations for the excited mode are:

$$\dot{a} = -\mu a + \beta_w a b^2 \sin(\gamma - \psi) + \frac{a^2}{4\omega} \Upsilon^{v1} \sin \gamma + \frac{b^2}{4\omega} \Upsilon^{v2} \sin \psi = 0 \tag{4.4.38}$$

$$a\dot{\gamma} = a\sigma - 3 f_v a + 3\alpha_v a^3 + 3\alpha_v{}^* a b^2 + 3\beta_v a b^2 + 3\beta_w a b^2 \cos(\gamma - \psi) + \frac{3a^2}{4\omega} \Upsilon^{v1} \cos \gamma + \frac{3b^2}{4\omega} \Upsilon^{v2} \cos \psi = 0 \tag{4.4.39}$$

$$\dot{b} = b[-\mu + \beta_w a^2 \sin(\psi - \gamma) + \frac{a}{4\omega} \Upsilon^w \sin \psi] = 0 \tag{4.4.40}$$

$$b\dot{\psi} = b[\sigma - f_v - 2 f_w + \alpha_v a^2 + 2\alpha_v b^2 + \alpha_v{}^* b^2 + 2\alpha_v{}^* a^2 + \beta_v b^2 + 2\beta_v a^2 + \beta_w b^2 \cos(\gamma - \psi) + 2\beta_w a^2 \cos(\psi - \gamma) + \frac{a}{4\omega} \Upsilon^{v1} \cos \gamma + \frac{b^2}{4\omega a} \Upsilon^{v2} \cos \psi + \frac{a}{2\omega} \Upsilon^w \cos \psi] = 0 \tag{4.4.41}$$

There are three possible solutions: (1) $a = 0, b = 0$; (2) $a \neq 0, b = 0$; (3) $a \neq 0, b \neq 0$. The planar motion, the second one, can be obtained simply by setting $b = \psi = 0$ to give:

$$\sigma = 3 f_v - 3\alpha_v a^2 \pm \frac{3}{4\omega} \sqrt{(a\Upsilon^{v1})^2 - (4\mu\omega)^2} \tag{4.4.42}$$

For the nonplanar solution, procedures similar to those for the subharmonic resonance of order two are used to find the steady-state responses. Instead of obtaining an eighth-order polynomial of b as in the previous case, we get a twenty-fourth order polynomial of b with ψ in its coefficients. We vary ψ from 0 to 2π to find the corresponding solutions for b and in turn to find the rest of the variables. The numerical results will be given in the next chapter.

5 Numerical Examples

In this chapter, numerical solutions of the first-order equations, eqs (4.2.5) and (4.2.6) for soft excitation, and eqs (4.3.5) and (4.3.6) for hard excitation, are described. It should be noted that only the resonance amplitudes, a_n and b_n, will be discussed and plotted in the results of secondary resonances. The particular solution with amplitude E_n in the second term of eq (4.3.5) always exists in the in-plane direction and will not be plotted.

We choose a steel beam with square cross section to investigate the response under a harmonic, distributed force. The dimensions and material properties of the beam are chosen as follows: 240 *in* in length; 2.4 *in* in depth; 2.4 *in* in width; density, ρg, of 0.28 lbf/in^3; Young's modulus, E, of 30×10^6 lbf/in^2.

Some parameters are varied. The first one is the damping coefficient. We choose a variety of damping coefficients to study the influence of damping on the frequency response. Damping will be expressed in terms of a proportion of critical damping, ζc_{cr}, as stated in Appendix F. The damping parameter ζ can be measured through the decrement of the amplitude of free vibration, or specifically, the logarithmic decrement δ. Thus, in this dissertation, the damping capacity will be described in terms of the logarithmic decrement.

The second parameter to be varied is the the magnitude of the force. In order to provide a physical idea about the dynamic force, we will express its magnitude in terms of the weight of the beam. The numerical value of the weight of the beam is 0.2688.

The stability of the response can be examined either by computing the eigenvalues of the Jacobian matrix or by using the Routh-Hurwitz criterion. Five resonances are investigated: primary resonance, superharmonic resonances of orders two and three, and subharmonic resonances of orders two and three.

5.1 Stationary Solutions

5.1.1.1 Frequency Response for a Primary Resonance of the First Mode

The forcing frequency is near the first natural frequency. Three levels of force, 0.001W, 0.0005W and 0.0001W (where W denotes the weight of the beam), are chosen to examine the response to a primary-resonance excitation. Damping is considered light, and three values of the logarithmic decrement, 0.0002, 0.002 and 0.02, are used.

Figures 5.1a and 5.1b show the frequency-response curves for in-plane and out-of-plane motions, respectively. The force magnitude is chosen to be 0.001W and damping is assumed to be such that the logarithmic decrement is equal to 0.0002. The vertical axis stands for the amplitudes of the modes, $\hat{\varepsilon}a_1$ or $\hat{\varepsilon}b_1$, or in-plane and out-of-plane modes, respectively, where a_1 and b_1 are obtained from the method of multiple scales. They are scaled by $1/\hat{\varepsilon}$ when the method of multiple scales is applied. To obtain physical values, we need to multiply them by $\hat{\varepsilon}$. Hence, a value of $\hat{\varepsilon}a_1 = 0.1$ in the diagram means the modal amplitude is 0.1 compared with 1, the dimensionless length of the beam. If $\hat{\varepsilon}$ is chosen to be 0.01, then $a_1 = 10$ in the results of the method of multiple

scales. The horizontal axis stands for the deviation from the linear natural frequency, or the detuning $\hat{\varepsilon}^2\sigma$. A value $\hat{\varepsilon}^2\sigma = 0.01$ means the frequency is 3.52602 if the linear natural frequency is 3.51602, and thus the value of σ from the method of multiple scales is 100. Here we use capital letters on curves of the amplitude of the in-plane component and lower case letters on curves of the corresponding amplitude of the out-of-plane component.

In Figure 5.1a, the branch ABCDEF corresponds to planar motion ($b_1 = 0$), while the branch BGHIE is associated with nonplanar motion ($b_1 \neq 0$). The planar response bends to the right here as the nonlinear geometric terms dominate the response. Hence, the first mode is of hardening type. The segment EI is indistinguishable from part of segment HI, but their corresponding phases are different. For planar motion subjected to an in-plane disturbance, segments AC and DF are stable, but segment DC is unstable. But if the planar motion is perturbed by an out-of-plane disturbance, segments BC and DE also become unstable. In other words, nonplanar motion should bifurcate from B and E, and this does occur. The bifurcation points can be found analytically by seting the equation for b, eq (G.1) in Appendix G, to zero (for details, see Appendix G). The calculations show the bifurcation points occur at $\hat{\varepsilon}^2\sigma = 0.003913$, $\hat{\varepsilon}a = 0.02081$, and $\hat{\varepsilon}^2\sigma = 0.001908$, $\hat{\varepsilon}a = 0.03640$. The calculations show a very good agreement with the result in Figure 5.1a. For the nonplanar motion, segments BG and HI are stable but segments GH and EI are unstable. We found that in those unstable regions, there is at least one eigenvalue of the Jacobian matrix having positive real part.

If the forcing frequency is increased from a point below the region of resonance, the amplitude of the planar motion initially increases, while the amplitude of the out-of-plane component remains zero; the response is planar. At point B, the planar response becomes unstable, and whirling motion rapidly develops as the frequency continues to increase. Between B and G, the amplitude of the in-plane component decreases while the amplitude of the out-of-plane component increases. At G, the amplitude jumps to G′ and then both in-plane and out-of-plane components increase until point I is reached. At I, the amplitude a_1 jumps to I′. The whirling motion disappears, and a small-amplitude, planar response is exhibited.

If the frequency of excitation is swept down from a point above the region of resonance, the motion initially will be planar with a small amplitude. The amplitude of the in-plane component will increase until point E is reached, where its amplitude jumps to E′ (where point E′ is almost indistinguishable from point E in Figure 5.1a, but their corresponding phases are quite different). At the same time, the amplitude of the out-of-plane component jumps from e to e′ in Figure 5.1b, and whirling motion develops rapidly. Following another jump at H, the amplitude of the out-of-plane component decreases to zero when point B is reached, the motion becomes planar, and the amplitude of the in-plane component decreases as the forcing frequency continues to decrease.

Figure 5.2 shows frequency-response curves of the first mode for both in-plane and out-of-plane motions when the force magnitude is the same as that in Figure 5.1, 0.001W, but damping is increased so that the logarithmic decrement is equal to 0.002. The planar response is stable everywhere if it is subjected to only an in-plane perturbation. In other words, a jump does not occur in the planar motion after the tip point C of planar motion is reached. But if an out-of-plane perturbation is applied, the response between points B and E becomes unstable and whirling motion develops. The calculation of bifurcation points shows that point B is located at $\hat{\varepsilon}^2\sigma = 0.002152$ and $\hat{\varepsilon}a = 0.02529$, and point E is located at $\hat{\varepsilon}^2\sigma = 0.003316$ and $\hat{\varepsilon}a = 0.02150$. For the nonplanar motion, segment BI (bi) is stable but segment IE (ie) is unstable (points I and E on the curve of planar motion are indistinguishable from each other).

If the frequency of excitation is swept up from a point below the region of resonance, the motion initially will be planar and the amplitude will increase until B is reached. At point B, the amplitude of the in-plane component starts to decrease, while the amplitude of the out-of-plane component grows from zero rapidly. Beyond point H, the amplitude of the in-plane component begins to increase. On the contrary, the amplitude of the out-of-plane part begins to decrease rapidly to zero when point E is reached. Whirling motion disappears and the motion becomes planar. Beyond point E, nonplanar motion is not possible, and planar motion is stable, no matter what kind of perturbation is applied. As the frequency continues to increase, the amplitude of the planar component decreases gradually.

If the forcing frequency is swept down from a point above the region of resonance, the motion will be planar until point E is reached, where the planar motion becomes unstable, and then a jump from E to I (e to i) occurs. Whirling motion develops suddenly with a large amplitude of the out-of-plane component. Whirling motion will continue to exist until point B is reached. Below point B, the motion will be planar again.

If damping is increased so that the logarithmic decrement is equal to 0.02 and the force magnitude is still kept equal to 0.001W, the motion will be strictly planar. Nonplanar motion is not possible under such circumstances. The calculation of bifurcation points shows the nonexistence of a real solution, and it implies that a bifurcation point does not exist in this case. The frequency-response curve is shown in Figure 5.3.

The effects of damping on primary resonance are as follows: (1) the maximum amplitude is approximately proportional to the inverse of the damping coefficient; (2) the smaller the damping, the more prominent the whirling motion becomes; (3) the smaller the damping, the more the maximum amplitude shifts to a higher frequency.

Next, the influence of the level of the excitation is investigated. First we decrease the force magnitude to 0.0005W and assume damping is such that the logarithmic decrement is equal to 0.0002. Under these conditions, whirling motion is still possible. The frequency-response curves are shown in Figures 5.4a and 5.4b. The responses are similar to those in Figures 5.1a and 5.1b but with a different scale.

If the magnitude of the excitation is further decreased to 0.0001W and the logarithmic decrement is still equal to 0.0002, whirling motion still exists. The frequency-response curves of the first mode for both in-plane and out-of-plane components are shown in Figure 5.5. The stability analysis indicates that nonplanar motion should bifurcate from points B and E, and it agrees with the calculations of bifurcation points very well. The calculations show that point B is located at $\hat{\varepsilon}^2\sigma = 0.002131$ and $\hat{\varepsilon}a = 0.01054$, and point E is located at $\hat{\varepsilon}^2\sigma = 0.002600$ and $\hat{\varepsilon}a = 0.01394$. If the frequency of excitation is swept up from point A, the motion will be planar until B is reached. Then whirling motion grows rapidly until G is reached, where it loses stability. Between G and H, both in-plane and out-of-plane motions are unstable with two pairs of complex conjugate eigenvalues.

The real part of one of the eigenvalues is positive. This indicates that a Hopf bifurcation should occur at point G and H, and this suggests that either limit cycles or chaotic motions may exist in this region. After point H, steady nonplanar motion is possible again. At point I, the amplitude jumps to I′ and whirling motion disappears. After point I′, the motion becomes planar and the amplitude of the planar motion decreases gradually.

The effects of the amplitude of the force on primary resonance are as follows: (1) the maximum modal amplitude is approximately proportional to the level of the force; (2) the larger the force, the more prominent the whirling motion becomes; (3) the larger the force, the more the maximum amplitude shifts toward a higher frequency.

5.1.1.2 Frequency Response for a Primary Resonance of the Second Mode

For the second mode, the frequency-response curve of planar motion, A-B-C-D-E-F, bends to the left. This is because the nonlinear inertia terms dominate the response, and hence, the second mode is of softening type. Figures 5.6a and 5.6b show the responses of in-plane and out-of-plane motions, respectively. The force magnitude is 0.005W and damping is such that the logarithmic decrement is equal to 0.0002. When the forcing frequency is swept up, a possible route is A-B-B′-D-E-F or A-B-B′-D-H-I-F, where point I is located at $\hat{\varepsilon}^2\sigma = 1$, which is outside of Figure 5.6a. The numerical integration shows the difficulty to obtain point I. The domain of attraction of point I is small, and probably the motion at point I is physically unrealistic. Before I is reached, the amplitude will jump down, and motion will become planar again. If the forcing frequency is swept down, a possible route is F-E-E′-H-D-C-A, where point C is located at $\hat{\varepsilon}^2\sigma = -8$. The numerical integration also shows the difficulty to obtain motion at point c, and the resonance will probably cease to exist before point C is reached. When the frequency is between D and H, both in-plane and out-of-plane motions are unstable. The eigenvalues of the Jacobian matrix between G and H are two pairs of complex conjugate values with one real part being positive. Hopf bifurcation should

occur at G and H. This implies that either limit cycles or chaotic motions may exist in this unstable region.

When the damping is increased so that the logarithmic increment is equal to 0.002 and the force is still 0.005W, the amplitude is decreased and the size of the arc DH is also decreased. The results are shown in Figures 5.7a and 5.7b. Essentially, the shapes of the response curves are similar to those in Figures 5.6a and 5.6b. If the damping is increased so that the logarithmic decrement is equal to 0.02, only planar motion exists, as shown in Figure 5.8.

The effect of decreasing the magnitude of the force can be seen by comparing Figures 5.6a and 5.9a. The forces are 0.005W and 0.001W, respectively. For the smaller force, not only the amplitude is smaller but also the unstable region of the upper branch in the planar motion, DE, is smaller. This indicates that the nonplanar motion is less likely to happen during the passage through the unstable region DE for a small force. Besides, because the unstable region, DE, is decreased, the motions between D and H are no longer unstable only. Stable motions become possible everywhere in this case. If the force is further decreased to 0.0005W, the unstable region almost vanishes, and the nonplanar motion is not likely to happen between the bifurcation points D and E. The results are shown in Figures 5.10a and 5.10b.

5.1.2.1 Frequency Response for a Superharmonic Resonance of Order Two of the First Mode

Because the magnitude of the force needed to excite a secondary resonance is much larger than that for a primary resonance, the levels of force are chosen to be W, 0.5W and 0.1W in this section. Since the same materials as in primary resonance are used to investigate the response, the same values of the logarithmic decrement, 0.0002, 0.002 and 0.02, will be used. Because primary resonance, superharmonic resonance of order two, and superharmonic resonance of order three

share the same modulation equations, as given in eqs (4.4.12)-(4.4.15), but with different values of coefficients, all of the above resonances have similar frequency-response curves. In the first case, the magnitude of the force is chosen to be equal to the weight of the beam and damping is assumed to be such that the logarithmic decrement is equal to 0.0002. Figures 5.11a and 5.11b show the frequency-response curves of in-plane and out-of-plane motions ($\hat{\varepsilon}a_1$ and $\hat{\varepsilon}b_1$ versus $\hat{\varepsilon}^2\sigma$), respectively. The forcing frequency is near one-half of the frequency of the first mode. The responses are similar to those in Figures 5.1a and 5.1b for primary resonance except the magnitudes of the amplitudes are different.

In Figure 5.12, damping is increased such that the logarithmic decrement is 0.002, while the force is kept equal to the weight of the beam. It is observed that the size of the unstable region decreases. Also, the jump phenomenon of the planar motion does not occur. If the forcing frequency is swept up from point A, the amplitude of the planar motion will grow until B is reached, where a nonplanar motion starts to develop. Whirling motion exists until point I is reached. Beyond I, there is no out-of-plane solution and the planar motion is stable. The amplitude jumps to I′ and the motion becomes planar again. As the forcing frequency is swept away from the region of resonance, the amplitude of the planar motion decreases gradually. On the contrary, if we sweep the frequency of excitation down from point F, the motion initially will be planar. When E is reached, out-of-plane motion develops suddenly with a jump from e to e′ but with only little change in the in-plane component. Whirling motion exists until point B is reached, where the amplitude of the out-of-plane motion becomes zero. The motion becomes planar and the amplitude decreases as the forcing frequency is swept away from the region of resonance.

If damping is increased so that the logarithmic decrement is equal to 0.02, and the force is kept equal to the weight of the beam, the damping will be too large for whirling motion to exist. The frequency-response curve for planar motion is shown in Figure 5.13. The effects of damping on superharmonic resonance of order two are the same as those for primary resonance.

Next, we investigate the influence of the magnitude of force on the frequency response. We decrease the force to half of the weight of the beam and put the logarithmic decrement equal to 0.0002, as in Figure 5.11. Under these conditions, whirling motion still exists. The

frequency-response curves, as shown in Figures 5.14a and 5.14b, are similar to those in Figures 5.1a and 5.1b, and Figures 5.11a and 5.11b except in the segment GH, where both in-plane and out-of-plane motions are unstable. The eigenvalues of the Jacobian matrix are two pairs of complex conjugate values with one positive real part. Hopf bifurcation theory predicts that the amplitudes and phases will modulate between G and H. In other words, this suggests that either limit cycles or chaotic motions may occur in this region.

If the magnitude of the force is further decreased to one-tenth of the weight of the beam and the logarithmic decrement is kept at 0.0002, as in Figure 5.11, the force will be too small to excite a whirling motion. Hence, only planar motion exists, as shown in Figure 5.15. The effects of the level of force on superharmonic resonance of order two are similar to those for primary resonance.

5.1.2.2 Frequency Response for a Superharmonic Resonance of Order Two of the Second Mode

For the same reason as stated for primary resonance, the force level chosen to excite a second mode of superharmonic resonance must be higher than that for a first mode. Hence, the force levels are chosen to be 5W, 2W and W. The response of the second mode is similar to that for primary resonance. The effects of the force and damping are also analogous to those for primary resonance. Figure 5.16 shows the frequency response when the force is 5W and the logarithmic decrement is 0.0002. The response curves are similar to those in Figure 5.6 except that the bifurcation points D and E are closer. Consequently, unlike Figure 5.6, both in-plane and out-of-plane motions are no longer all unstable when the frequency is between D and H. Instead, both stable in-plane and out-of-plane motions are possible in this region. Stable motions exist everywhere in this case. Figure 5.17 shows the result when the force is kept at 5W but the logarithmic decrement is increased to 0.002. The response curves are similar to those in Figure 5.9. When the logarithmic decrement

is further increased to 0.02, only planar motion exists, as shown in Figure 5.18. In Figure 5.19, the force is put at 2W but the logarithmic decrement is kept at 0.0002. It is noted that the decrease of the force level will cause the decrease of the size of the unstable region, DE. It turns out that the whirling motion will be less likely to happen when the forcing frequency is swept across this region. A special situation found in this resonance occurs when the force is equal to the weight and the damping is such that the logarithmic decrement is equal to 0.0002, as shown in Figures 5.20a and 5.20b. In this case, bifurcation points do not exist (the calculations of bifurcation points show no real solution of the bifurcation points). This means that the out-of-plane component does not grow from zero amplitude. If the nonplanar motion occurs, the out-of-plane amplitude may suddenly jump to a high amplitude. Numerical integration indicates that the whirling motion is very difficult to excite and may rarely be manifested for this case.

5.1.3.1 Frequency Response for a Superharmonic Resonance of Order Three of the First Mode

The frequency of excitation is near one-third of the frequency of the first mode. Whirling is less likely to occur in superharmonic resonance of order three than in superharmonic resonance of order two under the same level of force. The levels of force chosen in this resonance, 5W, W and 0.5W, are thus larger than those in superharmonic resonance of order two. Damping is assumed to be the same as in the previous resonances, in which the logarithmic decrements are 0.0002, 0.002 and 0.02.

Figures 5.21a and 5.21b show the frequency-response curves of in-plane and out-of-plane motions, respectively. The logarithmic decrement is equal to 0.0002, and the force is 5W. Essentially, the response is similar to those in Figures 5.1a and 5.1b, and Figures 5.11a and 5.11b except for the out-of-plane component. In this case, one of the vertical tangent points of the out-of-plane component, point G, moves outside of the envelope of the planar motion. Hence, at

point G when a jump occurs, there are two possibilities. The amplitude will either jump to G′, a planar motion, or jump to G″, another whirling motion, depending on the initial conditions. Similarly, when a jump occurs at point E, two choices are possible. The amplitude will either jump to point E′ or point E″ depending on the initial conditions. Both point E′ and point E″ correspond to nonplanar motions, but with different amplitudes. If we sweep up the forcing frequency from point A, there are two possible routes. The first is route A-B-G- G′-F. The second is route A-B-G-G″-I-F. There are also two possible routes, either route F-E-E′-H-H′-B-A or route F-E-E″-B-A, when the forcing frequency is swept down from point F.

In Figures 5.22a and 5.22b, the force is 5W and the logarithmic decrement is 0.002. As mentioned in the previous section, both primary resonance and superharmonic resonance of orders two and three have similar frequency-response curves. We note that the frequency-response curves in Figures 5.22a and 5.22b are similar to those in Figures 5.1a and 5.1b, and Figures 5.11a and 5.11b.

In Figure 5.23, the logarithmic decrement is equal to 0.02, but the force is kept at 5W. The response curves are similar to those in Figure 5.2 except that all out-of-plane motions are stable. It is observed that the amplitude decreases as the damping increases.

If the force is decreased to the weight of the beam and the logarithmic decrement is kept at 0.0002, the frequency-response curves, as shown in Figure 5.24, are similar to those in Figure 5.5 for primary resonance. Hopf bifurcation should also occur at points G and H.

If the force is further decreased to 0.5W and all other parameters are not changed from those in Figures 5.21a and 5.21b, the motion will be strictly planar. The frequency-response curve is shown in Figure 5.25.

5.1.3.2 Frequency Response for a Superharmonic Resonance of Order Three of the Second Mode

The effects of the force and damping on the second mode are similar to those for primary resonance. The results are shown in Figures 5.26a - 5.30. Because the unstable region DE on the upper branch of planar motion is small, the whirling motion is not likely to happen when the forcing frequency is swept across this region.

5.1.4.1 Frequency Response for a Subharmonic Resonance of Order Two of the First Mode

As mentioned earlier in Section 4.4.2, four types of steady-state solutions may exist in this resonance. In the first one, both the in-plane and out-of-plane components of the motion are zero, i.e., a trivial solution is possible for the homogeneous part in eqs (4.3.5) and (4.3.6). In other words, the resonance is not activated. It is noted that the particular solutions in eqs (4.3.5) and (4.3.6) are always nonzero if the force magnitude is nonzero. Thus the beam will vibrate in the in-plane direction with a frequency of excitation which is close to twice the natural frequency. In the second type, the in-plane component (the amplitude is denoted as a_p in the figures) exists but the out-of-plane component remains zero. The motion will be planar and thus have two frequencies, a frequency equal to half of the frequency of excitation and a frequency of excitation, which is close to twice the natural frequency. In the third case the in-plane component is zero, but the out-of-plane component (the amplitude is denoted as b_p in the figures) is nonzero. The beam will whirl in this situation. The frequency in the in-plane direction is equal to the forcing frequency, which is close to twice the natural frequency, and the frequency in the out-of-plane direction is equal to half of the forcing frequency. In the last type of steady-state solution, both in-plane and

out-of-plane components (in the figures, they are denoted as a_n and b_n, respectively) are nonzero. Whirling motion occurs in this case. In addition to having a frequency of excitation, which is close to twice the natural frequency, a second frequency of half of the forcing frequency is added to the in-plane motion. The frequency in the out-of-plane component of the motion is still equal to half of the forcing frequency.

From the solution for the in-plane motion, eq (4.4.31), we know that the magnitude of the force must exceed a minimum or critical value to activate the subharmonic resonance of order two. It is observed that the magnitude needed to excite the subharmonic resonance is much larger than that for a superharmonic resonance of order two. In contrast, the superharmonic resonance always exists. Thus the forces chosen here are 10W, 5W and W. Damping is still assumed to be light, and the corresponding logarithmic decrements are 0.0002, 0.002 and 0.02.

Figure 5.31 shows the frequency-response curves when the forcing frequency is near twice the natural frequency of the first mode. The magnitude of force used is 10W and damping is such that the logarithmic decrement is equal to 0.0002. For the first mode, the types two ($a_p \neq 0$) and three ($b_p \neq 0$) motions bend to the right. The nonlinear geometric terms dominate the response, and hence, the first mode is of the hardening type. In this case, the upper branch of the type two motion is stable and the lower branch is unstable, no matter what type of disturbance is applied. The upper branch of the type three motion is stable if subjected to an out-of-plane disturbance (note: the motion of b_p is in the out-of-plane direction). When subjected to an in-plane disturbance, the upper branch becomes unstable beyond point h, while the lower branch is always unstable, no matter what type of disturbance is applied. For the type four motion ($a_n \neq 0$ and $b_n \neq 0$), only segment LM is stable. We found that at least one of the eigenvalues of the Jacobian matrix in those unstable regions is a positive real number (the four eigenvalues are either four real numbers with two of them being positive or one complex conjugate pair with a negative real part and two real numbers with one being positive) except those between K and L, where they are two pairs of complex conjugate values with one positive real part. Thus, at K and L a Hopf bifurcation occurs, and it suggests the existence of either limit cycles or chaotic motions in between. For type one motion ($a_p = b_p = a_n = b_n = 0$), segment BC is unstable for the in-plane motion. But because the equations

for the in-plane and the out-of-plane motions are uncoupled in this type, segment BC is stable for the out-of-plane motion. Hence, the stabilities of the trivial solutions in two directions need not be consistent. Similarly, segment de is unstable for the out-of-plane motion, but is stable for the in-plane motion. When the forcing frequency is swept up from point A, the amplitudes of both in-plane and out-of-plane components initially will be zero, i.e., the solution is of type one-- trivial solution. But due to the existence of the particular solution, the motion will be planar. When B is reached, the amplitude of the in-plane component starts to grow but the amplitude of the out-of-plane component remains zero. The motion is planar of type two. The motion will remain planar until C′ is reached. After C′, the amplitude of the in-plane component will continue to increase (type two) or will drop to zero (type one). The type two motion is always possible after point B. But it is noted that the motion with a large amplitude at a large deviation from resonance frequencies is physically unrealistic, because a large amplitude will have destroyed the structure, and resonance is not supposed to occur everywhere. After point d, the trivial solution of the out-of-plane component becomes unstable, but that of the in-plane component is stable. Thus, whirling motion develops rapidly. The motion is of type three. Beyond K, the whirling motion becomes unstable until L is reached. Between K and e, only type two motion exists. Between e and N, the trivial solution becomes possible again in addition to type two motion. A whirling motion (type four), a trivial solution (type one) and a planar motion (type two) are possible after point L. When the frequency is swept across the resonance region, possible changes of the motion could be A-(1)-B-(2)-C-(1,2)-d-(2,3)-K-(2)-e-(1,2)-N-(1,2,4)-F, where the numbers inside brackets stand for the types. The type of the motion is determined by the initial conditions when there is more than one possible motion.

When damping is increased so that the logarithmic decrement is equal to 0.002, the frequency-response curves only change slightly, as shown in Figure 5.32. But if damping is further increased so that the logarithmic decrement is equal to 0.02, the resonance is not excited.

Next, the influence of the level of the force is examined. We decrease the magnitude of the force to 5W and keep the same damping as in Figure 5.31. The response curves, as shown in Figure 5.33, resemble those in Figure 5.31, except that the curves, a_p and b_p, come closer together.

If the magnitude of the force is decreased to W, the amplitude of type one motion, a_p, will move to the inside of that of type two motion, b_p. The response curves are shown in Figure 5.34. Besides, the upper branch of type one motion, BG, becomes unstable. The possible route could be A-(1)-d-(3)-C-(1,3)-L-(1,3,4)-F, when the forcing frequency is swept across the resonance region. When there is more than one possible motion, the type of motion is decided by the initial conditions. The effects of the level of force on subharmonic resonance of order two are as follows: (1) the curves of types two and three motions come closer together if the force level is decreased; (2) the type two curves will move to a higher frequency when the force is decreased, and if the force is small enough, the amplitudes of type two motion will move inside of that of type three motion; (3) the stable type four curves will not bifurcate from the other types of curves if the force is decreased to a certain value. In other words, it will be isolated, and hence, the type four motion is difficult to excite during passage through resonance region.

5.1.4.2 Frequency Response for a Subharmonic Resonance of Order Two of the Second Mode

There are also four possible solutions in the second mode, as those described in the first mode. The same force levels and damping coefficients are used as those for the first mode. The amplitudes of type two (a_p) and type three (b_p) motions bend to the left, because the nonlinear inertia terms dominate the response. For the second and higher modes, the responses are of the softening type. Figure 5.35 shows the response when the force is 10W and the logarithmic decrement is 0.0002. In this case, the upper branch of type two motion is stable if subjected to an in-plane disturbance. But, when an out-of-plane disturbance is applied, segment CK becomes unstable. The upper branch of type three motion is stable if subjected to an out-of-plane disturbance, while segment mj becomes unstable when an in-plane disturbance is applied (note: the type two motion is in the

out-of-plane direction). The lower branches of types two and three motions are stable, no matter what type of disturbance is applied. For the type four motion, branch KL is stable but branch MN is unstable. All of the unstable regions contain at least one eigenvalue of the Jacobian matrix with a positive real number. No Hopf bifurcation occurs in this case. A possible route, when the frequency is swept across the region of resonance, is A-(1,2)-B-(2)-k-(4)-M-(3,4)-e-(1,4)-F, where between points k and e, the motion is nonplanar only (either type three or four). The type of motion is decided by the initial conditions when more than one type of motion is possible.

When the damping is increased, the amplitudes of the type four motion (a_n and b_n) become smaller and bounded, as can be seen in Figure 5.36. Beyond point N, only the trivial solution is possible. When the logarithmic decrement is as large as 0.02, no resonance is excited.

When the force is decreased, the upper branch and the lower branch of both types two and three come closer. In addition, the curves of those two types also come closer. The response curves are shown in Figure 5.37. If the force is further decreased to be equal to the weight, as shown in Figure 5.38, the upper branch of type two motion will move to the left of the lower branch of type three motion. It turns out that type four motion no longer bifurcates from the type two motion. But, it still bifurcates from type three motion. Consequently, the eigenvalues of the Jacobian matrix in the unstable region KL become two pairs of complex conjugates with one positive and one negative real part. Hopf bifurcation occurs at points K and L, and this suggests that either limit cycles or chaotic motions may exist in this region. Besides, the amplitudes of type four motion come closer together, smaller and bounded. Possible routes are A-(1,2)-B-(2)-C-(1)-K-(1)-L-(1,4)-M-(1,3,4)-d-(3,4)-e-(1,4)-N-(1)-F, and the type of motion is decided by the initial conditions.

5.1.5.1 Frequency Response for a Subharmonic Resonance of Order Three of the First Mode

We use the same levels of force, 10W, 5W and W, as those in the subharmonic resonance of order two to investigate the frequency response in this section. Damping is the same as in the previous sections. As mentioned in Section 4.4.3, three possible solutions are the trivial, planar and nonplanar solutions. Trival and planar motions are always possible, no matter how large the damping and how small the force. This can be observed from the modulation equations, eqs (4.4.38)-(4.4.41), and the solution for the planar motion, eq (4.4.42).

In Figure 5.39 the frequency-response curves are given when the forcing frequency is near three times the natural frequency of the first mode. The magnitude of the force is 10W and the logarithmic decrement is 0.0002. For the first mode, the response curve bends to the right because nonlinear geometric terms dominate the response. Hence, the first mode is of hardening type. In this case, part of the upper branch of the planar motion, EF, is stable, no matter what type of disturbance is applied. The lower branch, BI, and part of the upper branch, BE, of the planar motion are unstable. For the nonplanar motion, only segment GH is stable. The eigenvalues of the Jacobian matrix of those unstable regions have at least one positive real number except along segment JG, where there are two pairs of complex conjugate eigenvalues, one with a positive and one with a negative real part. It is noted that point G is a Hopf-bifurcation point. This suggests that between points J and G, limit cycles and possibly chaotic motions exist. The possible routes are A-(1)-E-(1,2)-G-(1,2,3)-F, D or H when the forcing frequency is swept up from point A or swept down from point D (the numbers inside the brackets denote the type of motion). After point G, all three solutions are possible. But, because the amplitude of the branch, EF, is larger than 0.3, probably the motion above point E is physically unrealistic.

The response does not change much if the logarithmic decrement is increased to 0.002. The only obvious result is that the lowest point of the planar motion, B, and point C of nonplanar motion lift up a little, as can be seen in Figure 5.40.

If the logarithmic decrement is as large as 0.02, as shown in Figure 5.41, one branch of the nonplanar motion moves to the right, far away from the region of resonance and thus is not shown in Figure 5.41. Because of the large deviation of the forcing frequency from the resonance region, the motion probably is physically unrealistic and may not occur. Near the resonance region, the only stable solutions are the trivial solution and segment EF of the planar motion. The trivial solution is always possible. Possible routes are A-(1)-E-(1,2)-F or D as the frequency is swept up from point A or swept down from point D. But, because the amplitude of the stable planar motion, EF, is too large to be physically realistic, resonance is less likely to occur in this case.

Next, the effect of the level of the force is examined. In Figure 5.42, the force is decreased to 5W, but the logarithmic decrement is kept at 0.0002. Comparing Figures 5.42 and 5.39, we find that the upper and lower branches of the planar motion come closer together and become smaller. Basically, the frequency-response curves are similar in those two figures.

If the magnitude of the force is as small as W, as shown in Figure 5.43, the regions of both the planar and nonplanar motions will become narrow. Furthermore, part of the amplitude of the nonplanar motion moves inside the envelope of the planar motion, and more of the upper branch of the planar motion, EK, becomes unstable. For the nonplanar motion, only segments CG and HK are stable. The eigenvalues of the Jacobian matrix between points G and H are two pairs of complex conjugates, one with a positive and one with a negative real part. Points G and H are Hopf-bifurcation points, and hence, limit cycles and possibly chaotic motions exist in this region. When the forcing frequency is swept up or down through the resonance region, the possible routes are A-(1)-C-(1,3)-G-(1)-H-(1,3)-K-(1,2)-F or D.

5.1.5.2 Frequency Response for a Subharmonic Resonance of Order Three of the Second Mode

The same levels of force and damping as for the first mode are used for the second mode. The frequency-response curves for planar motion of the second mode bend to the left because the nonlinear inertial terms dominate the motion, and hence the second mode belongs to the softening type. The frequency response shown in Figure 5.44 is typical for this resonance. The different forces and dampings only change the size of the response curves; they still retain their shape. In Figure 5.44 the response is shown when the force is 10W and the logarithmic decrement is 0.0002. The upper branch of the planar motion, BJ, is stable when it is subjected to an in-plane disturbance. But segment DJ becomes unstable if an out-of-plane disturbance is applied. The nonplanar motion will bifurcate from point D, and this does occur. The lower branch of the planar motion is unstable, no matter what type of disturbance is applied. For the nonplanar motion, segments FG and GH are indistinguishable from each other, but their corresponding phases are quite different. Segment FG is stable, while segment GH is unstable. The size of loop I is too small to be recognized in Figure 5.44, but it is a stable nonplanar motion. The possible stable solutions are the trivial solution, planar motion (branch BD), and nonplanar motion (branch ED, branch GH, and loop I). Possible routes are A-(1)-E-(1,3)-D-(1,2)-B-(1)-G-(1,3)-H or C when the forcing frequency is swept across the region of resonance.

In Figure 5.45, the logarithmic decrement is increased to 0.002. The response curves are similar to those in Figure 5.44 except points B, K and G, where all three points lift up. Besides, the frequency at point K is lower, while that of point G is higher. When the damping is further increased so that the logarithmic decrement is 0.02, points B, K and G in Figure 5.46 move even higher and farther from the region of resonance than those in Figure 5.45 (point K is outside of Figure 5.46). The stable nonplanar motions exist in a large region. This is unreasonable and not likely to happen in the physical world, and it is suggested that only planar motion is possible when the logarithmic decrement is as large as 0.02. The same physically unrealistic phenomena happen

when the force is reduced to 5W and W, as can be seen in Figures 5.47 and 5.48, respectively. When the force is not large enough, nonplanar motion is not possible.

5.2 *Non-Stationary Solutions*

In this section, the non-stationary responses are investigated by integrating the modulation equations and the original differential equations. For primary resonance and superharmonic resonance of orders two and three, eqs (4.4.12) - (4.4.15) are used. For subharmonic resonance of order two, eqs (4.4.26) - (4.4.29) are used. For subharmonic resonance of order three, eqs (4.4.38) - (4.4.41) are used. In some cases, the time histories of the modal amplitudes are determined by numerical integration of the differential equations, eqs (3.35) and (3.36), and are compared with those from the modulation equations.

Various rates of sweep for both acceleration and deceleration will be examined. The effects of a persistent random disturbance, including the size of the disturbance, will be discussed. Also, the dependence of the maximum amplitudes on the sweep rate, damping coefficient and force magnitude will be discussed.

5.2.1.1 Frequency Response of a Primary Resonance of the First Mode

For the first mode of primary resonance, we choose Figure 5.4 to examine the passage through resonance region. The force used in Figure 5.4 is 0.0005W and damping is such that the logarithmic decrement is 0.0002. A linear variation of the forcing frequency is assumed, i.e., $\Omega = \Omega_0 + \lambda t$, where Ω_0 is the initial forcing frequency; λ stands for the rate of sweep. Three rates of sweep, 1.E-8, 1.E-7

and 1.E-6, are used for both acceleration and deceleration. The capital letter, E, stands for exponent of base ten. In Figures 5.49a - 5.49c, the responses are shown for sweep rates of 1.E-8, 1.E-7 and 1.E-6, respectively. The initial conditions are as follows: $\hat{\varepsilon}a_0 = 0.0001$, $\hat{\varepsilon}b_0 = \gamma_0 = \psi_0 = 0$. For a very small rate, e.g., 1.E-8, without any disturbance in the out-of-plane direction, the amplitude follows the planar steady-state solution. As the forcing frequency is swept up, the amplitude follows the route A-B-C-J′-F. After reaching the top point C, it jumps down suddenly to point J′.

In Figure 5.49b, the rate of sweep is increased to 1.E-7. As the forcing frequency is swept up, the amplitude of the motion still tends to follow the planar stationary solution. But before it can reach the top point C, a jump occurs. The amplitude jumps from point J to J′. If the rate of sweep is further increased to 1.E-6, as shown in Figure 5.49c, the amplitude does not follow the planar stationary response any more after it starts to increase. Instead, it grows to a certain maximum amplitude and then oscillates down to the steady-state value. The maximum amplitude occurs past the first natural frequency for all sweep rates because the first mode is of hardening type. The maximum amplitude of the acceleration is a function of the sweep rate, damping coefficient, force magnitude and initial conditions. Figure 5.50 shows the dependence of the maximum amplitudes of response on the sweep rates with three damping coefficients, corresponding to logarithmic decrements of 2.E-4, 4.E-4 and 2.E-2. It is observed that the maximum amplitude is approximately proportional to the inverse of the damping when the rate is small. This is because the non-stationary amplitude nearly coincides with the stationary amplitude, and the stationary amplitude has the proportional characteristic. When the rate is large, this proportional characteristic does not hold. In Figure 5.51, the maximum amplitude is given as a function of sweep rate for three force levels. It can be seen that the maximum amplitude is approximately proportional to the level of force except for the curve with force equal to 0.0005W around the sweep rate 2.5E-7.

Next, deceleration is examined. Figures 5.52a - 5.52c show the non-stationary responses with sweep rates -1.E-8, -1.E-7 and -1.E-6, respectively. When decelerating with a sweep rate equal to -1.E-8 without any disturbance in the out-of-plane direction, as shown in Figure 5.52a, the amplitude follows the planar stationary response until point E is reached. After the jump at E, it oscillates around J and then coincides with the planar stationary response again. In Figure 5.52b,

the rate is increased in magnitude to -1.E-7, and the amplitude leaves the stationary response earlier than it does in Figure 5.52a. An overshoot around the stationary response occurs. When the rate is further increased to -1.E-6, as shown in Figure 5.52c, the non-stationary response leaves the stationary response earlier than in the previous two cases. The amplitude grows to a certain maximum value and then oscillates down to zero gradually. The maximum amplitude of the deceleration is also a function of sweep rate, damping coefficient, force magnitude and initial conditions. The dependence of the maximum amplitude on the sweep rate is shown in Figure 5.53. The results for three logarithmic decrements, 2.E-4, 4.E-4 and 2.E-3, for damping are shown. Generally, the larger the damping, the smaller the maximum amplitude. Figure 5.54 shows the dependence of the maximum amplitude on the sweep rate for three force levels. The maximum amplitude is approximately proportional to the level of force when the rate of deceleration is large, e.g., -1.E-6. As the sweep rate is decreased in magnitude, the proportional characteristic vanishes.

The effects of disturbance on acceleration and deceleration are investigated next. The disturbance is assumed to be persistent, random and in both in-plane and out-of-plane directions. The size of the persistent random disturbance is limited within a small value, for example, 0.0001. The IMSL subroutine DRNUNF is manipulated to generate random numbers between -1 and 1, and then these random numbers are multiplied by 0.0001. Thus the lower and upper bounds of the persistent random disturbance are -0.0001 and 0.0001, respectively. The persistent random disturbance is included in the previous cases with the same initial conditions. Figures 5.55a, 5.55b and 5.55c show the non-stationary amplitudes of the in-plane component of the motion, the out-of-plane component of the motion and the total amplitude (square root of the amplitudes of in-plane and out-of-plane components), respectively. The sweep rate is equal to 1.E-8. Out-of-plane motion occurs wherever it is possible as predicted in the stationary response. The non-stationary motion coincides with the stationary amplitude except for the tip region of the nonplanar part around point I. It is concluded that the persistent random disturbance causes this early jump. The amplitude follows the route A-B-H-J-J′. It is observed when comparing Figure 5.55c with Figure 5.49a that the persistent random disturbance is beneficial to decrease the maximum amplitude when the sweep rate is small. When the persistent random disturbance is put in a motion with sweep rate

1.E-7, as shown in Figures 5.56a - 5.56c, the amplitude of the in-plane component tends to follow the stationary planar motion after point B is reached, while the out-of-plane component tends to remain zero. After a short penetration of the out-of-plane amplitude into the unstable zero-amplitude region, the motion becomes nonplanar. After a short fluctuation, the non-stationary amplitude follows the stationary nonplanar amplitude. The persistent random disturbance also has the benefit of decreasing the maximum amplitude under this situation. Figures 5.57a - 5.57c show the motion under the persistent random disturbances with a sweep rate equal to 1.E-6. Nonplanar motion occurs due to the disturbance. However, the amplitude of the motion in Figure 5.57c (square root of $(\hat{\varepsilon}a_1)^2 + (\hat{\varepsilon}b_1)^2$) shows a similar response to that in Figure 5.49c, which is planar without persistent random disturbance. It implies that the effect of the persistent random disturbance on the maximum amplitude is insignificant when the rate of sweep is as large as 1.E-6.

Figure 5.58 shows the dependence of the maximum amplitude on the sweep rate of acceleration for three situations. One is with only an initial disturbance in the in-plane direction. In other words, the initial conditions are $\hat{\varepsilon}a_0 = 0.0001$, $\hat{\varepsilon}b_0 = \gamma_0 = \psi_0 = 0$. The second is also without disturbance but with initial conditions $\hat{\varepsilon}a_0 = \hat{\varepsilon}b_0 = 0.0001$, $\gamma_0 = \psi_0 = 0$. The third is with a persistent random disturbance limited within a bound of 0.0001. In the second situation, because an initial disturbance exists in the out-of-plane direction and damping is small (where the logarithmic decrement is 0.0002), nonplanar motion becomes possible when the sweep rate is smaller than a critical rate. In this situation, the critical rate is approximate by 5.2E-7. But this does not imply that the nonplanar motion will always exist when the sweep rate is below the critical rate. The results show the possibility of planar motion below the critical rate; for instance, at rate 4.9E-7 the amplitude of the second situation coincides with that of the first situation, which is strictly planar. It is concluded that below the critical rate both planar and nonplanar motions are possible when an initial disturbance is applied. When the rate is above the critical rate, only planar motion is possible if there is only an initial disturbance.

When a persistent random disturbance is applied, as in the third situation, nonplanar motion is always possible below the critical rate. But the amplitude of the nonplanar motion does not always remain on the branch HI in Figure 5.55a. At some rates, nonplanar motion exists in a form

similar to that shown in Figure 5.57. For instance, Figure 5.59 shows the amplitude response at rate 8.5E-7; the amplitude does not follow the branch HI. Because only one sequence of random numbers is used to produce the above result, it is believed that the amplitude may follow the branch HI at the same rate if another sequence of random numbers is used. Figure 5.60 shows the result with a different sequence of random numbers. The amplitude does follow the branch HI with this sequence. The critical rate depends on the size of the persistent random disturbance. Figure 5.61 shows the dependence of the maximum amplitude on the sweep rate and the size of the persistent random disturbance. The sizes of disturbance used are 1.E-5, 1.E-4 and 1.E-3, and the critical rates are approximately 7.8E-7, 9.E-7 and above 1.E-6, respectively.

Figures 5.62a - 5.64c show the responses when the frequency is decreased and there is a small persistent random disturbance, with rates -1.E-8, -1.E-7 and -1.E-6, respectively. When the rate is -1.E-8, as shown in Figures 5.62a - 5.62c, the non-stationary amplitude closely follows the stationary route F-E-H-B-A. Comparing Figure 5.62c with Figure 5.52a, we find that the persistent random disturbance decreases the amplitude in this case. Because instead of a jump from point E to J, as that in Figure 5.52a, the amplitude of the in-plane component follows the nonplanar motion, route E-H-B. The disturbance also has the benefit of decreasing the amplitude when the sweep rate is -1.E-7, as one can see by comparing Figures 5.63c and 5.52b. But when the sweep rate is as large as -1.E-6, as shown in Figures 5.64a - 5.64c, the effect of such a small persistent random disturbance is insignificant. The disturbance causes nonplanar motion and decreases the in-plane amplitude a little. But the total amplitude is similar to that in Figure 5.52c. It is concluded that the effect of this disturbance on the amplitude is more significant for a small sweep rate.

Figure 5.65 shows the maximum amplitude versus the sweep rate of deceleration for three situations: (1) initial disturbance with size 0.0001 in the in-plane direction only ($\hat{\varepsilon}a_0 = 0.0001$); (2) initial disturbance with size 0.0001 in both in-plane and out-of-plane directions ($\hat{\varepsilon}a_0 = \hat{\varepsilon}b_0 = 0.0001$); (3) a persistent random disturbance with bound 0.0001. The amplitude of the second situation coincides with that of the first situation because the damping, in which the logarithmic decrement is equal to 2.E-3, is relatively large so that the initial disturbance decays immediately. Also, it is almost not possible to reach branch HI in Figure 5.55a, no matter how large

the disturbance is. Hence, the effect of initial disturbance in the out-of-plane direction is not significant. In the third situation, the persistent random disturbance causes the amplitude to tend to follow the nonplanar route E-H-B in Figure 5.55a after point E is reached when the sweep rate is small. Figure 5.66 shows the effect of the size of the persistent random disturbance on the maximum amplitude. All amplitudes with persistent random disturbances are below those with only an initial disturbance except at a few points, where it is believed that the random sequence causes an exception. It can be concluded that the persistent random disturbance tends to decrease the maximum amplitude in the deceleration of the first mode of primary resonance by changing the motion from a planar motion to a nonplanar one. In the planar motion, a jump phenomenon causes a larger amplitude than the nonplanar motion does, in which a small amplitude occurs.

5.2.1.2 Frequency Response of a Primary Resonance of the Second Mode

For the second mode, Figure 5.7 is chosen to examine the passage through resonance region. The same parameters as used for the first mode are varied. Because the second mode is of a softening type, deceleration might cause a larger amplitude than acceleration when the sweep rate is small. Deceleration is examined first. In Figures 5.67a - 5.67c the amplitude response is shown for the rates -1.E-6, -1.E-5 and -1.E-4, respectively. The initial conditions are zero for $\hat{\varepsilon}b_0$, γ_0 and ψ_0 while $\hat{\varepsilon}a_0$ is 0.0001. There is no disturbance in both in-plane and out-of-plane directions.

Without a disturbance, the amplitude follows the planar stationary response very closely under a small sweep rate, e.g., -1.E-6 (Figure 5.67a). A jump occurs when the top point C is reached. When the sweep rate is decreased to -1.E-5 (Figure 5.67b), before the amplitude can reach the top point C, it jumps down, When the rate is further decreased to -1.E-4 (Figure 5.67c), it is too fast to remain on the planar stationary response. After reaching a certain maximum value, the amplitude oscillates down to a small value. The maximum amplitude occurs at frequencies lower than the

second natural frequency for all sweep rates because of the softening characteristic. The dependence of the maximum amplitude on the sweep rate is shown in Figures 5.68 and 5.69 for various damping coefficients and force magnitudes, respectively. Three logarithmic decrements, 1.E-3, 2.E-3 and 5.E-3, for damping are chosen in Figure 5.68. For the steady-state response, the maximum amplitude of the planar motion is approximately proportional to the inverse of the damping. The non-stationary amplitude coincides with that of the stationary one when the sweep rate is small (for example, the response shown in Figure 5.67a with a small rate -1.E-6). When the sweep rate is large, the non-stationary amplitude does not follow the branch FC in Figure 5.67a; for instance, the response with a large rate, -1.E-4, is shown in Figure 5.67c. Thus, the proportional characteristic does not hold when the sweep rate is large. But in general, the larger the damping, the smaller the maximum amplitude. In Figure 5.69, three force magnitudes, 0.005W, 0.01W and 0.02W, are used. The proportional characteristic still holds when the sweep rate is small. Generally, the larger the level of force, the larger the maximum amplitude when the sweep rate is large.

The same rates as used in the deceleration but with positive sign will be used to investigate the acceleration. The rates used in Figures 5.70a - 5.70c are 1.E-6, 1.E-5 and 1.E-4, respectively. When the rate is 1.E-6 (Figure5.70a), the non-stationary response coincides with the stationary planar response if there is no disturbance in the out-of-plane direction except after a jump at the vertical tangent point, point B. After the jump the amplitude fluctuates a short while and then returns to the stationary planar response. When the sweep rate is increased to 1.E-5 (Figure 5.70b), the non-stationary response leaves the stationary response earlier than point B. Overshoot around the stationary response occurs. After the rate is increased to 1.E-4 (Figure 5.70c), overshoot around the stationary response does not occur. Instead, the amplitude oscillates down after reaching a certain maximum value. It is seen that the faster the sweep rate, the greater the shift of the maximum amplitude to a higher frequency. In Figure 5.71 the dependence of the maximum amplitude on the sweep rate is shown for three damping coefficients. It can be seen that the larger the damping, the smaller the maximum amplitude. Figure 5.72 shows the maximum amplitude versus sweep rate under three force levels, 0.005W, 0.01W and 0.02W. In general, the larger the level of the force, the larger the maximum amplitude.

Next, the effects of a disturbance are studied. The disturbance is also assumed to be persistent, random and in both in-plane and out-of-plane directions, as used in the first mode. In Figures 5.73a - 5.75c the non-stationary responses under a persistent random disturbance with a bound equal to 0.0001 are shown. The sweep rates used in Figures 5.73 - 5.75 are -1.E-6, -1.E-5 and -1.E-4, respectively. When the rate is small, the non-stationary amplitude tends to follow the stationary planar amplitude (the branch FC in Figure 5.67a). But in segment ED, the planar motion is unstable. Nonplanar motion grows after a short penetration of the unstable zero-amplitude region in Figure 5.67a, segment DE. After point D is reached, motion again tends to follow the planar motion. The disturbance causes the fluctuation, but basically the trend is as described above. When the rate is as small as -1.E-5 or even -1.E-4, as shown in Figures 5.74 and 5.75, nonplanar motion can only be produced by the persistent random disturbance.

In Figure 5.76 the maximum amplitude is shown as a function of the sweep rate for the same three situations represented in Figures 5.58 and 5.65. The amplitude of the second situation coincides with that of the first situation because of the same reasons as described for Figure 5.65. In the third situation, the persistent random disturbance is beneficial in decreasing the maximum amplitude when the sweep rate is small except at a few points, where it is concluded that the persistent random disturbance causes an exception. In Figure 5.77, three bounds of persistent random disturbance, 1.E-3, 1.E-4 and 1.E-5, are used. When the size of the disturbance is small, e.g., 1.E-5, the maximum amplitude is dominated by the planar motion. But when the disturbance is large, the maximum amplitude is dominated by the disturbance. In general, the disturbance does not have the benefit of decreasing the maximum amplitude in the deceleration of the second mode. This can be seen from Figure 5.77. But, when the sweep rate is small, sometimes the disturbance may break the tendency of following the branch FC in Figure 5.7. The maximum amplitude may be decreased when this occurs.

In Figures 5.78a - 5.80c the effect of the disturbance on the acceleration cases is shown. A small persistent random sequence of disturbances with bound 0.0001 is included in Figures 5.78a - 5.80c to examine the effect of the disturbance. It is found that the disturbance causes the same effect as it does in the deceleration cases. When the rate is small, the disturbance may cause nonplanar

motion. This depends on the random sequence and does not always occur. In Figure 5.81, three situations, as those used in Figure 5.76, are chosen. The effect of various disturbances is insignificant. In Figure 5.82, three bounds of disturbance are chosen. The effect of the size of the disturbance is the same as for deceleration.

5.2.2.1 Frequency Response of a Superharmonic Resonance of Order Two of the First Mode

Figure 5.14 is chosen to investigate the passage through the resonance region for superharmonic resonance of order two of the first mode. The force used in this case is 0.5W and the logarithmic decrement for damping is 0.0002. The forcing frequency is also assumed to be varied linearly, as was the case in primary resonance. Three sweep rates, 1.E-8, 1.E-7 and 1.E-6, are chosen for acceleration. The initial conditions are zero for $\hat{\varepsilon}b_0$, γ_0 and ψ_0, and $\hat{\varepsilon}a_0$ is equal to 0.0001 initially. Without any disturbance in the out-of-plane direction, the amplitude follows the planar steady-state solution closely when the sweep rate is as small as 1.E-8. As the frequency is swept up, the amplitude follows the route A-B-J-J′-F in Figure 5.83a. A jump occurs before the amplitude reaches the tip at point C. The jump will occur closer to point C when the sweep rate is smaller. After a short fluctuation around point J′, the amplitude settles down and nearly coincides with the planar steady-state motion again.

In Figure 5.83b the response is shown when the sweep rate is 1.E-7. Instead of following the planar motion closely, the amplitude deviates from the planar steady-state motion before point B is reached. It reaches a certain maximum amplitude and then oscillates down to a steady-state value. If the sweep rate is increased to 1.E-6, as is the case in Figure 5.83c, the amplitude leaves the planar steady-state motion earlier than in the previous figure. Furthermore, the amplitude no longer follows the planar stationary amplitude after it starts to grow. The maximum amplitude occurs past

twice the first natural frequency because of the hardening characteristic of the first mode. The maximum amplitude depends on the sweep rate, damping coefficient, force level and initial conditions.

Three rates, -1.E-8, -1.E-7 and -1.E-6, are chosen to examine the response for deceleration. In Figure 5.84a the sweep rate is -1.E-8. The amplitude follows the stationary planar response closely until point D is reached where a jump to the upper branch, which is stable when no out-of-plane disturbance is present, occurs. After reaching its maximum amplitude, the response exhibits a few oscillations and then coincides with the stationary planar motion again, because no out-of-plane disturbance is present. When the sweep rate is decreased to -1.E-7, as one can see in Figure 5.84b, the amplitude leaves the steady-state planar motion before point D is reached. After reaching a maximum value, it oscillates down with a large overshoot to a steady-state value. If the sweep rate is further decreased to -1.E-6, as can be seen in Figure 5.84c, the amplitude deviates from the stationary planar response earlier than it does in the previous two cases. It grows to a maximum value and then oscillates down to a steady-state value slowly. The maximum amplitude is also a function of sweep rate, damping coefficient, force magnitude and initial conditions.

Next, the effects of a continuous disturbance on acceleration and deceleration are examined. The disturbance is again assumed to be persistent, random and in both in-plane and out-of-plane directions. The bound of the persistent random disturbance is set at 0.0001. The persistent random disturbance is added to the previous cases with the same initial conditions. In Figure 5.85, the non-stationary response is shown when the sweep rate is 1.E-8. The non-stationary amplitude closely follows the stationary response initially. After point B is reached, the amplitude of the in-plane component tends to stay on the planar motion, while the out-of-plane amplitude tends to remain zero, for a short time. After a short penetration of the in-plane motion into the unstable zone, the motion becomes nonplanar. The motion continues to be nonplanar until point J is reached, where the jump occurs. The motion becomes planar with a small amplitude after point J′. It is believed that the motion could reach closer to tip point I if another sequence of random disturbances were used. It can be seen by comparing Figures 5.85 and 5.83a that the persistent random disturbance is beneficial to decrease the maximum amplitude when the sweep rate is as

small as 1.E-8, because the nonplanar motion avoids the large growth of the planar motion shown in Figure 5.83a.

When the sweep rate is increased to 1.E-7, as can be seen in Figure 5.86, the non-stationary planar motion penetrates the unstable region deeper than it does in Figure 5.85. After a short fluctuation, the amplitude closely follows the nonplanar motion until J is reached. After a jump from J to J′, the motion becomes planar again. In Figure 5.87, the results are shown when the sweep rate is increased to 1.E-6. The non-stationary amplitude is similar to that without the persistent random disturbance shown in Figure 5.83c, except the out-of-plane component of the motion is now excited. But the out-of-plane component only grows a little. The change of the maximum amplitude by the persistent random disturbance is insignificant in this case.

In Figure 5.88, the results for the deceleration subjected to a persistent random disturbance when the sweep rate is equal to -1.E-8 are plotted. The non-stationary amplitude follows the route F-E-H-B-A closely, as predicted by the stationary result, except that the amplitude oscillates after a jump from point e to e′ in part (b) when nonplanar motion begins to grow. The persistent random disturbance has the benefit of decreasing the maximum amplitude in this case because the nonplanar motion eliminates the big increase of the planar motion in Figure 5.84a. When the sweep rate is decreased to -1.E-7, as shown in Figure 5.89, the non-stationary amplitude leaves the stationary planar response earlier than it does in the previous case, and the out-of-plane component of the motion penetrates the unstable zero-amplitude region a short distance. After point B, the motion becomes planar gradually. In Figure 5.90, the sweep rate is decreased to -1.E-6. The persistent random disturbance causes the non-stationary amplitude to fluctuate around the stationary one before it grows. After the non-stationary amplitude grows, it shows a similar response to that in Figure 5.84c. It is noted that the change of the maximum amplitude is insignificant in this case when the persistent random disturbance is applied.

5.2.2.2 Frequency Response of a Superharmonic Resonance of Order Two of the Second Mode

Figure 5.17 is chosen to investigate the passage through resonance region for a superharmonic resonance of order two of the second mode. The force used in Figure 5.17 is 5W and the logarithmic decrement is 0.002 for damping. Because of the softening characteristics of the second mode, deceleration might cause a larger amplitude than acceleration does when the sweep rate is small. The deceleration is examined first. Three rates of sweep, -1.E-6, -1.E-5 and -1.E-4, are chosen for the cases of deceleration. The results are shown in Figures 5.91a, 5.91b and 5.91c, respectively. The initial conditions are the same as those used in the first mode. No persistent disturbance is applied in these cases.

In Figure 5.91a, the non-stationary response is shown when the sweep rate is -1.E-6. The non-stationary amplitude very nearly coincides with the stationary planar response. It follows the route F-E-D-C-A. A jump occurs at point C.

When the sweep rate is decreased to -1.E-5, as shown in Figure 5.91b, the non-stationary amplitude still follows the stationary planar response closely, but just before it reaches the tip point C, a jump occurs. If the sweep rate is further decreased to -1.E-4, the non-stationary amplitude no longer follows the stationary amplitude after it starts to grow. As one can see in Figure 5.91c, the non-stationary amplitude grows to a much smaller maximum value and then oscillates down to a small steady-state value. The maximum amplitude is a function of sweep rate, damping coefficient, force level and initial conditions.

The non-stationary responses for the cases of acceleration are examined next. In Figures 5.92a, 5.92b and 5.92c, the amplitudes of the responses are given for the sweep rates 1.E-6, 1.E-5 and 1.E-4, respectively. When the sweep rate is as small as 1.E-6, as one can see in Figure 5.92a, the non-stationary amplitude follows the route A-B-D-E-F closely except there is a jump at point B. After the jump, the non-stationary amplitude oscillates for a short while and then very nearly coincides with the stationary planar motion again. In Figure 5.92b, the sweep rate is increased to

1.E-5. The non-stationary amplitude leaves the stationary planar response before point B is reached. It grows to a certain maximum value and then oscillates down with a big overshoot to a small steady-state value. When the sweep rate is as large as -1.E-4, as shown in Figure 5.92c, the non-stationary amplitude deviates considerably from the stationary planar response after it grows. After reaching the maximum value, the non-stationary amplitude oscillates down slowly to a small steady-state value. The maximum amplitude also depends on sweep rate, damping coefficient, force magnitude and initial conditions.

The persistent random disturbances in both in-plane and out-of-plane directions are added to the previous cases to investigate their effect on the response. The bound of the persistent random disturbance is again set at 0.0001, and the initial conditions are the same as in the previous cases. In Figure 5.93, the amplitude of the non-stationary response is shown when the sweep rate is -1.E-6. The non-stationary amplitude fluctuates around the stationary planar curve before point E is reached. After the out-of-plane component of the motion jumps from e to e′, nonplanar motion is activated. The motion remains nonplanar until point g is reached, where the out-of-plane amplitude jumps down to a small value and the motion becomes essentially planar again. Below point G, nonplanar motion is essentially not active. The non-stationary amplitude follows the stationary planar response closely and grows to point J. After a jump from J to J′, the non-stationary amplitude becomes small. It is noted by comparing Figures 5.91a and 5.93 that the persistent random disturbance causes the non-stationary amplitude to jump earlier (before point C is reached) in this case. The jump might occur earlier or later depending on the random sequence. In general, the persistent random disturbance is beneficial to decrease the maximum amplitude when the sweep rate is as small as -1.E-6.

In Figure 5.94, the sweep rate is decreased to -1.E-5. The non-stationary amplitude follows the stationary planar response completely. Between points E and D, the stationary planar response is unstable, but the sweep rate is so fast that the nonplanar motion is not excited. After a jump from J to J′, the non-stationary amplitude becomes small. In this case, as one can see by comparing Figures 5.91b and 5.94, the persistent random disturbance is also beneficial to decrease the maximum amplitude. When the sweep rate is decreased to -1.E-4, as shown in Figure 5.95, the

non-stationary amplitude does not follow the stationary response after it starts to grow. After the in-plane component of the non-stationary motion reaches a certain maximum value, it oscillates down slowly to a small steady-state value. The out-of-plane resonance is not activated to a significant extent in this case. The change of the maximum amplitude due to the persistent random disturbance is insignificant when the sweep rate is as fast as -1.E-4, but it does change the shape of the non-stationary response slighily.

Next, the persistent random disturbance is added to the simulations shown above in Figures 5.92a - 5.92c. In Figure 5.96 the non-stationary response is shown when the sweep rate is 1.E-6. The amplitude of the non-stationary motion closely follows that of the stationary planar motion initially. After point D is reached, the nonplanar motion is activated. The non-stationary amplitude grows to point I and then jumps down to a small value, and thereafter the out-of-plane resonance of the non-stationary motion is no longer excited. It can be seen by comparing Figures 5.92a and 5.96 that the persistent random disturbance will increase the maximum amplitude when the sweep rate is as small as 1.E-6. In Figure 5.97, the sweep rate is increased to 1.E-5. The non-stationary response is similar to that without the persistent random disturbance in Figure 5.92b. The out-of-plane motion is not excited because the sweep rate is too fast and the unstable planar region is too narrow. In this case, the effect of the persistent random disturbance on the maximum amplitude is not significant. In Figure 5.98, the amplitude of the non-stationary response is given when the sweep rate is 1.E-4. The non-stationary response is similar to that in Figure 5.92c. The effect of the persistent random disturbance on the maximum amplitude is also not significant in this case, though it does change the shape of the response curve slightly.

5.3 Comparisons Between Results From the MMS and the Original Differential Equations

In this section, the time histories of the modal amplitudes are determined by numerical integration of the original differential equations, eqs (3.35) and (3.36), and are compared with those determined by the integration of the modulation equations. The cases chosen to be compared are those for which the same initial conditions can be used in both methods. For those cases with the persistent random disturbance, it is not possible to have exactly the same disturbance procedure in both methods. Because the result from the integration of the modulation equations describes the envelope of the time history of the modal amplitude, which is obtained from the integration of the original differential equations, adding the persistent random disturbance to the envelope is not equal to adding it to the actual amplitude, even if the rates of the persistent random disturbance are equal. Hence, consistent results from both methods are not expected. But the history of the modal amplitude with the persistent random disturbance still will be shown. Also, the case with initial disturbances in both in-plane and out-of-plane directions will be compared. For this case, the same initial conditions can be used for both methods. The first one is the case with only an initial disturbance in the in-plane direction, i.e., $\hat{\varepsilon}a_0 = 0.0001$, $\hat{\varepsilon}b_0 = \gamma_0 = \psi_0 = 0$.

5.3.1 Comparisons for Primary Resonance of the First Mode

For primary resonance, we first examine the case with only an initial disturbance in the in-plane direction when the sweep rate is 1.E-6. In Figure 5.99a the history of the modal amplitude is given. The diagram is shaded because of the slow change of the frequency. There are numerous points plotted in this diagram. It can be seen that the outline of the amplitude is similar to that from

the MMS (Method of Multiple Scales) in Figure 5.49c. In Figure 5.99b, the absolute peak values of the modal amplitude are plotted along with both stationary and non-stationary amplitudes from the MMS. The non-stationary results from both methods are overlayed and indistinguishable from each other. This shows very good agreement between the results. In Figure 5.100a, the history of the modal amplitude is given for the sweep rate 1.E-7, and the initial conditions are the same as in the previous case. Comparing the results from the two methods, as shown in Figure 5.100b, one can see the good agreement between the results.

In Figure 5.101a, the history of the modal amplitude for deceleration is shown when the sweep rate is -1.E-6. The absolute peak values of the modal amplitude are shown in Figure 5.101b along with stationary and non-stationary amplitudes from the MMS. As one can see in Figure 5.101b, the results from both methods again show very good agreement. When the sweep rate is increased to -1.E-7, as one can see in Figure 5.102, the results from both methods are also consistent. It can be concluded that the MMS works well for the first mode of primary resonance when there is only an in-plane initial disturbance applied.

Next, the results with both in-plane and out-of-plane initial disturbances are compared. Figures 5.103a and 5.103b show histories of the modal amplitude in the in-plane and out-of-plane directions, respectively. The rate of sweep is 1.E-6, and the initial conditions are $\hat{\varepsilon}a_0 = \hat{\varepsilon}b_0 = 0.0001$ and $\gamma_0 = \psi_0 = 0$. In this case, a noticeable motion in the out-of-plane direction is activated by the introduction of the out-of-plane initial disturbance. Comparing the outlines of the above modal amplitudes with the results from the MMS (as shown in Figures 5.103c and 5.103d), one can see that those results are similar. The maximum amplitude in the in-plane direction predicted by the original differential equations is 0.03767 at $\hat{\varepsilon}^2\sigma = 0.00457$, while that predicted by the MMS is 0.03802 at $\hat{\varepsilon}^2\sigma = 0.00460$. The maximum amplitude in the out-of-plane direction predicted by the original differential equations is 0.01817 at $\hat{\varepsilon}^2\sigma = 0.00818$, while that predicted by the MMS is 0.01477 at $\hat{\varepsilon}^2\sigma = 0.00933$. The result from the MMS in this case is less accurate than that in the case with only initial in-plane disturbance. In Figures 5.104a and 5.104b, the histories of modal amplitudes in the in-plane and out-of-plane directions are given, respectively, when the sweep rate is decreased to 1.E-7. The results from the MMS are shown in Figures 5.104c

and 5.104d. In this case, the modal amplitudes follow the branch HI (hi) in Figure 5.104c (5.104d) and grow to large amplitudes. From the comparisons between Figures 5.104a (5.104b) and 5.104c (5.104d), one can see that the results from the MMS come close to those from the integration of the original differential equations except at points J and I in Figure 5.104c. The results from the MMS underestimate the amplitudes in the out-of-plane direction at point J. The amplitude at point J predicted by the integration of the original differential equations is 0.06192 at $\hat{\varepsilon}^2\sigma = 0.00331$, while that from the MMS is 0.05129 at $\hat{\varepsilon}^2\sigma = 0.00340$. At point I, the actual modal amplitude jumps down earlier than MMS predicts. Although those differences exist, it still can be concluded that the MMS works well for primary resonance when both in-plane and out-of-plane initial disturbances are applied.

In Figures 5.105a and 5.105b, the histories of modal amplitudes in the in-plane and the out-of-plane directions are shown, respectively. The sweep rate of acceleration is 1.E-6 and the persistent random disturbances are added to both directions. In order to match the rate of the persistent random disturbance used in the MMS, which is 100 times per T_1 second (the slow time scale, which is equal to $\hat{\varepsilon}^2 t$), the rate for the integration of the original differential equations is set to 1 time per 100 second. The bound of the disturbance is set to 0.0001. Comparing Figure 5.105a (5.105b) with Figure 5.57a (5.57b), one can see that the outline of the modal amplitude in the former figure does not agree with the latter. The maximum amplitude in the in-plane direction is overestimated by the MMS, while that in the out-of-plane direction is underestimated by the MMS. The maximum amplitude in the in-plane direction in Figure 5.105a is 0.03691 and that in Figure 5.57a is 0.03813. The maximum amplitude in the out-of-plane direction in Figure 5.105b is 0.03258 and that in Figure 5.57b is 0.02637. The effect of the persistent random disturbance is obvious in this case, as can be seen by comparing Figures 5.105a (5.105b) and 5.103a (5.103b). The persistent random disturbance not only changes the shape of the modal amplitudes but also increases the amplitude in the out-of-plane direction significantly. The maximum amplitude in the out-of-plane direction in Figure 5.103b is 0.01817, which is much smaller than that in Figure 5.105b.

Figures 5.106a and 5.106b show the actual modal amplitudes in the in-plane and the out-of-plane directions, respectively. The sweep rate of deceleration is -1.E-6 and the rate and the

bound of the persistent random disturbance are the same as used in Figure 5.105. Although the same results from both methods are not expected, similar outlines were obtained.

5.3.2 Comparisons for Superharmonic Resonance of Order Two of the First Mode

For superharmonic resonance of order two, as described earlier in Section 4.3, the first-order solution of the modal amplitude can be approximated by combining the homogeneous part and the particular part. The result from the MMS shown in Section 5.2 is only the solution of the homogeneous part. In order to compare with the result from the integration of the original differential equations, the modal amplitude must be reconstructed by adding the homogeneous and particular parts.

In Figure 5.107a, the history of the modal amplitude from the integration of the original differential equations is shown. The sweep rate of acceleration is 1.E-6, and the initial conditions are $\hat{\varepsilon}a_0 = 0.0001$ and $\hat{\varepsilon}b_0 = \gamma_0 = \psi_0 = 0$. There is no other disturbance applied in this case. In Figure 5.107b, the reconstructed modal amplitude from the result of MMS is given. The sweep rate and initial conditions are the same as those in Figure 5.107a. As one can see by comparing Figures 5.107a and 5.107b, the result from the MMS predicts the modal amplitude in this case very well. Figures 5.108a and 5.108b show the modal amplitudes from the original differential equations and the reconstruction of the amplitude from the MMS, respectively, when the sweep rate is 1.E-7 and the same initial conditions as in the previous case are used. They again are in very good agreement with each other. In Figures 5.109a and 5.109b, the actual modal amplitude from the original differential equations and the reconstructed modal amplitude from the MMS are given, respectively, when the sweep rate of deceleration is -1.E-6 and the initial conditions are the same as in the previous two cases. In this case of deceleration, the results again show very good consistency. When

the sweep rate is increased to -1.E-7, as can be seen in Figures 5.110a and 5.110b, the results from the two methods again are in very good agreement. It can be concluded that the MMS works well when only an initial in-plane disturbance is applied.

Next, the results with both in-plane and out-of-plane initial disturbances are examined. The magnitude of the initial disturbance is 0.0001. The sweep rate used in Figure 5.111 is 1.E-6. In Figures 5.111a and 5.111b the histories of the modal amplitudes for the in-plane and the out-of-plane directions are given, respectively. Comparing with Figures 5.111c and 5.111d, which are the reconstructed modal amplitudes from the results of MMS, one can see that there is good consistency in the in-plane components of the motion. The out-of-plane components of the motion are not consistent, but, in comparison with the amplitude in the in-plane direction, the difference between these two components is relatively small. When the sweep rate is decreased to 1.E-7, as can be seen in Figures 5.112a and 5.112b, the modal amplitudes follow the branch HI (hi) in Figure 5.85a (5.85b) after they penetrate the unstable planar region. But the amplitudes from the MMS in Figures 5.112c - 5.112d show different results. The results from the MMS predict the amplitude closely until the detuning, $\hat{\varepsilon}^2\sigma$, is around 0.004. Thereafter, the amplitude does not grow to a large value. The reason for this difference could be the sensitivity of the MMS to the initial conditions. Due to the particular part involved in the MMS, the exact initial conditions for the original differential equations are hard to match with those for the MMS.

Next, the motion subjected to the persistent random disturbance is examined. In Figures 5.113a and 5.113b, the modal amplitudes in the in-plane and out-of-plane directions are shown, respectively. The sweep rate is 1.E-6, and the rate of the persistent random disturbance is 1 time per 100 seconds. Comparing Figures 5.113a and 5.113b with Figures 5.87a and 5.87b, one can see that the maximum amplitude in the out-of-plane direction is overestimated by the MMS. The maximum amplitude in the out-of-plane direction from the MMS is 0.005010 at $\hat{\varepsilon}^2\sigma = 0.01298$, but that from the integration of the original differential equations is 0.0018254 at $\hat{\varepsilon}^2\sigma = 0.01380$. But because the amplitude in the out-of-plane is relatively small compared with that in the in-plane direction, the difference is insignificant.

The deceleration with the persistent random disturbance is examined next. Figures 5.114a and 5.114b show the modal amplitudes in the in-plane and out-of-plane directions, respectively. The MMs results again overestimate the maximum amplitudes in the out-of-plane directions. In other words, the MMS overestimates the effect of the persistent random disturbance. The maximum amplitude in the out-of-plane direction from the MMS is 0.003926 at $\hat{\varepsilon}^2\sigma = -0.0068$, but that from the integration of the original differential equations is 0.001850 at $\hat{\varepsilon}^2\sigma = -0.0084$.

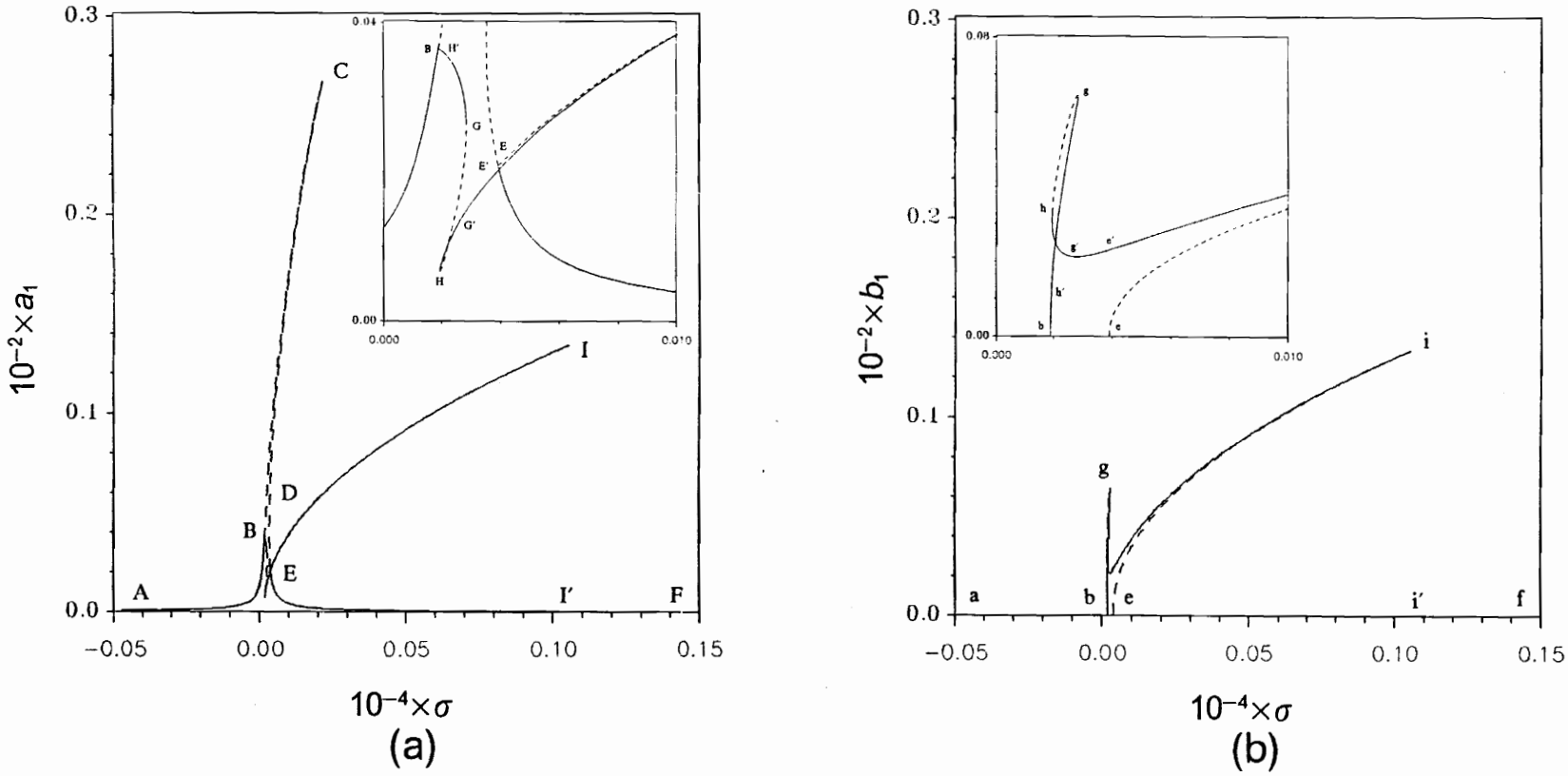

Figure 5.1 Response curves for primary resonance of the first mode. f = 0.001W, $\delta = 0.0002$; (a) in-plane component, (b) out-of-plane component.

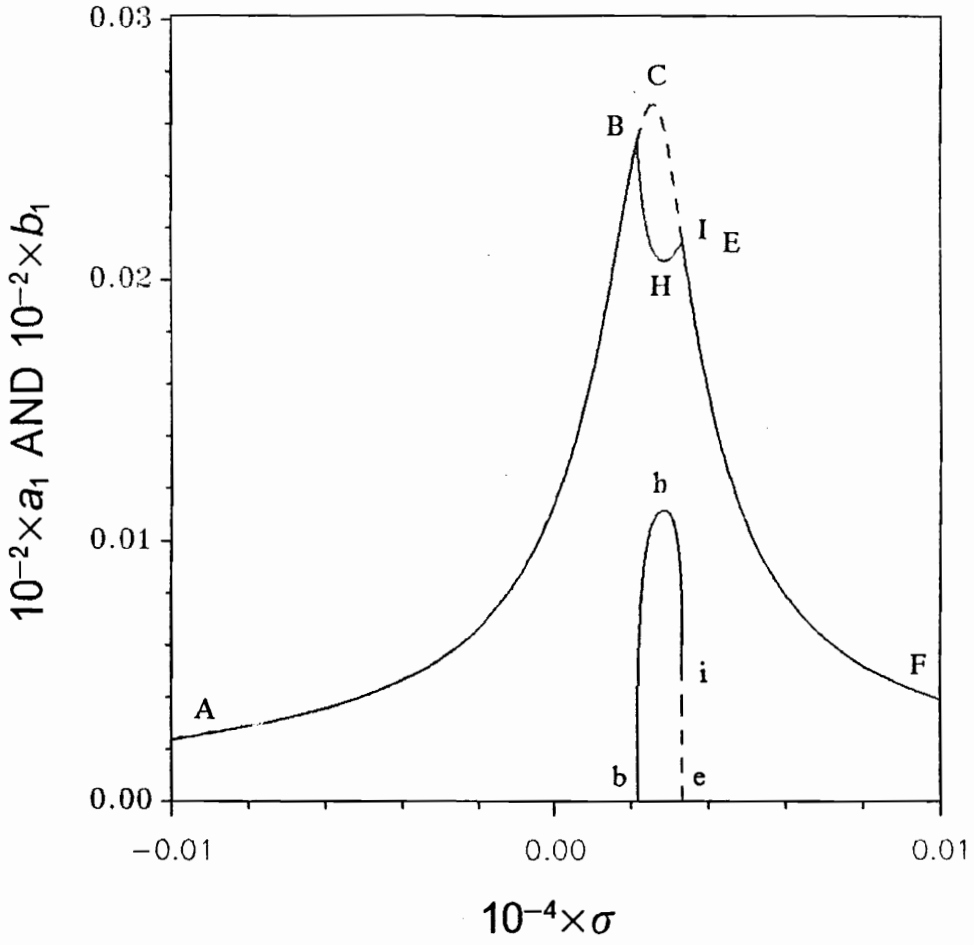

Figure 5.2 Response curves for primary resonance of the first mode. In-plane and out-of-plane components. f = 0.001W, $\delta = 0.002$.

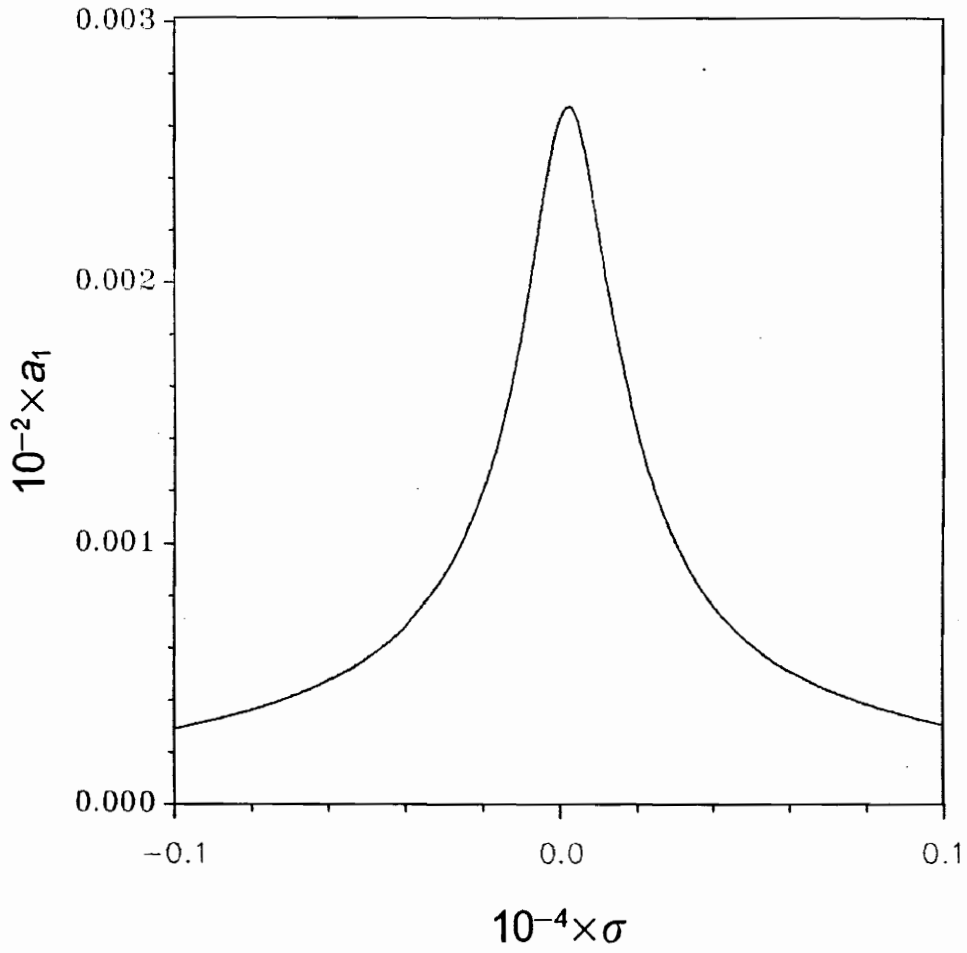

Figure 5.3 Response curves for primary resonance of the first mode. In-plane component. f = 0.001W, $\delta = 0.02$.

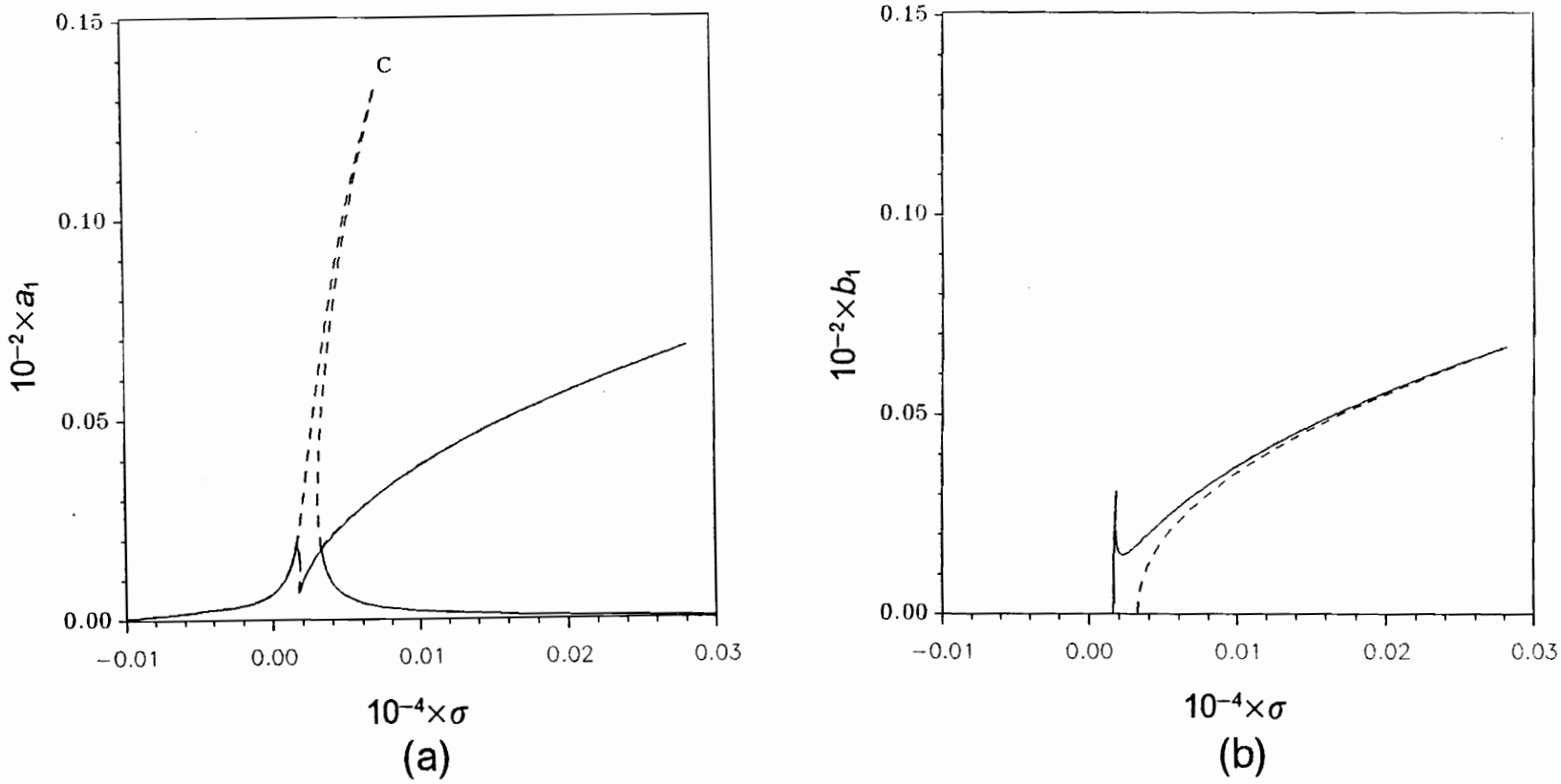

Figure 5.4 Response curves for primary resonance of the first mode. f = 0.0005W, $\delta = 0.0002$; (a) in-plane component, (b) out-of-plane component.

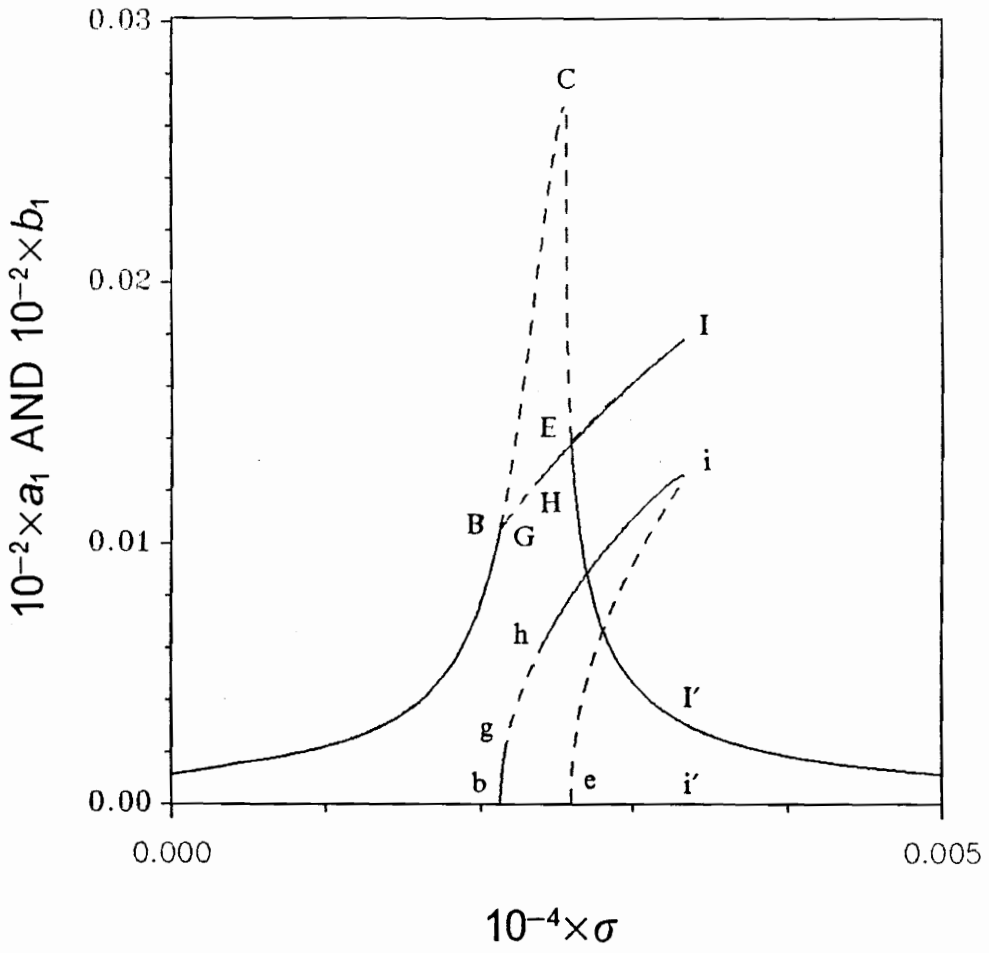

Figure 5.5 Response curves for primary resonance of the first mode. In-plane and out-of-plane components. f = 0.0001W, $\delta = 0.0002$.

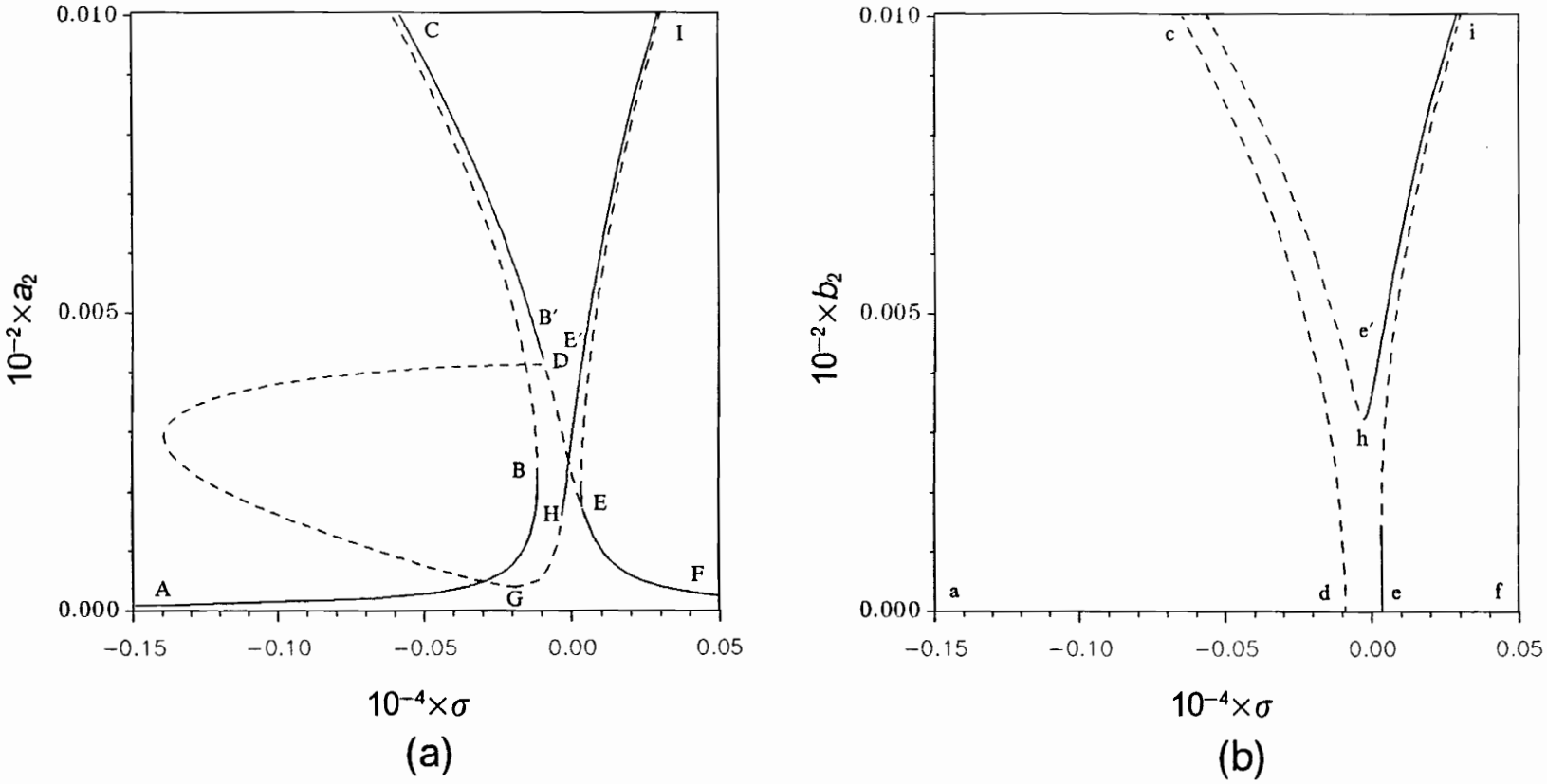

Figure 5.6 Response curves for primary resonance of the second mode. f = 0.005W, $\delta = 0.0002$; (a) in-plane component, (b) out-of-plane component.

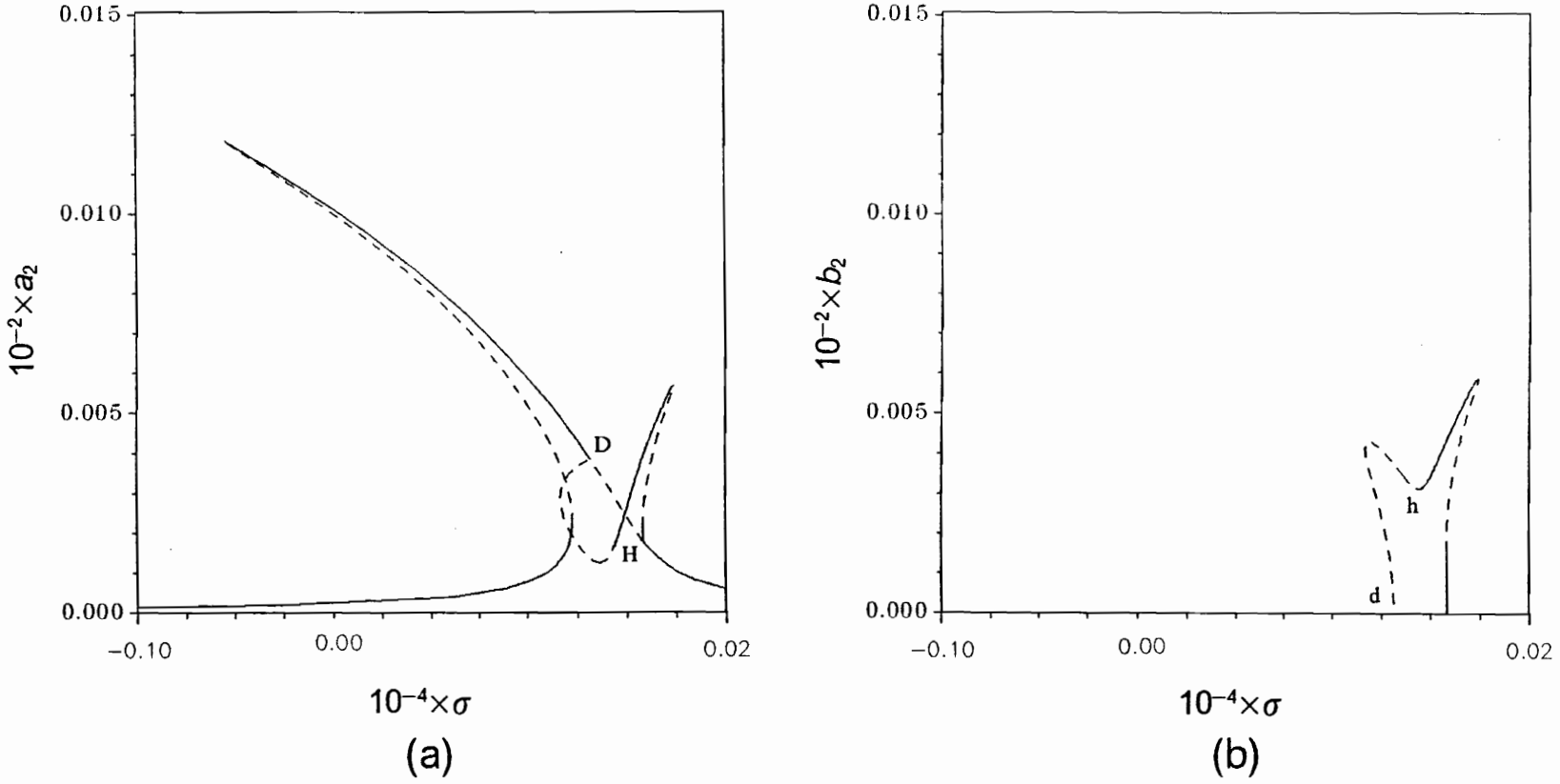

Figure 5.7 Response curves for primary resonance of the second mode. f = 0.005W, $\delta = 0.002$; (a) in-plane component, (b) out-of-plane component.

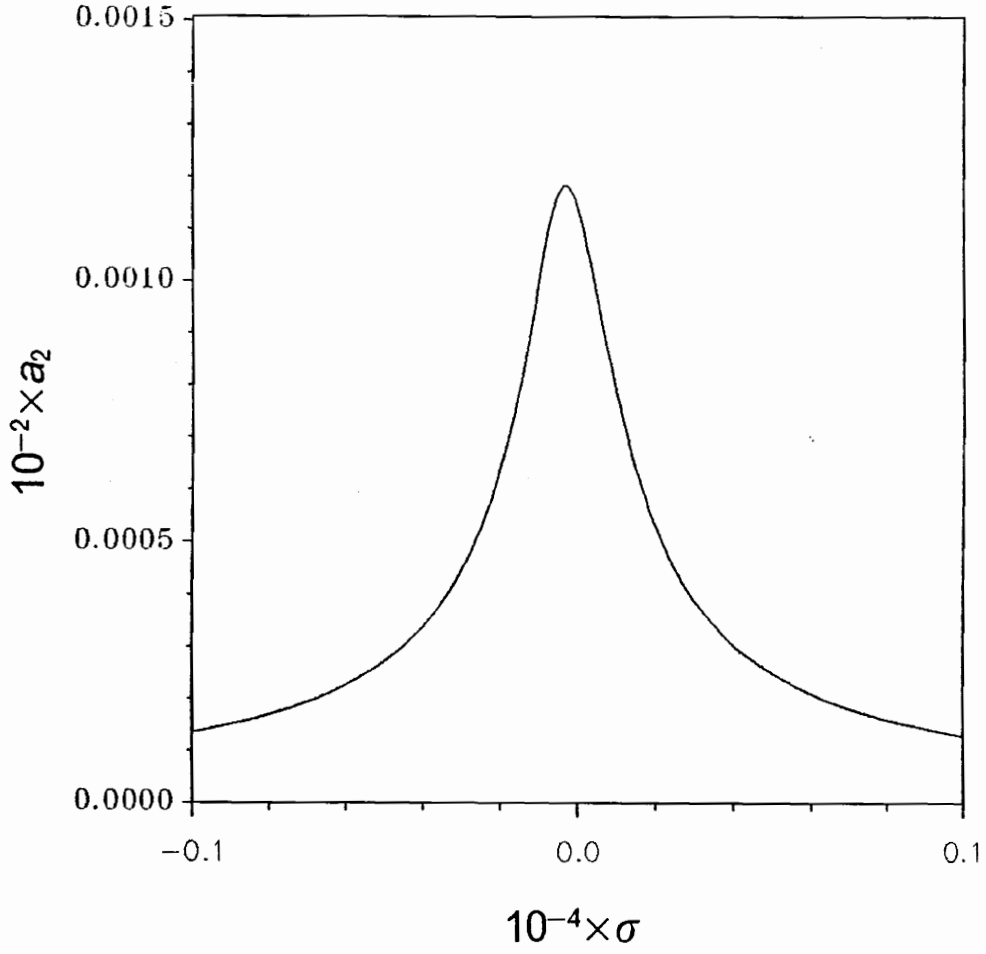

Figure 5.8 Response curves for primary resonance of the second mode. In-plane component. f = 0.005W, $\delta = 0.02$.

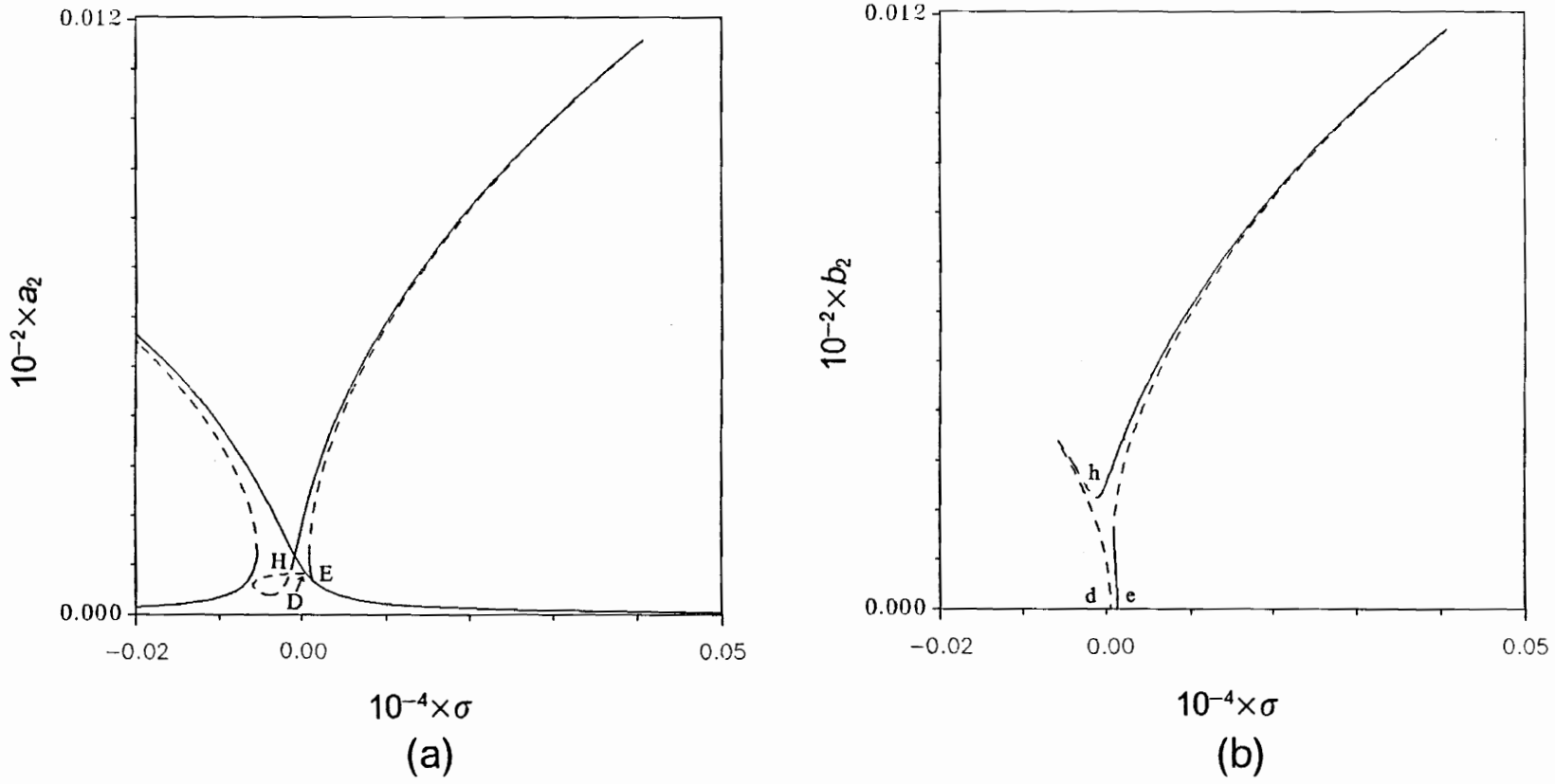

Figure 5.9 Response curves for primary resonance of the second mode. f = 0.001W, $\delta = 0.0002$; (a) in-plane component, (b) out-of-plane component.

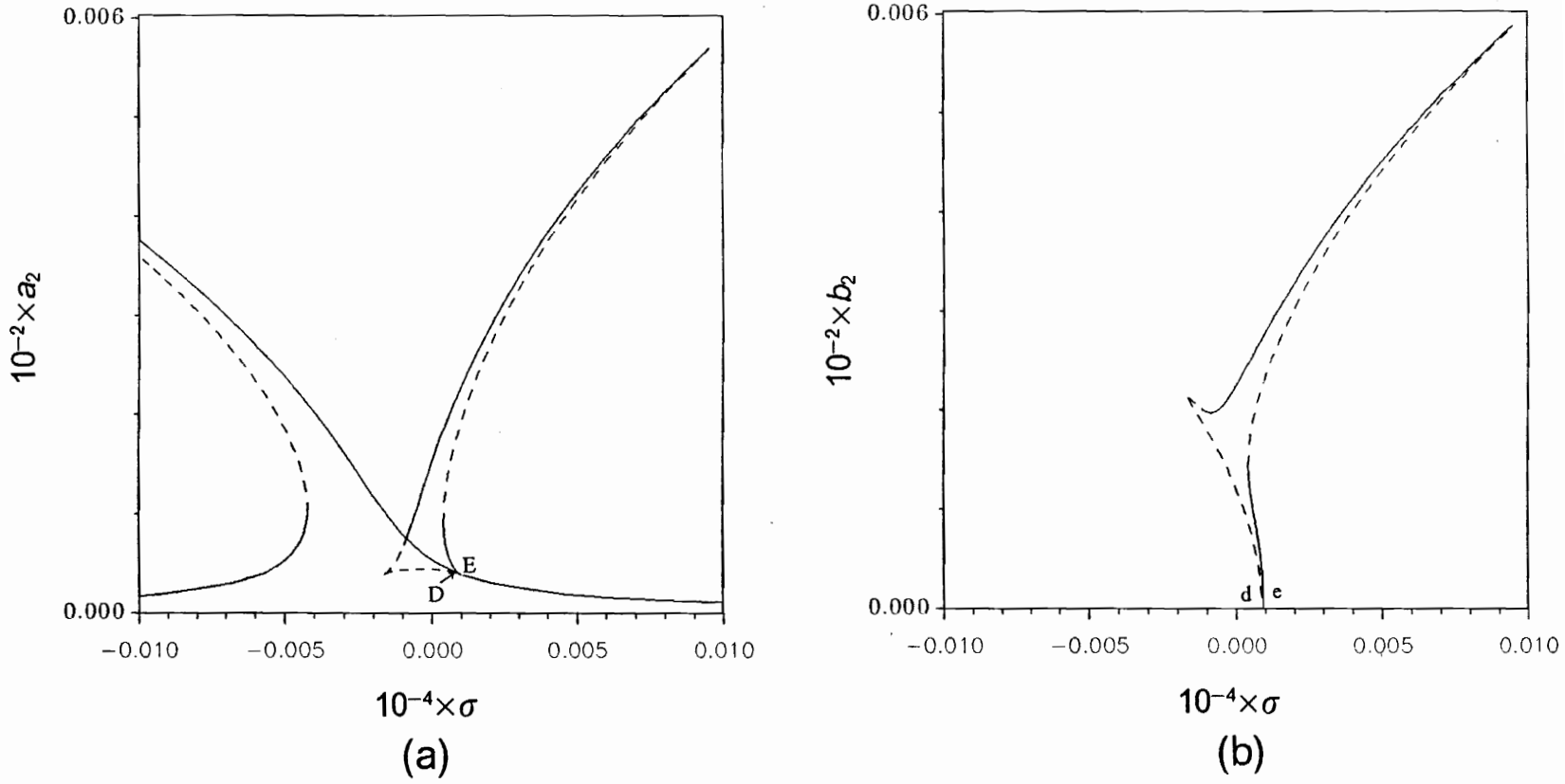

Figure 5.10 Response curves for primary resonance of the second mode. f = 0.0005W, $\delta = 0.0002$; (a) in-plane component, (b) out-of-plane component.

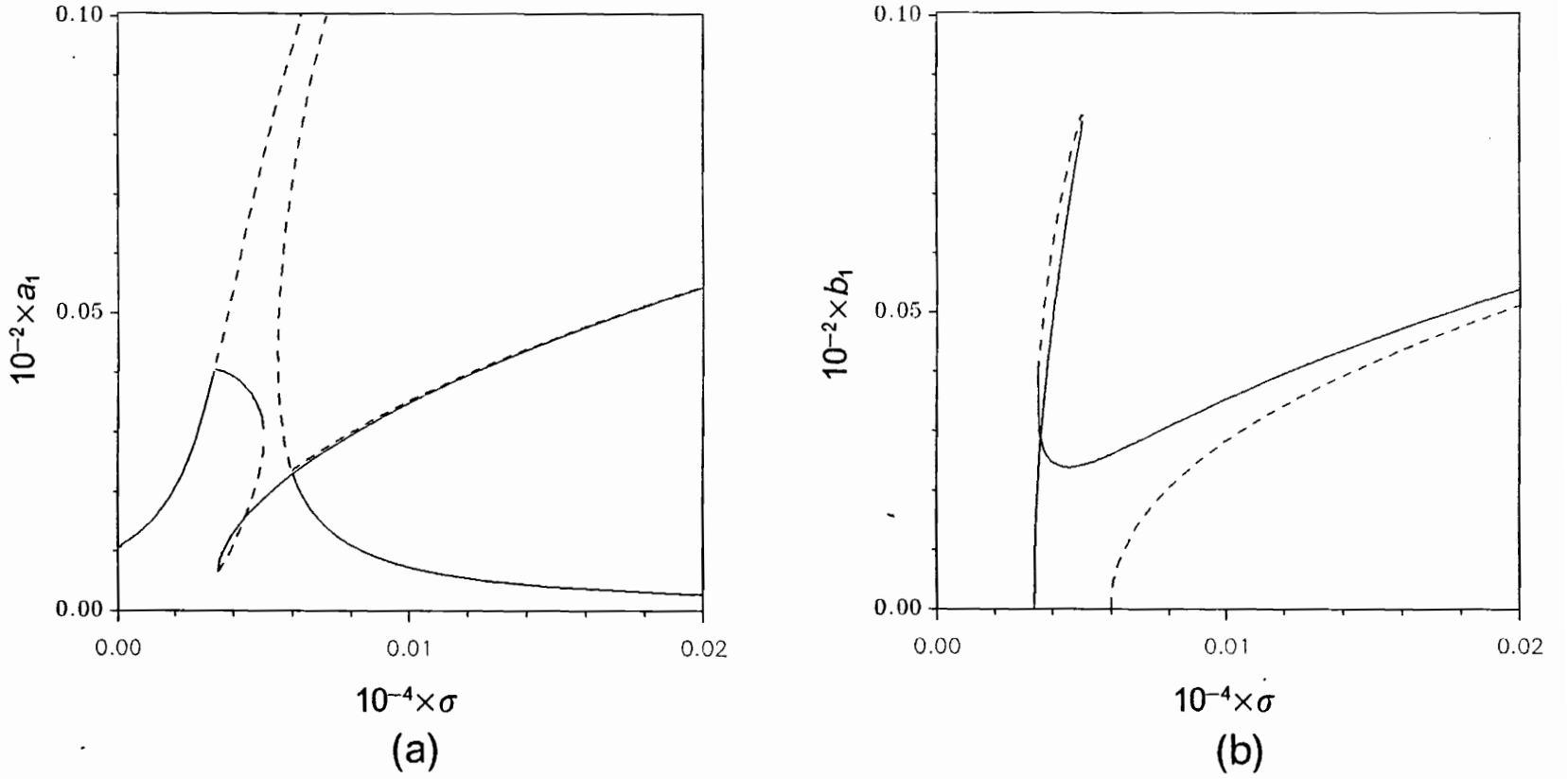

Figure 5.11 Response curves for superharmonic resonance of order two of the first mode. f = W, $\delta = 0.0002$; (a) in-plane component, (b) out-of-plane component.

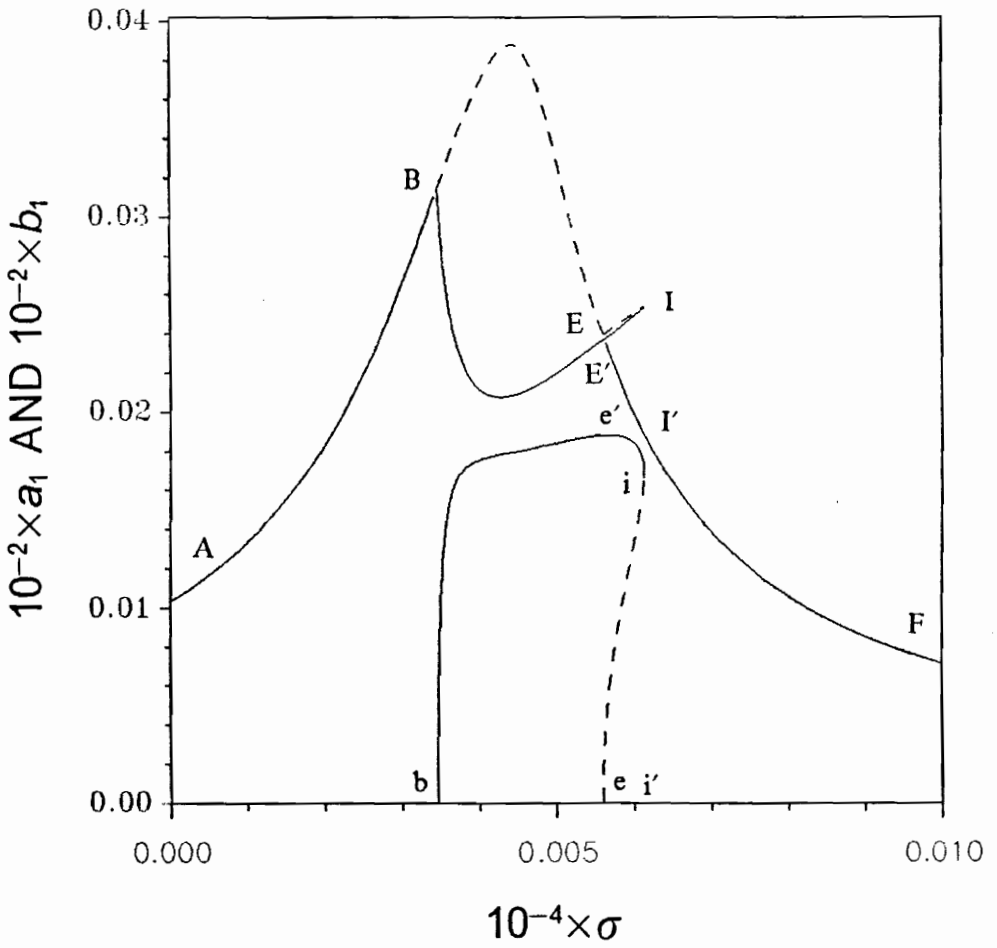

Figure 5.12 Response curves for superharmonic resonance of order two of the first mode. In-plane and out-of-plane components. f = W, $\delta = 0.002$.

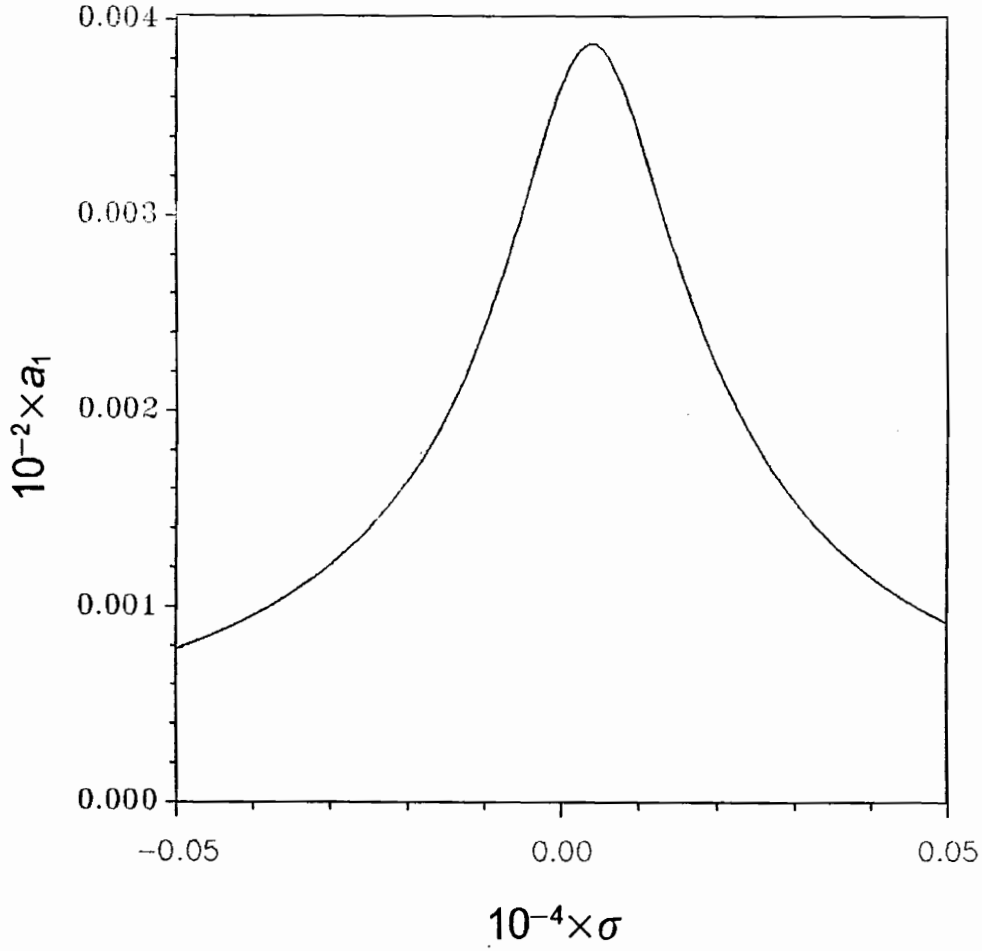

Figure 5.13 Response curves for superharmonic resonance of order two of the first mode. In-plane component. f = W, $\delta = 0.02$.

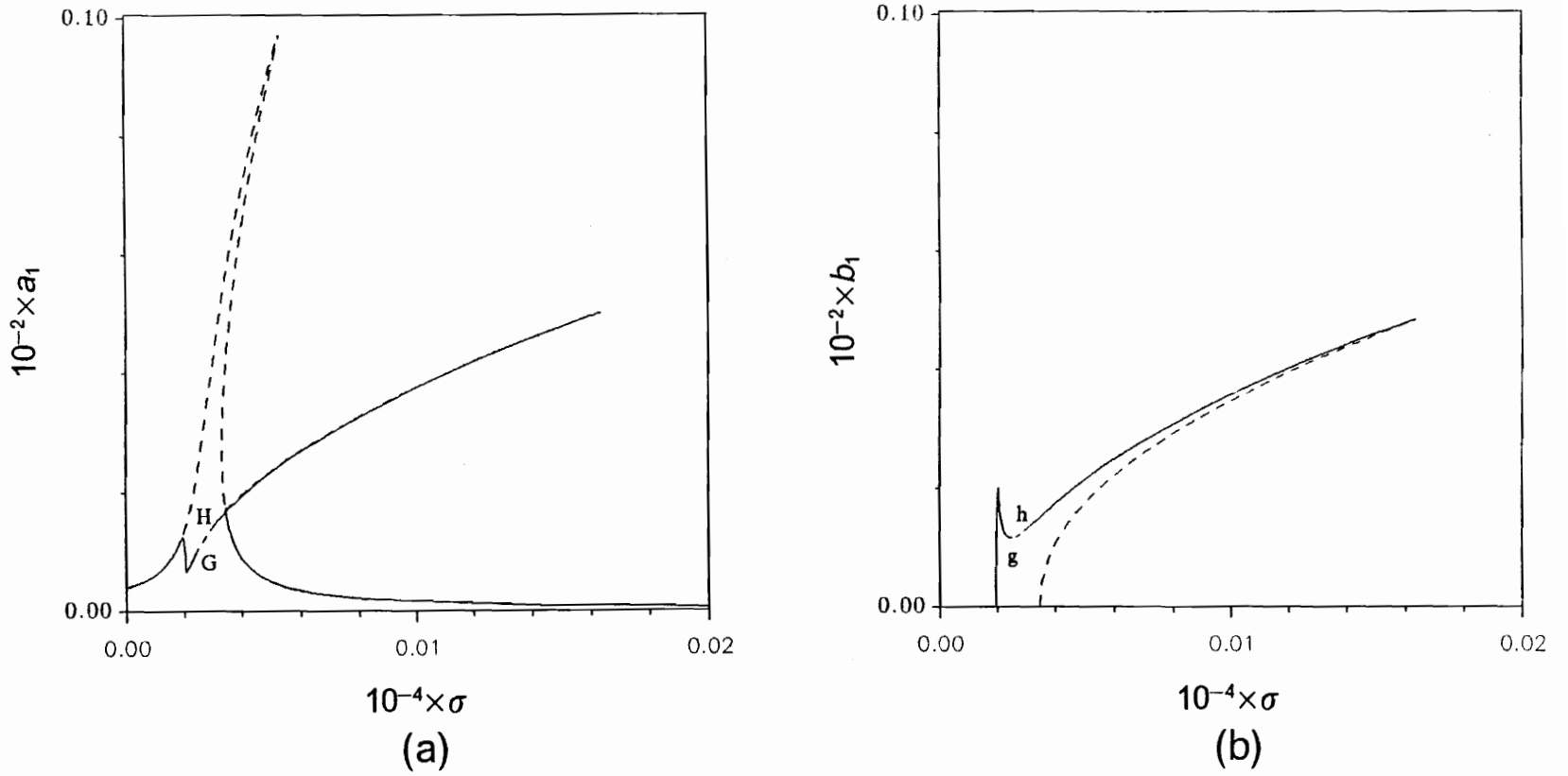

Figure 5.14 Response curves for superharmonic resonance of order two of the first mode. f = 0.5W, $\delta = 0.0002$; (a) in-plane component, (b) out-of-plane component.

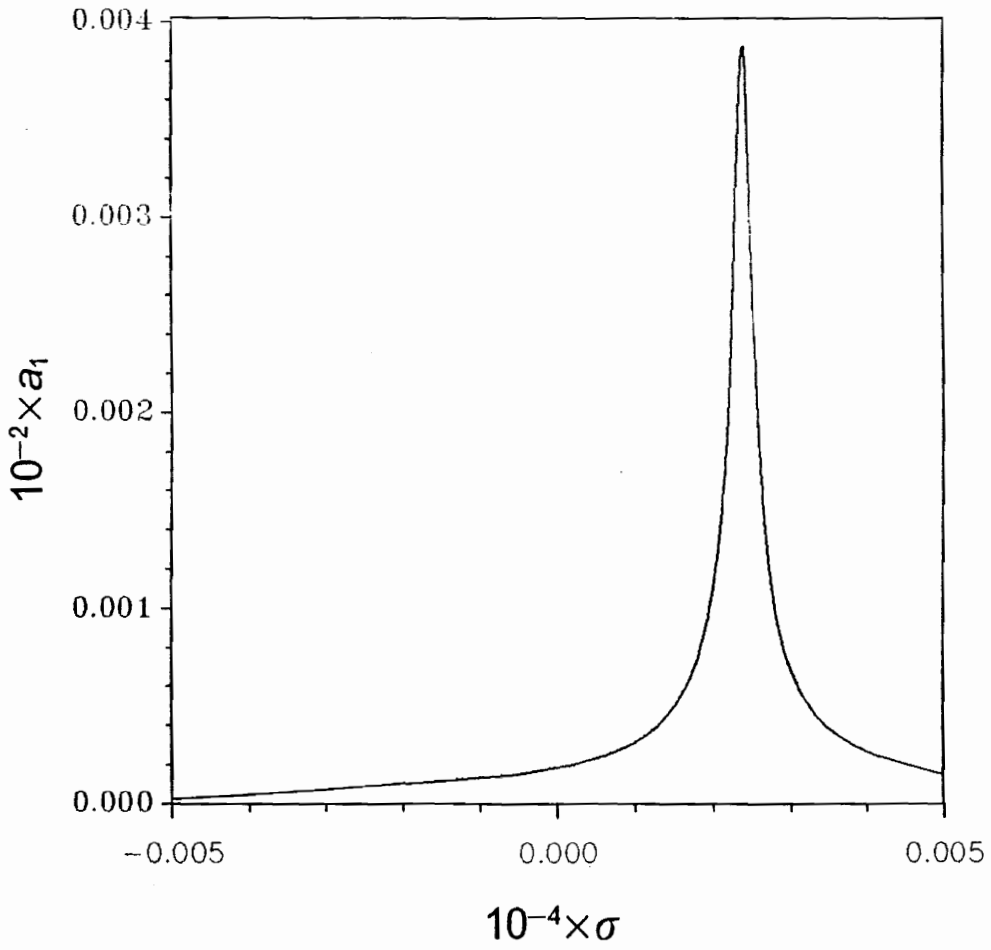

Figure 5.15 Response curves for superharmonic resonance of order two of the first mode. In-plane component. f = 0.1W, $\delta = 0.0002$.

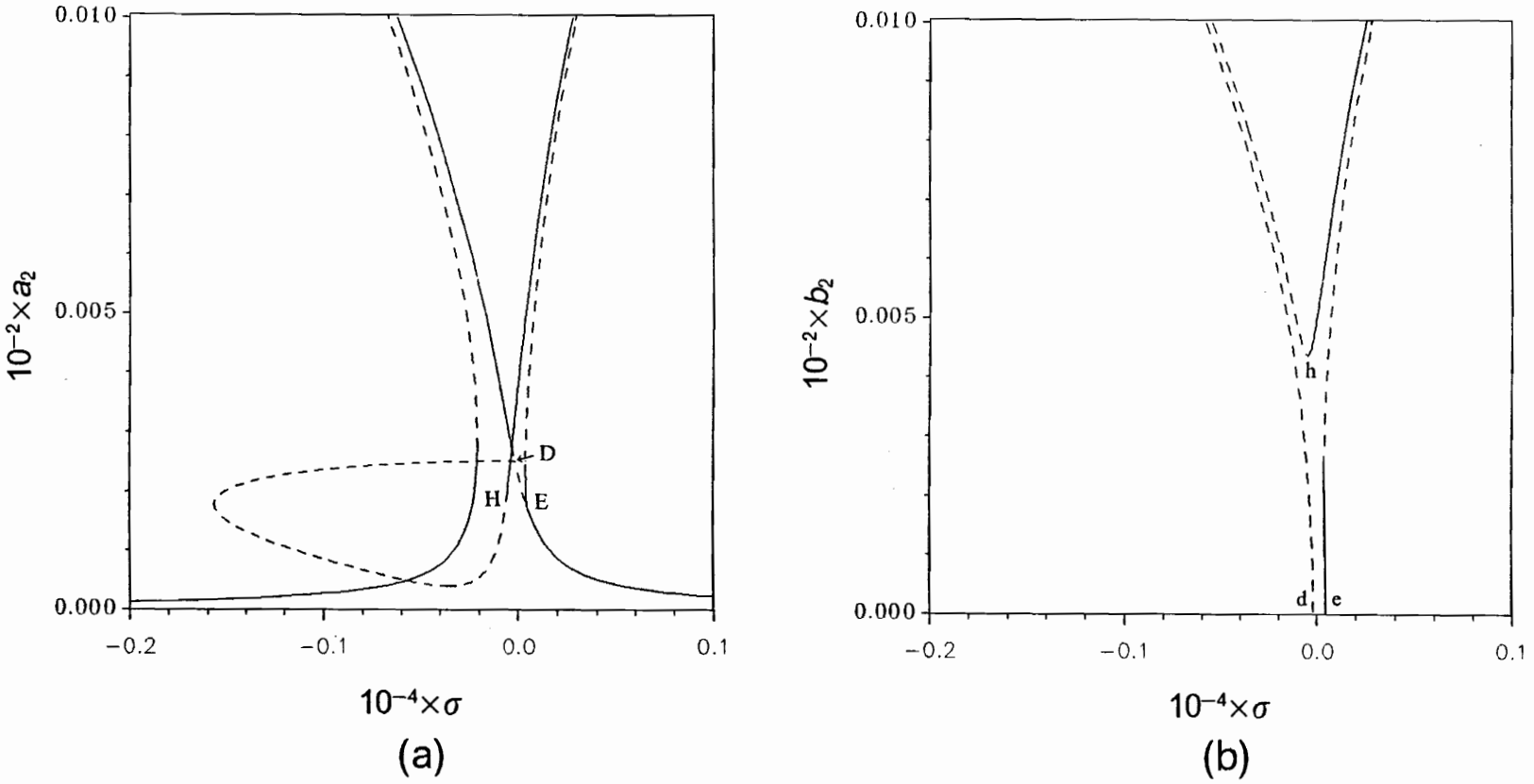

Figure 5.16 Response curves for superharmonic resonance of order two of the second mode. f = 5W, $\delta = 0.0002$; (a) in-plane component, (b) out-of-plane component.

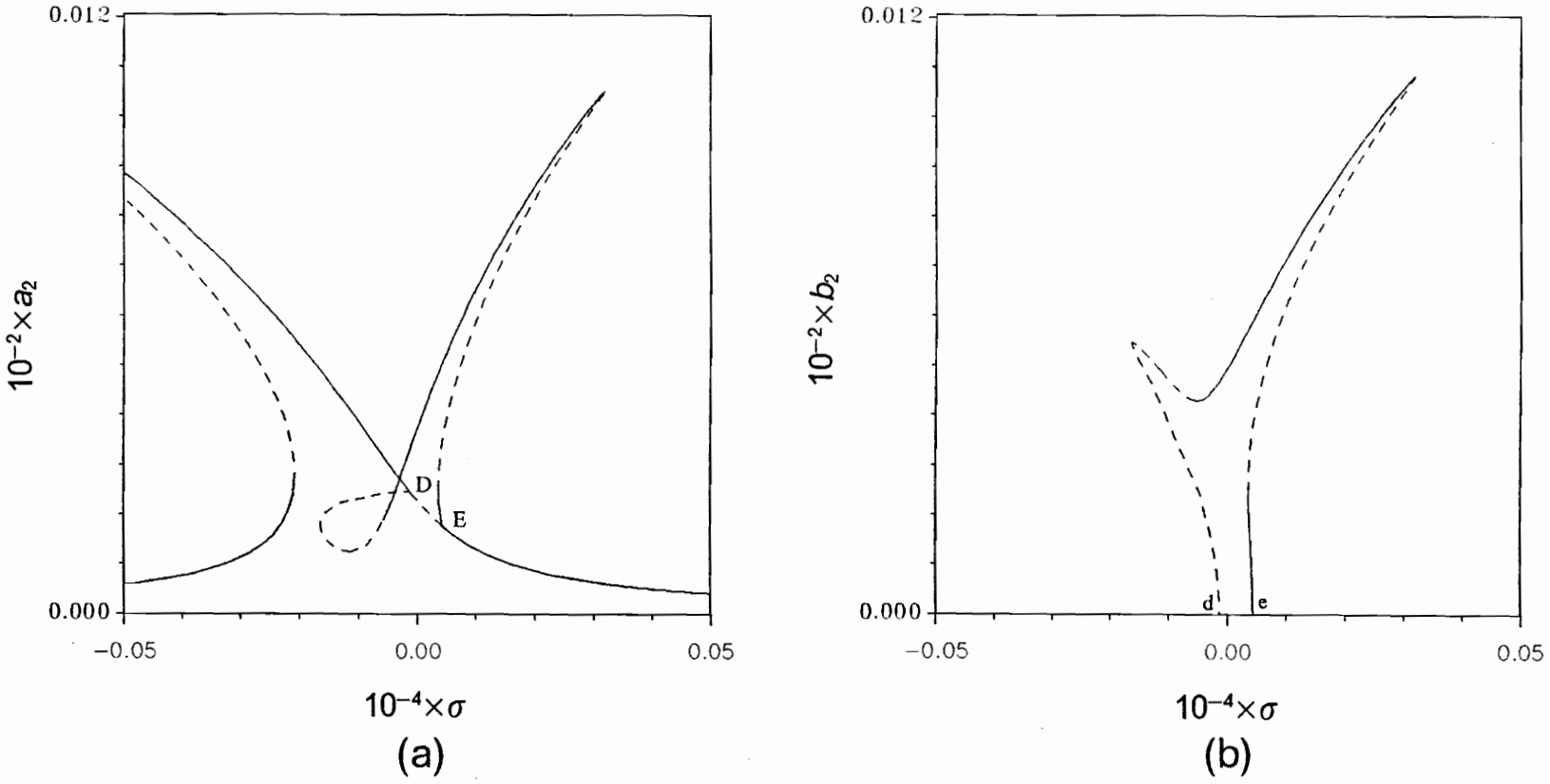

Figure 5.17 Response curves for superharmonic resonance of order two of the second mode. f = 5W, $\delta = 0.002$; (a) in-plane component, (b) out-of-plane component.

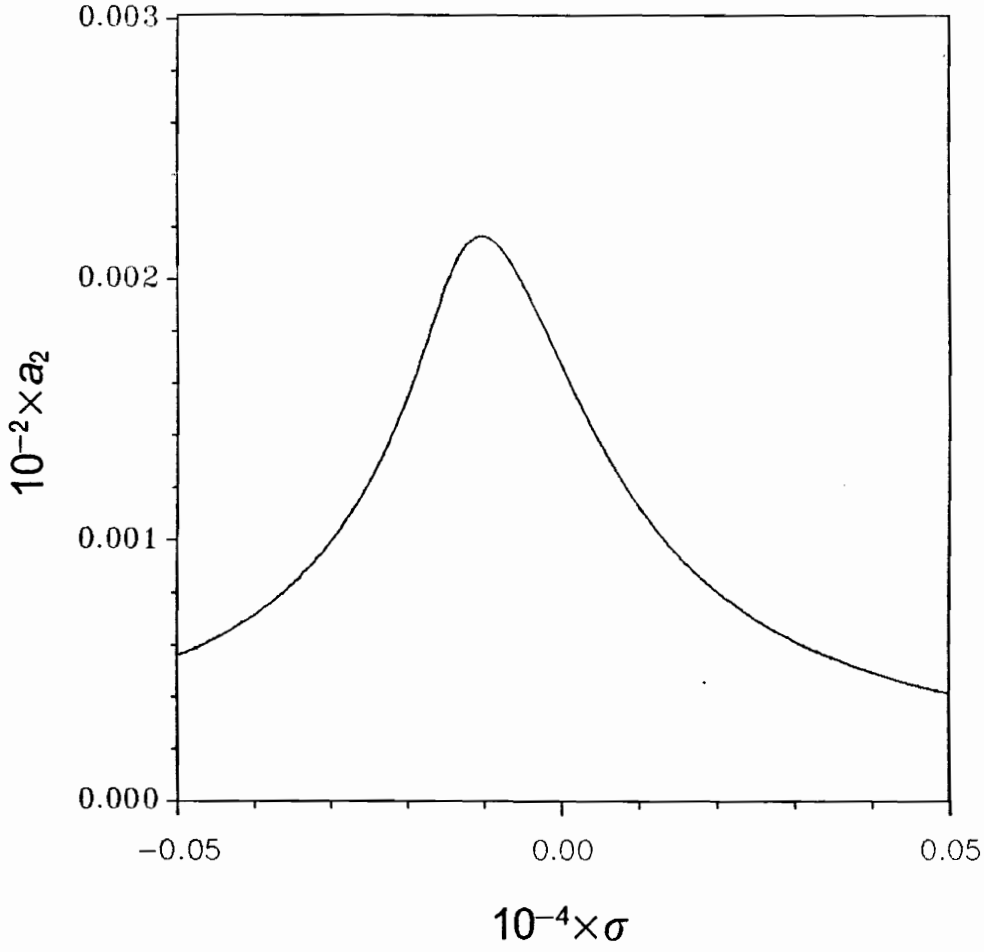

Figure 5.18 Response curves for superharmonic resonance of order two of the second mode. In-plane component. f = 5W, $\delta = 0.02$.

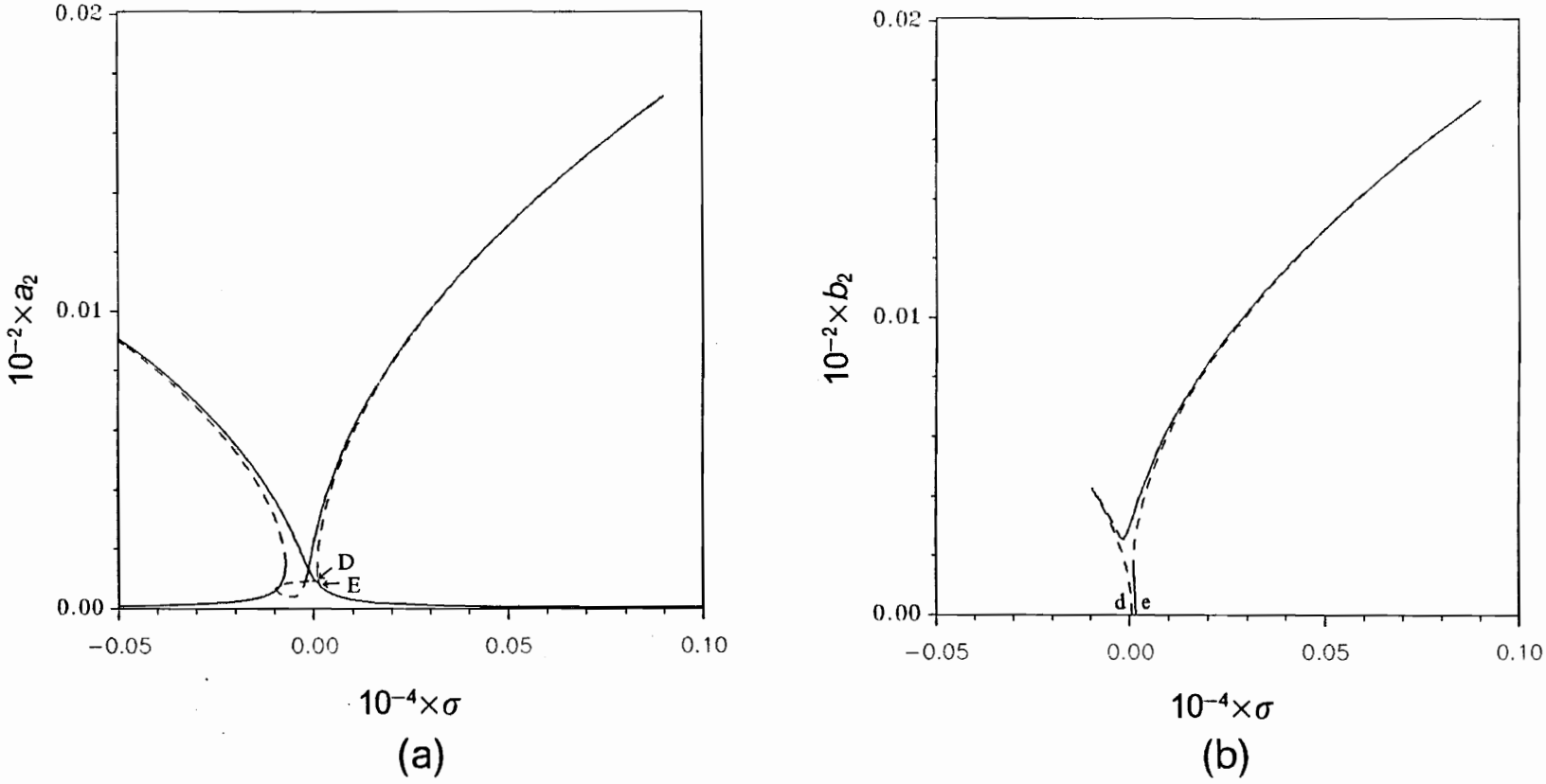

Figure 5.19 Response curves for superharmonic resonance of order two of the second mode. f = 2W, $\delta = 0.0002$; (a) in-plane component, (b) out-of-plane component.

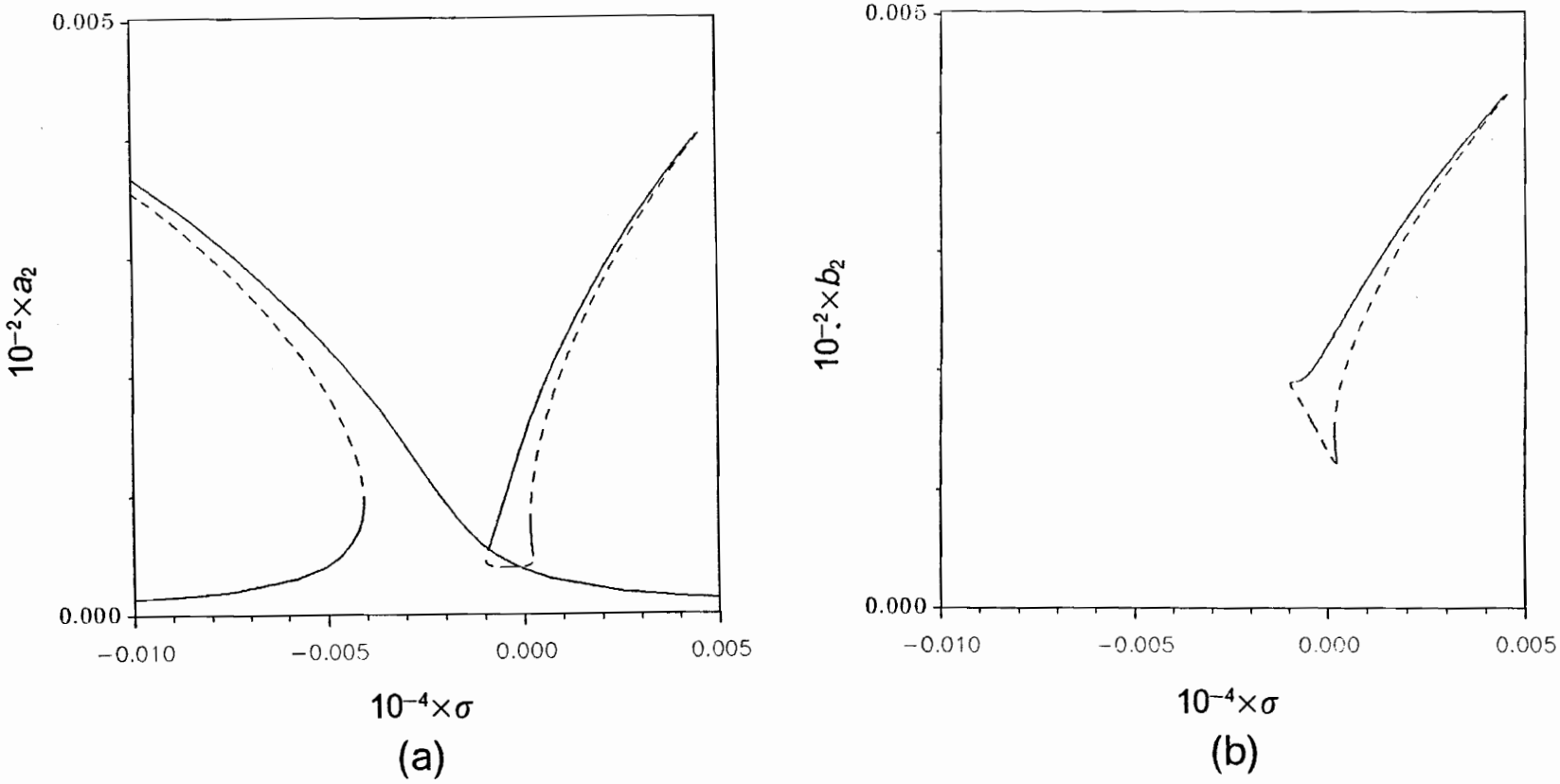

Figure 5.20 Response curves for superharmonic resonance of order two of the second mode. f = W, $\delta = 0.0002$; (a) in-plane component, (b) out-of-plane component.

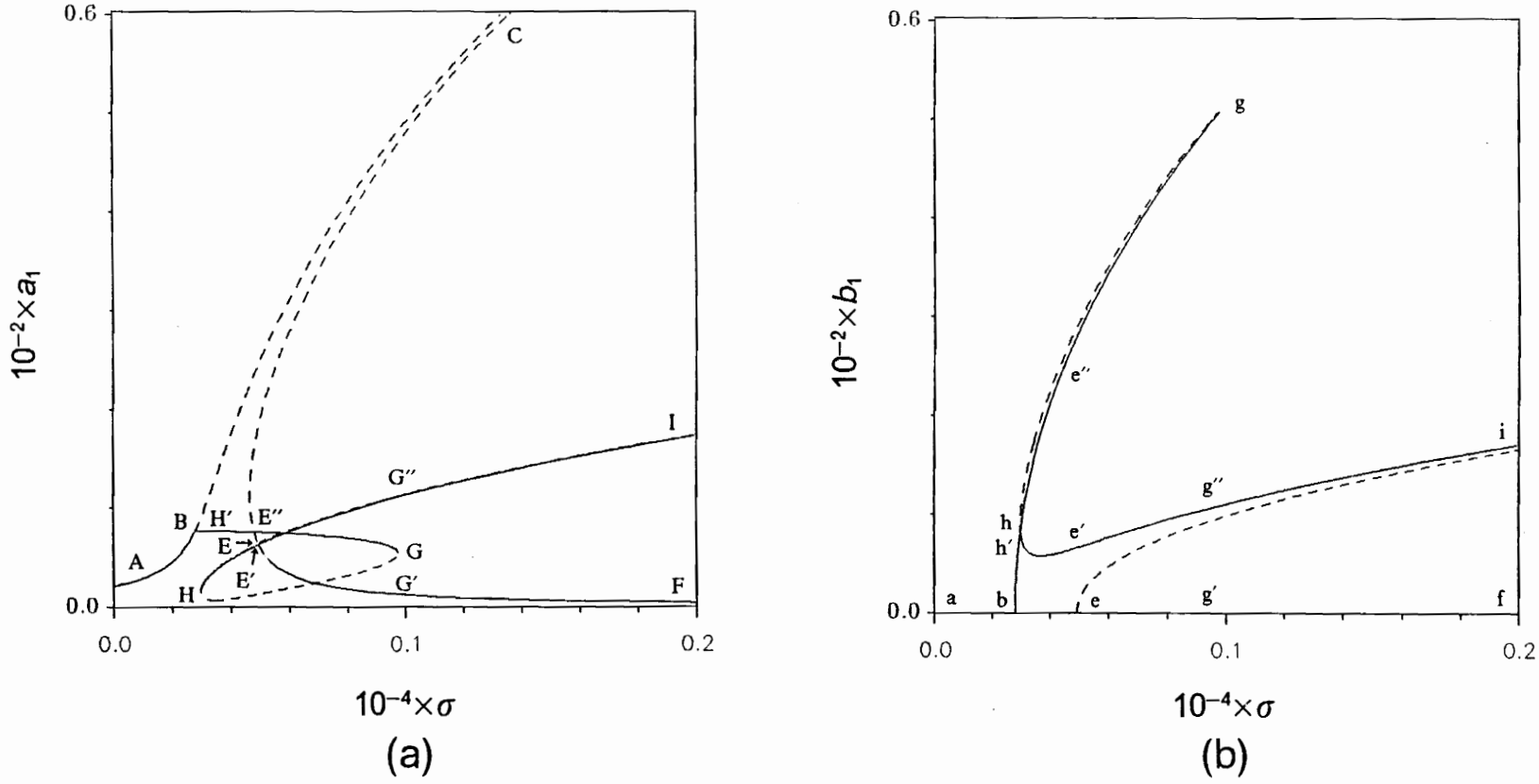

Figure 5.21 Response curves for superharmonic resonance of order three of the first mode. f = 5W, $\delta = 0.0002$; (a) in-plane component, (b) out-of-plane component.

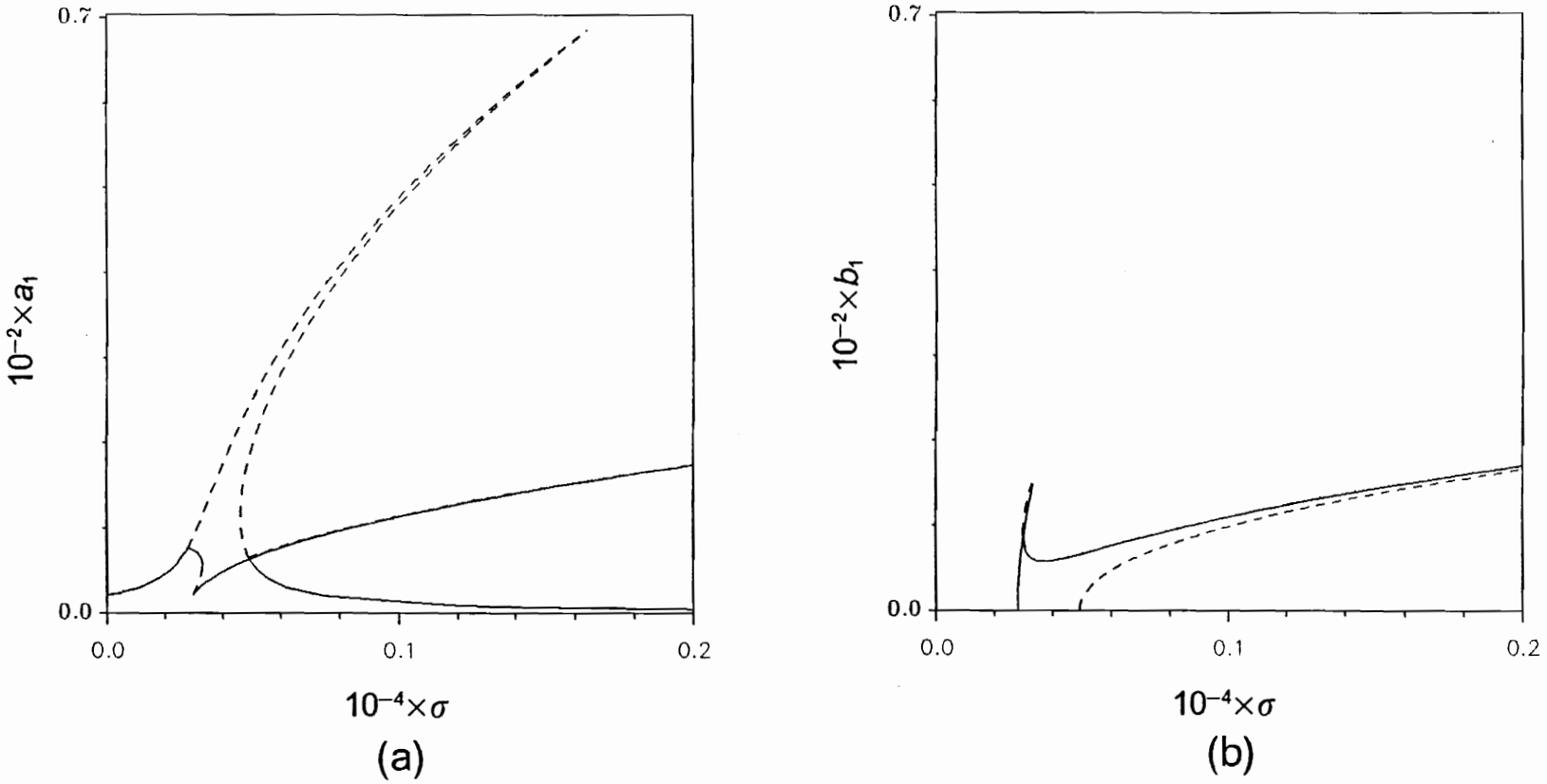

Figure 5.22 Response curves for superharmonic resonance of order three of the first mode. f = 5W, $\delta = 0.002$; (a) in-plane component, (b) out-of-plane component.

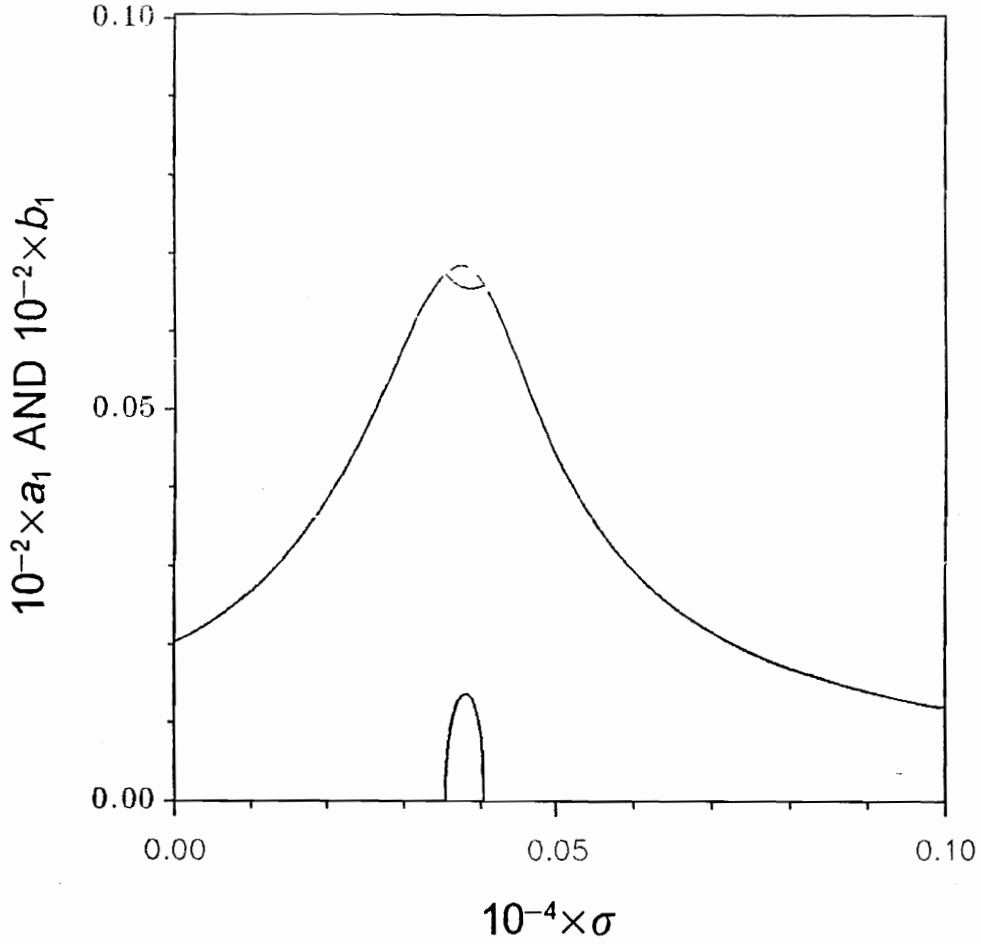

Figure 5.23 Response curves for superharmonic resonance of order three of the first mode. In-plane and out-of-plane components. f = 5W, $\delta = 0.02$.

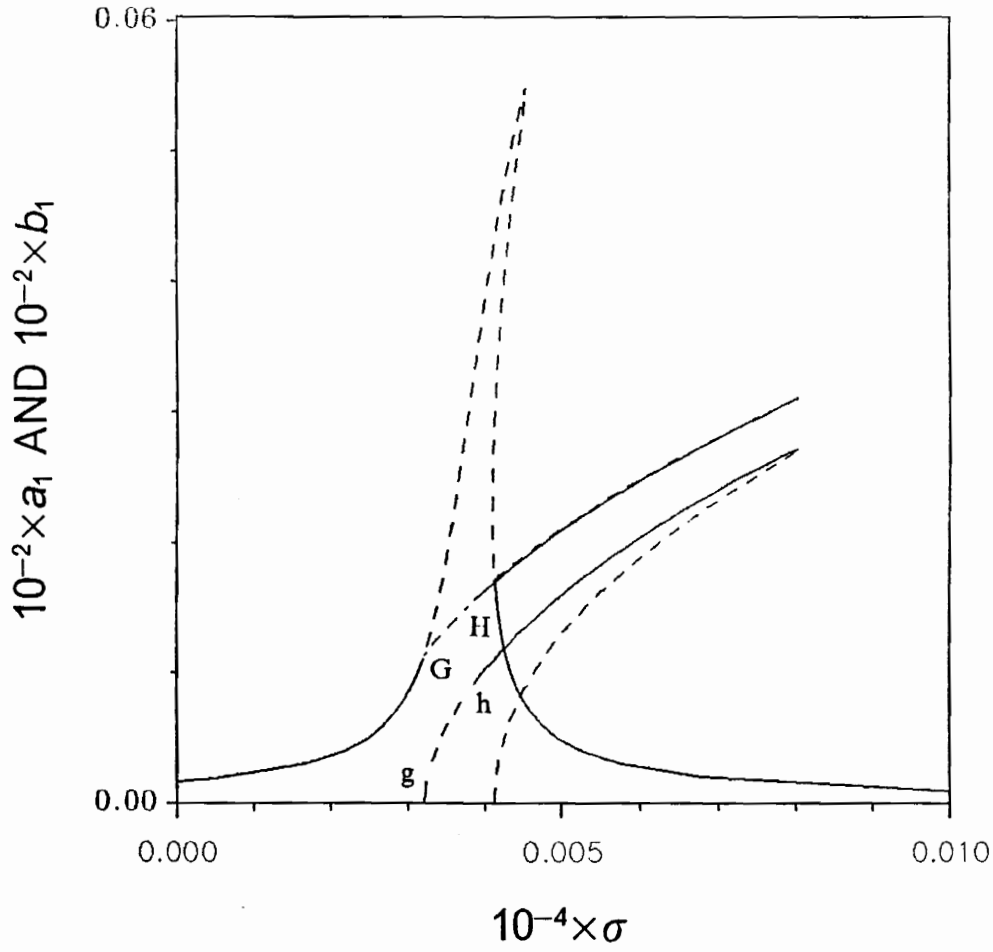

Figure 5.24 Response curves for superharmonic resonance of order three of the first mode. In-plane and out-of-plane components. f = W, $\delta = 0.0002$.

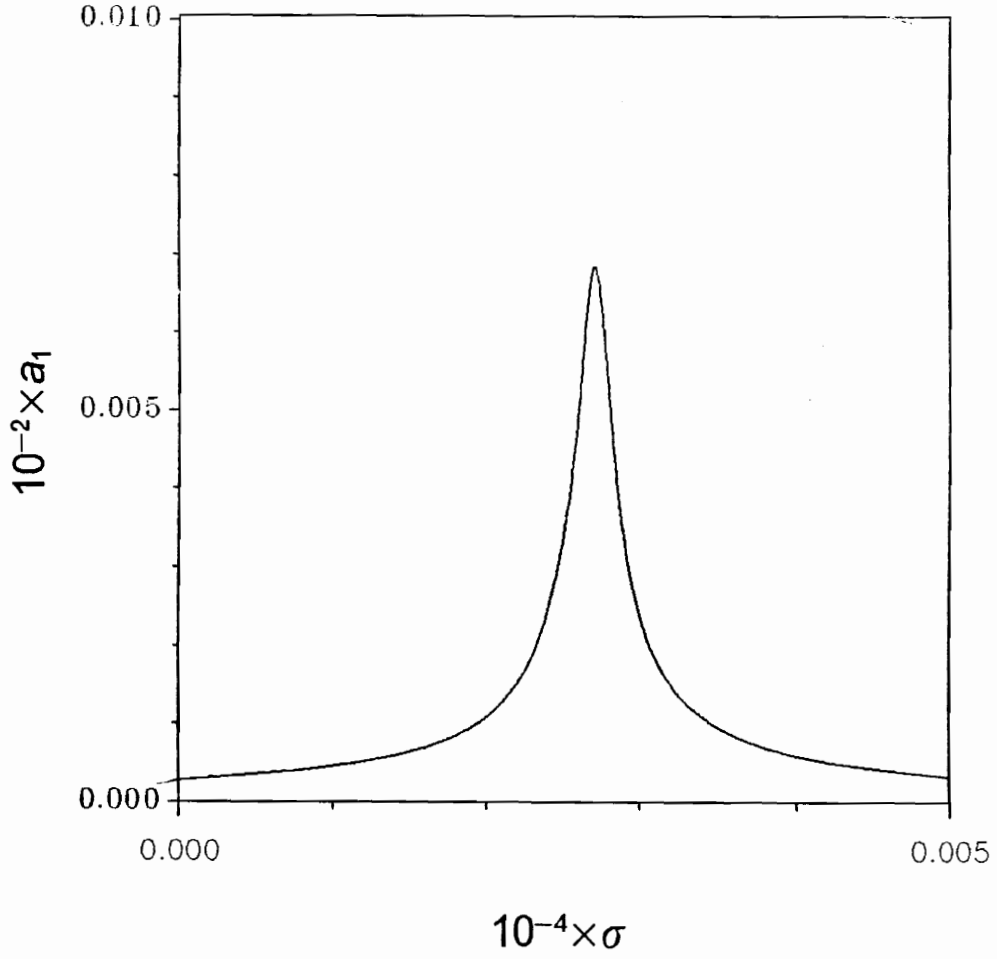

Figure 5.25 Response curves for superharmonic resonance of order three of the first mode. In-plane component. f = 0.5W, $\delta = 0.0002$.

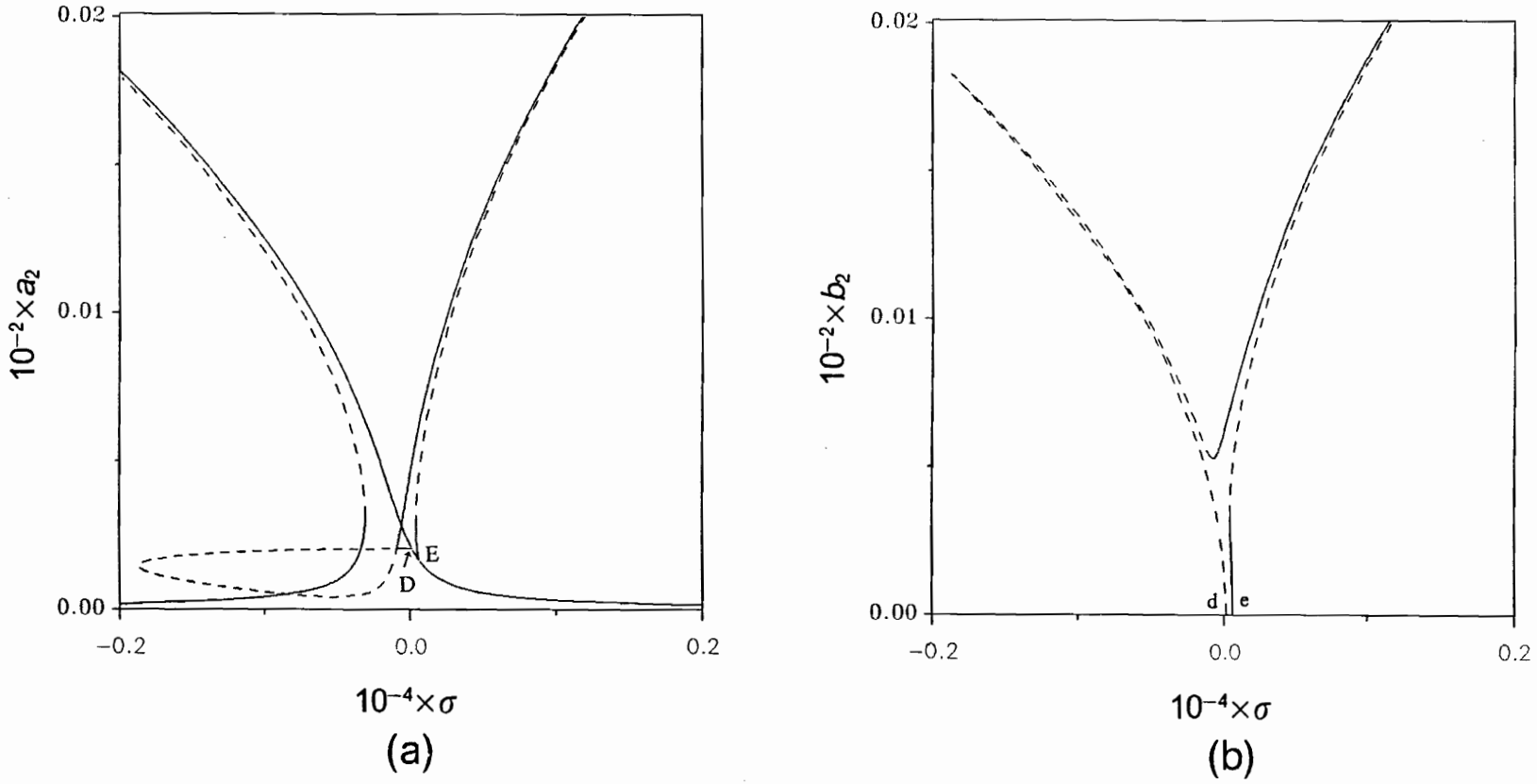

Figure 5.26 Response curves for superharmonic resonance of order three of the second mode. f = 5W, $\delta = 0.0002$; (a) in-plane component, (b) out-of-plane component.

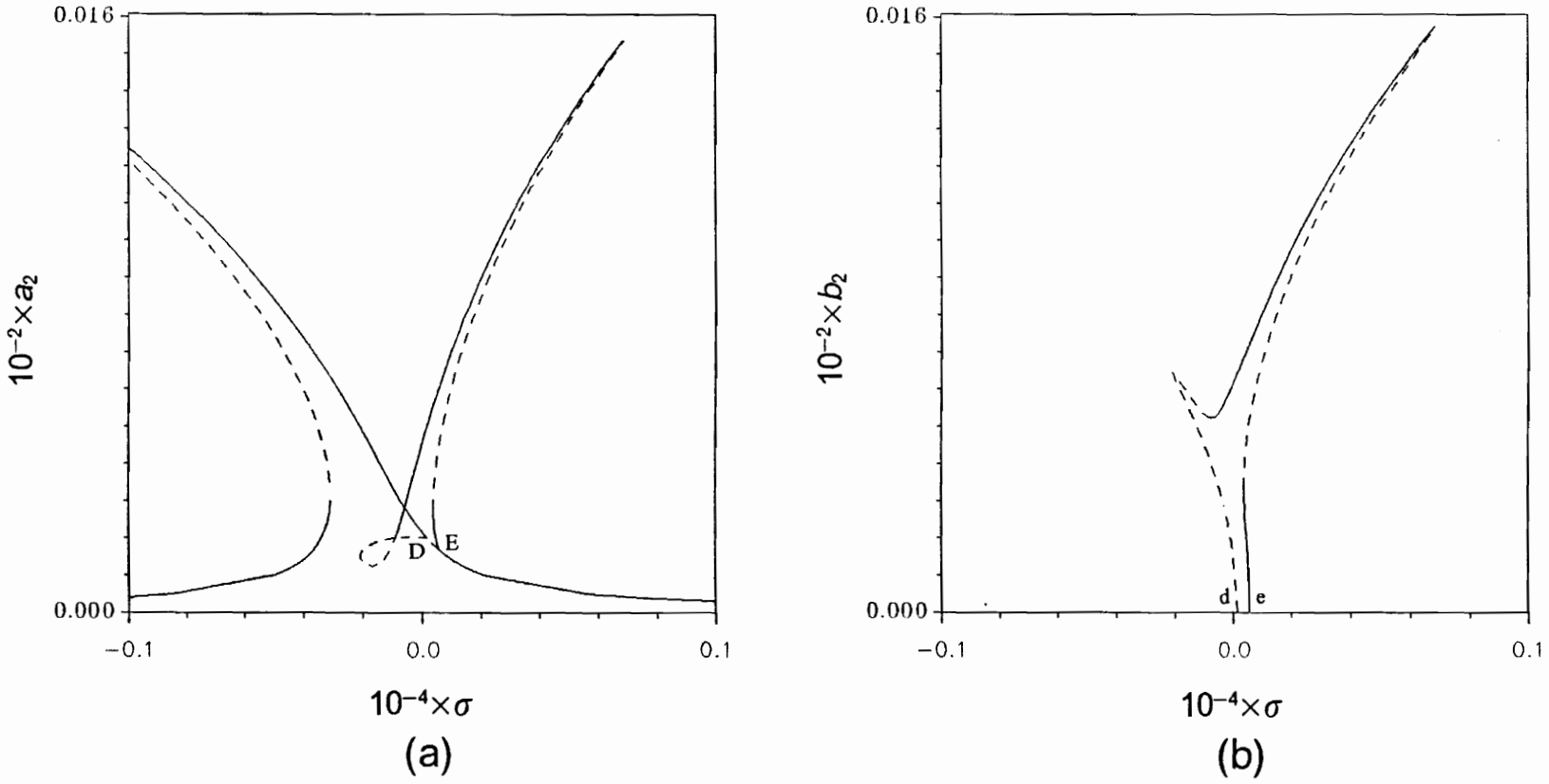

Figure 5.27 Response curves for superharmonic resonance of order three of the second mode. f = 5W, $\delta = 0.002$; (a) in-plane component, (b) out-of-plane component.

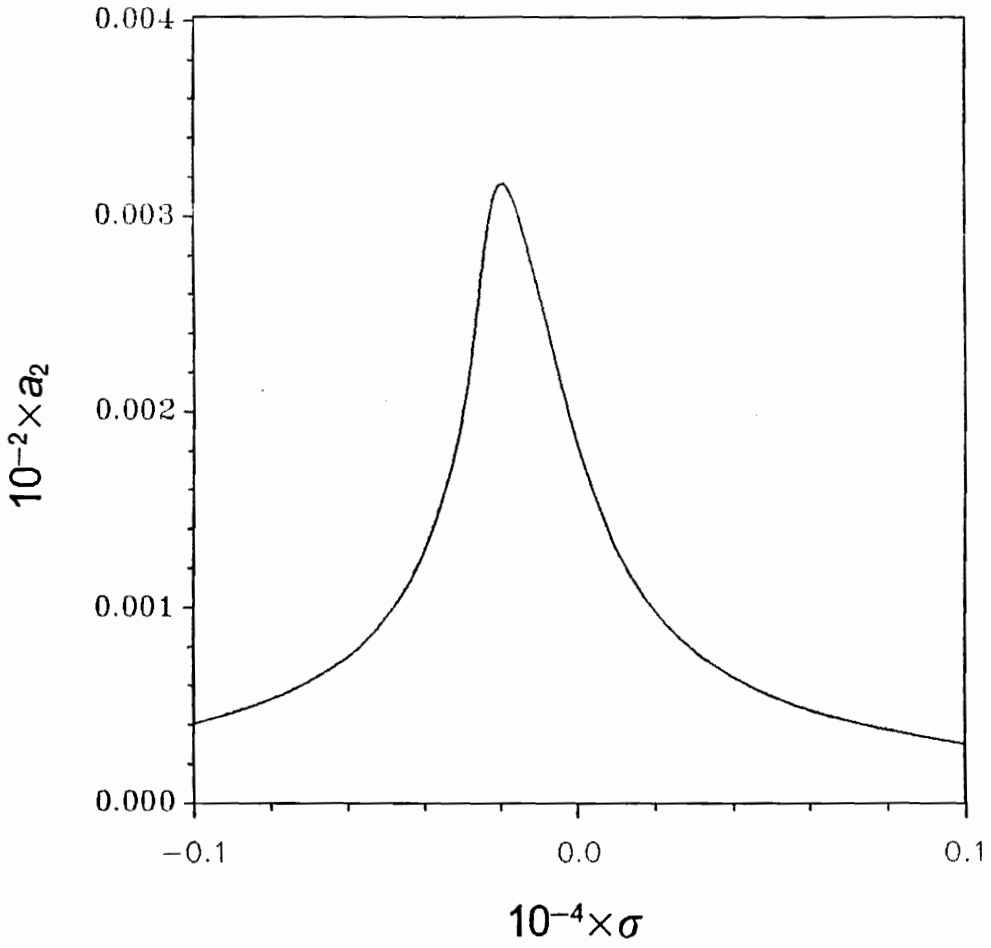

Figure 5.28 Response curves for superharmonic resonance of order three of the second mode. In-plane component. f = 5W, $\delta = 0.02$.

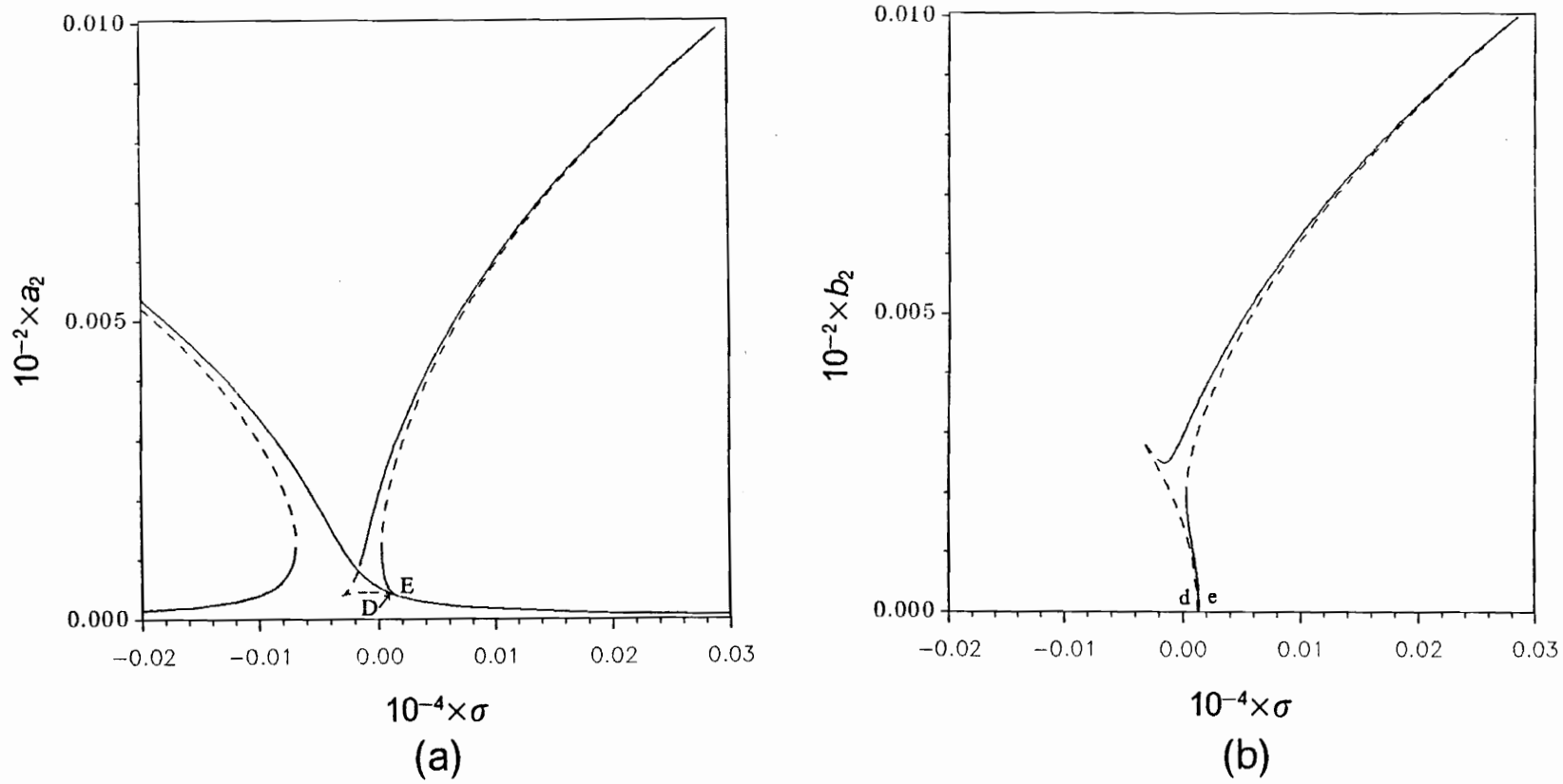

Figure 5.29 Response curves for superharmonic resonance of order three of the second mode. f = 2W, $\delta = 0.0002$; (a) in-plane component, (b) out-of-plane component.

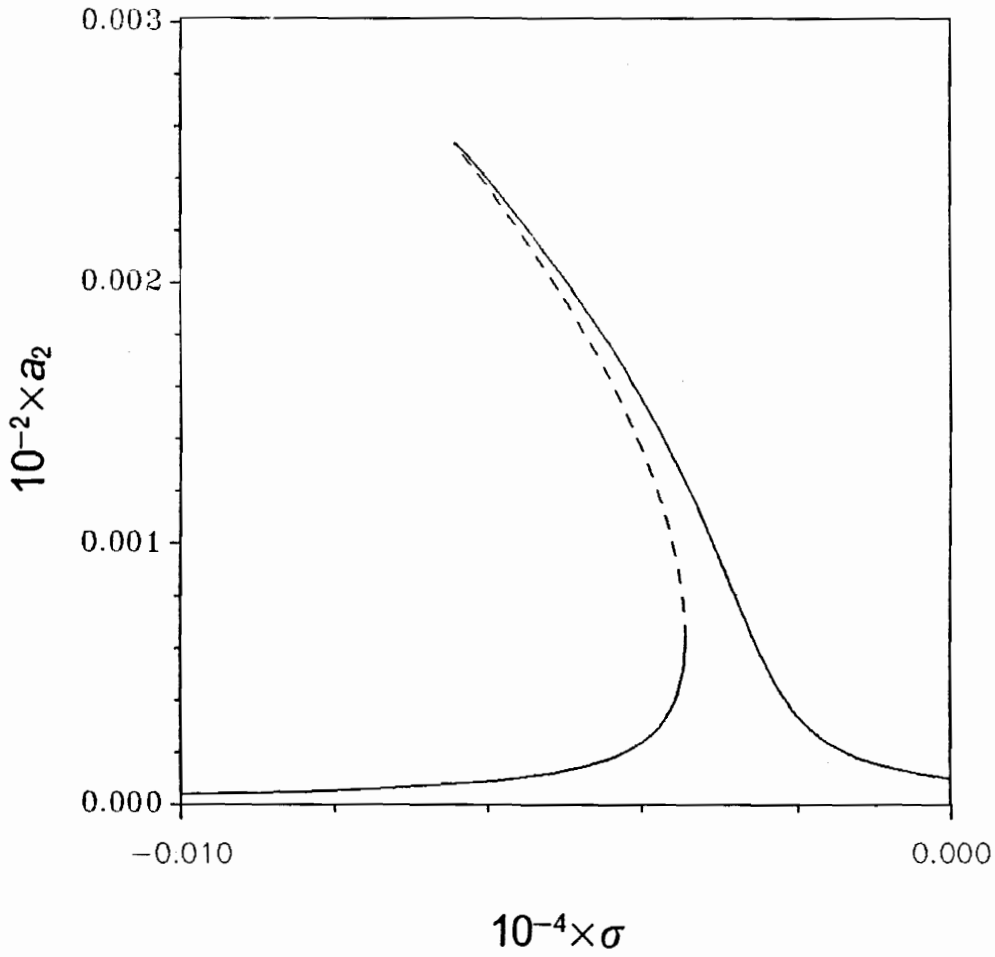

Figure 5.30 Response curves for superharmonic resonance of order three of the second mode. In-plane component. f = W, $\delta = 0.0002$.

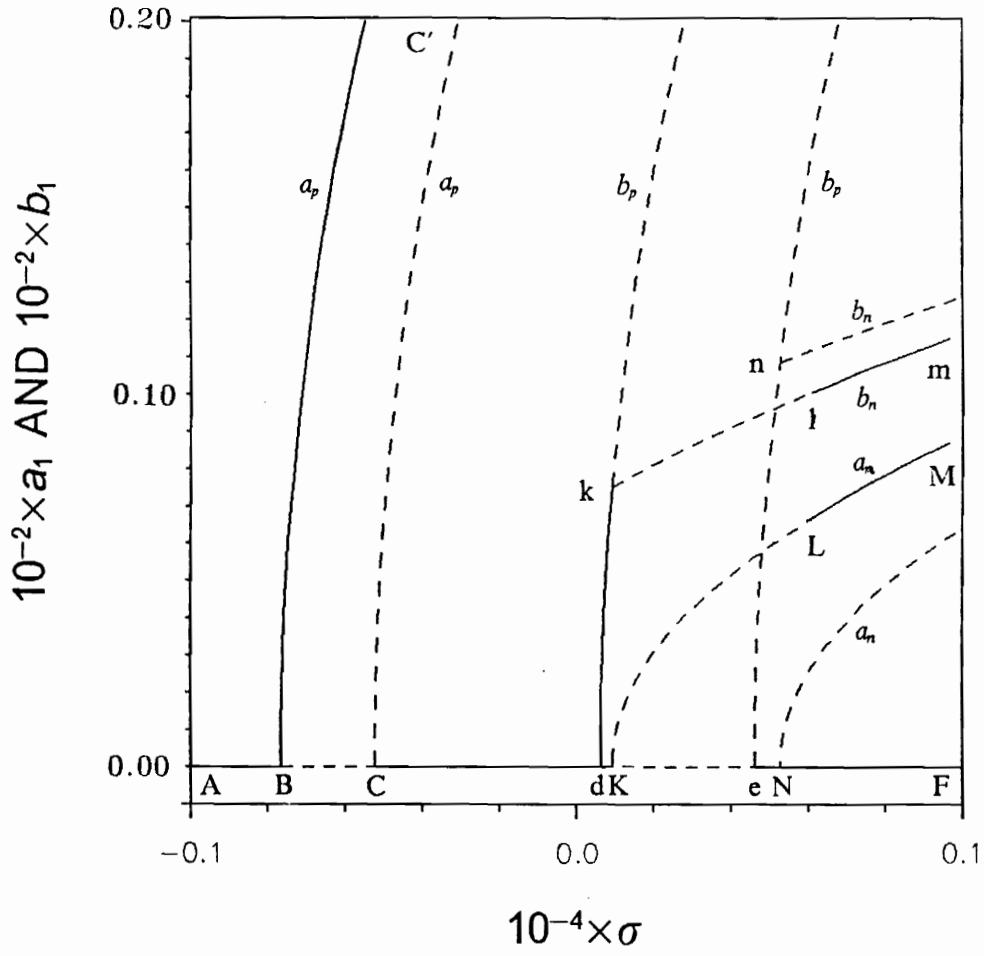

Figure 5.31 Response curves for subharmonic resonance of order two of the first mode. In-plane and out-of-plane components. f = 10W, $\delta = 0.0002$.

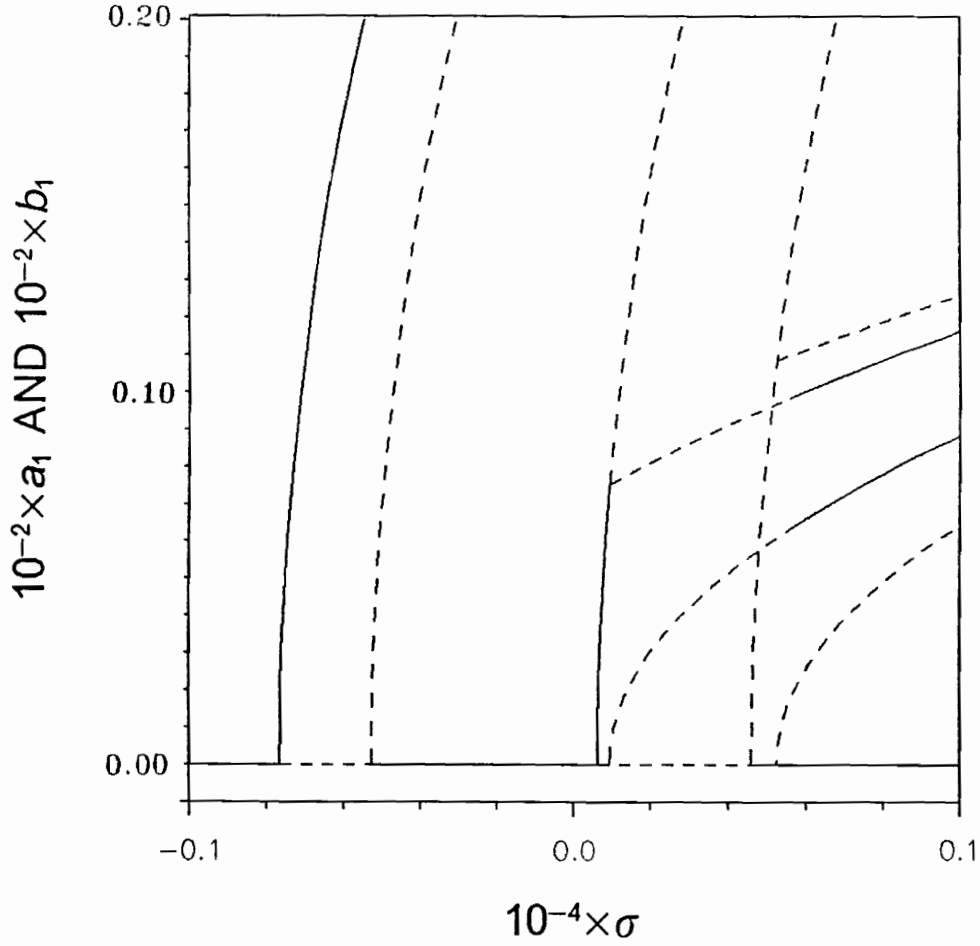

Figure 5.32 Response curves for subharmonic resonance of order two of the first mode. In-plane and out-of-plane components. f = 10W, $\delta = 0.002$.

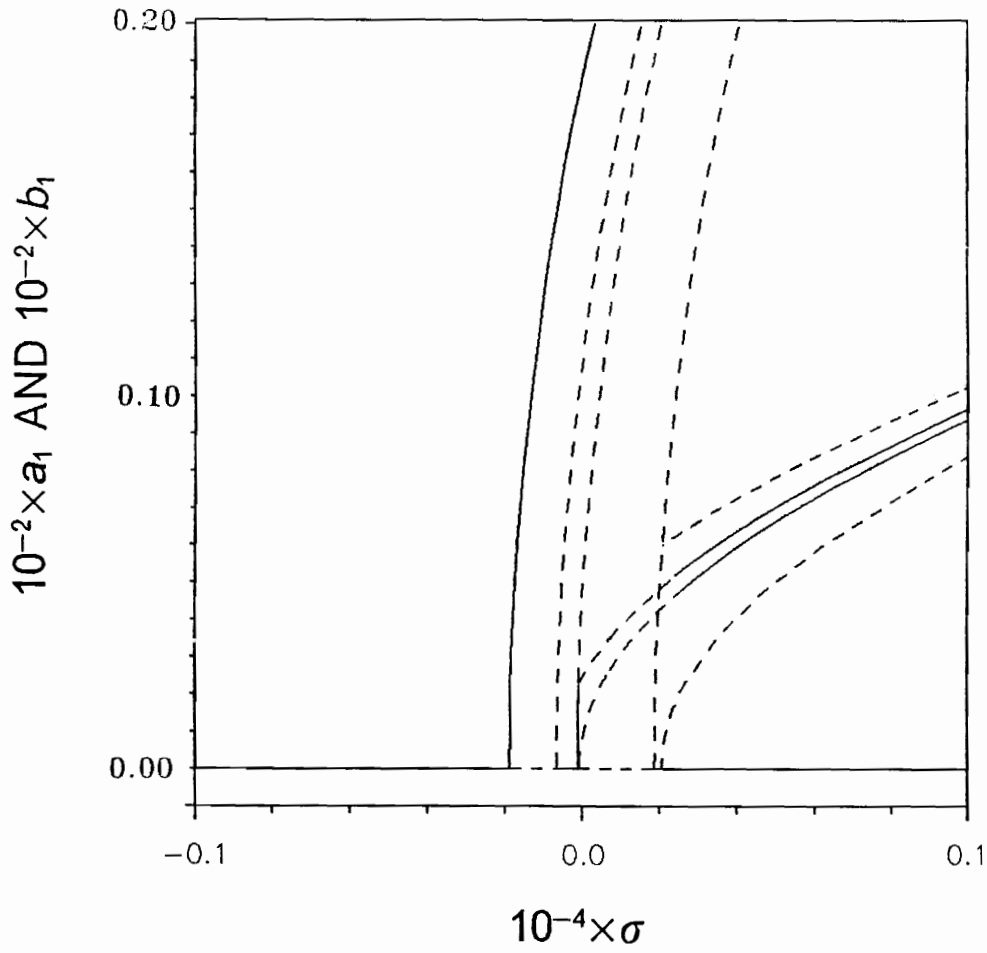

Figure 5.33 Response curves for subharmonic resonance of order two of the first mode. In-plane and out-of-plane components. f = 5W, $\delta = 0.0002$.

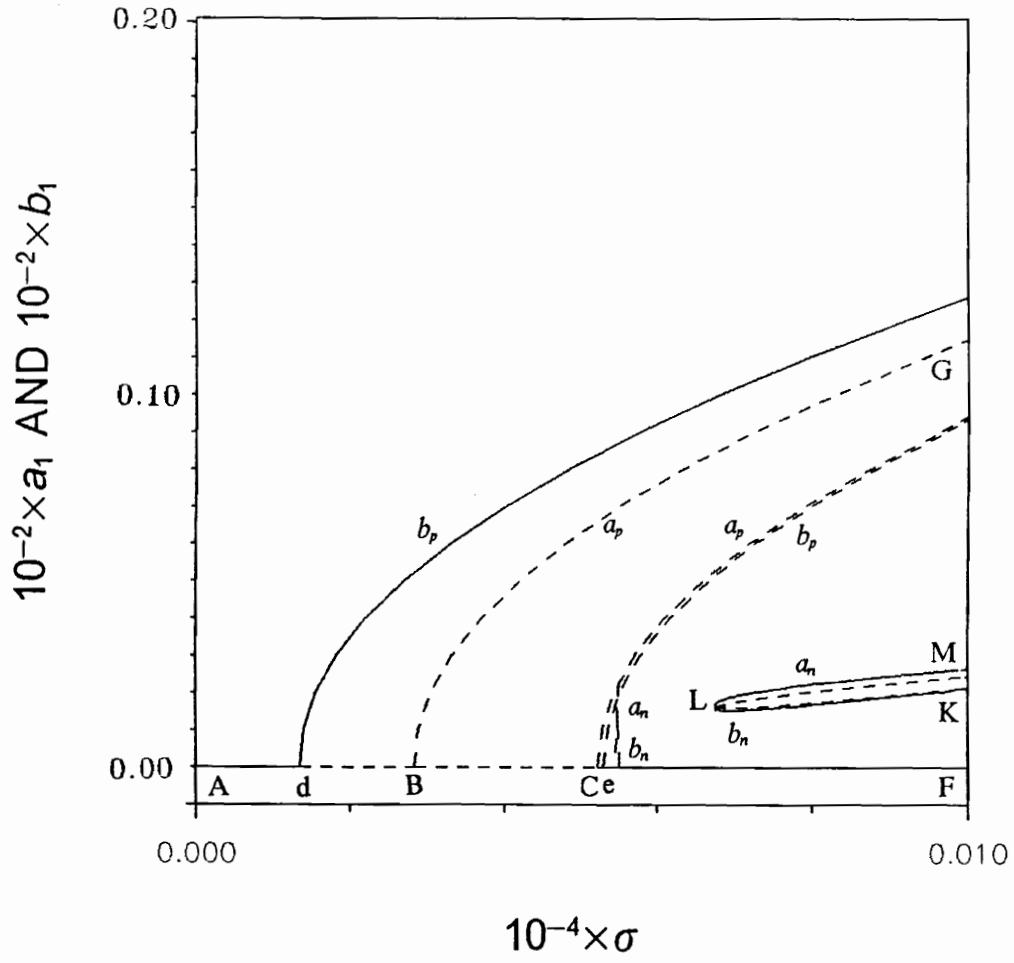

Figure 5.34 Response curves for subharmonic resonance of order two of the first mode. In-plane and out-of-plane components. f = W, $\delta = 0.0002$.

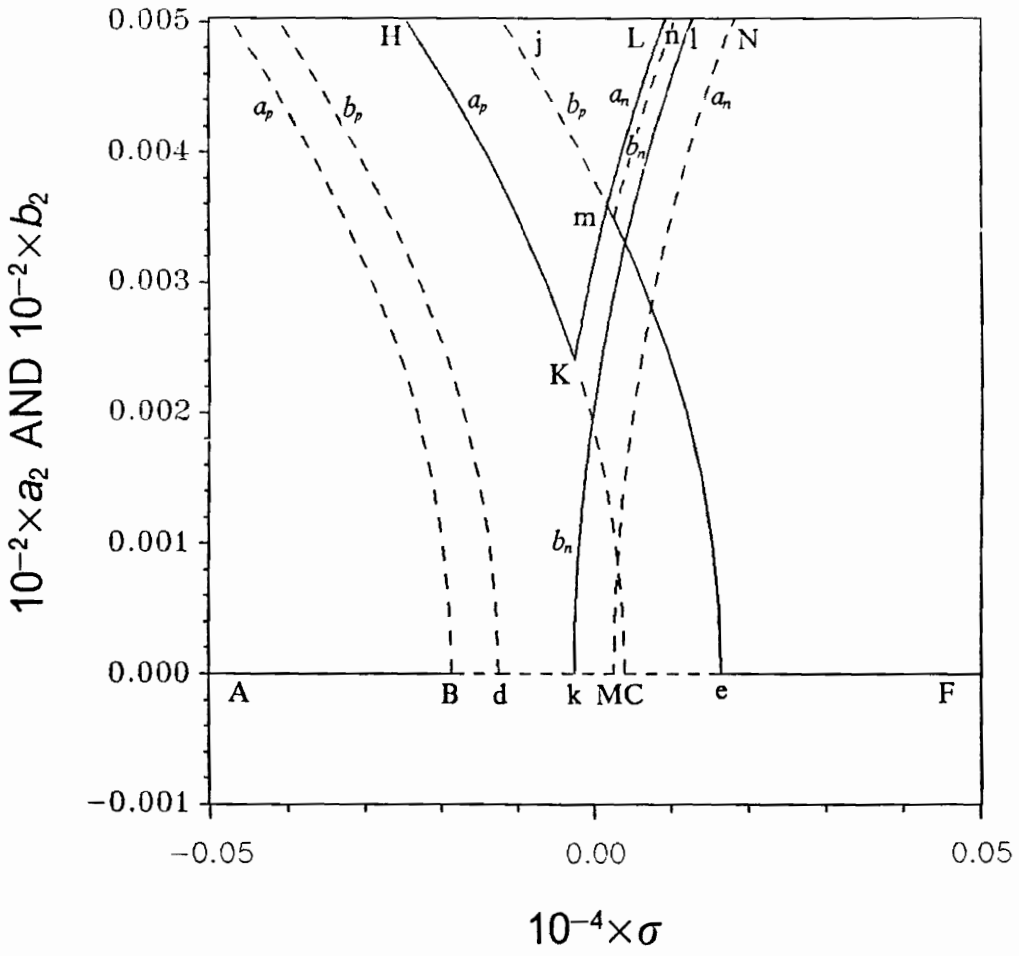

Figure 5.35 Response curves for subharmonic resonance of order two of the second mode. In-plane and out-of-plane components. f = 10W, $\delta = 0.0002$.

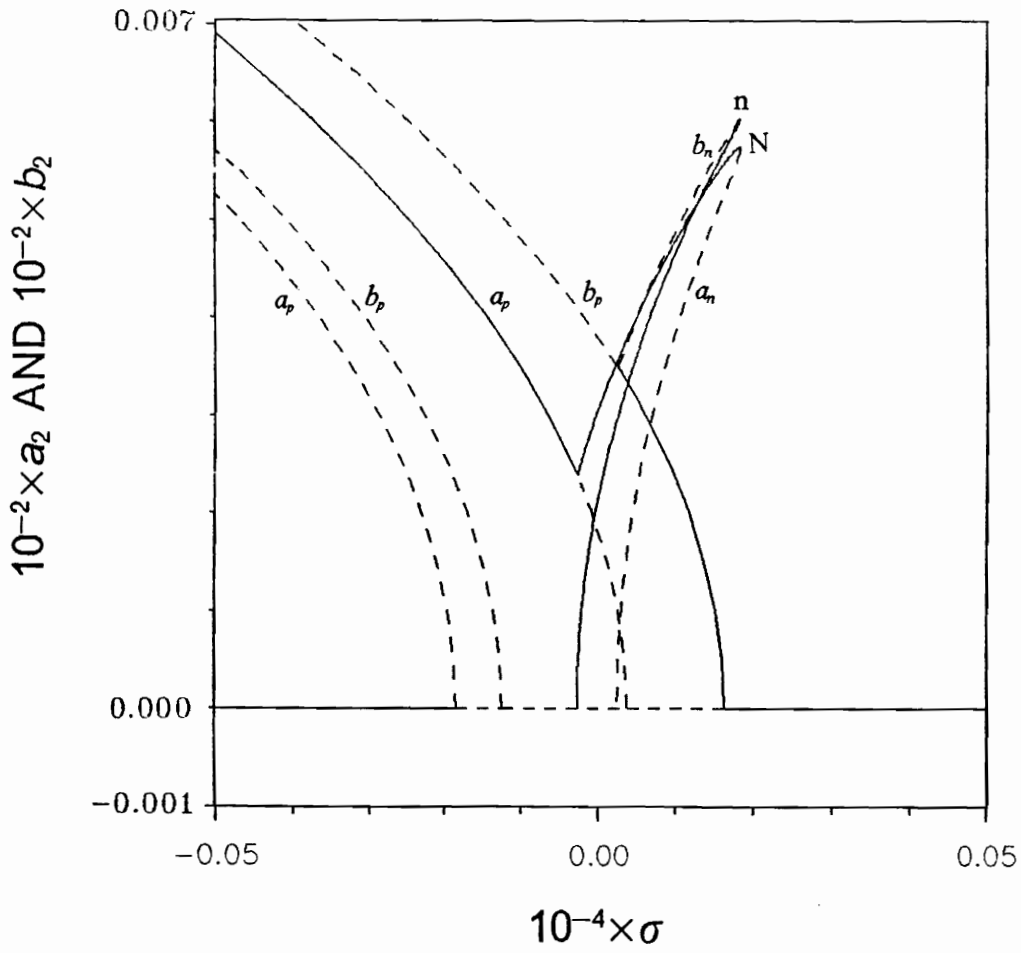

Figure 5.36 Response curves for subharmonic resonance of order two of the second mode. In-plane and out-of-plane components. f = 10W, $\delta = 0.002$.

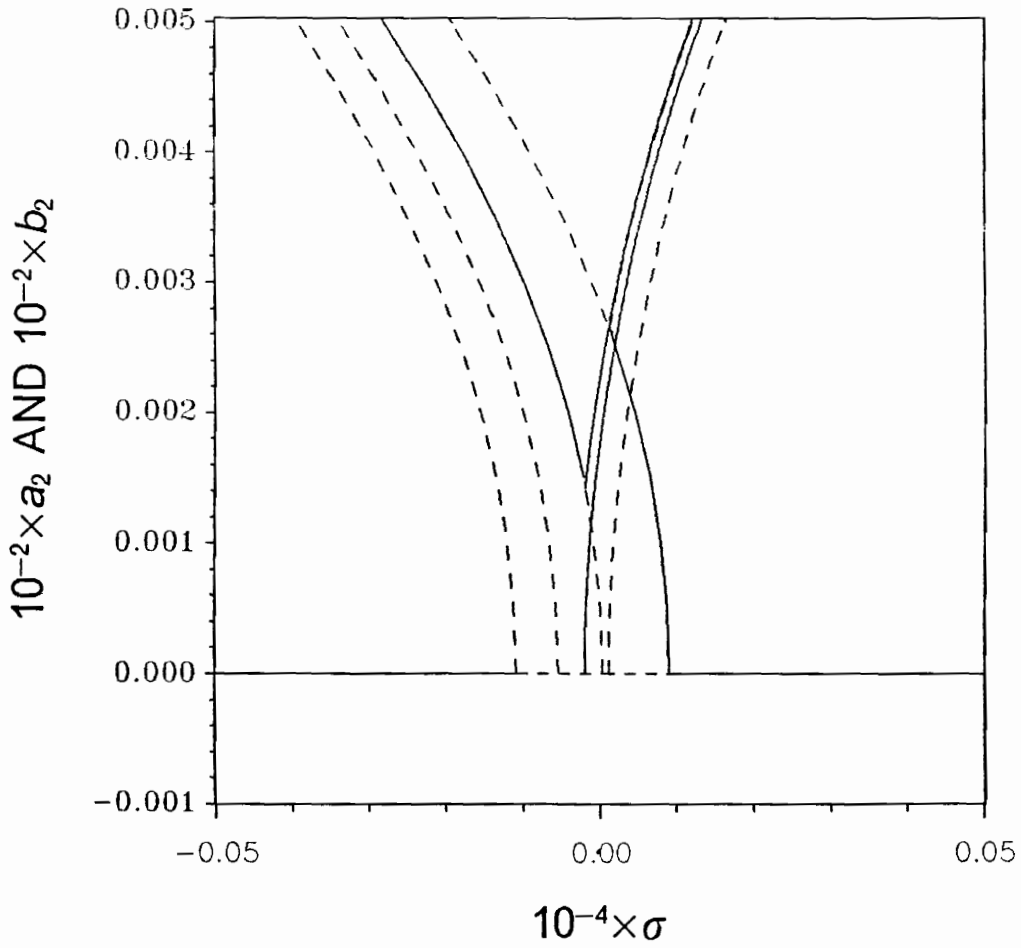

Figure 5.37 Response curves for subharmonic resonance of order two of the second mode. In-plane and out-of-plane components. f = 5W, $\delta = 0.0002$.

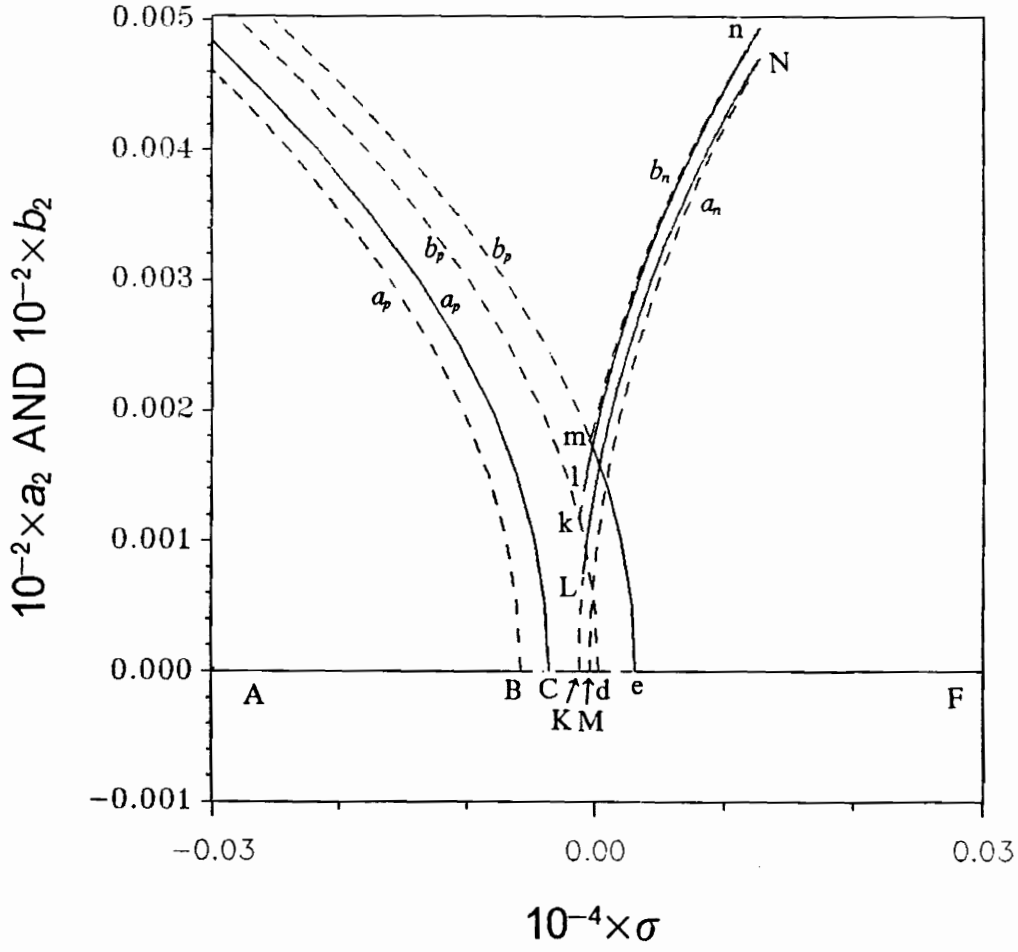

Figure 5.38 Response curves for subharmonic resonance of order two of the second mode. In-plane and out-of-plane components. f = W, $\delta = 0.0002$.

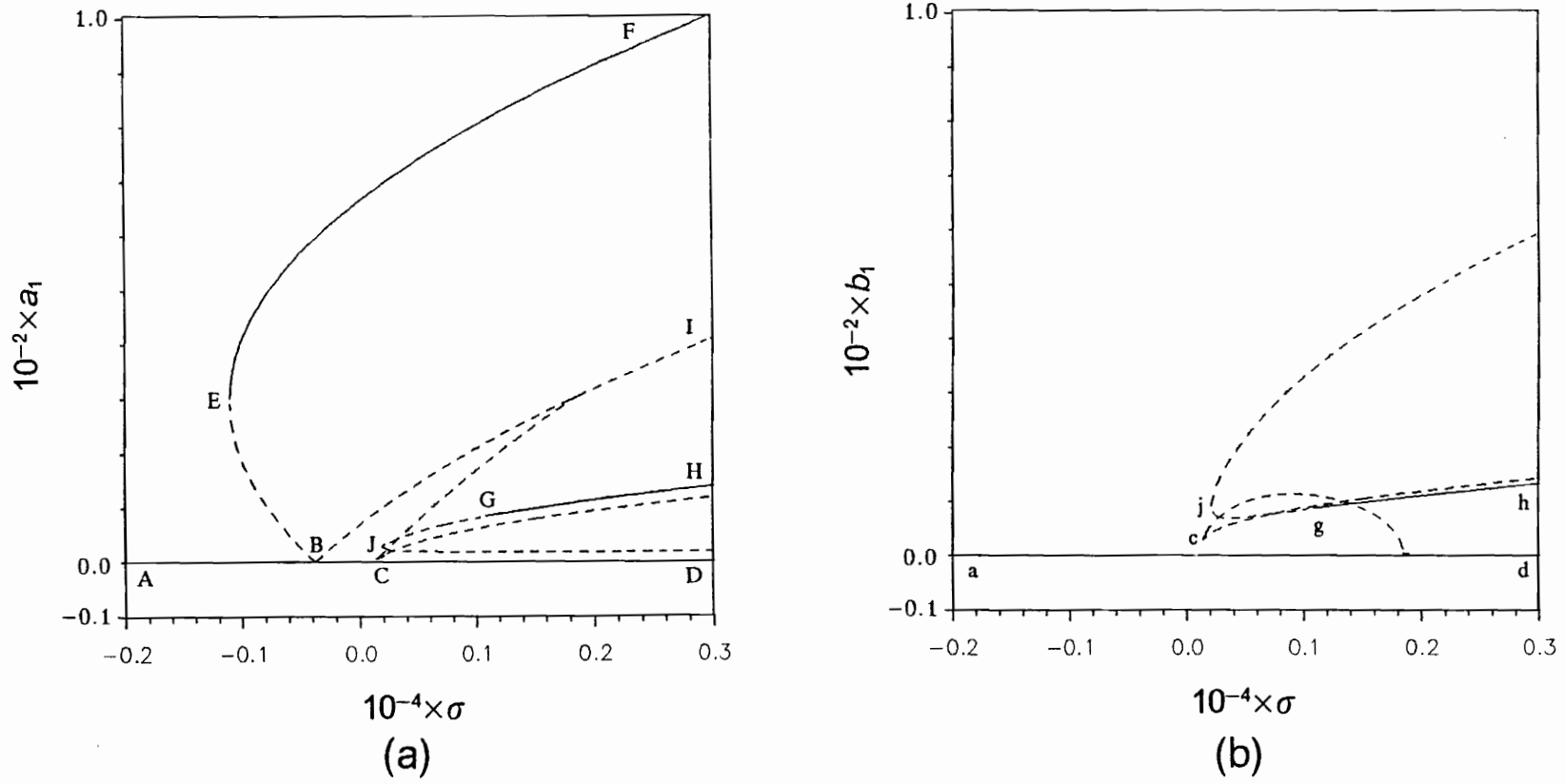

Figure 5.39 Response curves for subharmonic resonance of order three of the first mode. f = 10W, $\delta = 0.0002$; (a) in-plane component, (b) out-of-plane component.

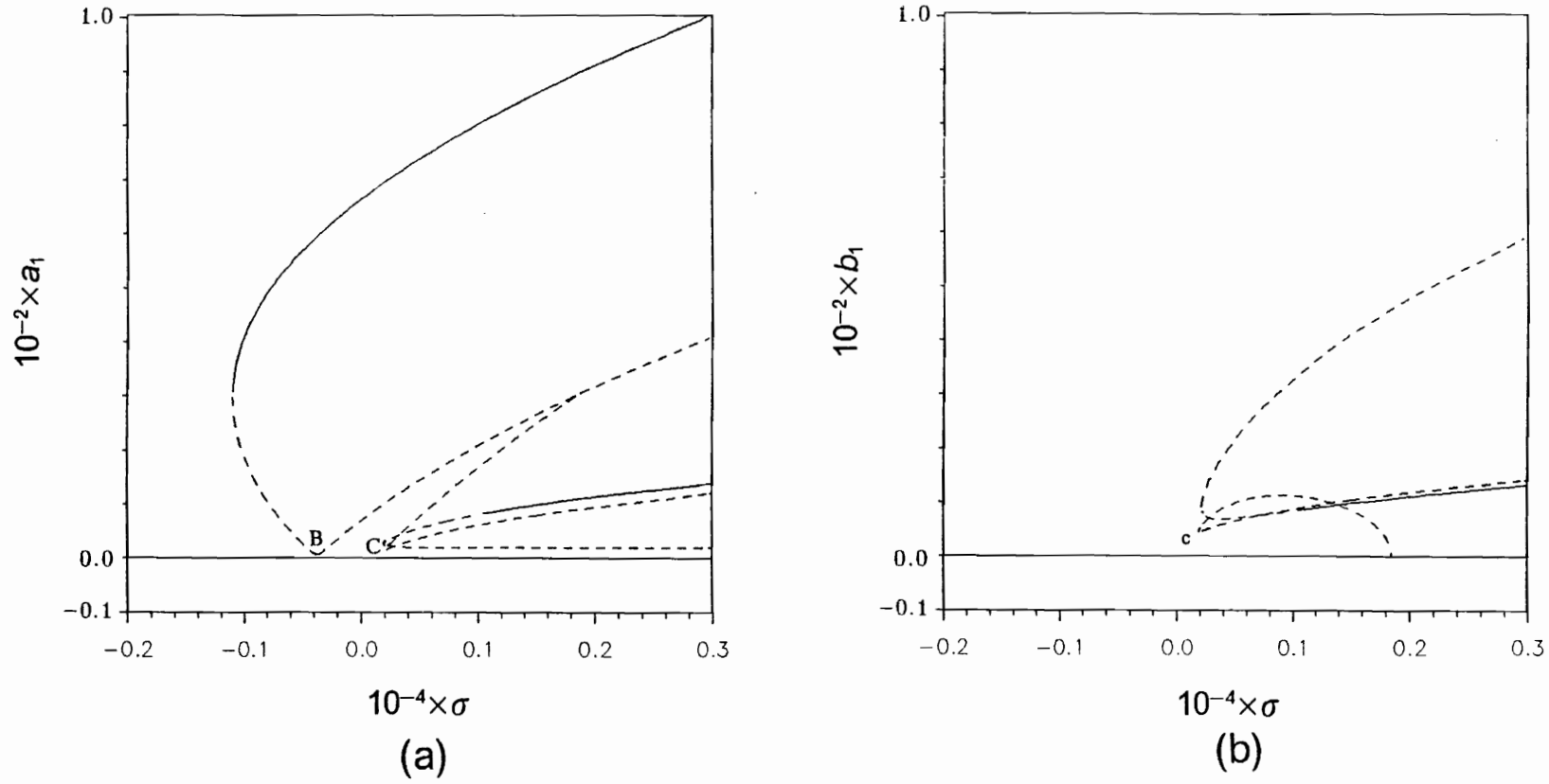

Figure 5.40 Response curves for subharmonic resonance of order three of the first mode. f = 10W, $\delta = 0.002$; (a) in-plane component, (b) out-of-plane component.

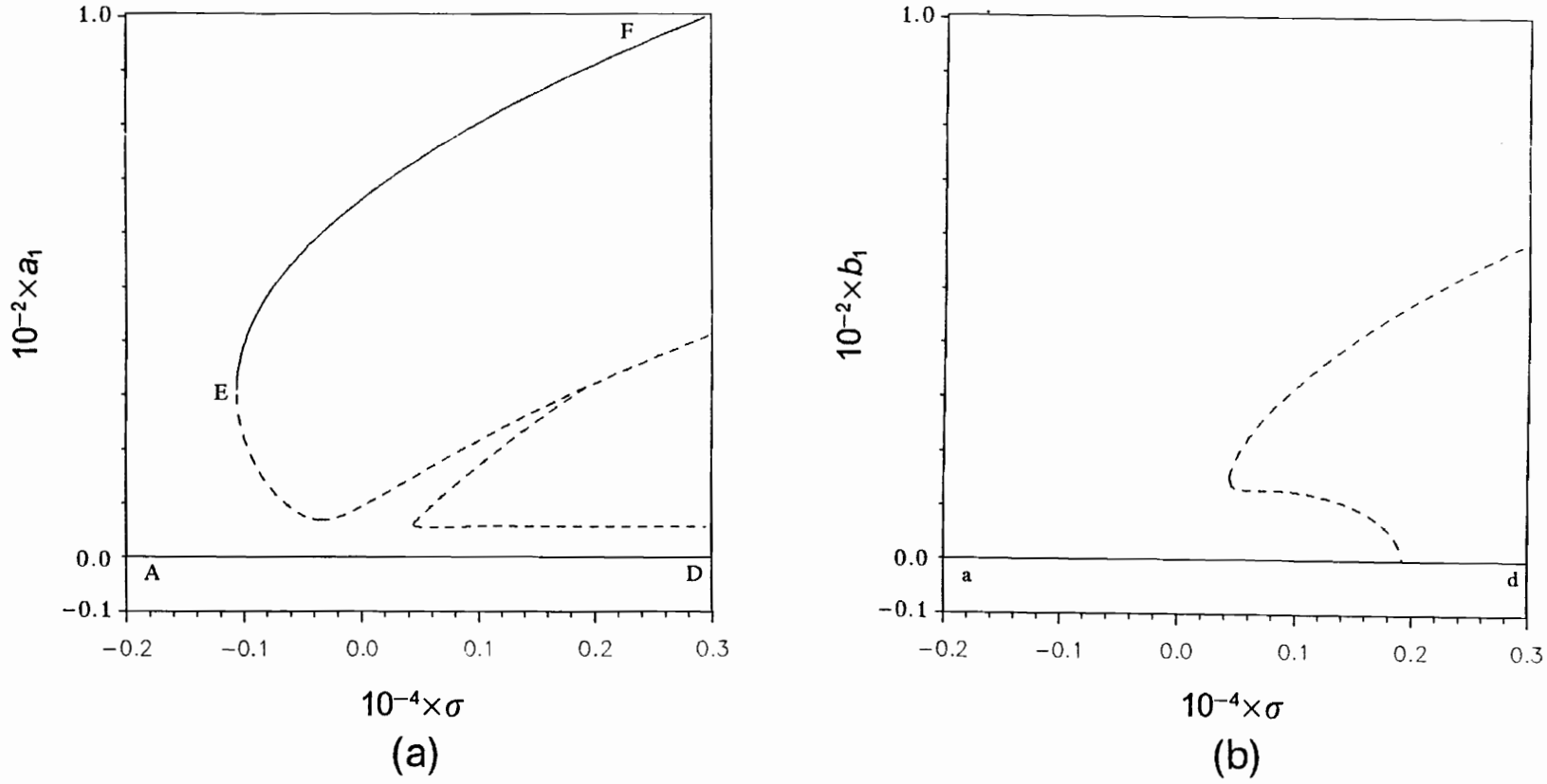

Figure 5.41 Response curves for subharmonic resonance of order three of the first mode. f = 10W, $\delta = 0.02$; (a) in-plane component, (b) out-of-plane component.

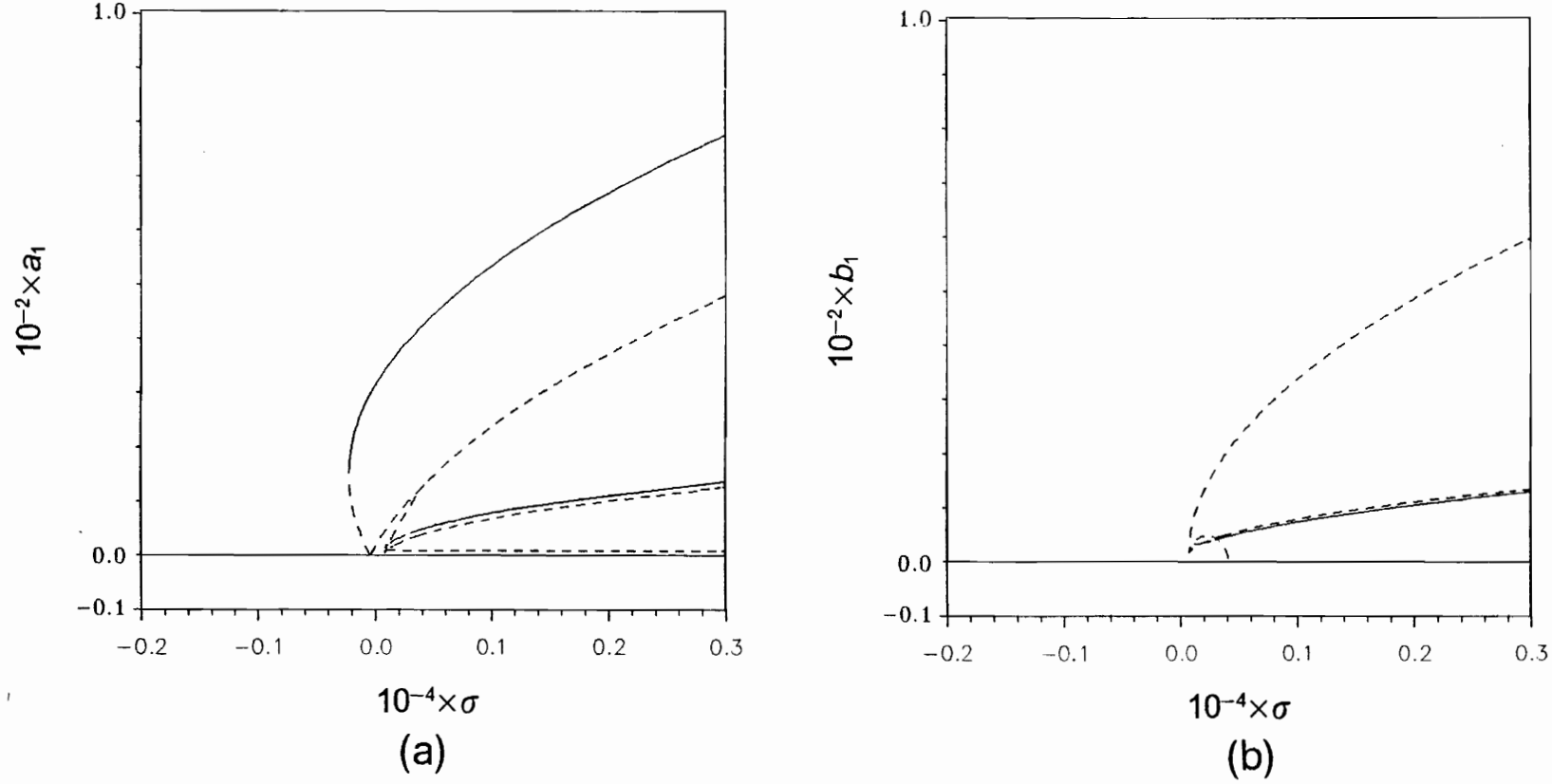

Figure 5.42 Response curves for subharmonic resonance of order three of the first mode. f = 5W, $\delta = 0.0002$; (a) in-plane component, (b) out-of-plane component.

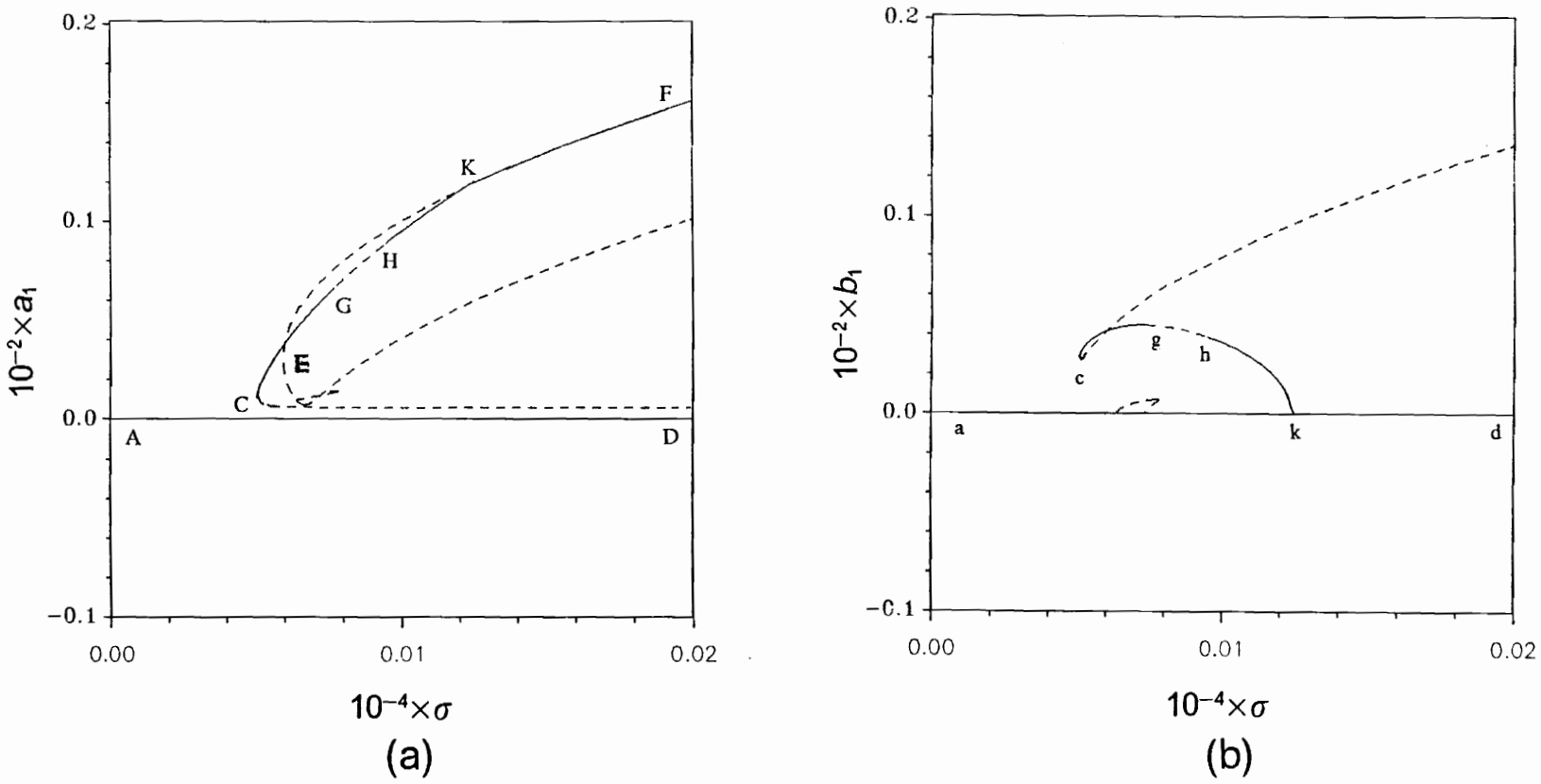

Figure 5.43 Response curves for subharmonic resonance of order three of the first mode. f = W, $\delta = 0.0002$; (a) in-plane component, (b) out-of-plane component.

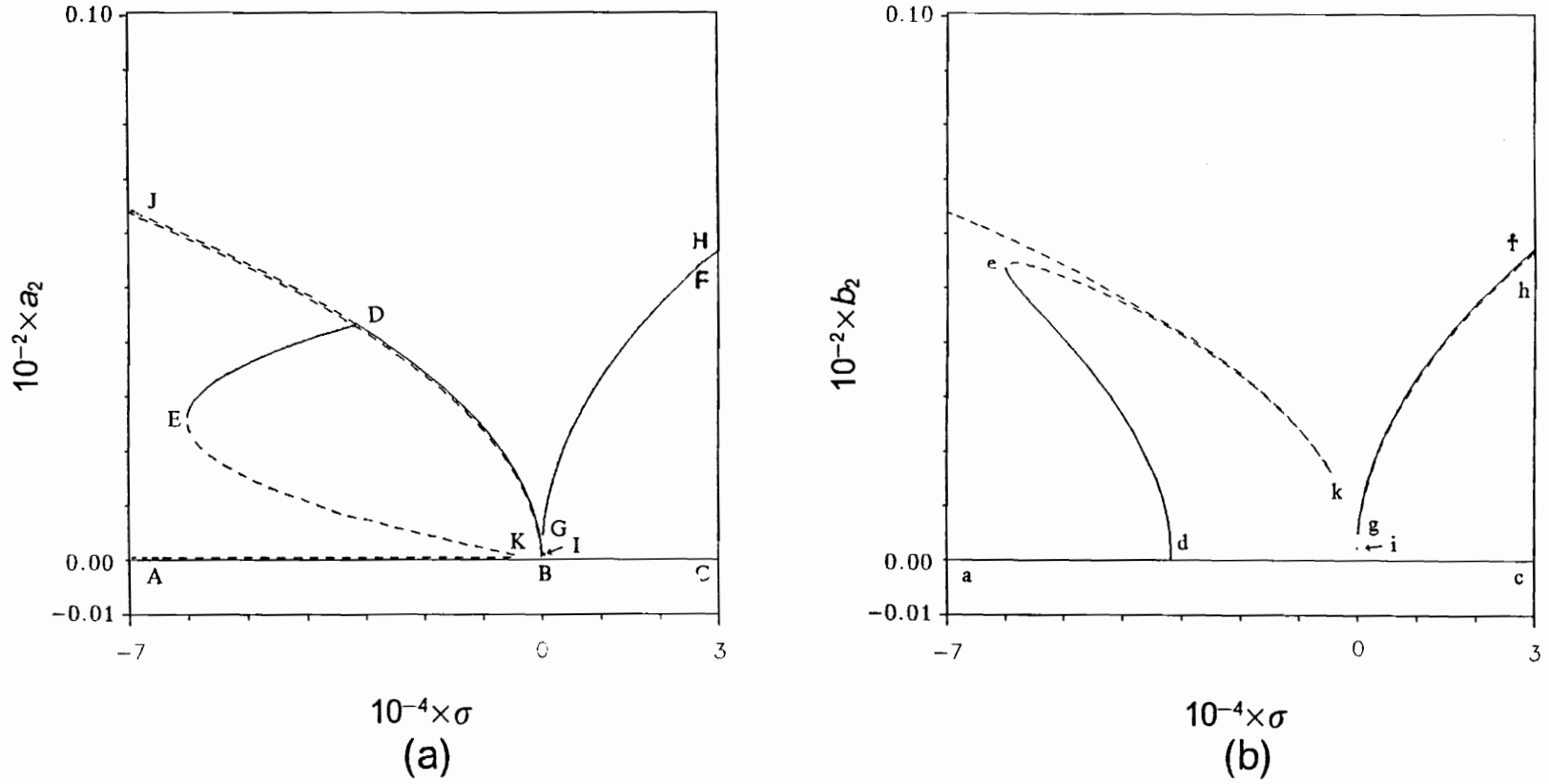

Figure 5.44 Response curves for subharmonic resonance of order three of the second mode. f = 10W, $\delta = 0.0002$; (a) in-plane component, (b) out-of-plane component.

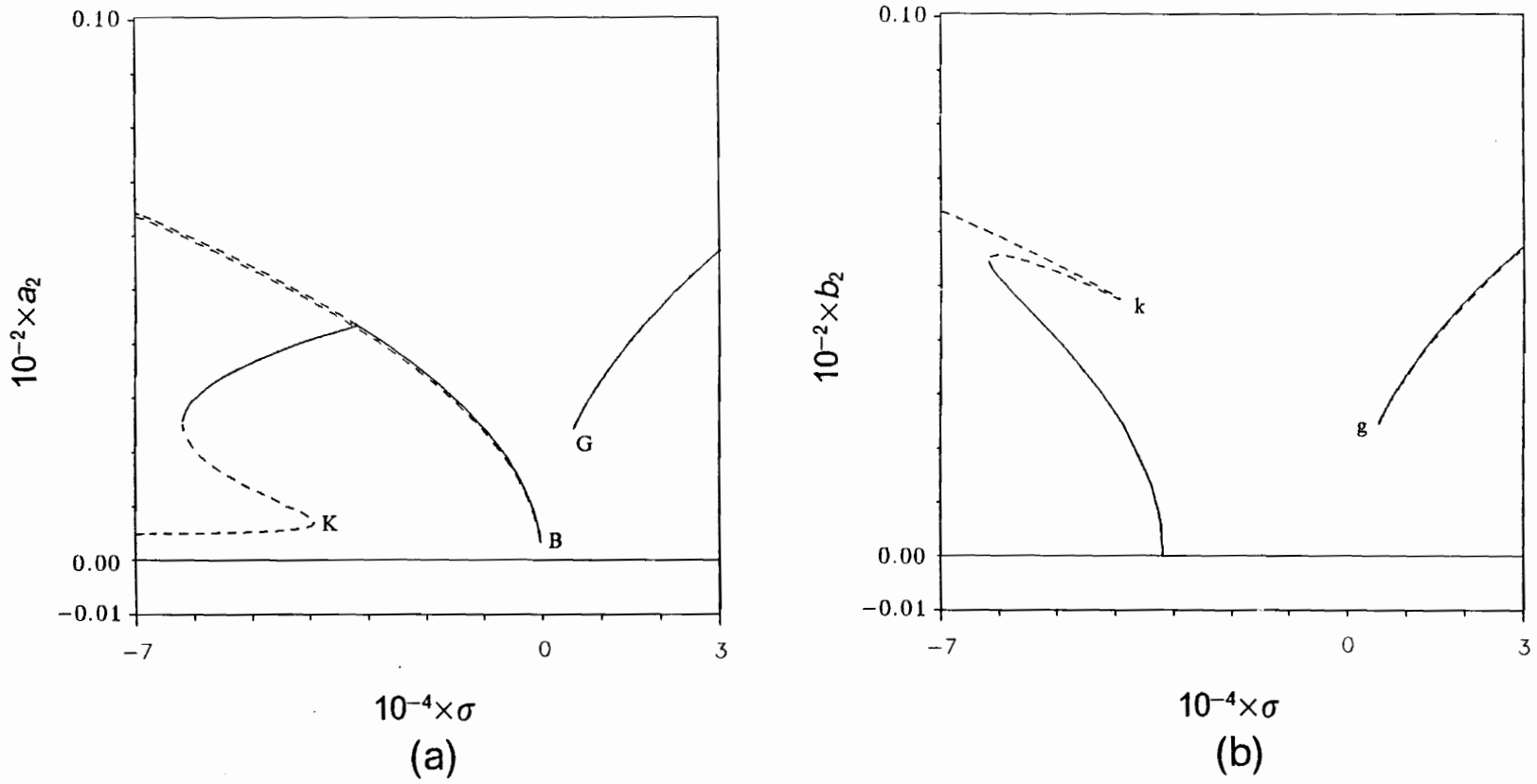

Figure 5.45 Response curves for subharmonic resonance of order three of the second mode. f = 10W, $\delta = 0.002$; (a) in-plane component, (b) out-of-plane component.

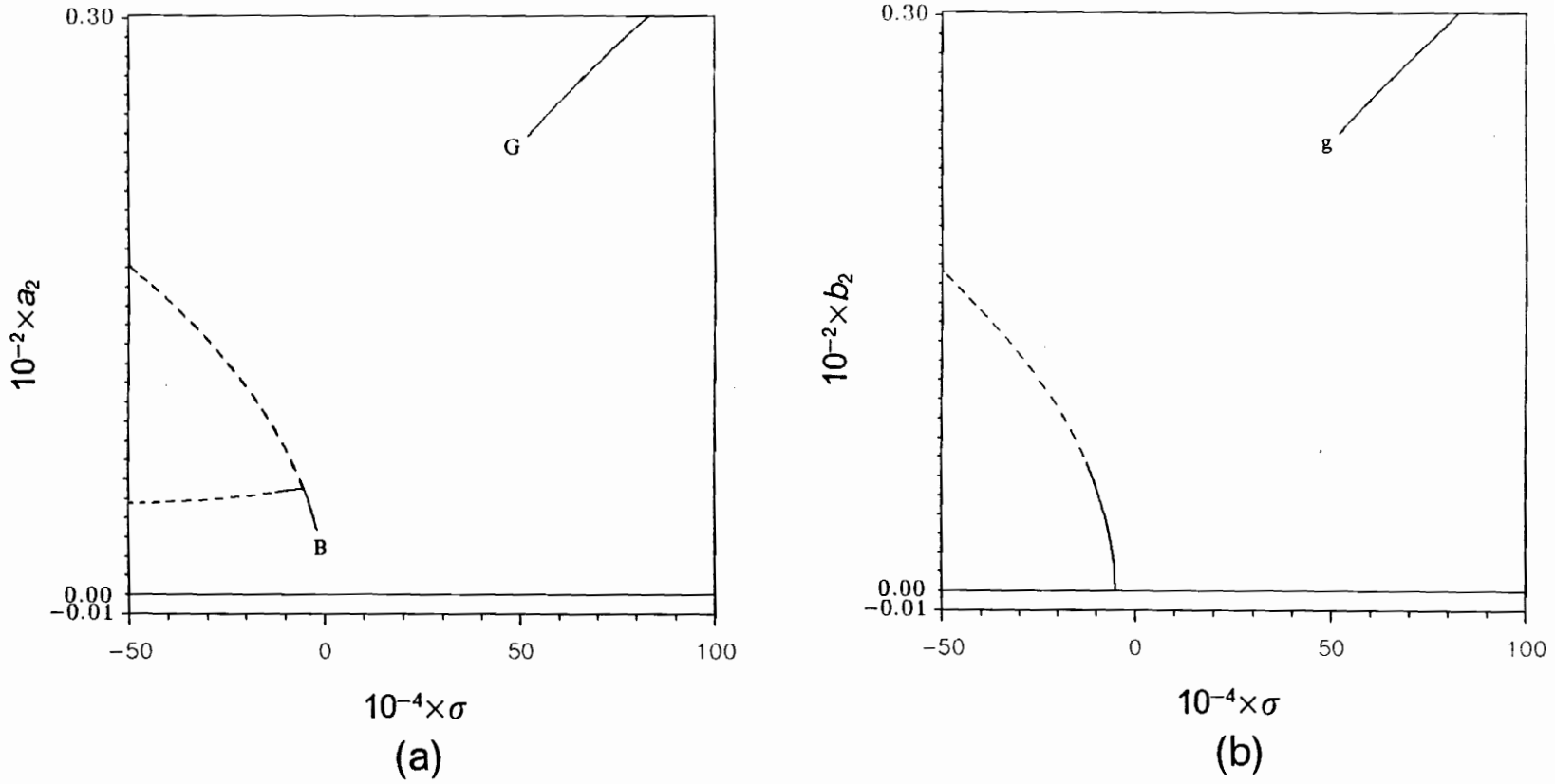

Figure 5.46 Response curves for subharmonic resonance of order three of the second mode. f = 10W, $\delta = 0.02$; (a) in-plane component, (b) out-of-plane component.

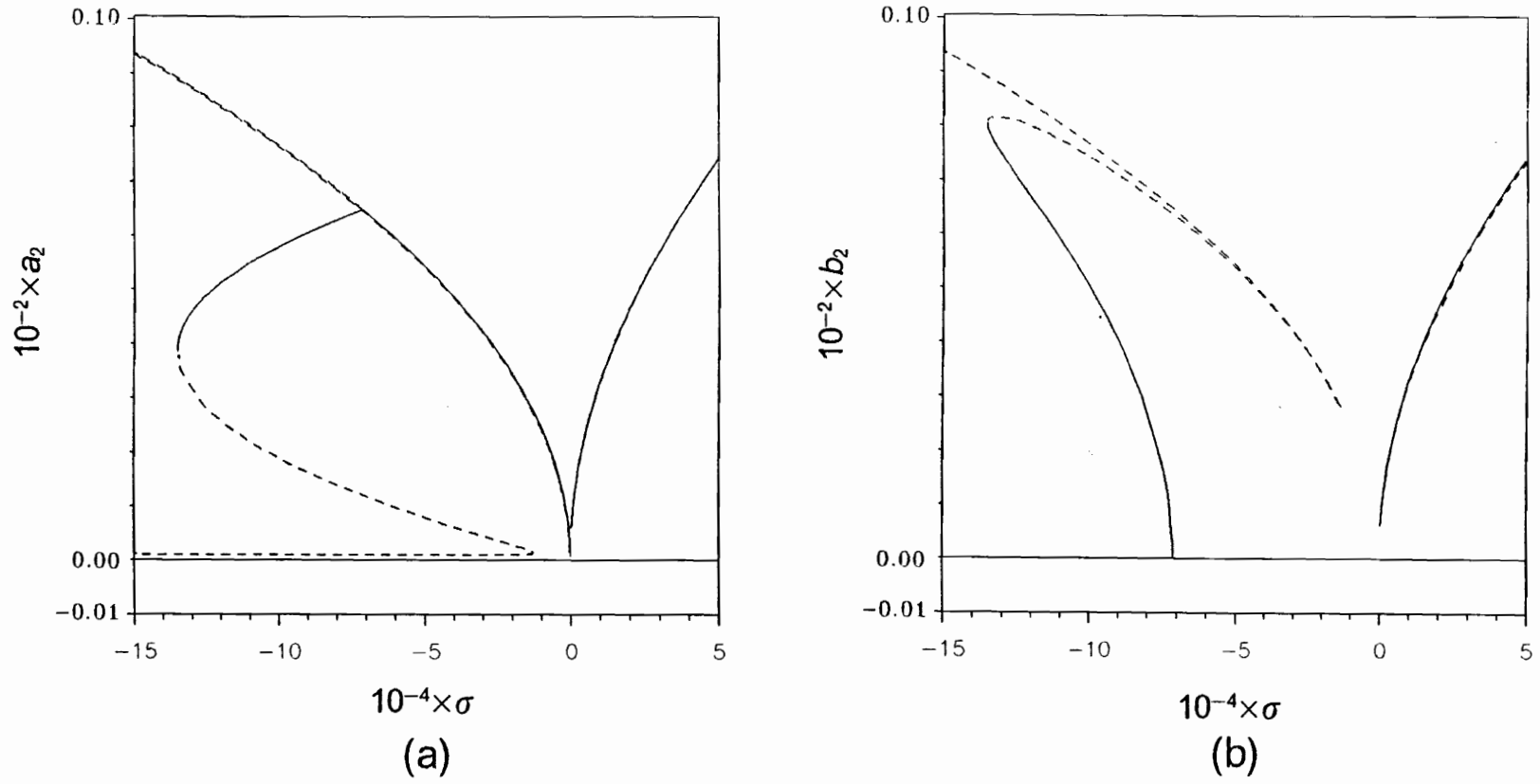

Figure 5.47 Response curves for subharmonic resonance of order three of the second mode. f = 5W, $\delta = 0.0002$; (a) in-plane component, (b) out-of-plane component.

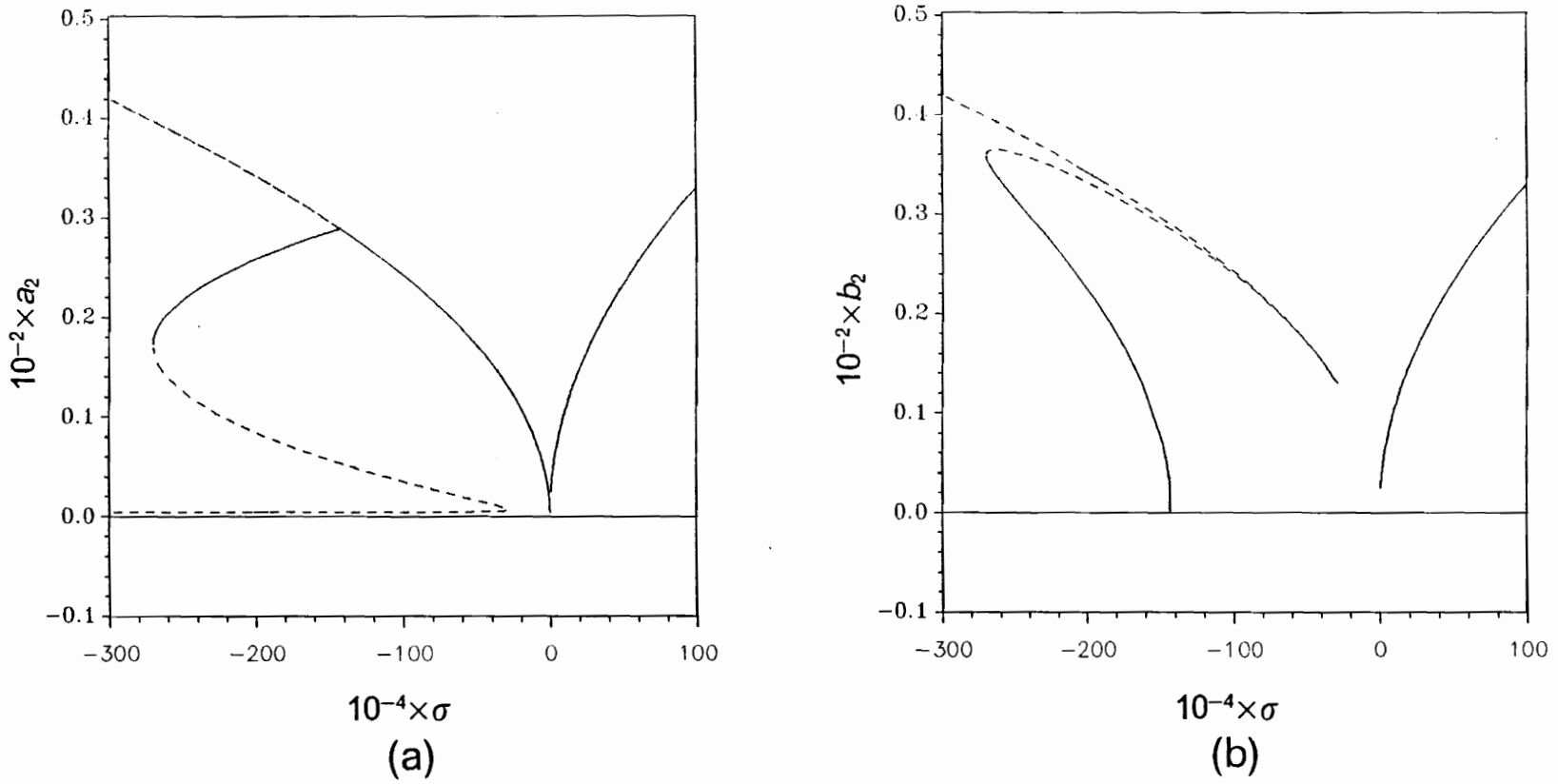

Figure 5.48 Response curves for subharmonic resonance of order three of the second mode. f = W, $\delta = 0.0002$; (a) in-plane component, (b) out-of-plane component.

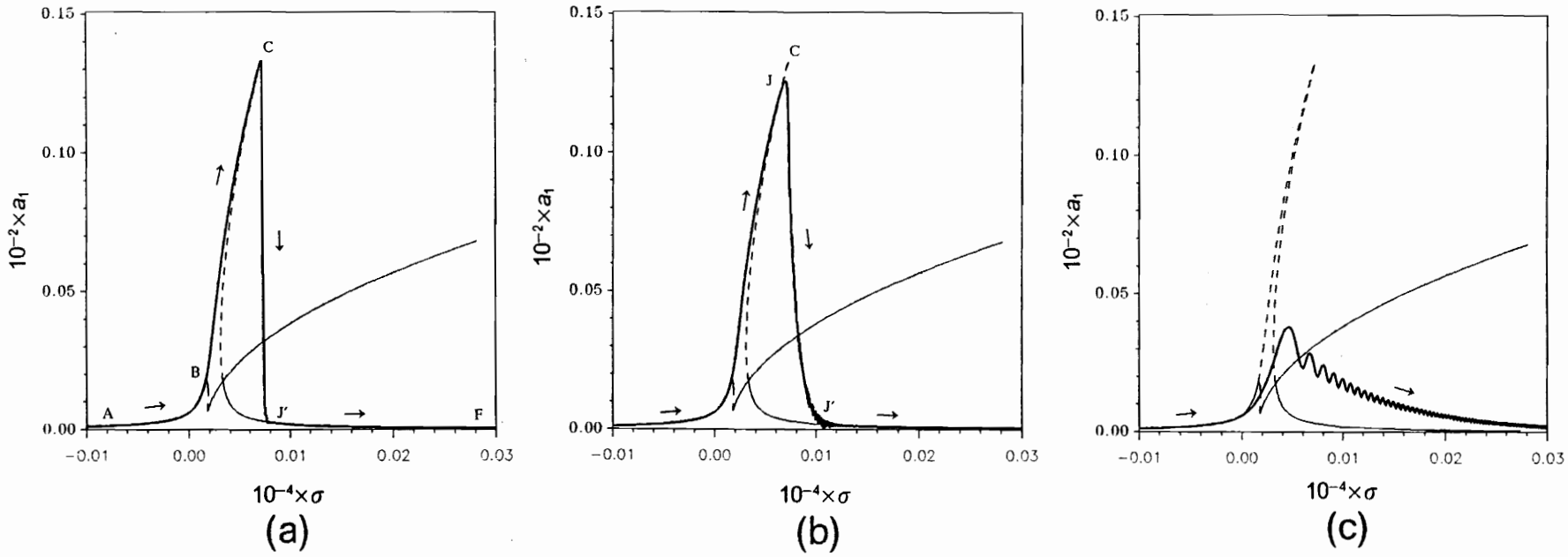

Figure 5.49 Comparison of non-stationary and stationary responses of the first mode for primary resonance with three sweep rates (acceleration). f = 0.0005W, $\delta = 0.0002$, $\hat{\varepsilon}a_0 = 0.0001$, $\hat{\varepsilon}b_0 = \gamma_0 = \psi_0 = 0$; (a) $\lambda = 1\times10^{-8}$, (b) $\lambda = 1\times10^{-7}$, (c) $\lambda = 1\times10^{-6}$.

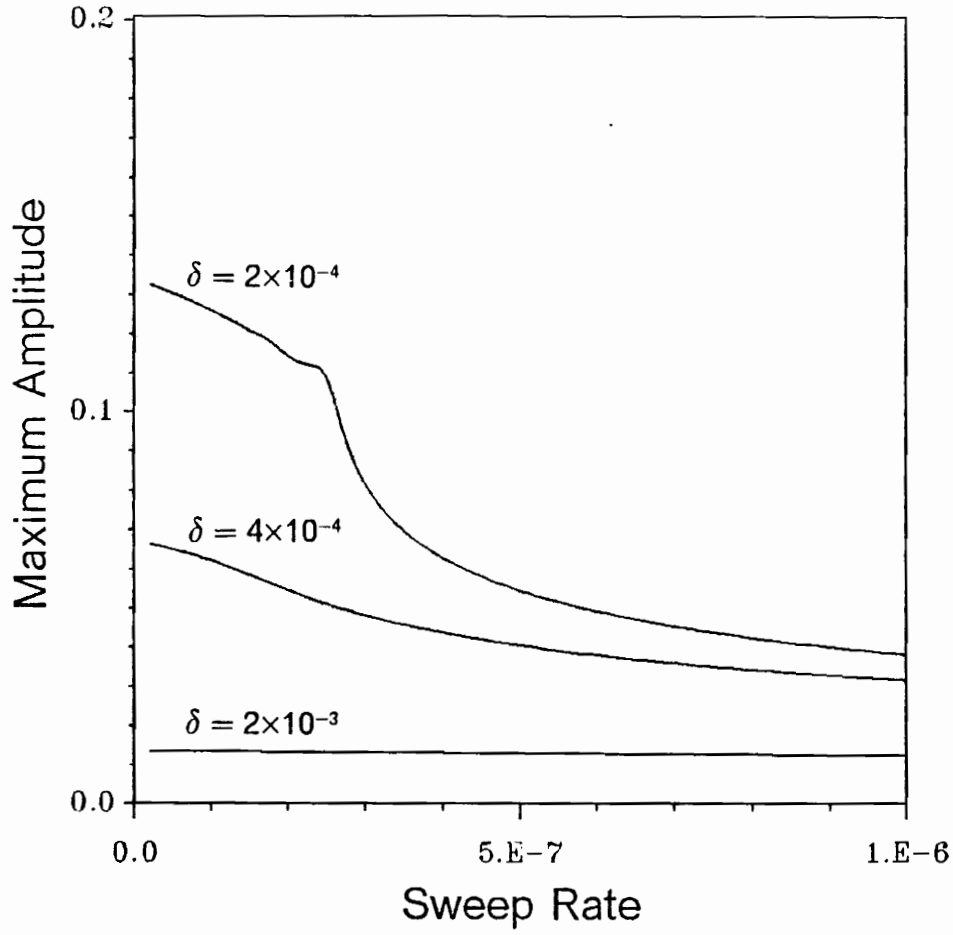

Figure 5.50 Dependence of the maximum amplitude on the sweep rate (acceleration) with three damping coefficients. First mode, primary resonance, f = 0.0005W, $\hat{\varepsilon}a_0 = 0.0001$, $\hat{\varepsilon}b_0 = \gamma_0 = \psi_0 = 0$.

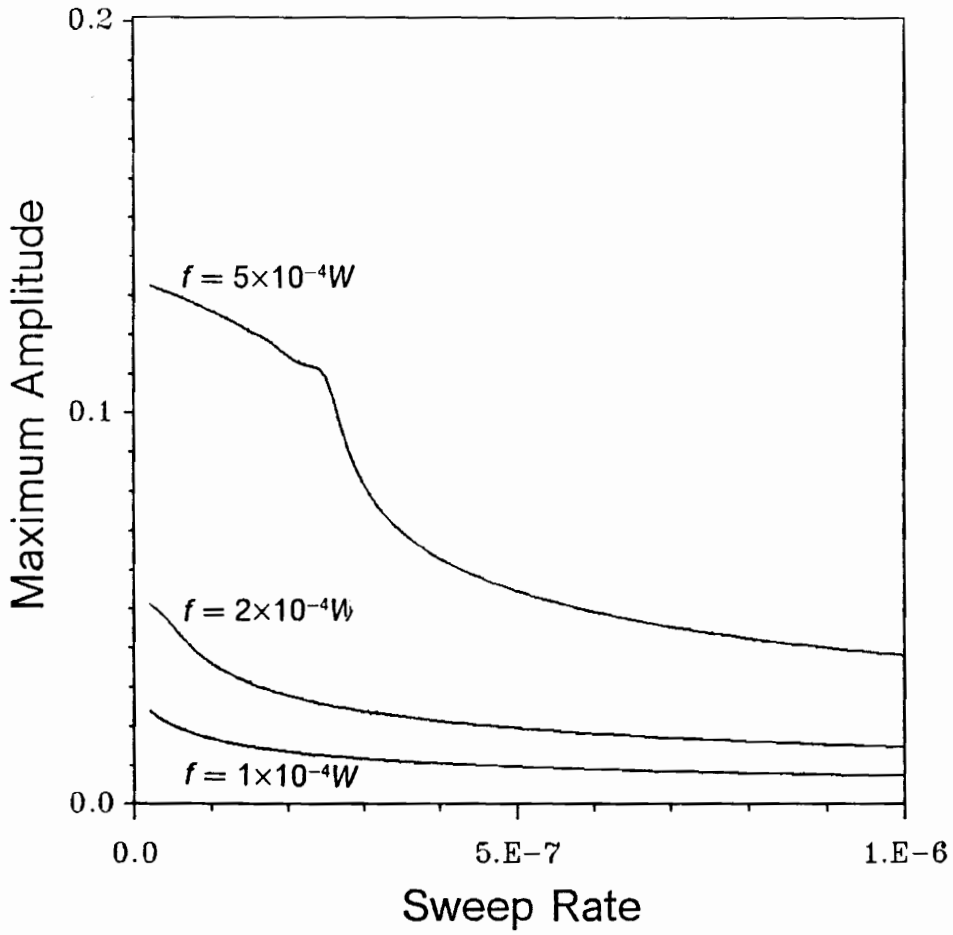

Figure 5.51 Dependence of the maximum amplitude on the sweep rate (acceleration) with three force levels. First mode, primary resonance, $\delta = 0.0002$, $\hat{\varepsilon}a_0 = 0.0001$, $\hat{\varepsilon}b_0 = \gamma_0 = \psi_0 = 0$.

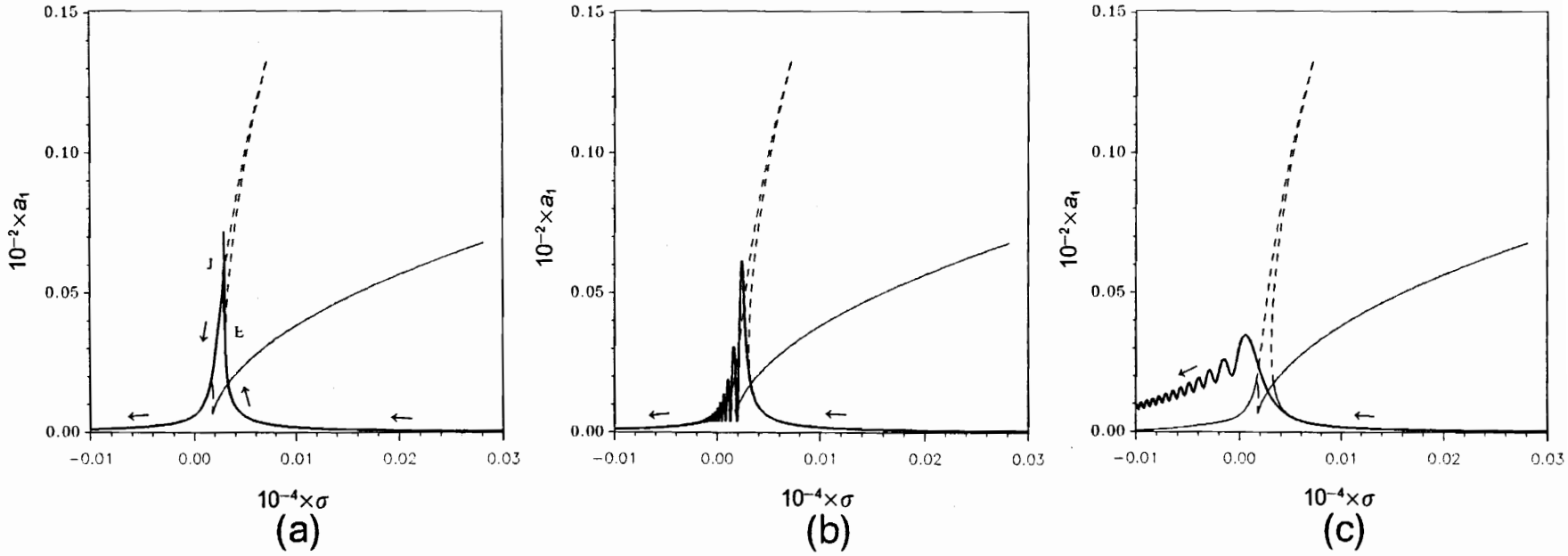

Figure 5.52 Comparison of non-stationary and stationary responses of the first mode for primary resonance with three sweep rates (deceleration). f = 0.0005W, $\delta = 0.0002$, $\hat{\varepsilon}a_0 = 0.0001$, $\hat{\varepsilon}b_0 = \gamma_0 = \psi_0 = 0$; (a) $\lambda = -1\times10^{-8}$, (b) $\lambda = -1\times10^{-7}$, (c) $\lambda = -1\times10^{-6}$.

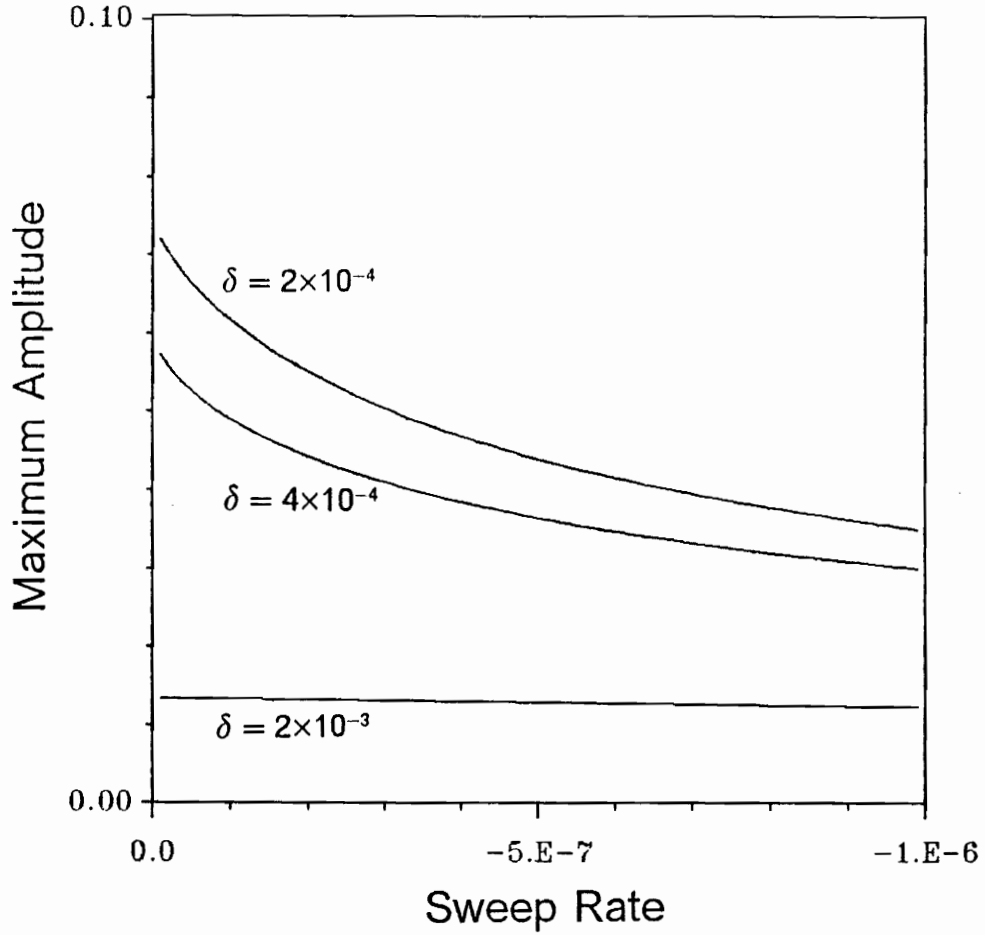

Figure 5.53 Dependence of the maximum amplitude on the sweep rate (deceleration) with three damping coefficients. First mode, primary resonance, f = 0.0005W, $\hat{\varepsilon}a_0 = 0.0001$, $\hat{\varepsilon}b_0 = \gamma_0 = \psi_0 = 0$.

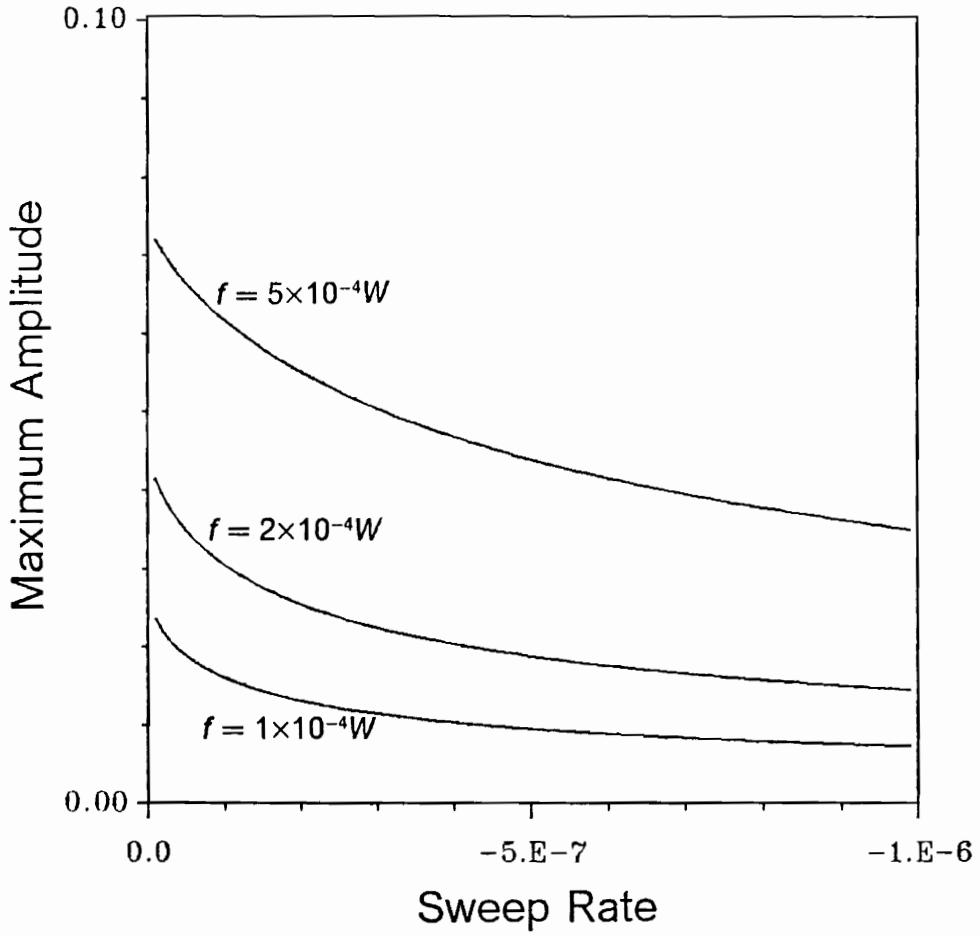

Figure 5.54 Dependence of the maximum amplitude on the sweep rate (deceleration) with three force levels. First mode, primary resonance, $\delta = 0.0002$, $\hat{\varepsilon}a_0 = 0.0001$, $\hat{\varepsilon}b_0 = \gamma_0 = \psi_0 = 0$.

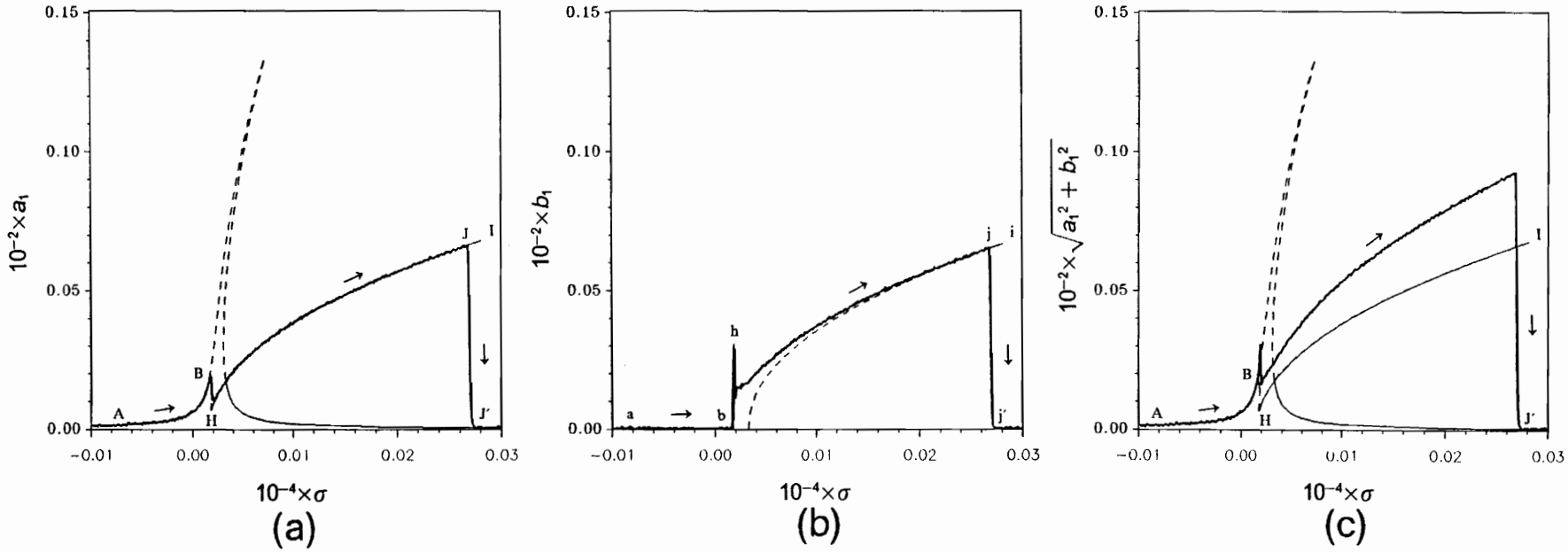

Figure 5.55 Comparison of non-stationary response subjected to persistent random disturbance and stationary response for sweep rate $\lambda = 1\times10^{-8}$. First mode, primary resonance, bound of the disturbance = 0.0001, f = 0.0005W, $\delta = 0.0002$, $\hat{\varepsilon}a_0 = 0.0001$, $\hat{\varepsilon}b_0 = \gamma_0 = \psi_0 = 0$; (a) in-plane component, (b) out-of-plane component, (c) total amplitude.

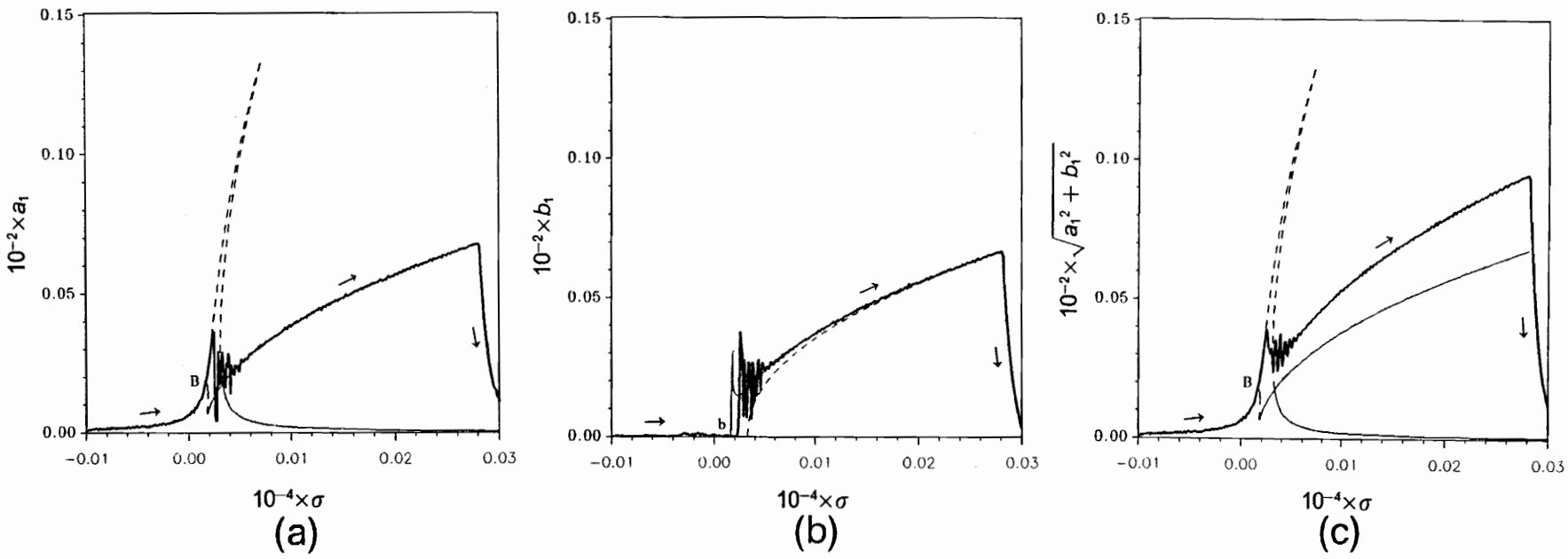

Figure 5.56 Comparison of non-stationary response subjected to persistent random disturbance and stationary response for sweep rate $\lambda = 1\times10^{-7}$. First mode, primary resonance, bound of the disturbance = 0.0001, f = 0.0005W, $\delta = 0.0002$, $\hat{\varepsilon}a_0 = 0.0001$, $\hat{\varepsilon}b_0 = \gamma_0 = \psi_0 = 0$; (a) in-plane component, (b) out-of-plane component, (c) total amplitude.

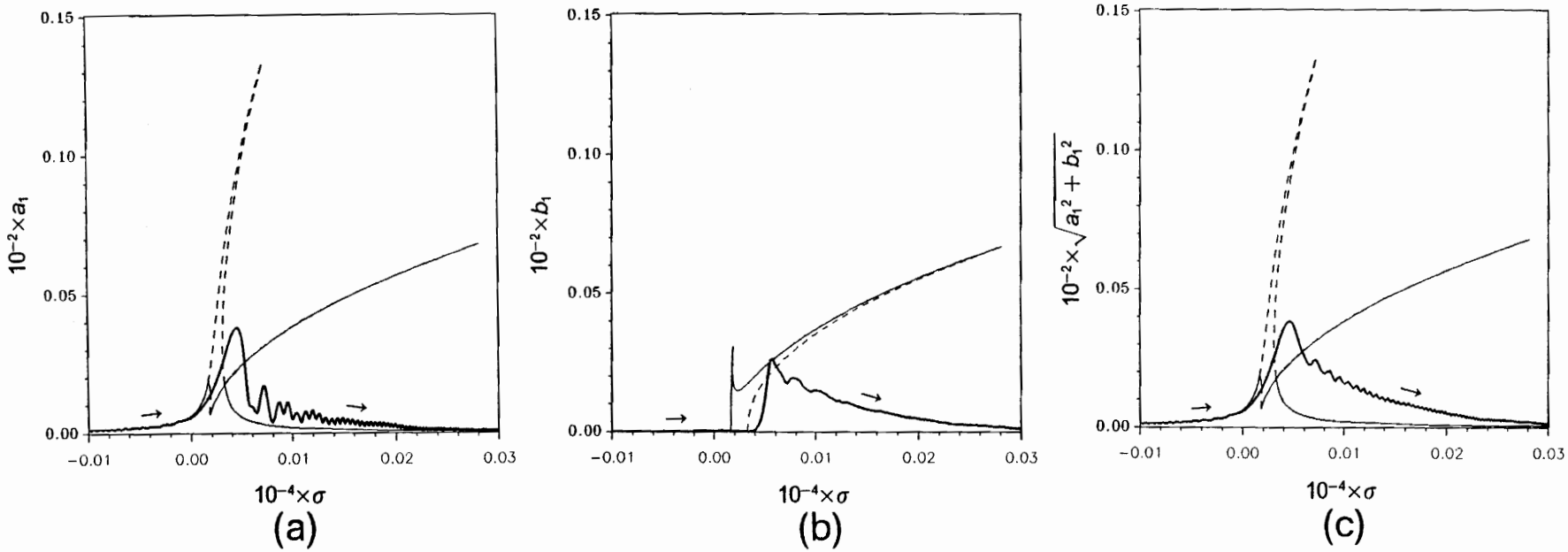

Figure 5.57 Comparison of non-stationary response subjected to persistent random disturbance and stationary response for sweep rate $\lambda = 1\times10^{-6}$. First mode, primary resonance, bound of the disturbance = 0.0001, f = 0.0005W, $\delta = 0.0002$, $\hat{\varepsilon}a_0 = 0.0001$, $\hat{\varepsilon}b_0 = \gamma_0 = \psi_0 = 0$; (a) in-plane component, (b) out-of-plane component, (c) total amplitude.

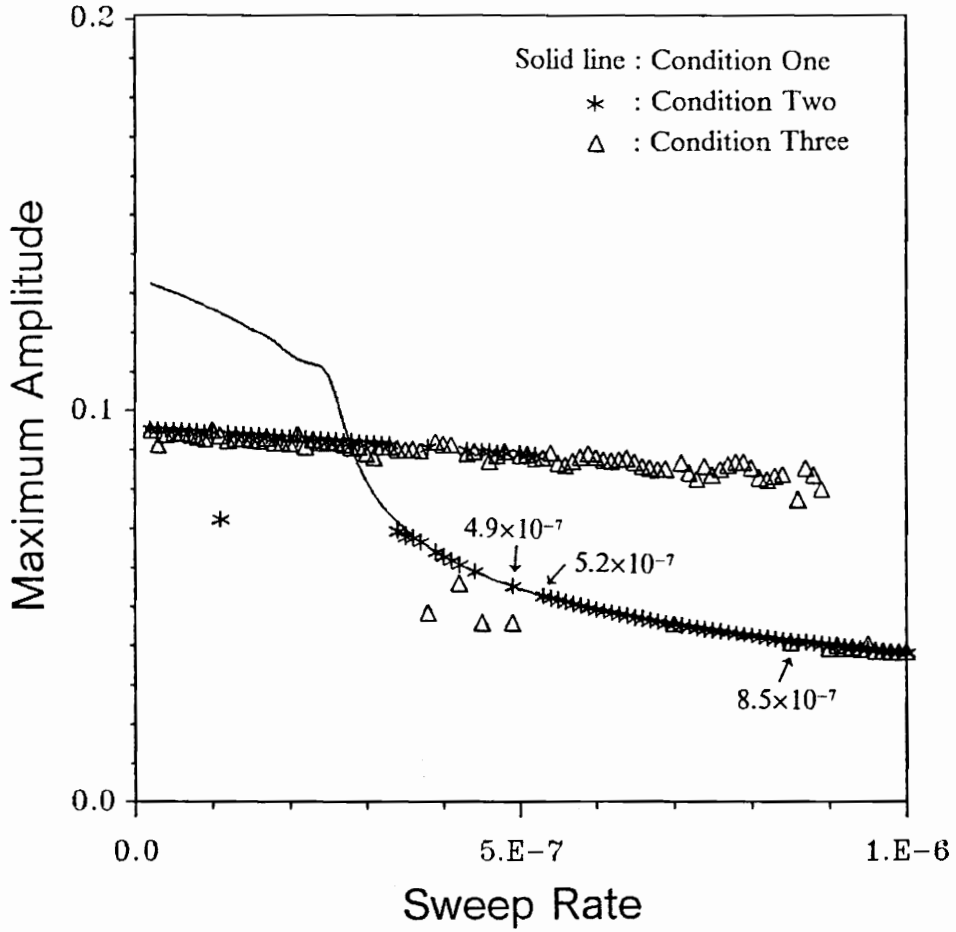

Figure 5.58 Dependence of the maximum amplitude on the sweep rate (acceleration) under three conditions. First mode, primary resonance, f = 0.0005W, $\delta = 0.0002$.

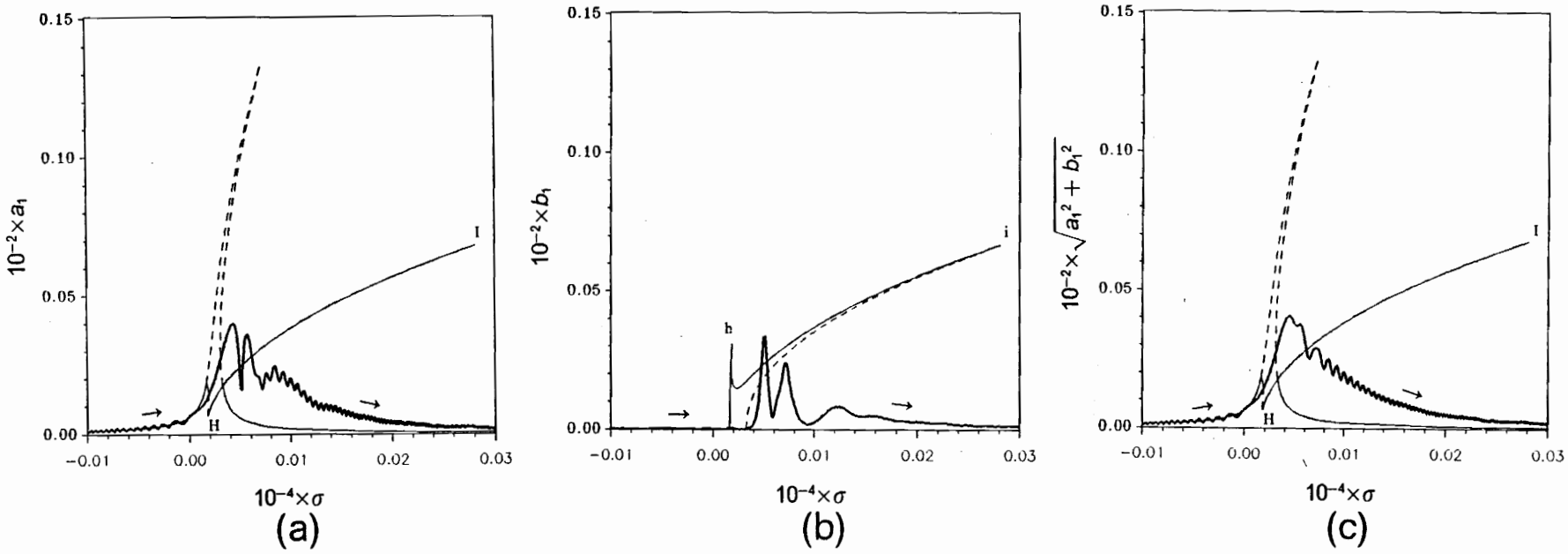

Figure 5.59 Comparison of non-stationary response subjected to persistent random disturbance and stationary response for sweep rate $\lambda = 1\times8.5^{-7}$. First mode, primary resonance, bound of the disturbance = 0.0001, f = 0.0005W, $\delta = 0.0002$, $\hat{\varepsilon}a_0 = 0.0001$, $\hat{\varepsilon}b_0 = \gamma_0 = \psi_0 = 0$; (a) in-plane component, (b) out-of-plane component, (c) total amplitude.

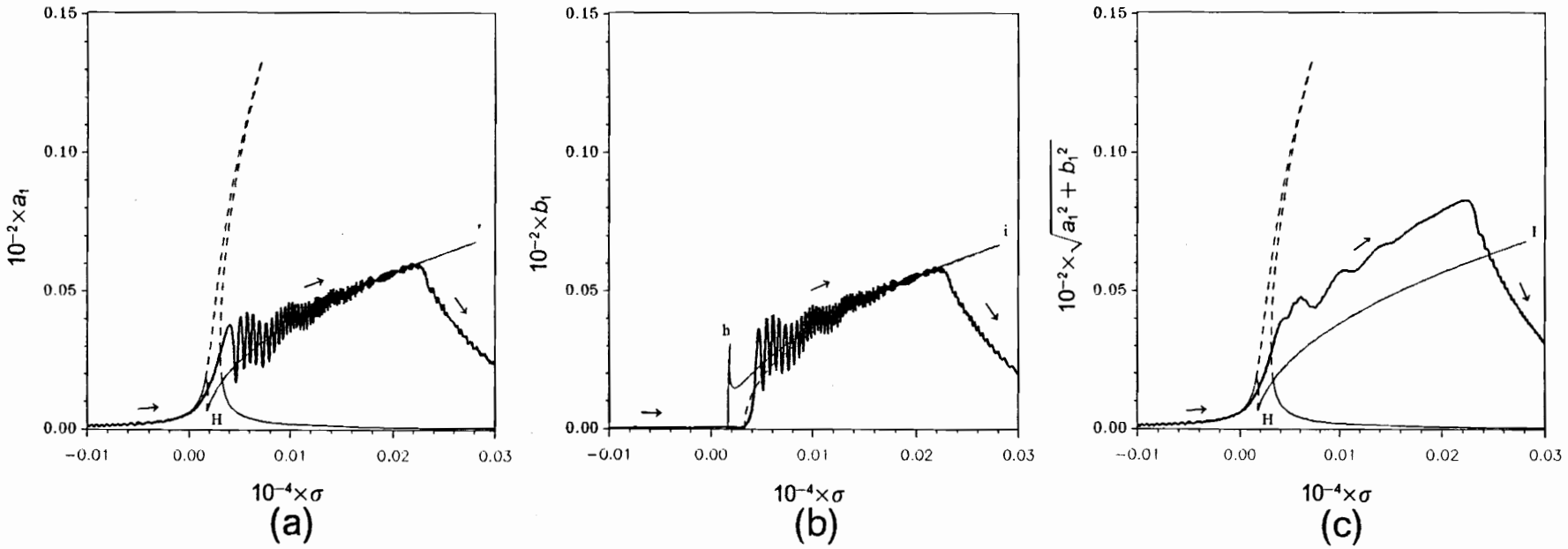

Figure 5.60 Comparison of non-stationary response subjected to persistent random disturbance (with different random sequence from that in Figure 5.59) and stationary response for sweep rate $\lambda = 1\times8.5^{-7}$. First mode, primary resonance, bound of the disturbance = 0.0001, f = 0.0005W, $\delta = 0.0002$, $\hat{\varepsilon}a_0 = 0.0001$, $\hat{\varepsilon}b_0 = \gamma_0 = \psi_0 = 0$; (a) in-plane component, (b) out-of-plane component, (c) total amplitude.

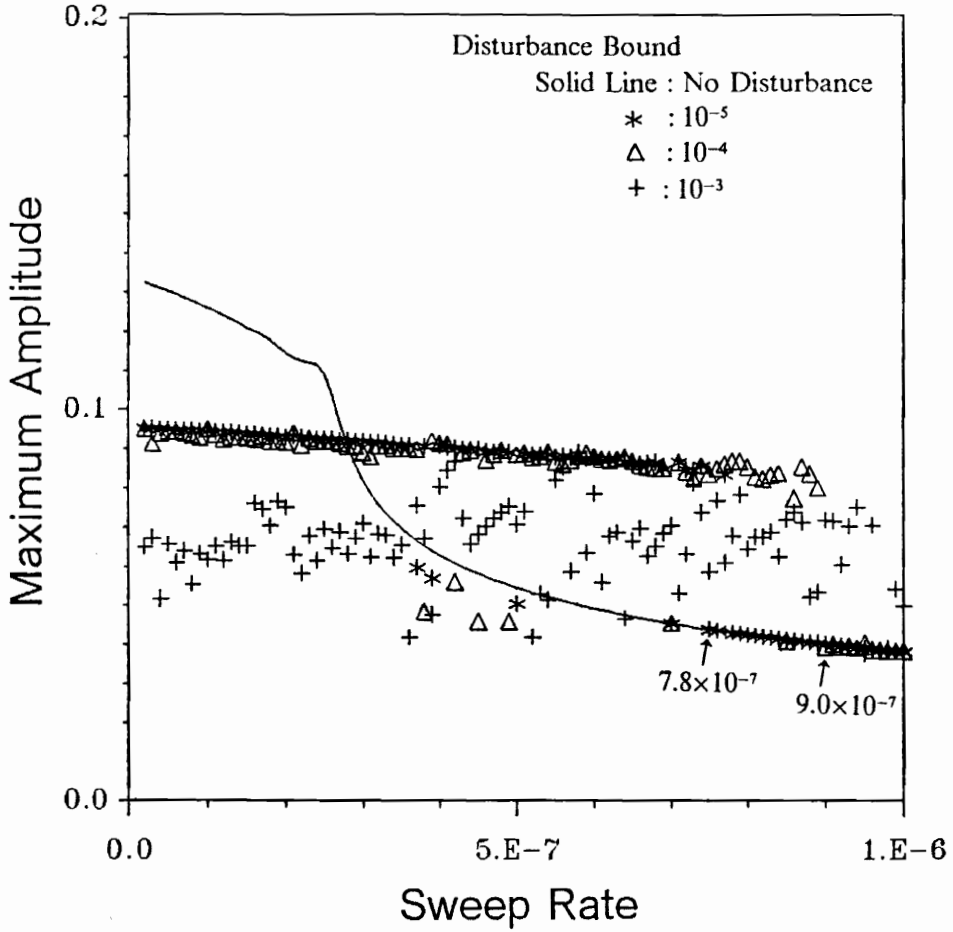

Figure 5.61 Dependence of the maximum amplitude on the sweep rate (acceleration) with four bounds of the persistent random disturbance. First mode, primary resonance, f = 0.0005W, $\delta = 0.0002$, $\hat{\varepsilon}a_0 = 0.0001$, $\hat{\varepsilon}b_0 = \gamma_0 = \psi_0 = 0$.

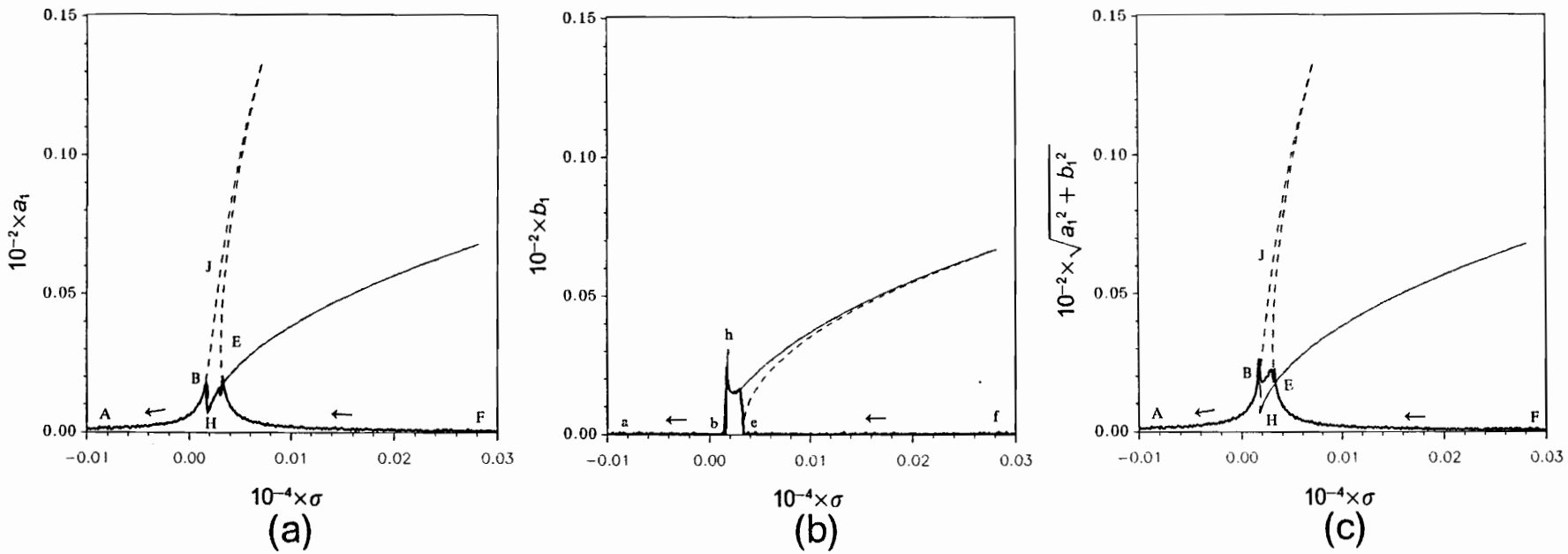

Figure 5.62 Comparison of non-stationary response subjected to persistent random disturbance and stationary response for sweep rate $\lambda = -1\times10^{-8}$. First mode, primary resonance, bound of the disturbance = 0.0001, f = 0.0005W, $\delta = 0.0002$, $\hat{\varepsilon}a_0 = 0.0001$, $\hat{\varepsilon}b_0 = \gamma_0 = \psi_0 = 0$; (a) in-plane component, (b) out-of-plane component, (c) total amplitude.

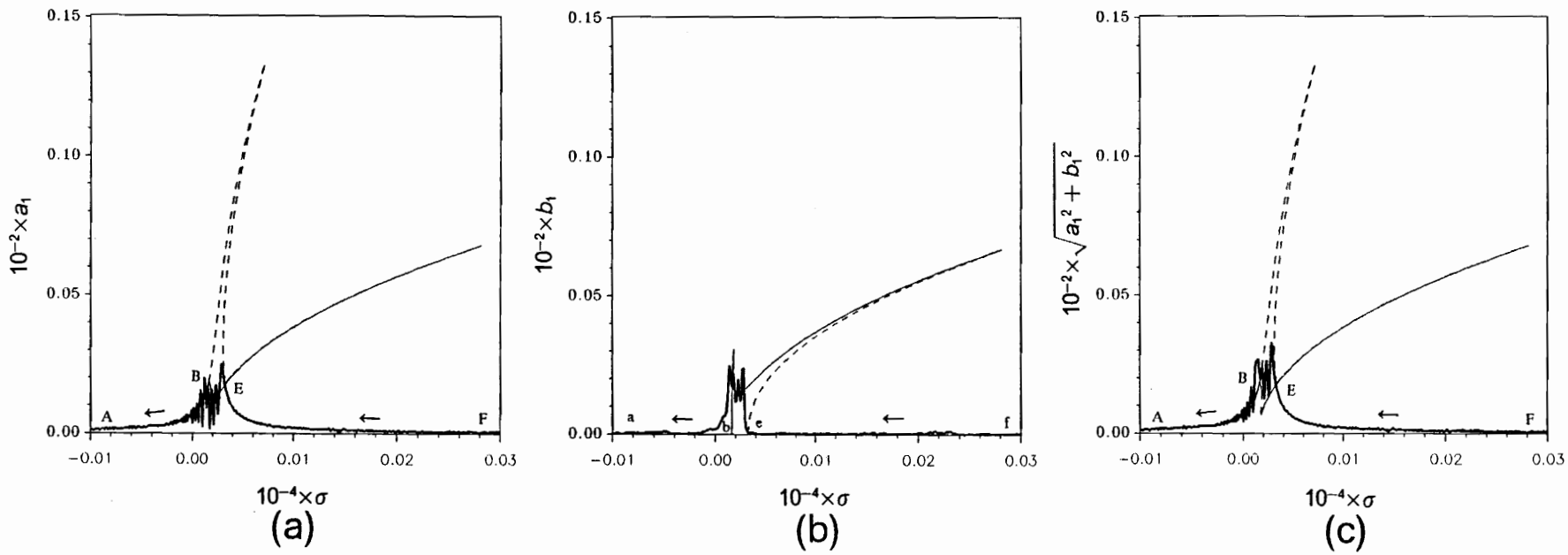

Figure 5.63 Comparison of non-stationary response subjected to persistent random disturbance and stationary response for sweep rate $\lambda = -1\times10^{-7}$. First mode, primary resonance, bound of the disturbance = 0.0001, f = 0.0005W, $\delta = 0.0002$, $\hat{\varepsilon}a_0 = 0.0001$, $\hat{\varepsilon}b_0 = \gamma_0 = \psi_0 = 0$; (a) in-plane component, (b) out-of-plane component, (c) total amplitude.

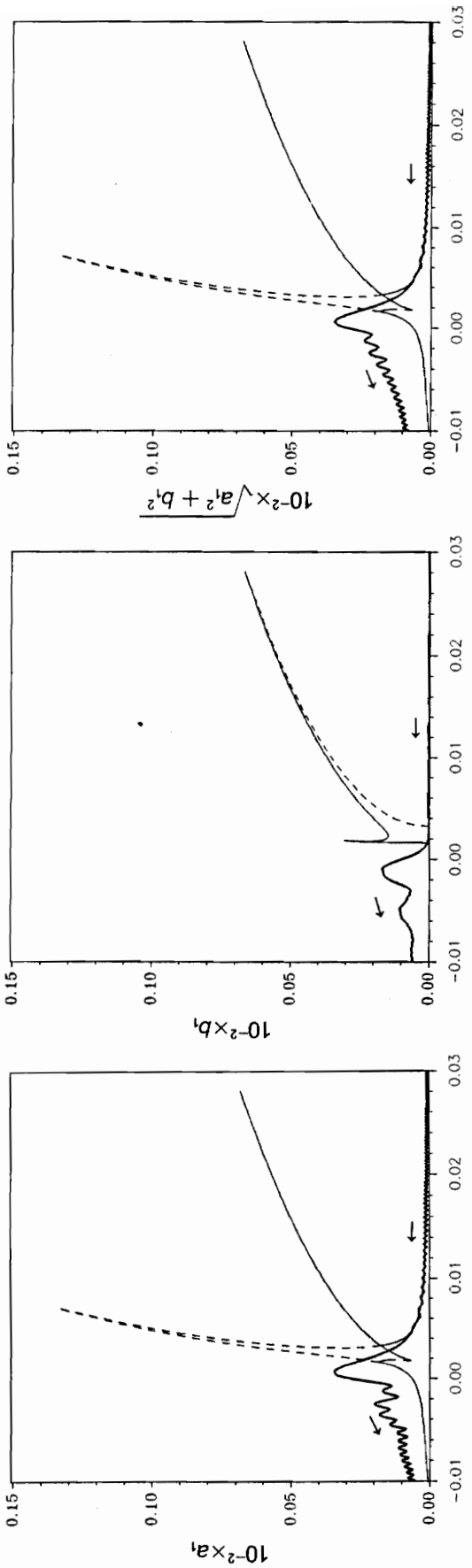

Figure 5.64 Comparison of non-stationary response subjected to persistent random disturbance and stationary response for sweep rate $\lambda = -1\times10^{-6}$. First mode, primary resonance, bound of the disturbance = 0.0001, f = 0.0005W, $\delta = 0.0002$, $\hat{\varepsilon}a_0 = 0.0001$, $\hat{\varepsilon}b_0 = \gamma_0 = \psi_0 = 0$; (a) in-plane component, (b) out-of-plane component, (c) total amplitude.

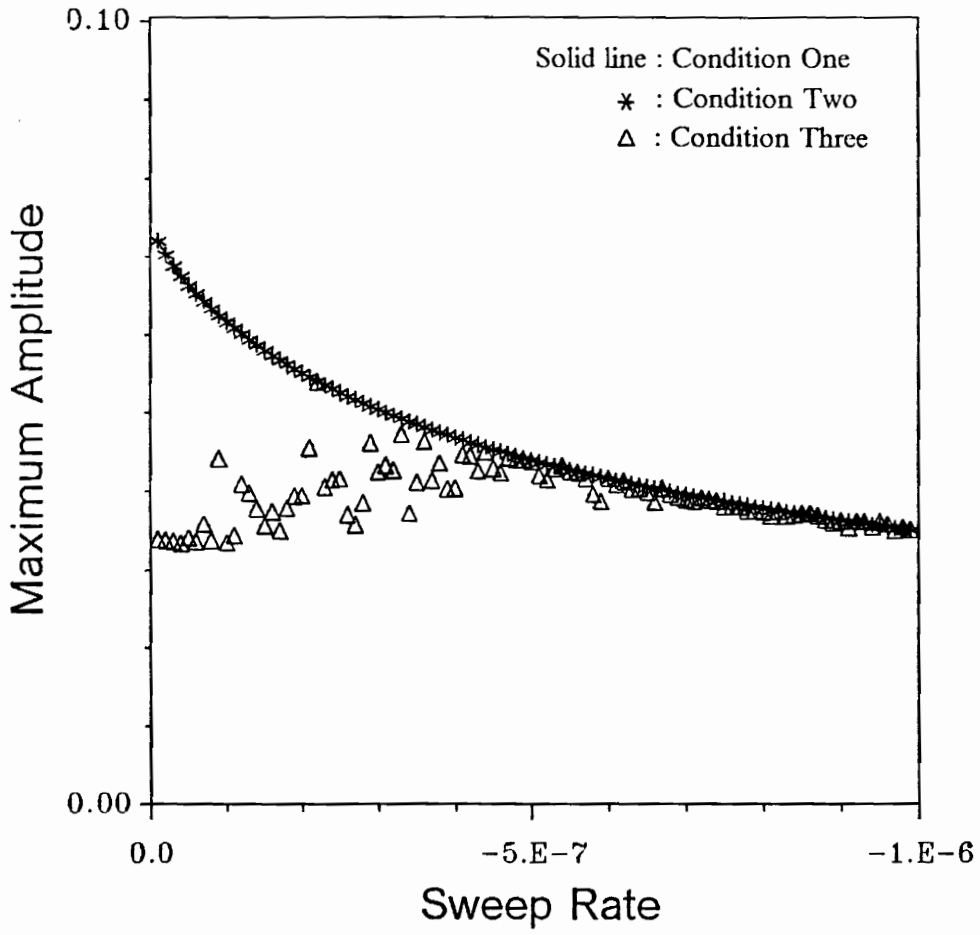

Figure 5.65 Dependence of the maximum amplitude on the sweep rate (deceleration) under three conditions. First mode, primary resonance, f = 0.0005W, $\delta = 0.0002$.

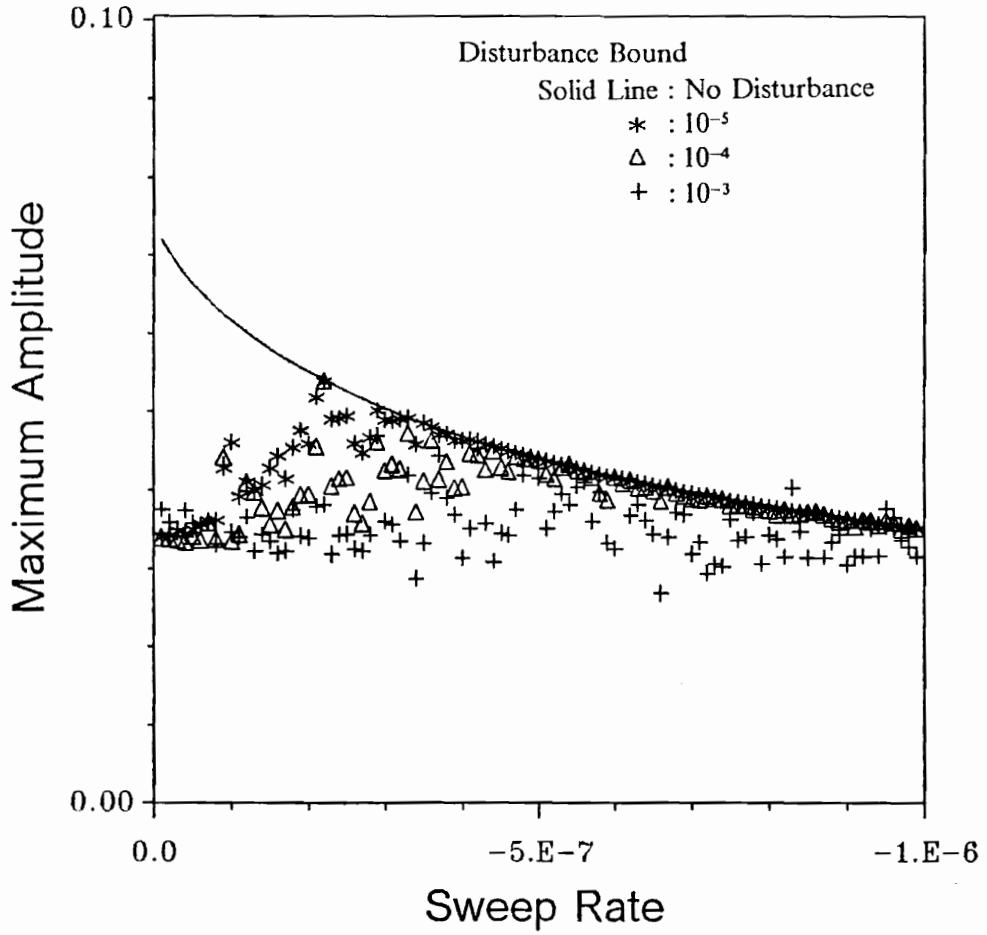

Figure 5.66 Dependence of the maximum amplitude on the sweep rate (deceleration) with four bounds of the persistent random disturbance. First mode, primary resonance, f = 0.0005W, $\delta = 0.0002$, $\hat{\varepsilon}a_0 = 0.0001$, $\hat{\varepsilon}b_0 = \gamma_0 = \psi_0 = 0$.

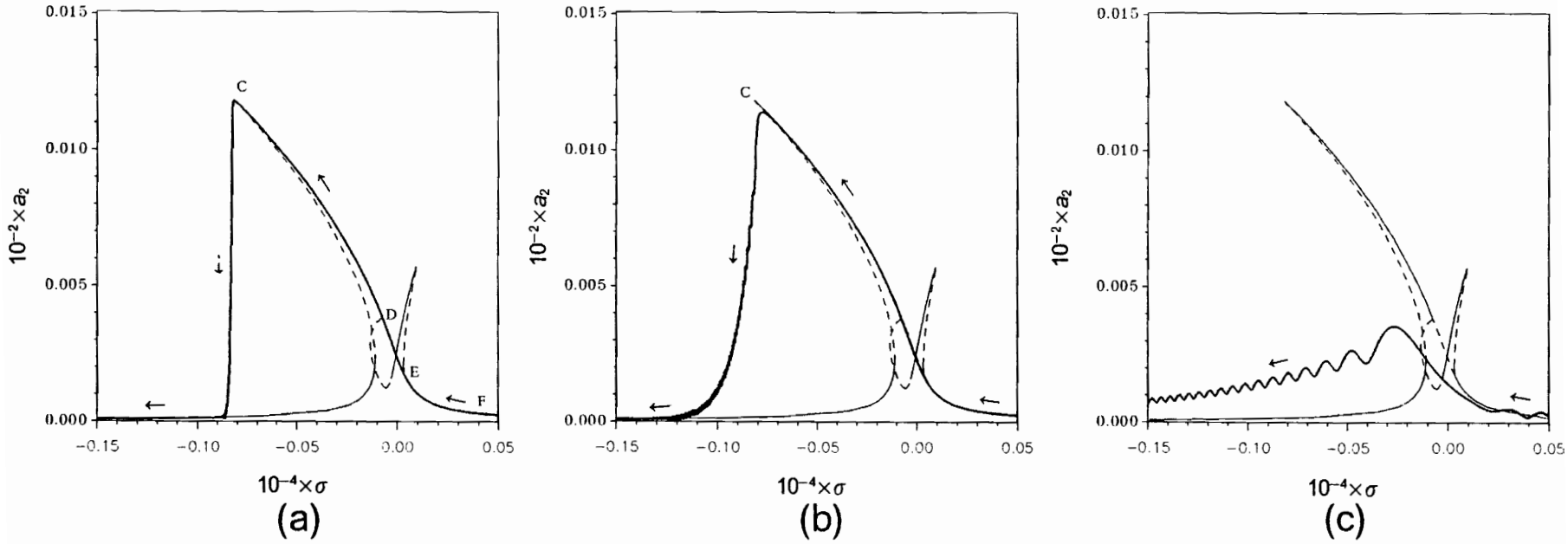

Figure 5.67 Comparison of non-stationary and stationary responses of the second mode for primary resonance with three sweep rates (deceleration). f = 0.005W, $\delta = 0.002$, $\hat{\varepsilon}a_0 = 0.0001$, $\hat{\varepsilon}b_0 = \gamma_0 = \psi_0 = 0$; (a) $\lambda = -1\times10^{-6}$, (b) $\lambda = -1\times10^{-5}$, (c) $\lambda = -1\times10^{-4}$.

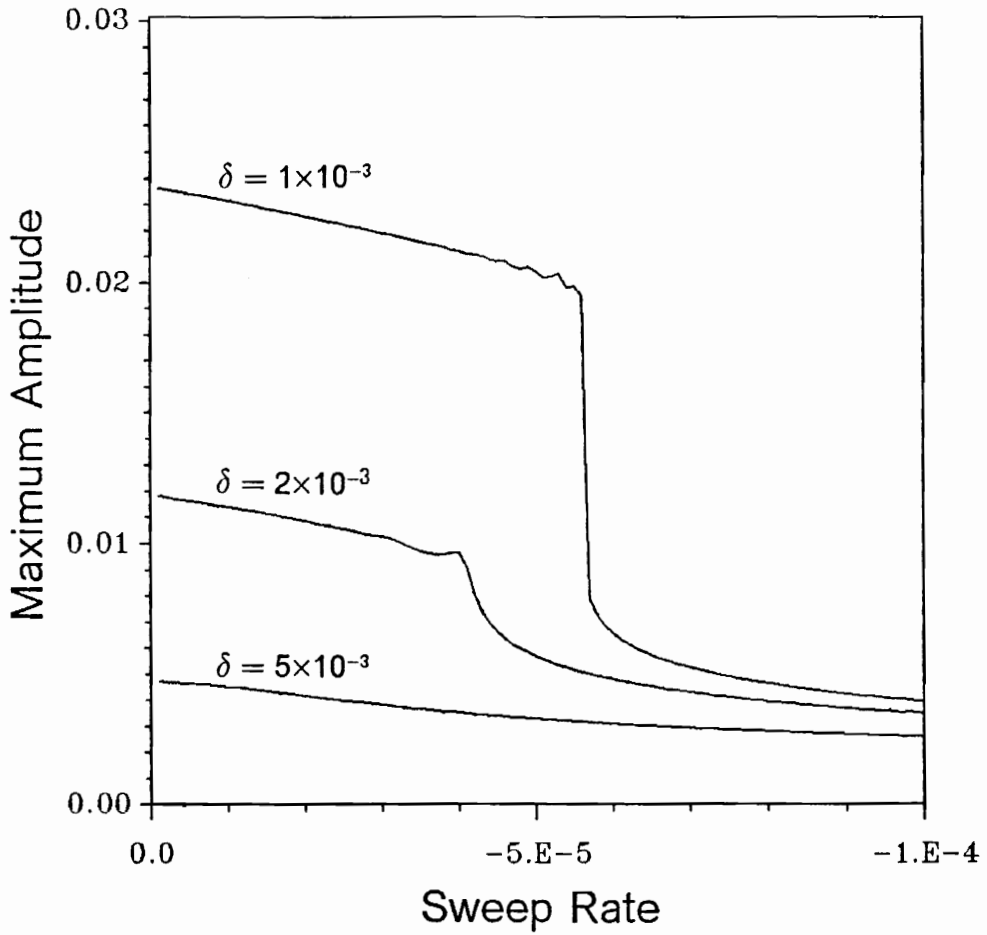

Figure 5.68 Dependence of the maximum amplitude on the sweep rate (deceleration) with three damping coefficients. Second mode, primary resonance, f = 0.005W, $\hat{\varepsilon}a_0 = 0.0001$, $\hat{\varepsilon}b_0 = \gamma_0 = \psi_0 = 0$.

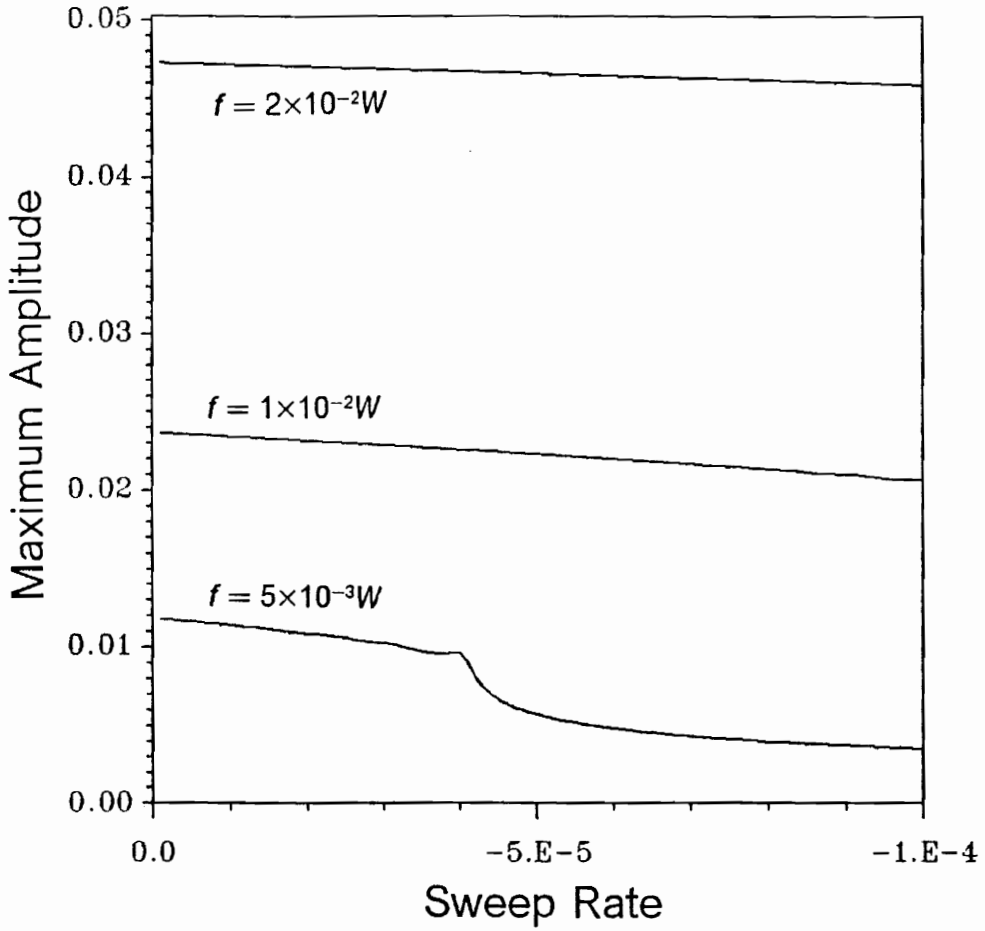

Figure 5.69 Dependence of the maximum amplitude on the sweep rate (deceleration) with three force levels. Second mode, primary resonance, $\delta = 0.002$, $\hat{\varepsilon}a_0 = 0.0001$, $\hat{\varepsilon}b_0 = \gamma_0 = \psi_0 = 0$.

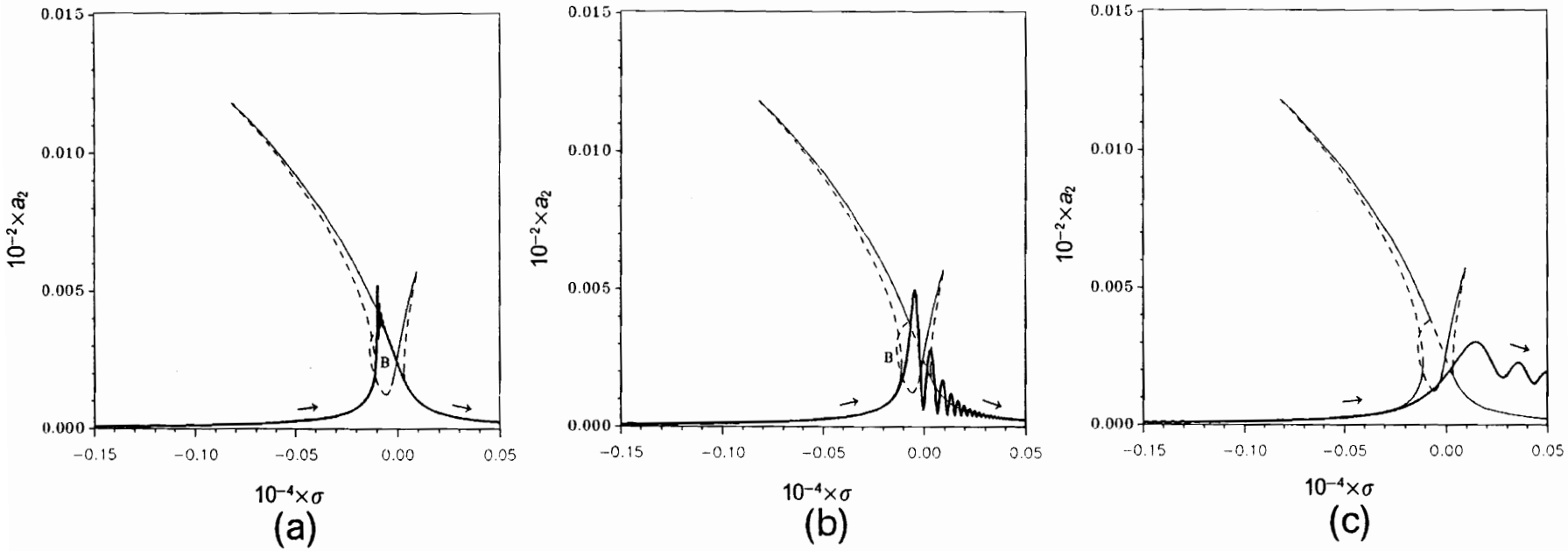

Figure 5.70 Comparison of non-stationary and stationary responses of the second mode for primary resonance with three sweep rates (accelcration). f = 0.005W, $\delta = 0.002$, $\hat{\varepsilon}a_0 = 0.0001$, $\hat{\varepsilon}b_0 = \gamma_0 = \psi_0 = 0$; (a) $\lambda = 1\times10^{-6}$, (b) $\lambda = 1\times10^{-5}$, (c) $\lambda = 1\times10^{-4}$.

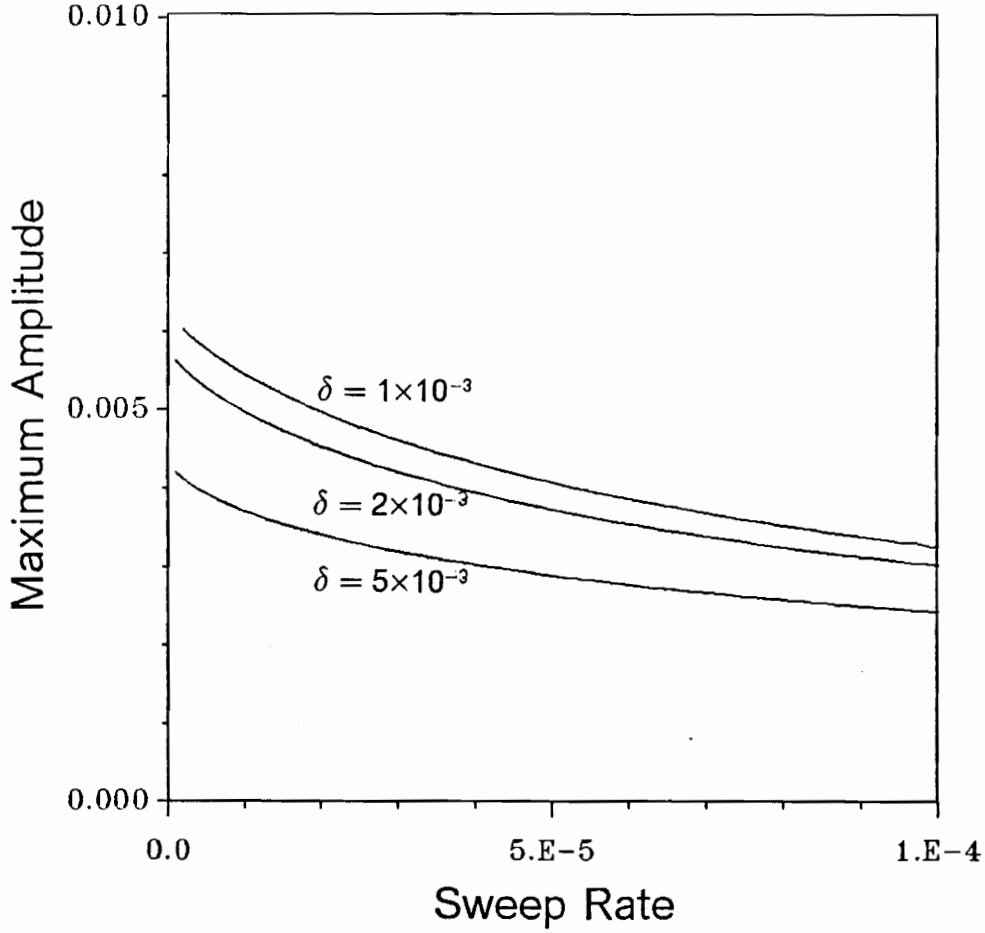

Figure 5.71 Dependence of the maximum amplitude on the sweep rate (acceleration) with three damping coefficients. Second mode, primary resonance, f = 0.005W, $\hat{\varepsilon}a_0 = 0.0001$, $\hat{\varepsilon}b_0 = \gamma_0 = \psi_0 = 0$.

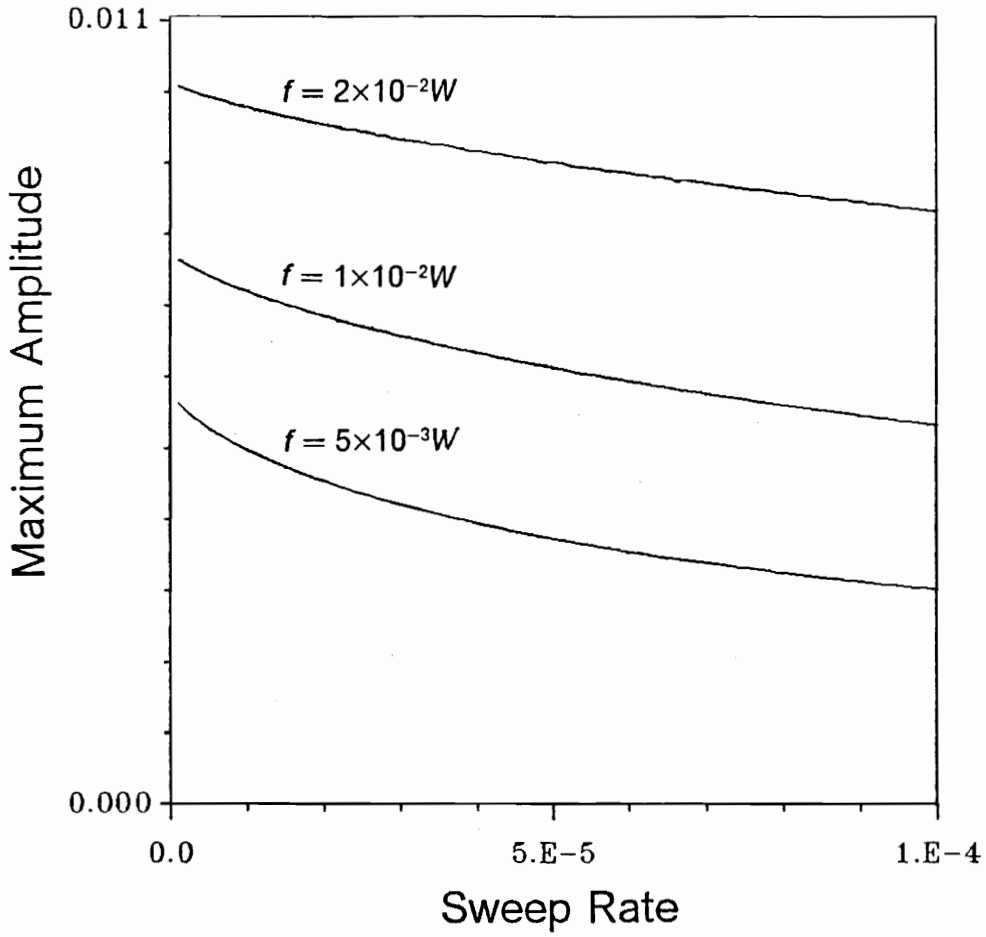

Figure 5.72 Dependence of the maximum amplitude on the sweep rate (acceleration) with three force levels. Second mode, primary resonance, $\delta = 0.002$, $\hat{\varepsilon}a_0 = 0.0001$, $\hat{\varepsilon}b_0 = \gamma_0 = \psi_0 = 0$.

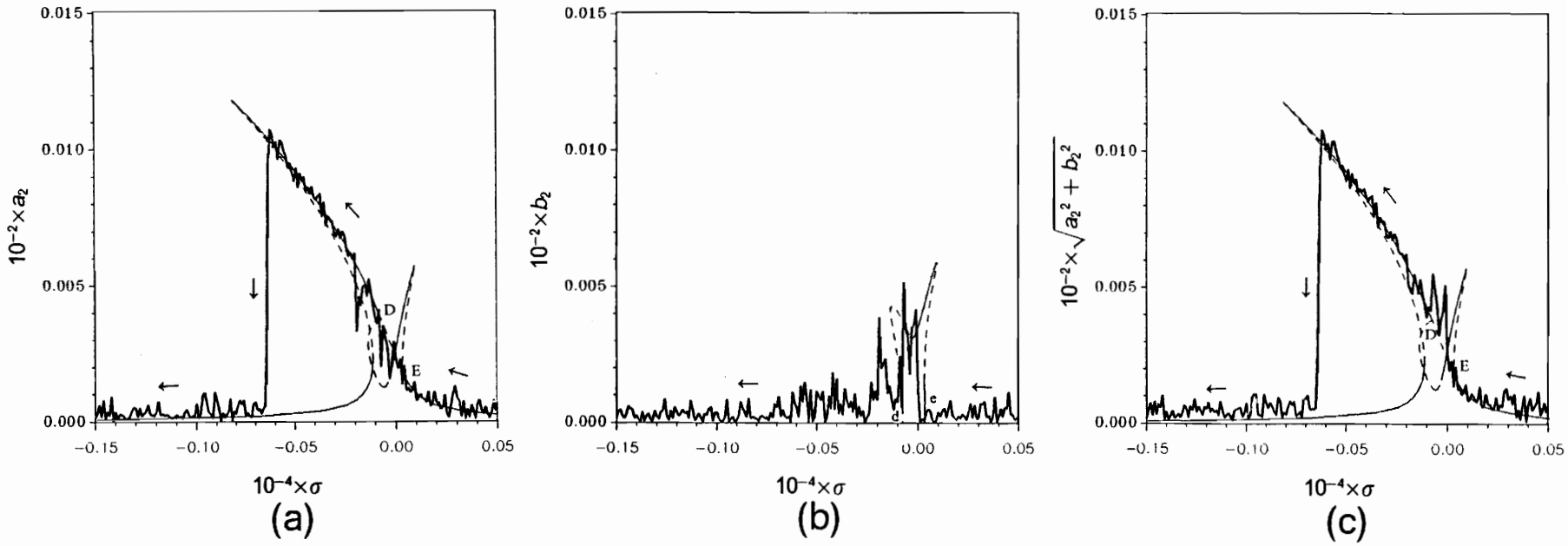

Figure 5.73 Comparison of non-stationary response subjected to persistent random disturbance and stationary response for sweep rate $\lambda = -1\times10^{-6}$. Second mode, primary resonance, bound of the disturbance = 0.0001, f = 0.005W, $\delta = 0.002$, $\hat{\varepsilon}a_0 = 0.0001$, $\hat{\varepsilon}b_0 = \gamma_0 = \psi_0 = 0$; (a) in-plane component, (b) out-of-plane component, (c) total amplitude.

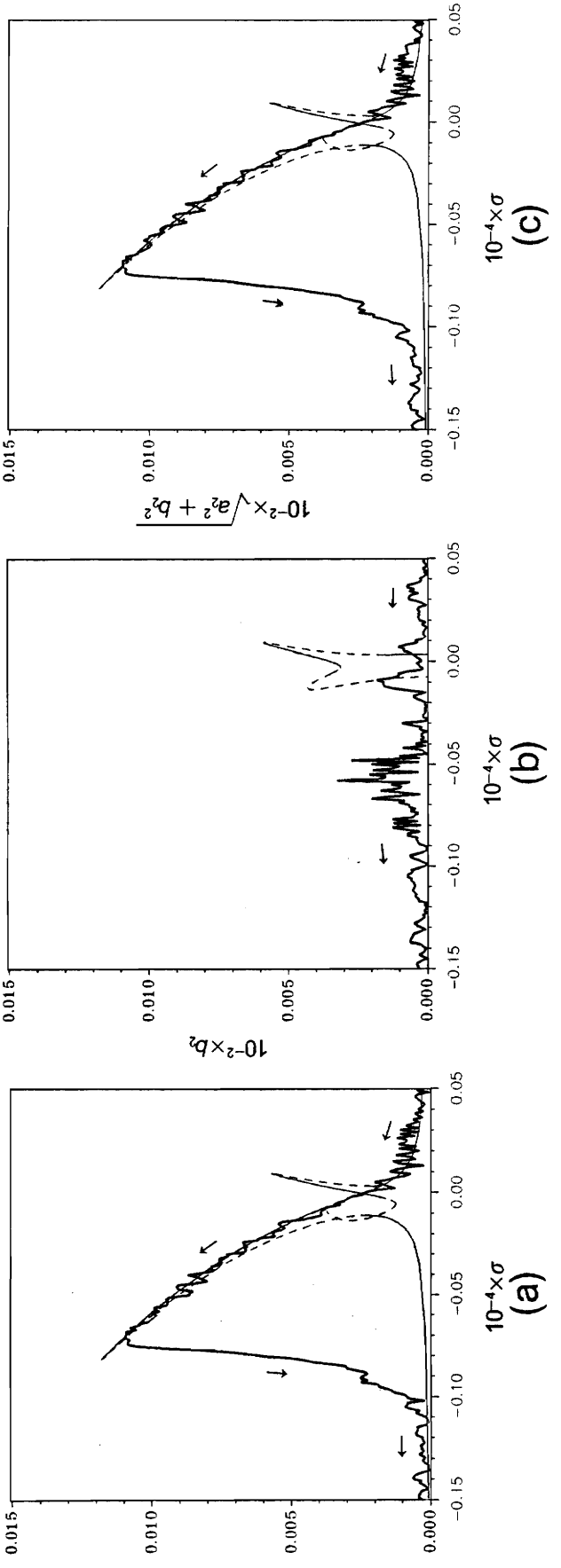

Figure 5.74 Comparison of non-stationary response subjected to persistent random disturbance and stationary response for sweep rate $\lambda = -1\times10^{-5}$. Second mode, primary resonance, bound of the disturbance = 0.0001, f = 0.005W, $\delta = 0.002$, $\hat{\varepsilon}a_0 = 0.0001$, $\hat{\varepsilon}b_0 = \gamma_0 = \psi_0 = 0$; (a) in-plane component, (b) out-of-plane component, (c) total amplitude.

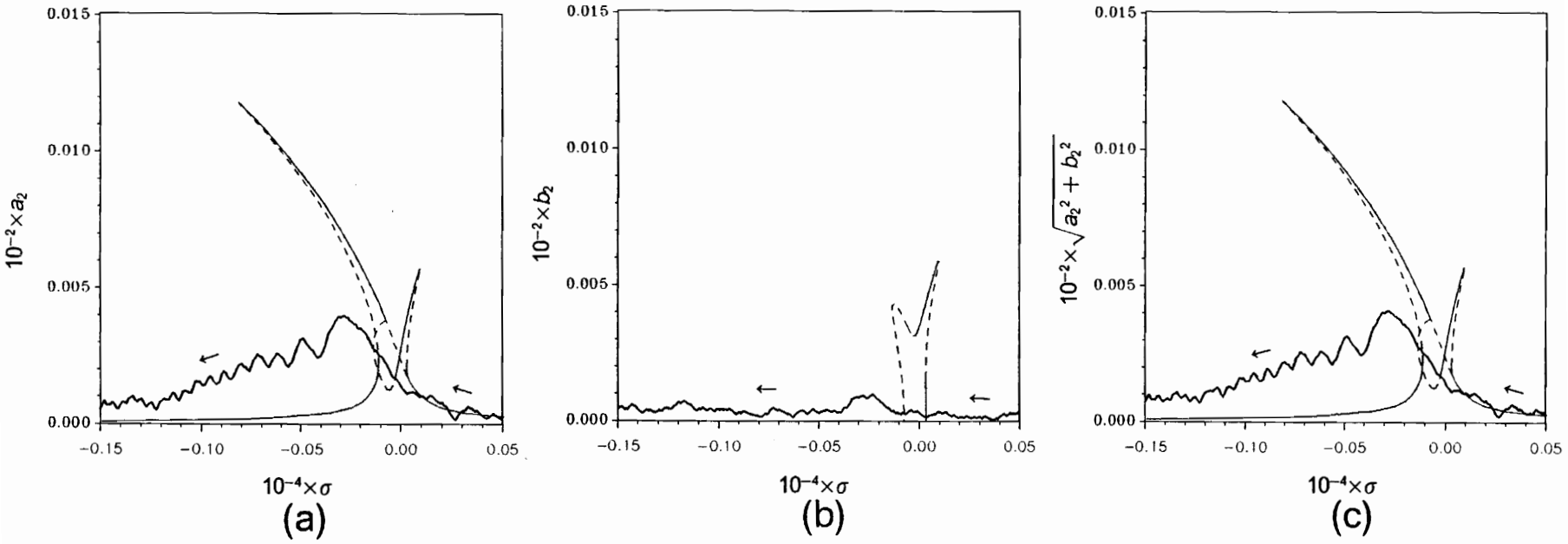

Figure 5.75 Comparison of non-stationary response subjected to persistent random disturbance and stationary response for sweep rate $\lambda = -1\times10^{-4}$. Second mode, primary resonance, bound of the disturbance = 0.0001, f = 0.005W, $\delta = 0.002$, $\hat{\varepsilon}a_0 = 0.0001$, $\hat{\varepsilon}b_0 = \gamma_0 = \psi_0 = 0$; (a) in-plane component, (b) out-of-plane component, (c) total amplitude.

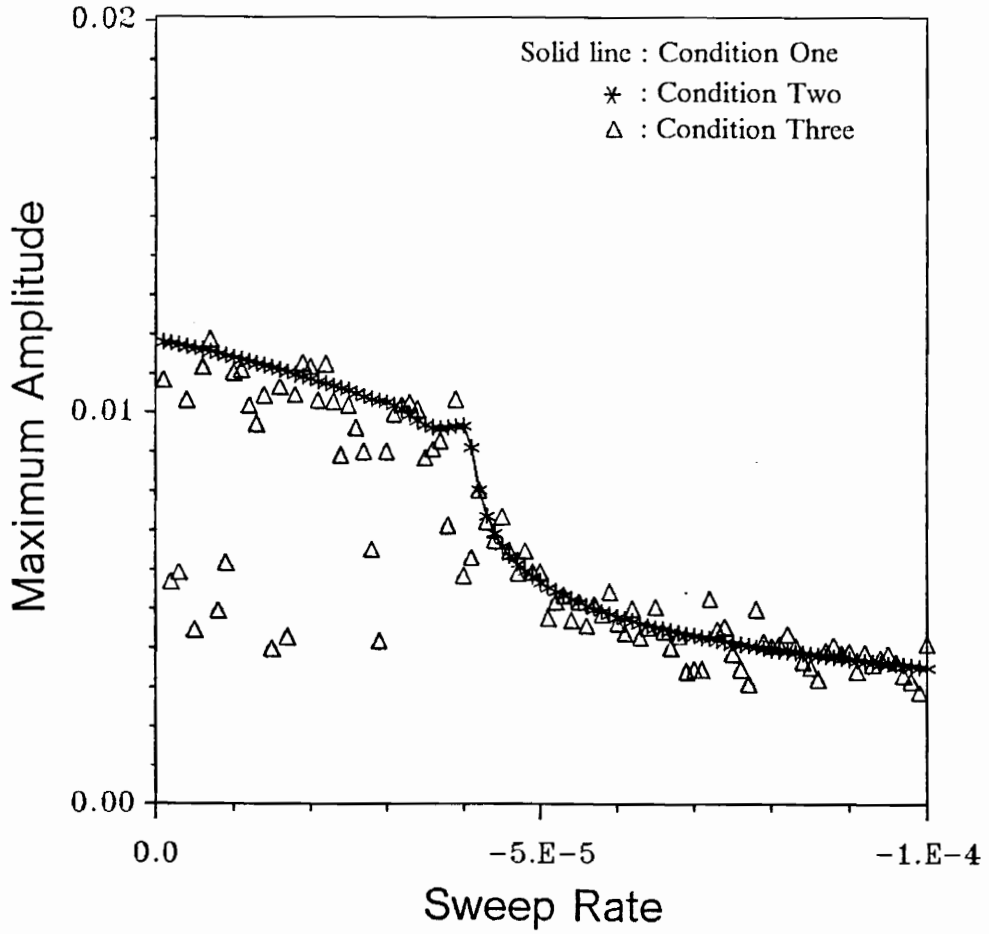

Figure 5.76 Dependence of the maximum amplitude on the sweep rate (deceleration) under three conditions. Second mode, primary resonance, f = 0.005W, $\delta = 0.002$.

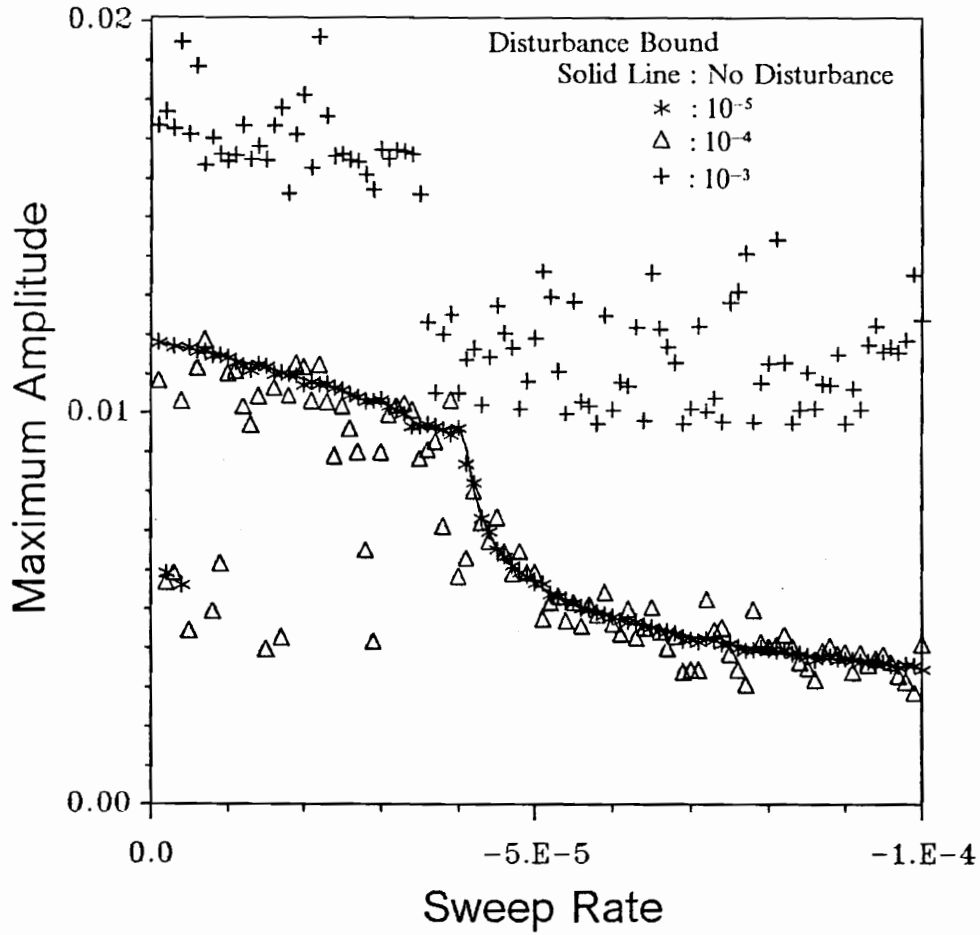

Figure 5.77 Dependence of the maximum amplitude on the sweep rate (deceleration) with four bounds of the persistent random disturbance. Second mode, primary resonance, f = 0.005W, $\delta = 0.002$, $\hat{\varepsilon}a_0 = 0.0001$, $\hat{\varepsilon}b_0 = \gamma_0 = \psi_0 = 0$.

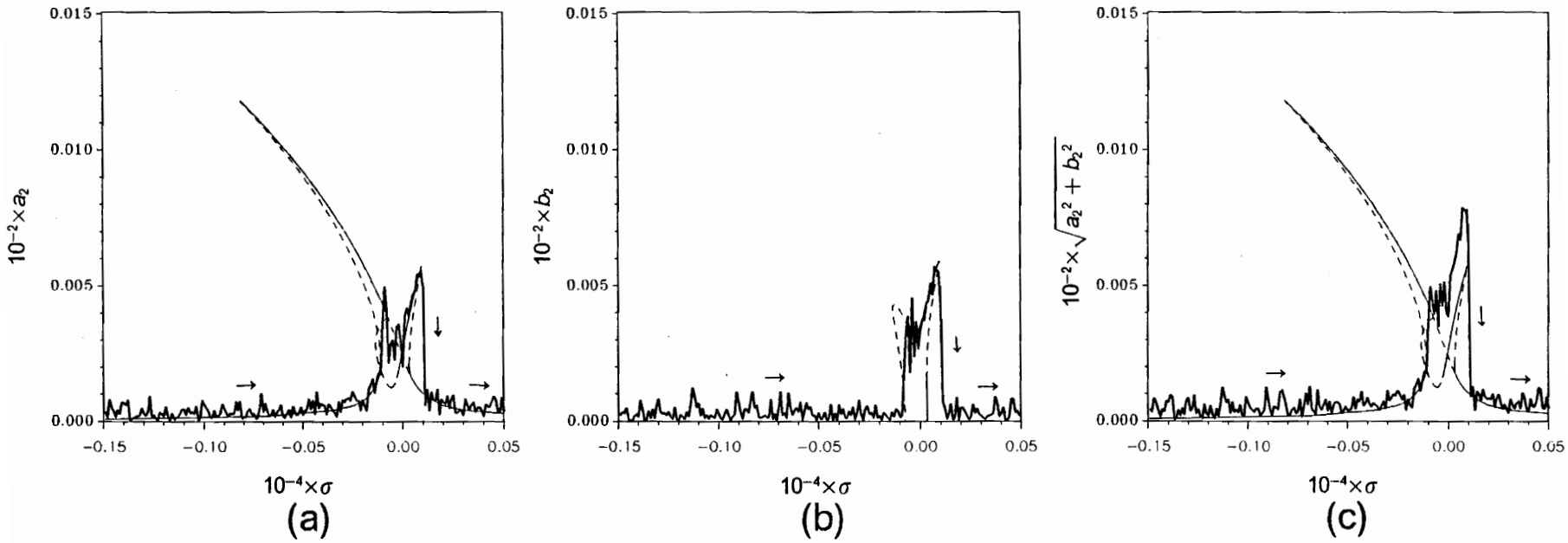

Figure 5.78 Comparison of non-stationary response subjected to persistent random disturbance and stationary response for sweep rate $\lambda = 1\times10^{-6}$. Second mode, primary resonance, bound of the disturbance = 0.0001, f = 0.005W, $\delta = 0.002$, $\hat{\varepsilon}a_0 = 0.0001$, $\hat{\varepsilon}b_0 = \gamma_0 = \psi_0 = 0$; (a) in-plane component, (b) out-of-plane component, (c) total amplitude.

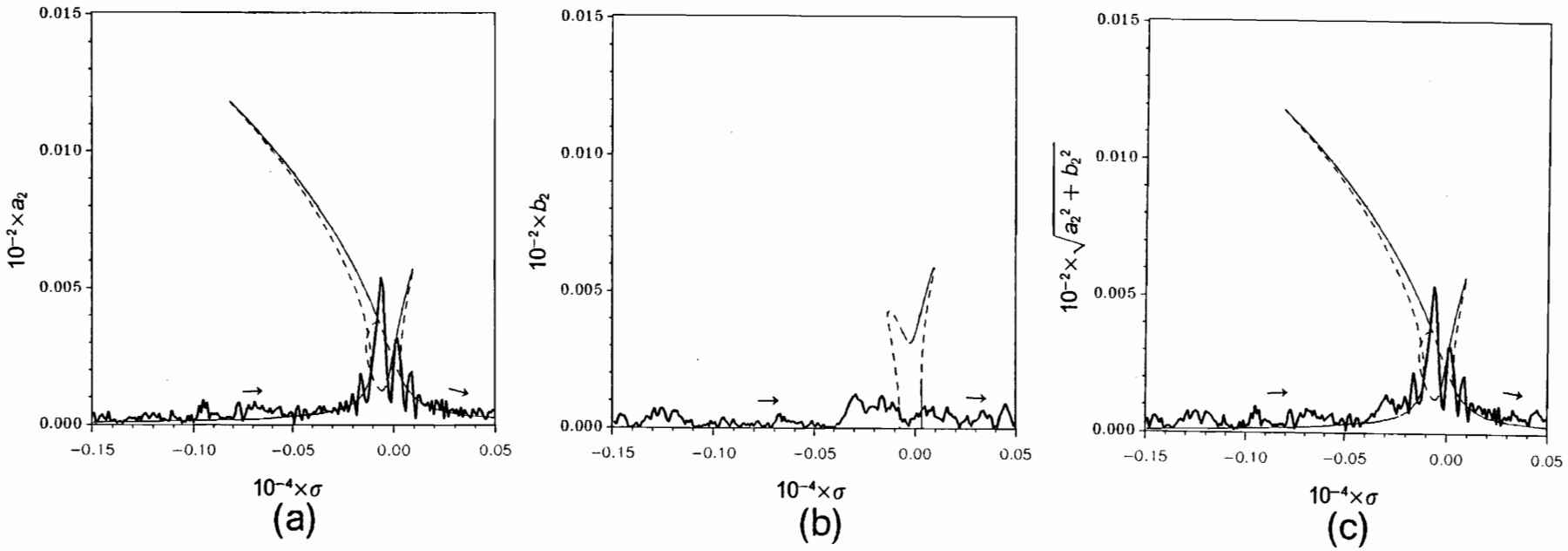

Figure 5.79 Comparison of non-stationary response subjected to persistent random disturbance and stationary response for sweep rate $\lambda = 1\times10^{-5}$. Second mode, primary resonance, bound of the disturbance = 0.0001, f = 0.005W, $\delta = 0.002$, $\hat{\varepsilon}a_0 = 0.0001$, $\hat{\varepsilon}b_0 = \gamma_0 = \psi_0 = 0$; (a) in-plane component, (b) out-of-plane component, (c) total amplitude.

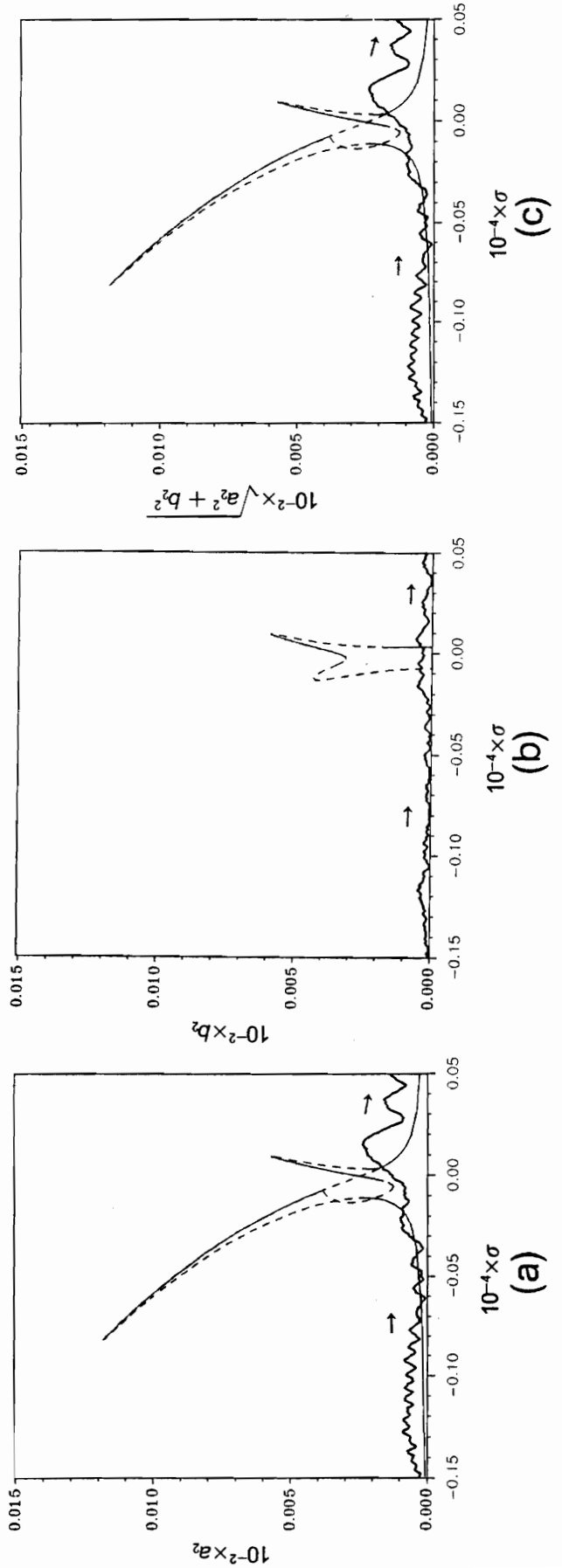

Figure 5.80 Comparison of non-stationary response subjected to persistent random disturbance and stationary response for sweep rate $\lambda = 1\times10^{-4}$. Second mode, primary resonance, bound of the disturbance = 0.0001, f = 0.005W, $\delta = 0.002$, $\hat{\varepsilon}a_0 = 0.0001$, $\hat{\varepsilon}b_0 = \gamma_0 = \psi_0 = 0$; (a) in-plane component, (b) out-of-plane component, (c) total amplitude.

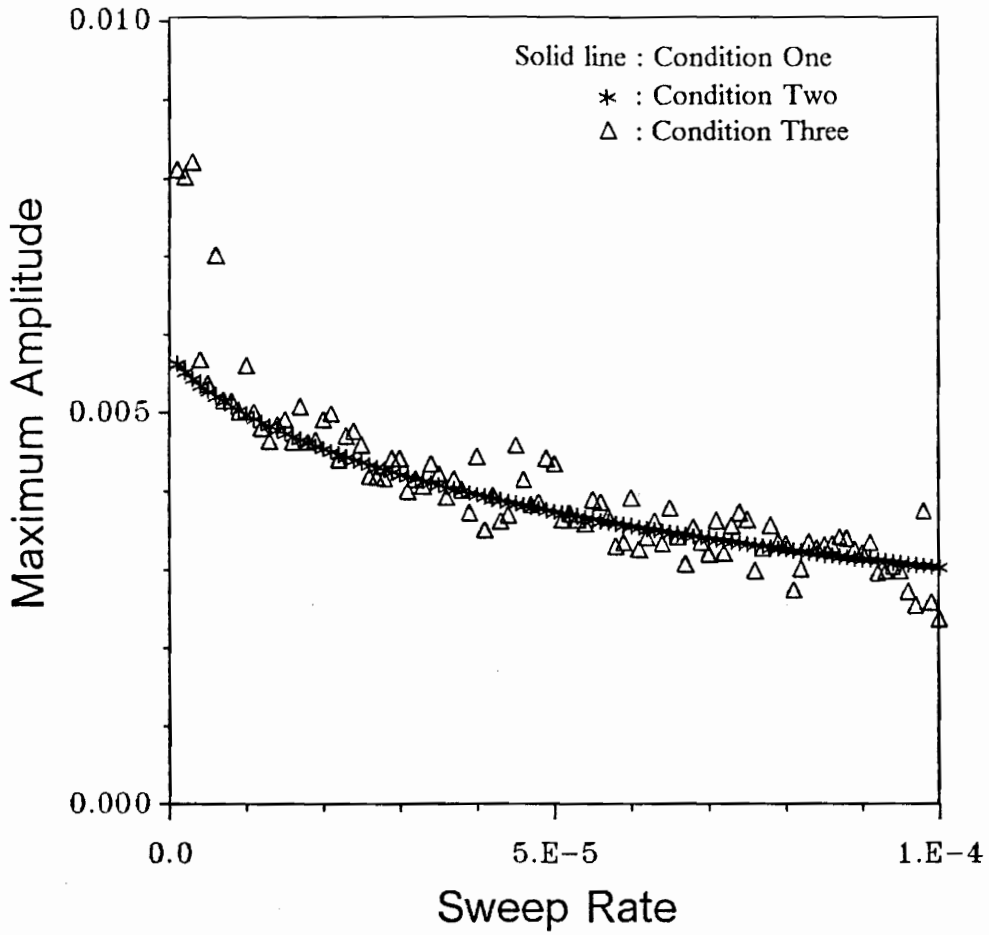

Figure 5.81 Dependence of the maximum amplitude on the sweep rate (acceleration) under three conditions. Second mode, primary resonance, f = 0.005W, $\delta = 0.002$.

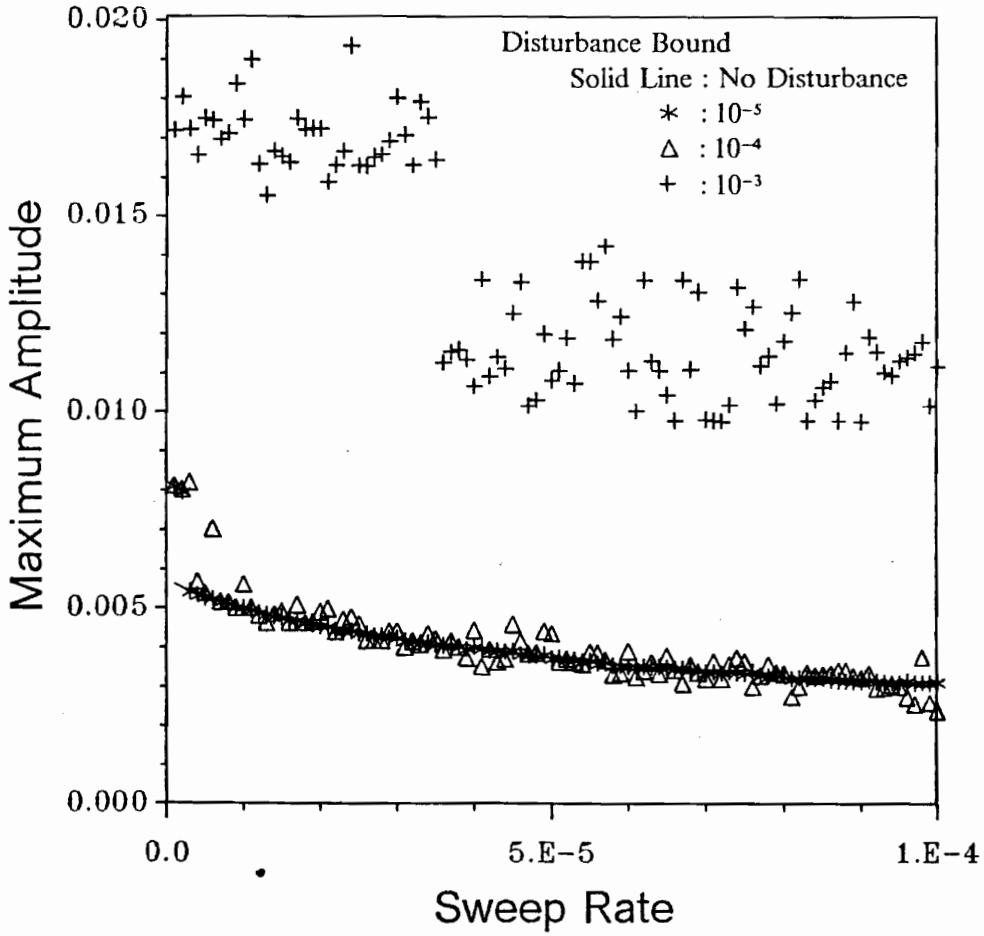

Figure 5.82 Dependence of the maximum amplitude on the sweep rate (acceleration) with four bounds of the persistent random disturbance. Second mode, primary resonance, f = 0.005W, $\delta = 0.002$, $\hat{\varepsilon}a_0 = 0.0001$, $\hat{\varepsilon}b_0 = \gamma_0 = \psi_0 = 0$.

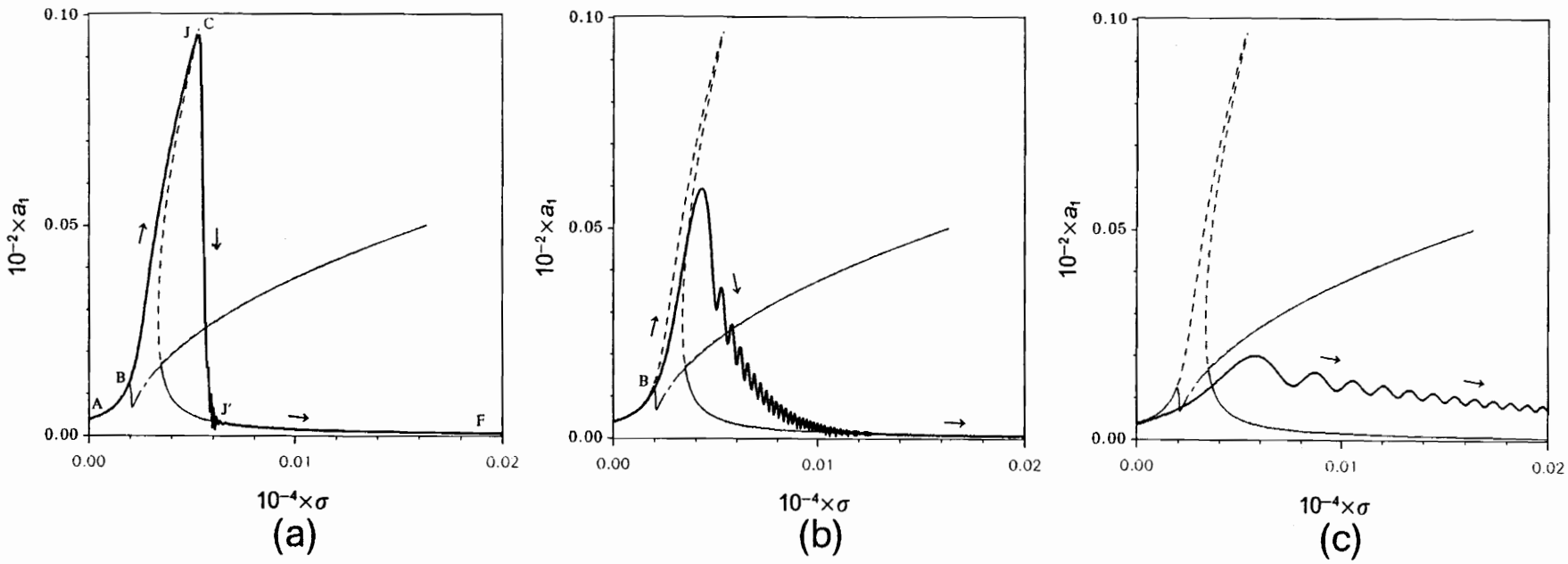

Figure 5.83 Comparison of non-stationary and stationary responses of the first mode for superharmonic resonance of order two with three sweep rates (acceleration). f = 0.5W, $\delta = 0.0002$, $\hat{\varepsilon}a_0 = 0.0001$, $\hat{\varepsilon}b_0 = \gamma_0 = \psi_0 = 0$; (a) $\lambda = 1\times10^{-8}$, (b) $\lambda = 1\times10^{-7}$, (c) $\lambda = 1\times10^{-6}$.

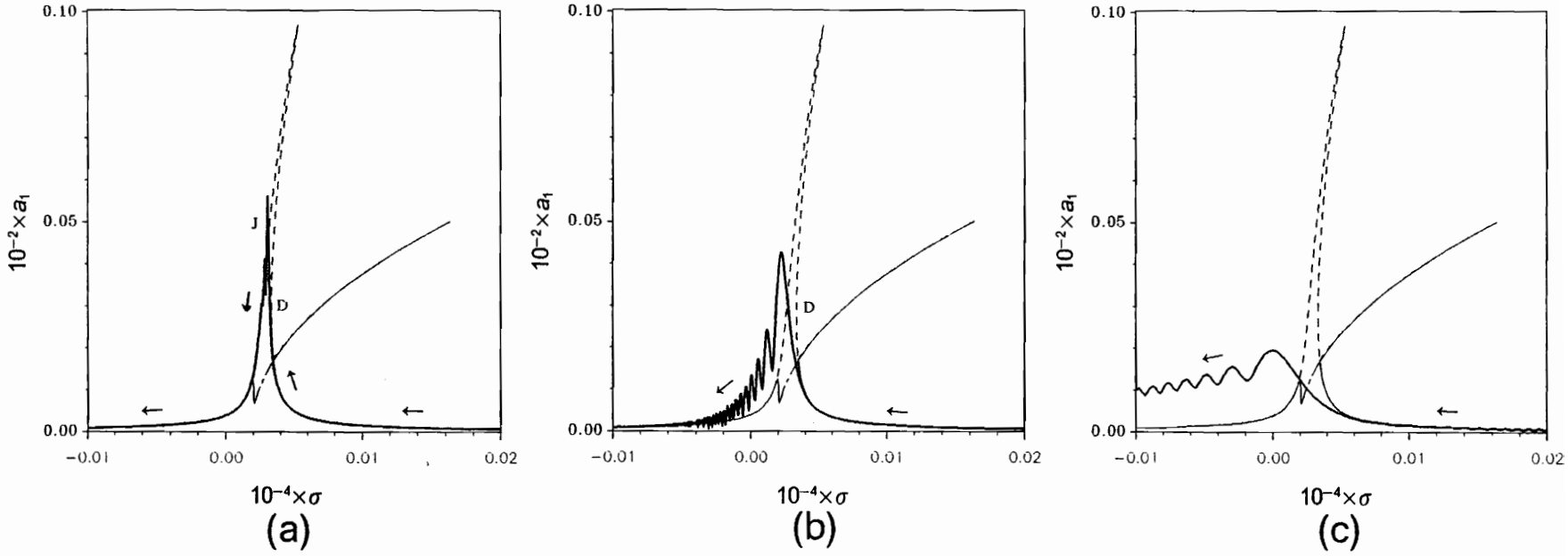

Figure 5.84 Comparison of non-stationary and stationary responses of the first mode for superharmonic resonance of order two with three sweep rates (deceleration). f = 0.5W, $\delta = 0.0002$, $\hat{\varepsilon}a_0 = 0.0001$, $\hat{\varepsilon}b_0 = \gamma_0 = \psi_0 = 0$; (a) $\lambda = -1\times10^{-8}$, (b) $\lambda = -1\times10^{-7}$, (c) $\lambda = -1\times10^{-6}$.

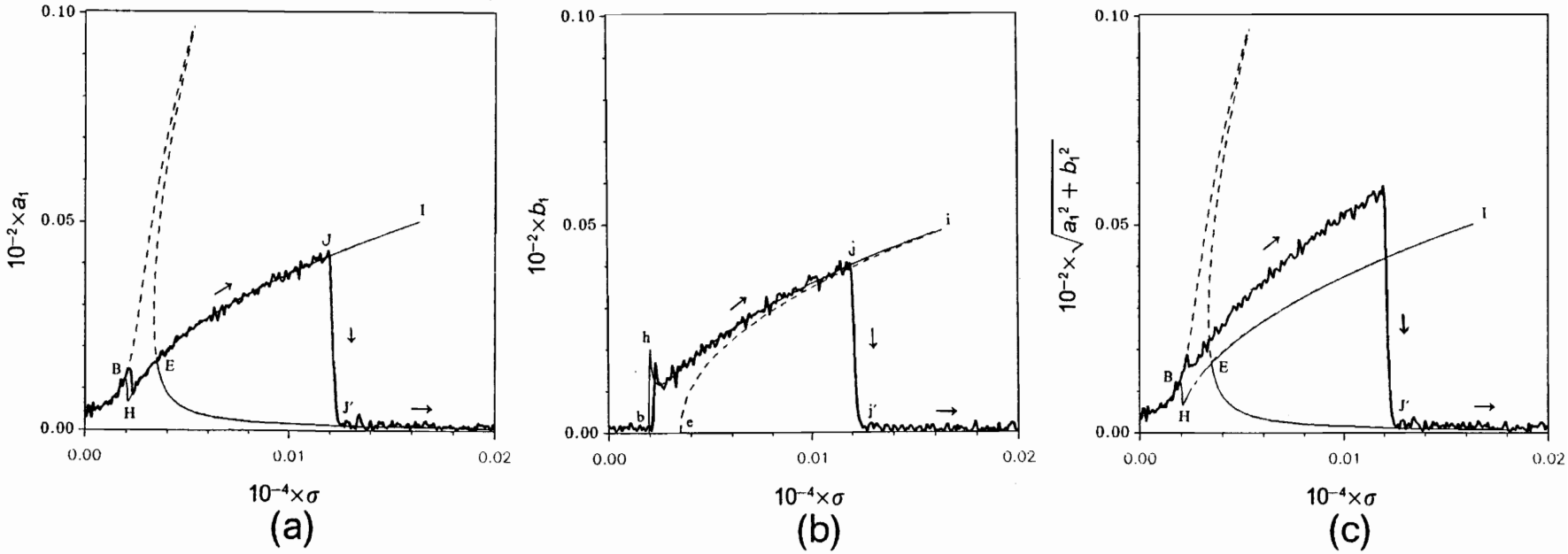

Figure 5.85 Comparison of non-stationary response subjected to persistent random disturbance and stationary response for sweep rate $\lambda = 1\times10^{-8}$. First mode, superharmonic resonance of order two, bound of the disturbance = 0.0001, f = 0.5W, $\delta = 0.0002$, $\hat{\varepsilon}a_0 = 0.0001$, $\hat{\varepsilon}b_0 = \gamma_0 = \psi_0 = 0$; (a) in-plane component, (b) out-of-plane component, (c) total amplitude.

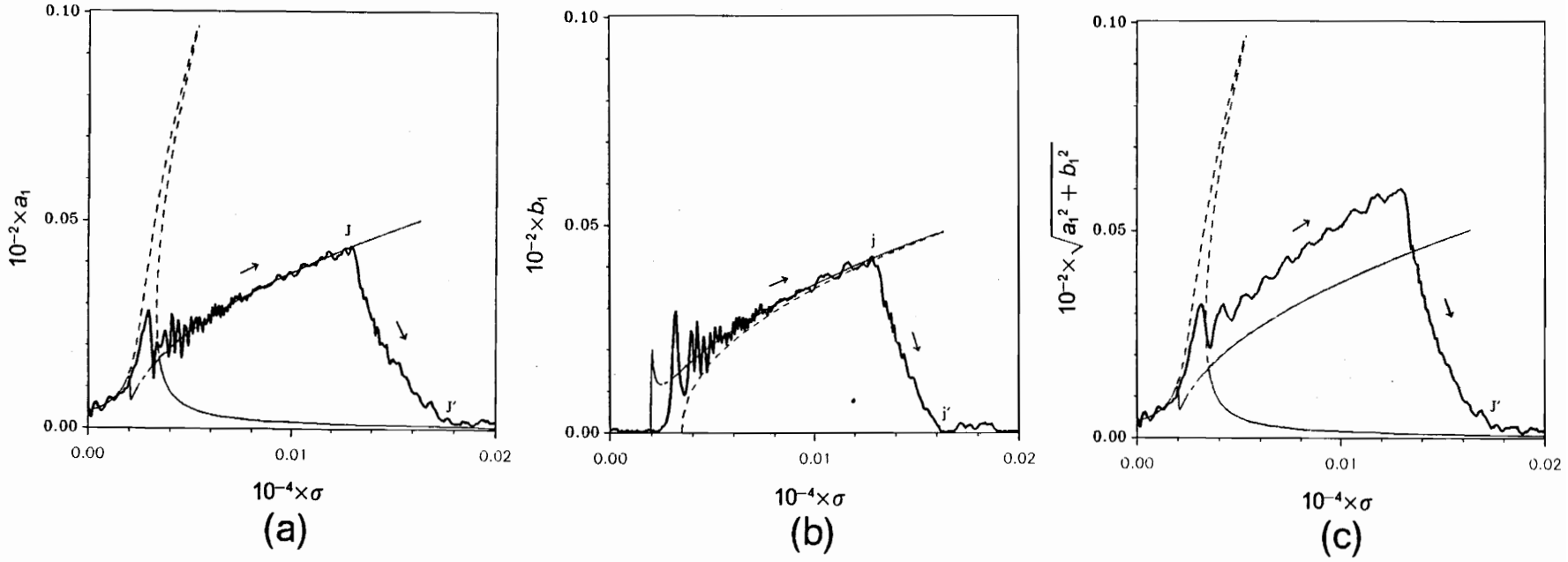

Figure 5.86 Comparison of non-stationary response subjected to persistent random disturbance and stationary response for sweep rate $\lambda = 1\times10^{-7}$. First mode, superharmonic resonance of order two, bound of the disturbance = 0.0001, f = 0.5W, $\delta = 0.0002$, $\hat{\varepsilon}a_0 = 0.0001$, $\hat{\varepsilon}b_0 = \gamma_0 = \psi_0 = 0$; (a) in-plane component, (b) out-of-plane component, (c) total amplitude.

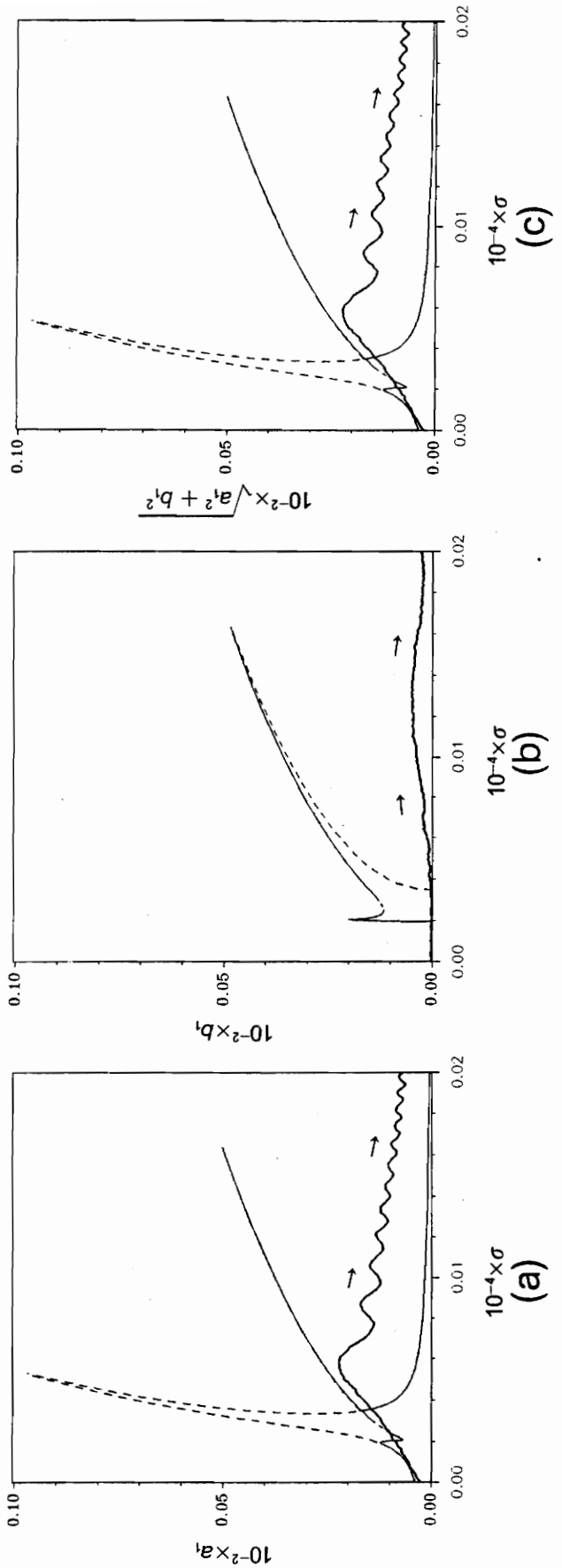

Figure 5.87 Comparison of non-stationary response subjected to persistent random disturbance and stationary response for sweep rate $\lambda = 1\times10^{-6}$. First mode, superharmonic resonance of order two, bound of the disturbance = 0.0001, f = 0.5W, $\delta = 0.0002$, $\hat{\varepsilon}a_0 = 0.0001$, $\hat{\varepsilon}b_0 = \gamma_0 = \psi_0 = 0$; (a) in-plane component, (b) out-of-plane component, (c) total amplitude.

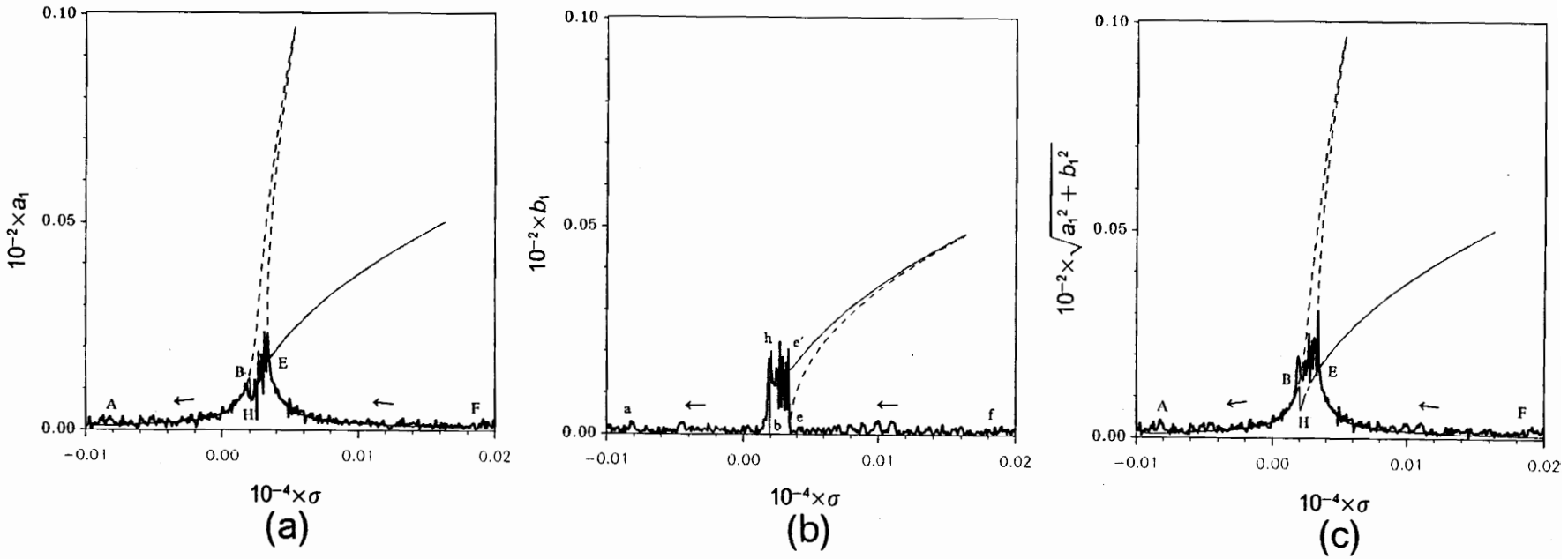

Figure 5.88 Comparison of non-stationary response subjected to persistent random disturbance and stationary response for sweep rate $\lambda = -1\times10^{-8}$. First mode, superharmonic resonance of order two, bound of the disturbance = 0.0001, f = 0.5W, $\delta = 0.0002$, $\hat{\varepsilon}a_0 = 0.0001$, $\hat{\varepsilon}b_0 = \gamma_0 = \psi_0 = 0$; (a) in-plane component, (b) out-of-plane component, (c) total amplitude.

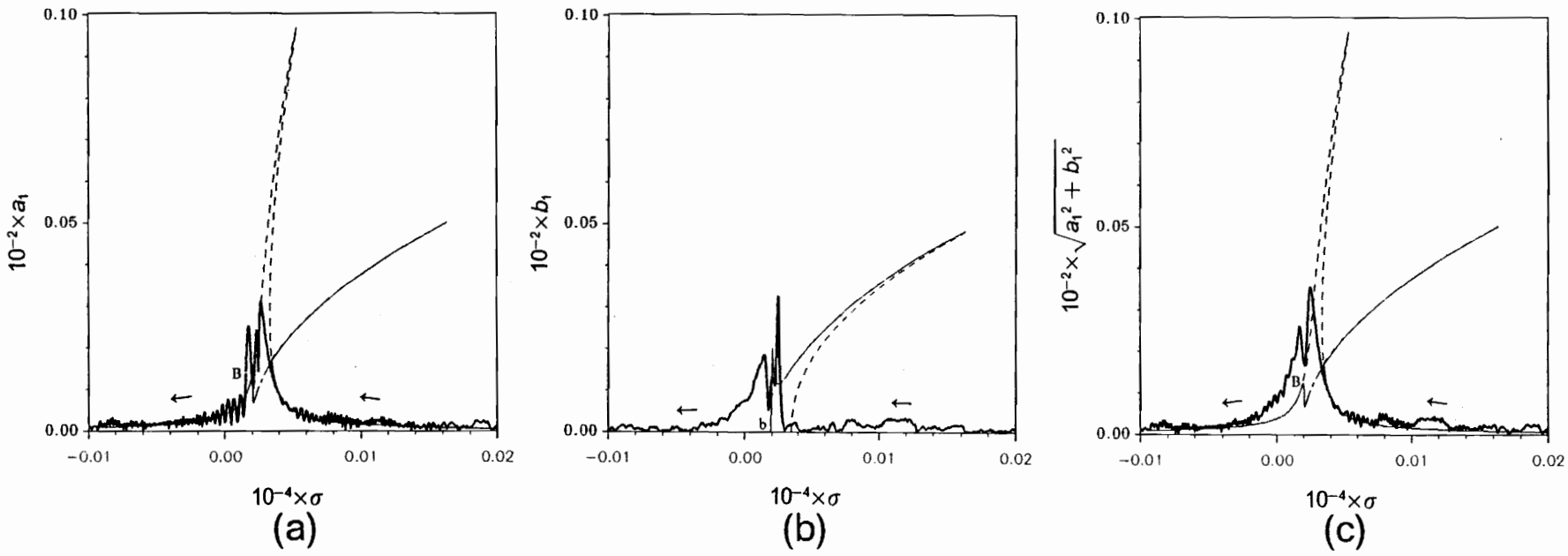

Figure 5.89 Comparison of non-stationary response subjected to persistent random disturbance and stationary response for sweep rate $\lambda = -1\times10^{-7}$. First mode, superharmonic resonance of order two, bound of the disturbance = 0.0001, f = 0.5W, $\delta = 0.0002$, $\hat{\varepsilon}a_0 = 0.0001$, $\hat{\varepsilon}b_0 = \gamma_0 = \psi_0 = 0$; (a) in-plane component, (b) out-of-plane component, (c) total amplitude.

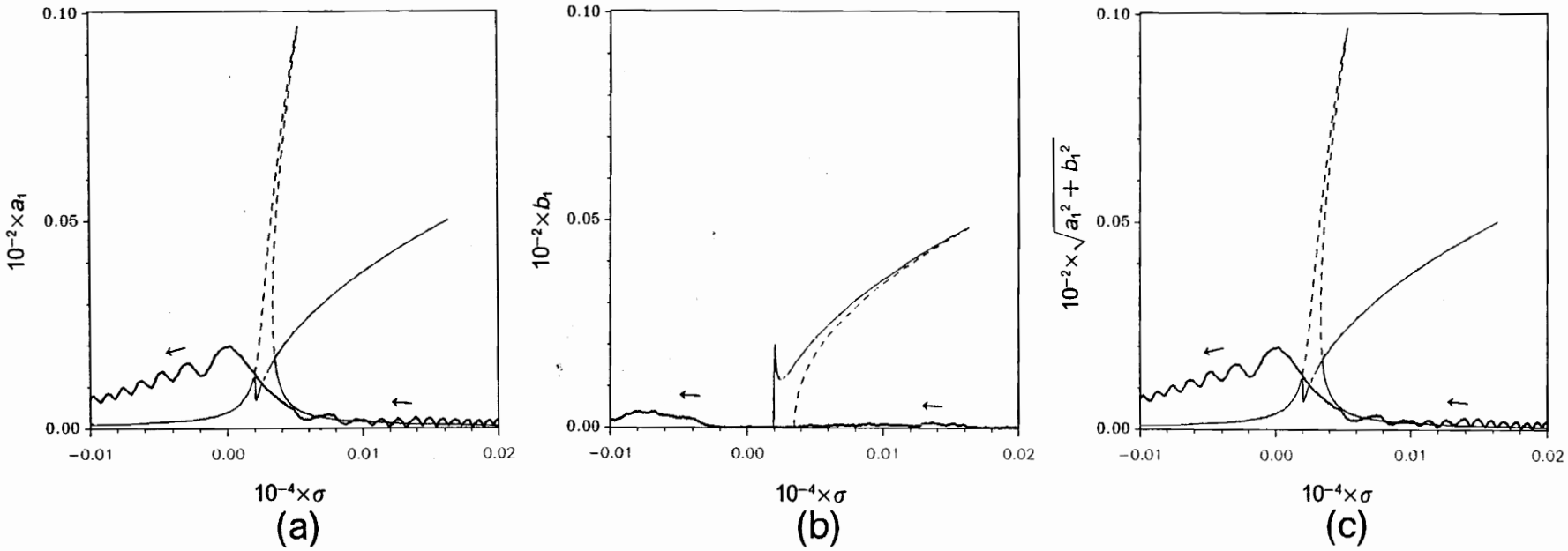

Figure 5.90 Comparison of non-stationary response subjected to persistent random disturbance and stationary response for sweep rate $\lambda = -1\times10^{-6}$. First mode, superharmonic resonance of order two, bound of the disturbance = 0.0001, f = 0.5W, $\delta = 0.0002$, $\hat{\varepsilon}a_0 = 0.0001$, $\hat{\varepsilon}b_0 = \gamma_0 = \psi_0 = 0$; (a) in-plane component, (b) out-of-plane component, (c) total amplitude.

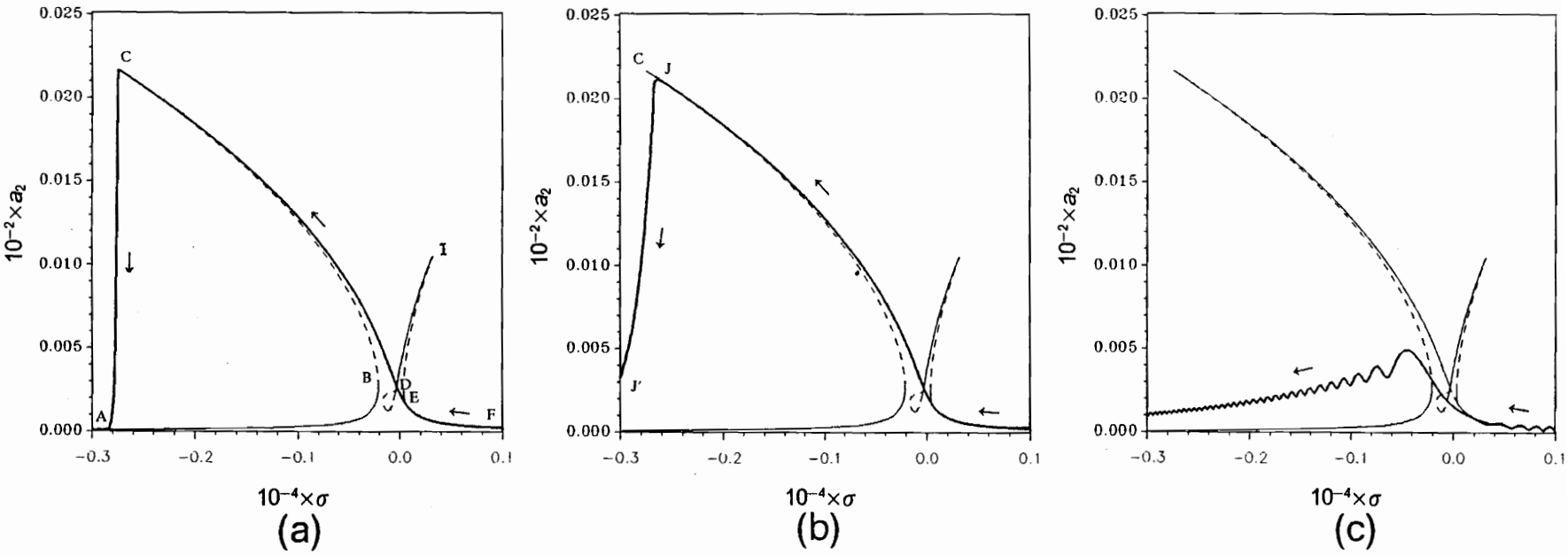

Figure 5.91 Comparison of non-stationary and stationary responses of the second mode for superharmonic resonance of order two with three sweep rates (deceleration). f = 5W, $\delta = 0.002$, $\hat{\varepsilon}a_0 = 0.0001$, $\hat{\varepsilon}b_0 = \gamma_0 = \psi_0 = 0$; (a) $\lambda = -1\times10^{-6}$, (b) $\lambda = -1\times10^{-5}$, (c) $\lambda = -1\times10^{-4}$.

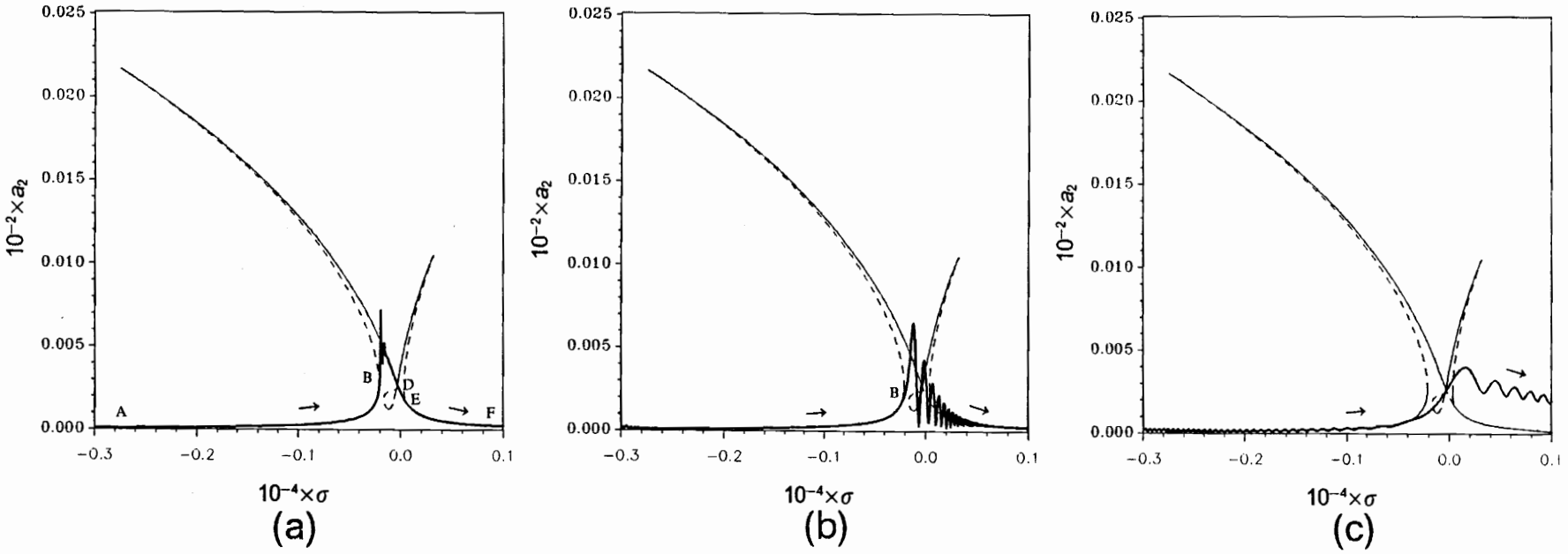

Figure 5.92 Comparison of non-stationary and stationary responses of the second mode for superharmonic resonance of order two with three sweep rates (acceleration). f = 5W, $\delta = 0.002$, $\hat{\varepsilon}a_0 = 0.0001$, $\hat{\varepsilon}b_0 = \gamma_0 = \psi_0 = 0$; (a) $\lambda = 1\times10^{-6}$, (b) $\lambda = 1\times10^{-5}$, (c) $\lambda = 1\times10^{-4}$.

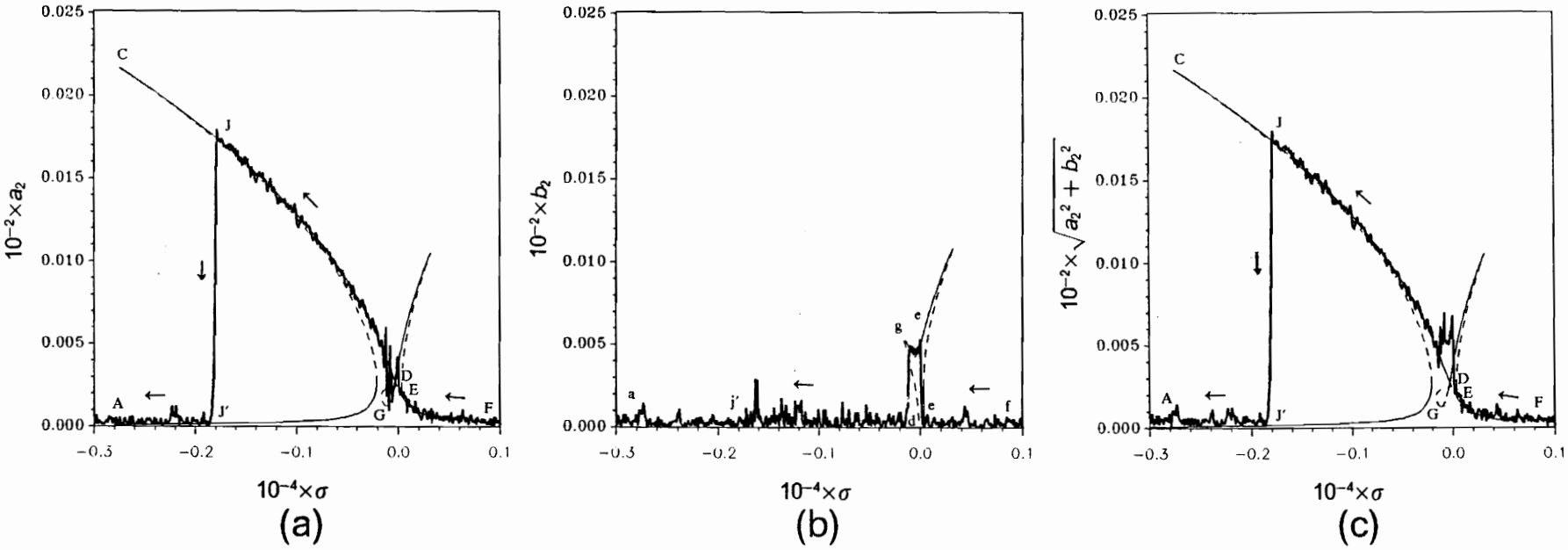

Figure 5.93 Comparison of non-stationary response subjected to persistent random disturbance and stationary response for sweep rate $\lambda = -1\times10^{-6}$. Second mode, superharmonic resonance of order two, bound of the disturbance = 0.0001, f = 5W, $\delta = 0.002$, $\hat{\varepsilon}a_0 = 0.0001$, $\hat{\varepsilon}b_0 = \gamma_0 = \psi_0 = 0$; (a) in-plane component, (b) out-of-plane component, (c) total amplitude.

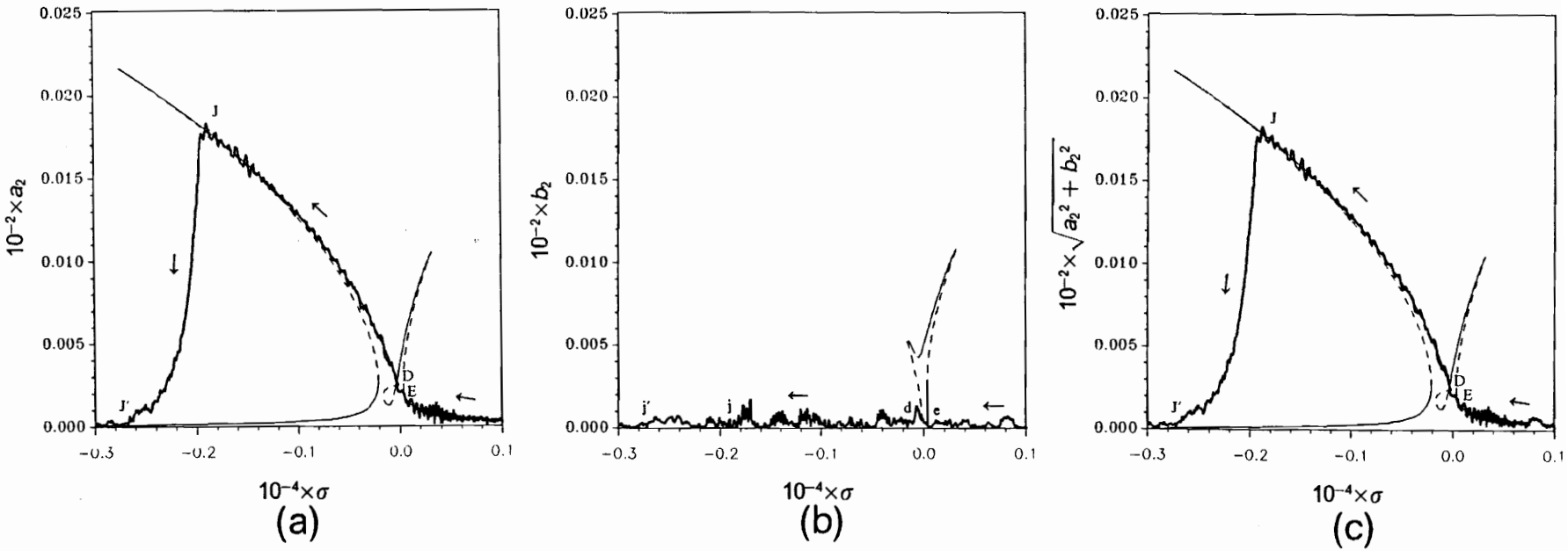

Figure 5.94 Comparison of non-stationary response subjected to persistent random disturbance and stationary response for sweep rate $\lambda = -1\times10^{-5}$. Second mode, superharmonic resonance of order two, bound of the disturbance = 0.0001, f = 5W, $\delta = 0.002$, $\hat{\varepsilon}a_0 = 0.0001$, $\hat{\varepsilon}b_0 = \gamma_0 = \psi_0 = 0$; (a) in-plane component, (b) out-of-plane component, (c) total amplitude.

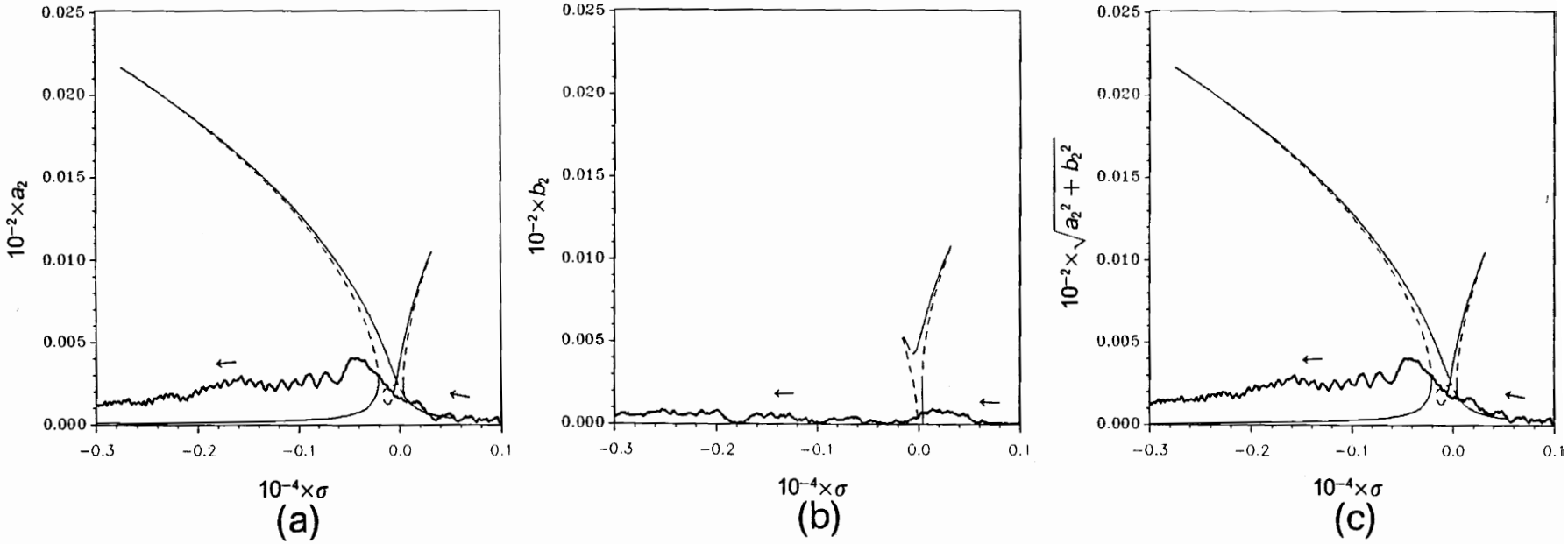

Figure 5.95 Comparison of non-stationary response subjected to persistent random disturbance and stationary response for sweep rate $\lambda = -1\times10^{-4}$. Second mode, superharmonic resonance of order two, bound of the disturbance = 0.0001, f = 5W, $\delta = 0.002$, $\hat{\varepsilon}a_0 = 0.0001$, $\hat{\varepsilon}b_0 = \gamma_0 = \psi_0 = 0$; (a) in-plane component, (b) out-of-plane component, (c) total amplitude.

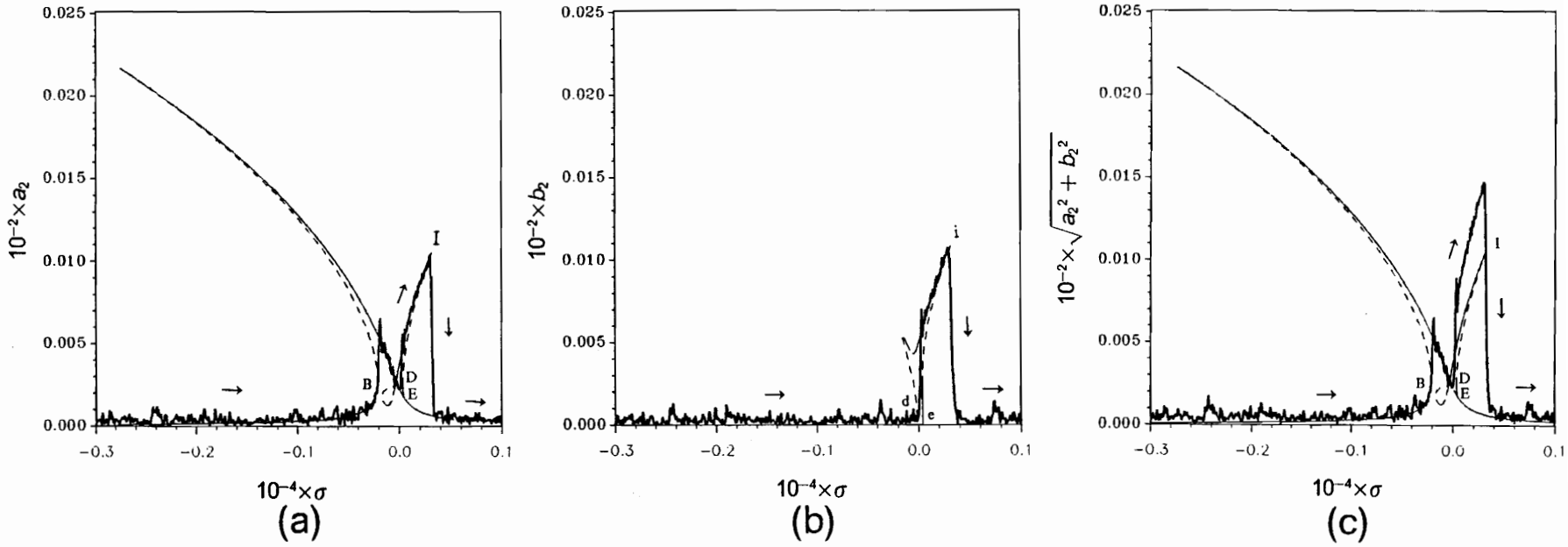

Figure 5.96 Comparison of non-stationary response subjected to persistent random disturbance and stationary response for sweep rate $\lambda = 1\times10^{-6}$. Second mode, superharmonic resonance of order two, bound of the disturbance = 0.0001, f = 5W, $\delta = 0.002$, $\hat{\varepsilon}a_0 = 0.0001$, $\hat{\varepsilon}b_0 = \gamma_0 = \psi_0 = 0$; (a) in-plane component, (b) out-of-plane component, (c) total amplitude.

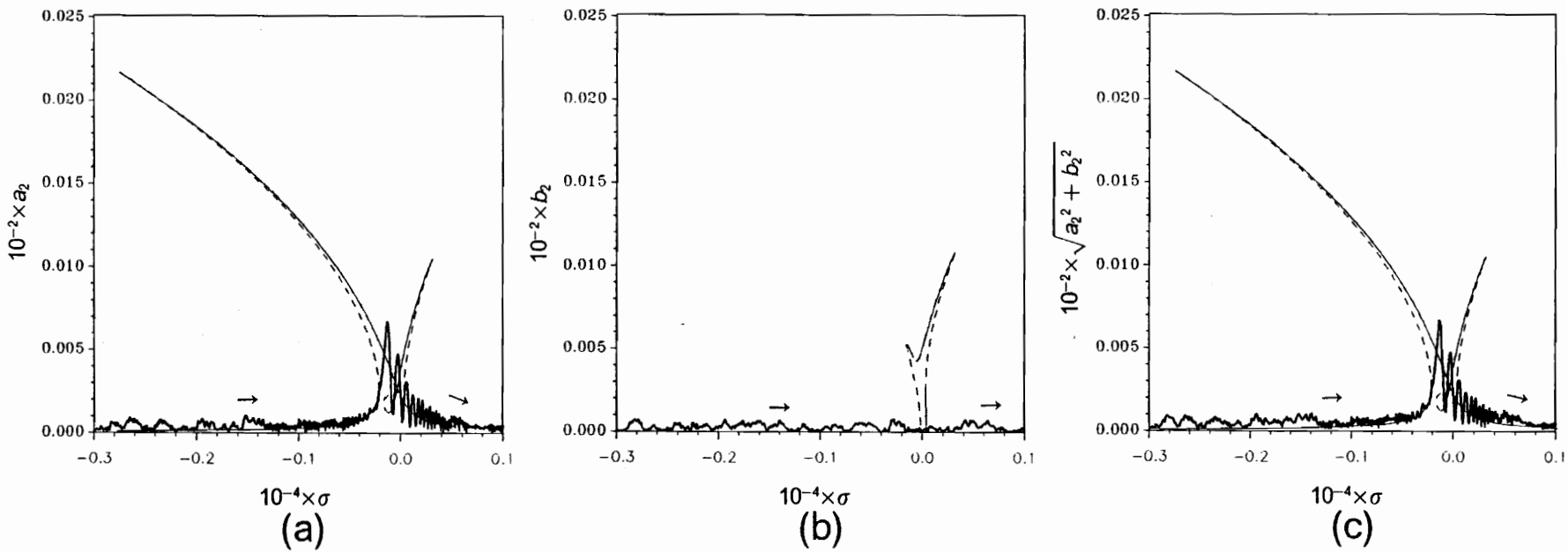

Figure 5.97 Comparison of non-stationary response subjected to persistent random disturbance and stationary response for sweep rate $\lambda = 1\times10^{-5}$. Second mode, superharmonic resonance of order two, bound of the disturbance = 0.0001, f = 5W, $\delta = 0.002$, $\hat{\varepsilon}a_0 = 0.0001$, $\hat{\varepsilon}b_0 = \gamma_0 = \psi_0 = 0$; (a) in-plane component, (b) out-of-plane component, (c) total amplitude.

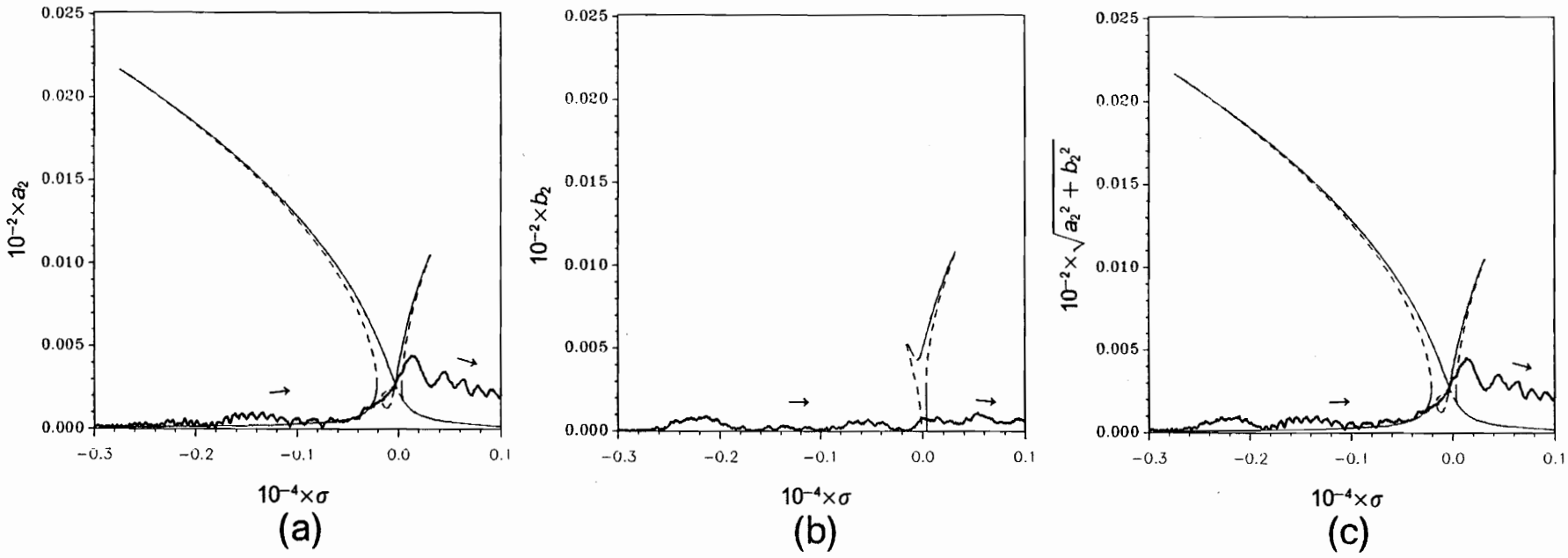

Figure 5.98 Comparison of non-stationary response subjected to persistent random disturbance and stationary response for sweep rate $\lambda = 1\times10^{-4}$. Second mode, superharmonic resonance of order two, bound of the disturbance = 0.0001, f = 5W, $\delta = 0.002$, $\hat{\varepsilon}a_0 = 0.0001$, $\hat{\varepsilon}b_0 = \gamma_0 = \psi_0 = 0$; (a) in-plane component, (b) out-of-plane component, (c) total amplitude.

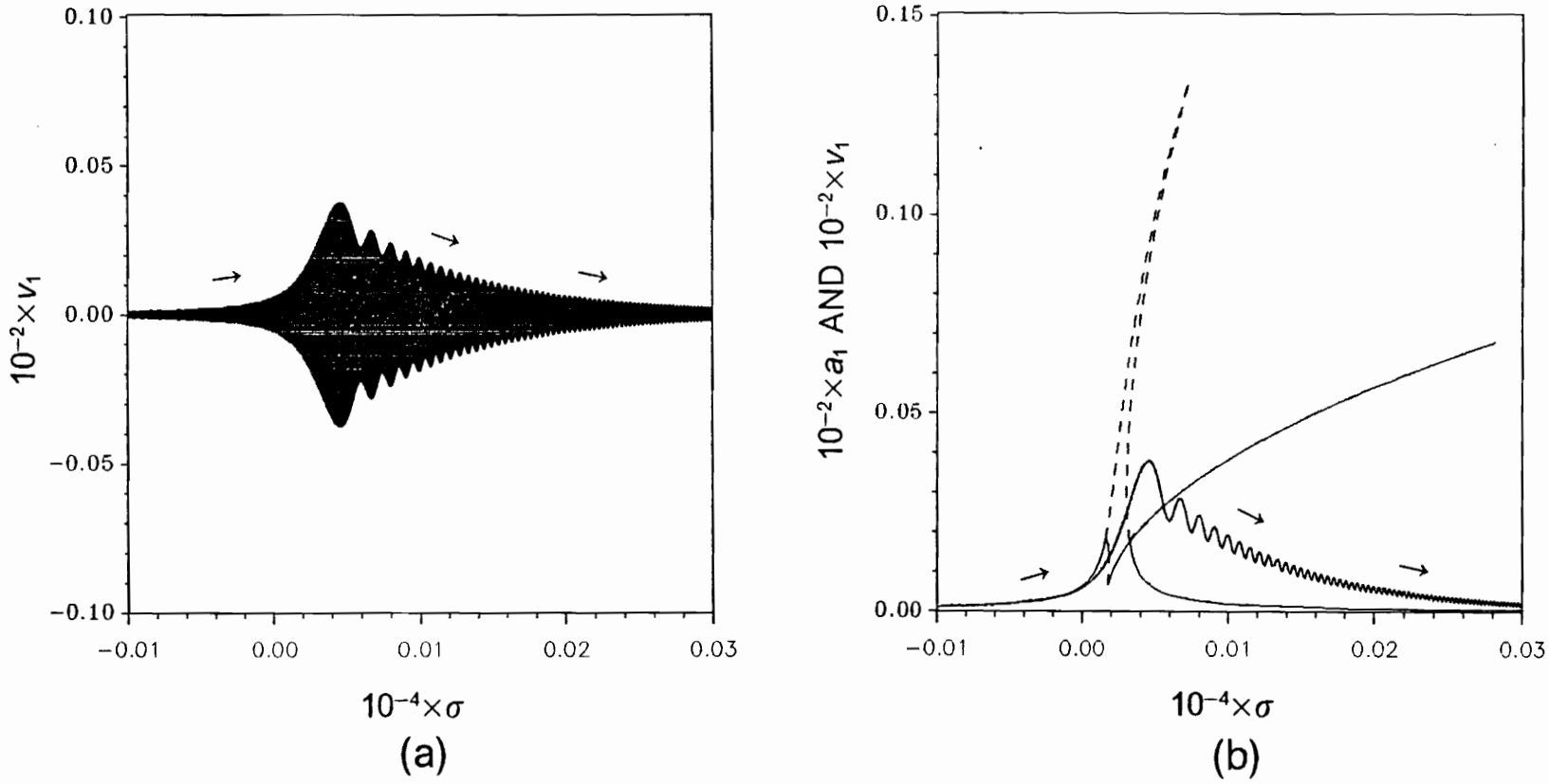

Figure 5.99 Comparison of the amplitudes from the integration of the original differential equations and the MMS. First mode, primary resonance, f = 0.0005W, $\delta = 0.0002$, $\hat{\varepsilon}a_0 = 0.0001$, $\hat{\varepsilon}b_0 = \gamma_0 = \psi_0 = 0$, $\lambda = 1\times10^{-6}$; (a) amplitude from the integration of the original differential equations, (b) stationary amplitude, non-stationary amplitude from the MMS and the outline from (a).

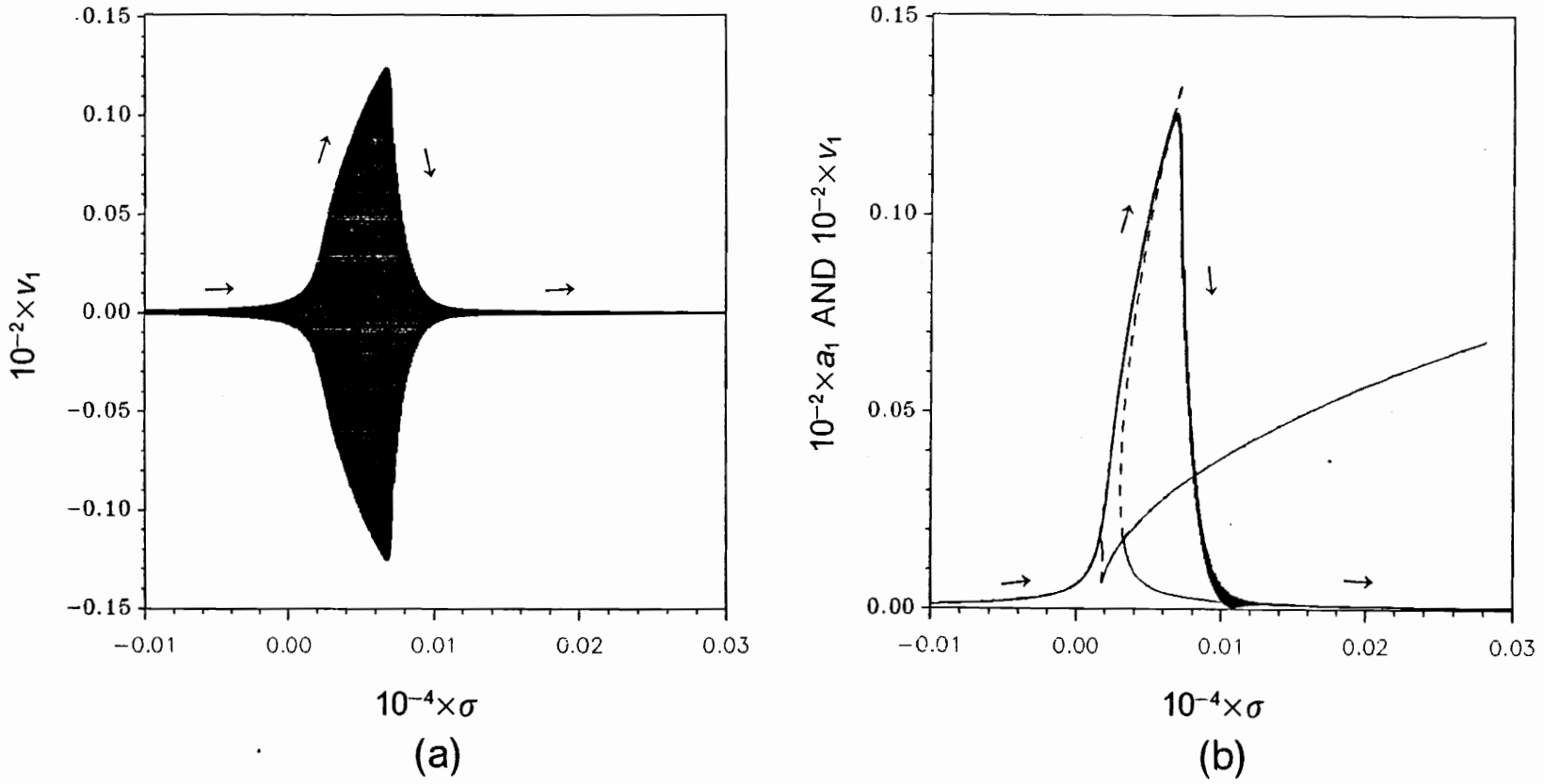

Figure 5.100 Comparison of the amplitudes from the integration of the original differential equations and the MMS. First mode, primary resonance, f = 0.0005W, $\delta = 0.0002$, $\hat{\varepsilon}a_0 = 0.0001$, $\hat{\varepsilon}b_0 = \gamma_0 = \psi_0 = 0$, $\lambda = 1\times10^{-7}$; (a) amplitude from the integration of the original differential equations, (b) stationary amplitude, non-stationary amplitude from the MMS and the outline from (a).

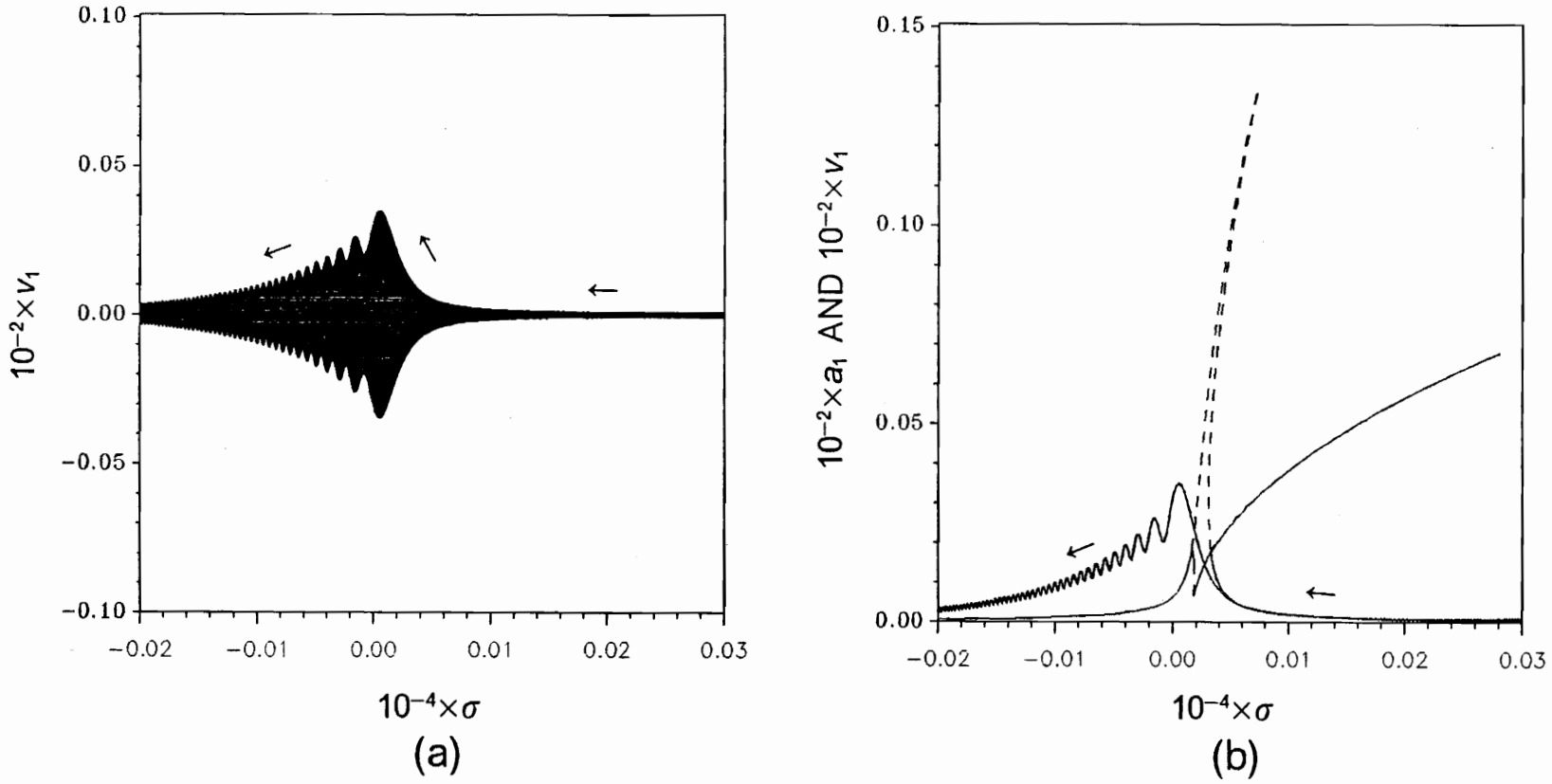

Figure 5.101 Comparison of the amplitudes from the integration of the original differential equations and the MMS. First mode, primary resonance, f = 0.0005W, $\delta = 0.0002$, $\hat{\varepsilon}a_0 = 0.0001$, $\hat{\varepsilon}b_0 = \gamma_0 = \psi_0 = 0$, $\lambda = -1\times10^{-6}$; (a) amplitude from the integration of the original differential equations, (b) stationary amplitude, non-stationary amplitude from the MMS and the outline from (a).

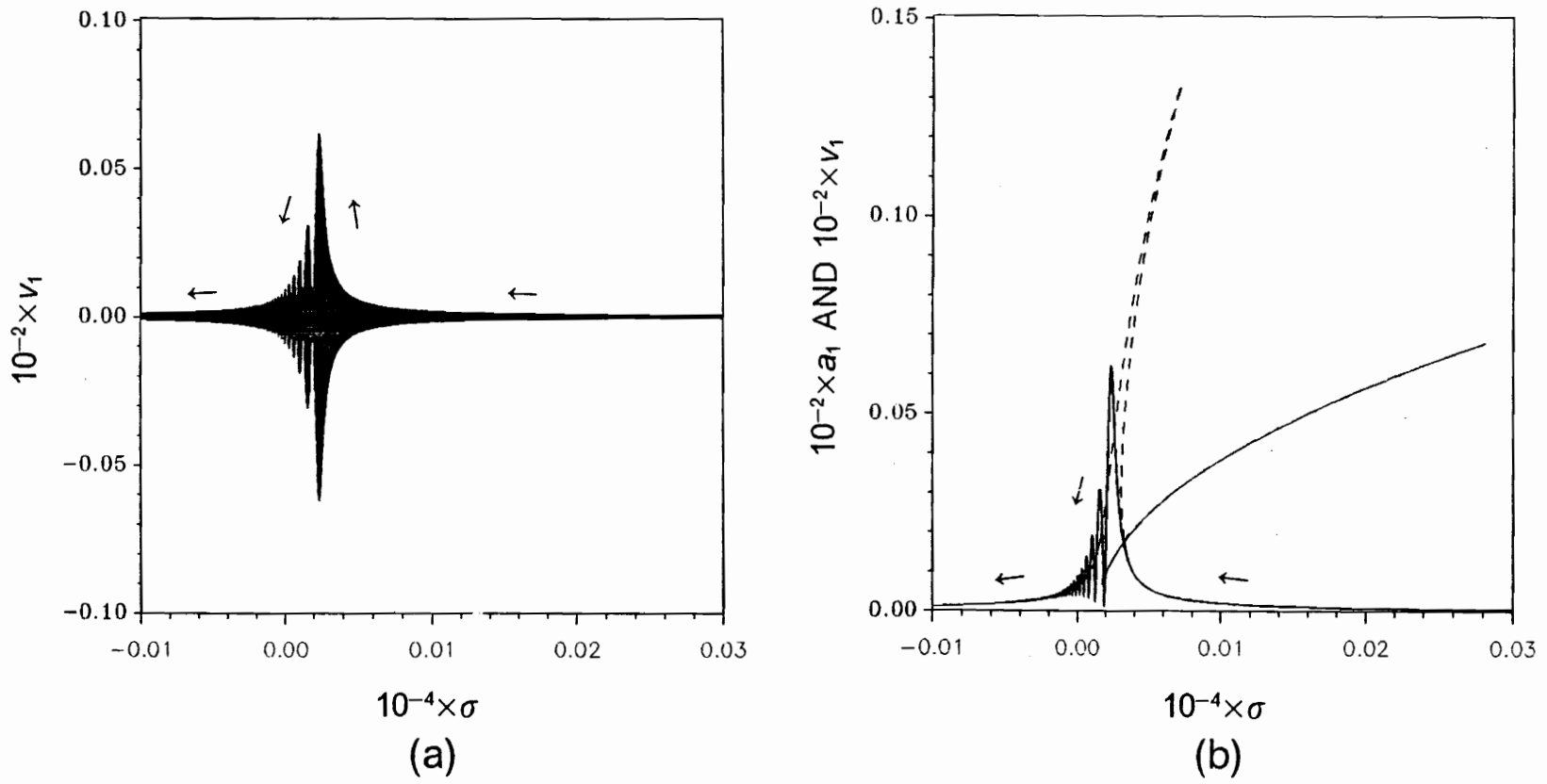

Figure 5.102 Comparison of the amplitudes from the integration of the original differential equations and the MMS. First mode, primary resonance, f = 0.0005W, $\delta = 0.0002$, $\hat{\varepsilon}a_0 = 0.0001$, $\hat{\varepsilon}b_0 = \gamma_0 = \psi_0 = 0$, $\lambda = -1\times10^{-7}$; (a) amplitude from the integration of the original differential equations, (b) stationary amplitude, non-stationary amplitude from the MMS and the outline from (a).

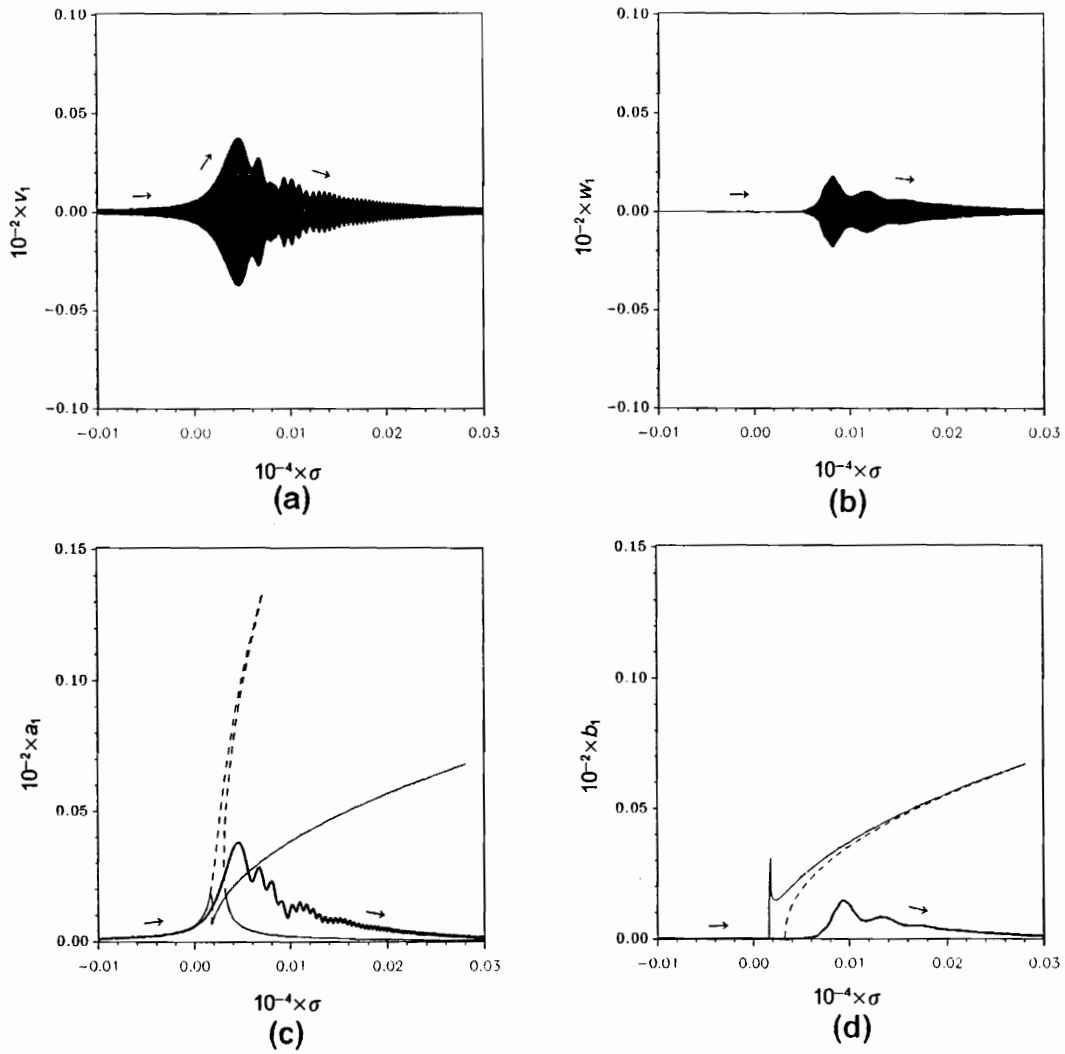

Figure 5.103 Comparison of the amplitudes from the integration of the original differential equations and the MMS. First mode, primary resonance, f = 0.0005W, $\delta = 0.0002$, $\hat{\varepsilon}a_0 = \hat{\varepsilon}b_0 = 0.0001$, $\gamma_0 = \psi_0 = 0$, $\lambda = 1\times10^{-6}$; (a) in-plane component, (b) out-of-plane component of the amplitude from the integration of the original differential equations; (c) in-plane component, (d) out-of-plane component of stationary and non-stationary amplitudes from the MMS.

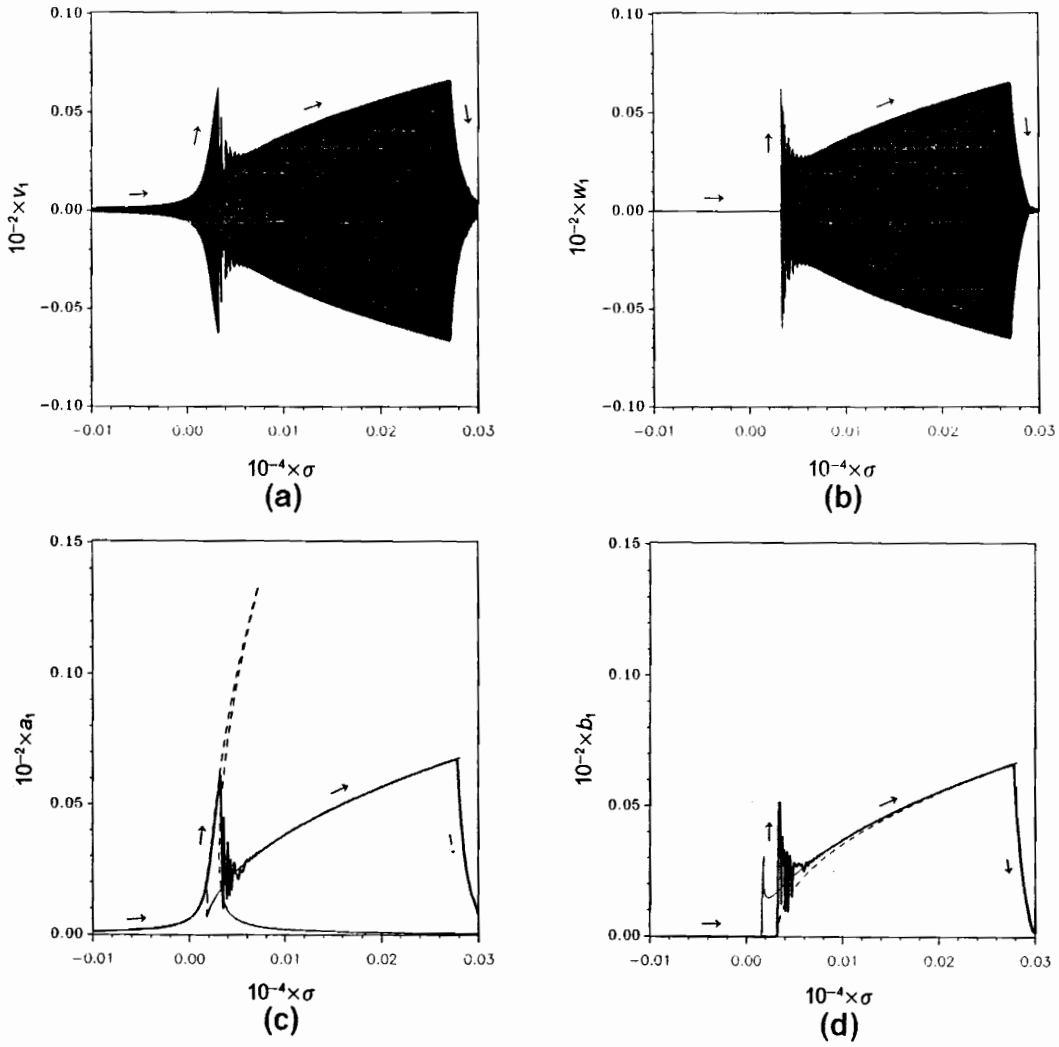

Figure 5.104 Comparison of the amplitudes from the integration of the original differential equations and the MMS. First mode, primary resonance, f = 0.0005W, $\delta = 0.0002$, $\hat{\varepsilon}a_0 = \hat{\varepsilon}b_0 = 0.0001$, $\gamma_0 = \psi_0 = 0$, $\lambda = 1\times10^{-7}$; (a) in-plane component, (b) out-of-plane component of the amplitude from the integration of the original differential equations; (c) in-plane component, (d) out-of-plane component of stationary and non-stationary amplitudes from the MMS.

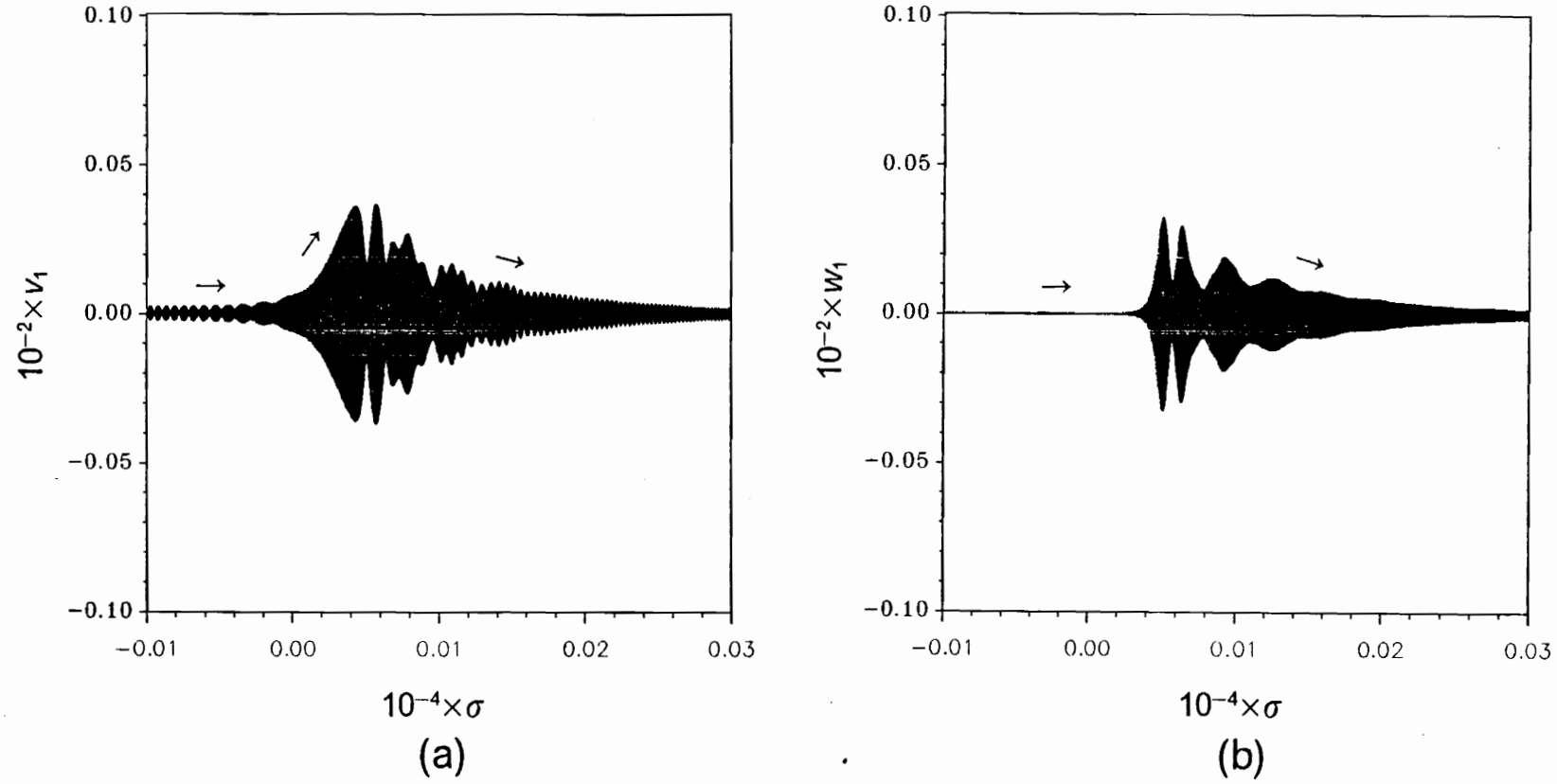

Figure 5.105 amplitudes from the integration of the original differential equations. First mode, primary resonance, f = 0.0005W, $\delta = 0.0002$, $\hat{\varepsilon}a_0 = 0.0001$, $\hat{\varepsilon}b_0 = \gamma_0 = \psi_0 = 0$, $\lambda = 1\times10^{-6}$, bound of the persistent random disturbance = 0.0001; (a) in-plane component, (b) out-of-plane component.

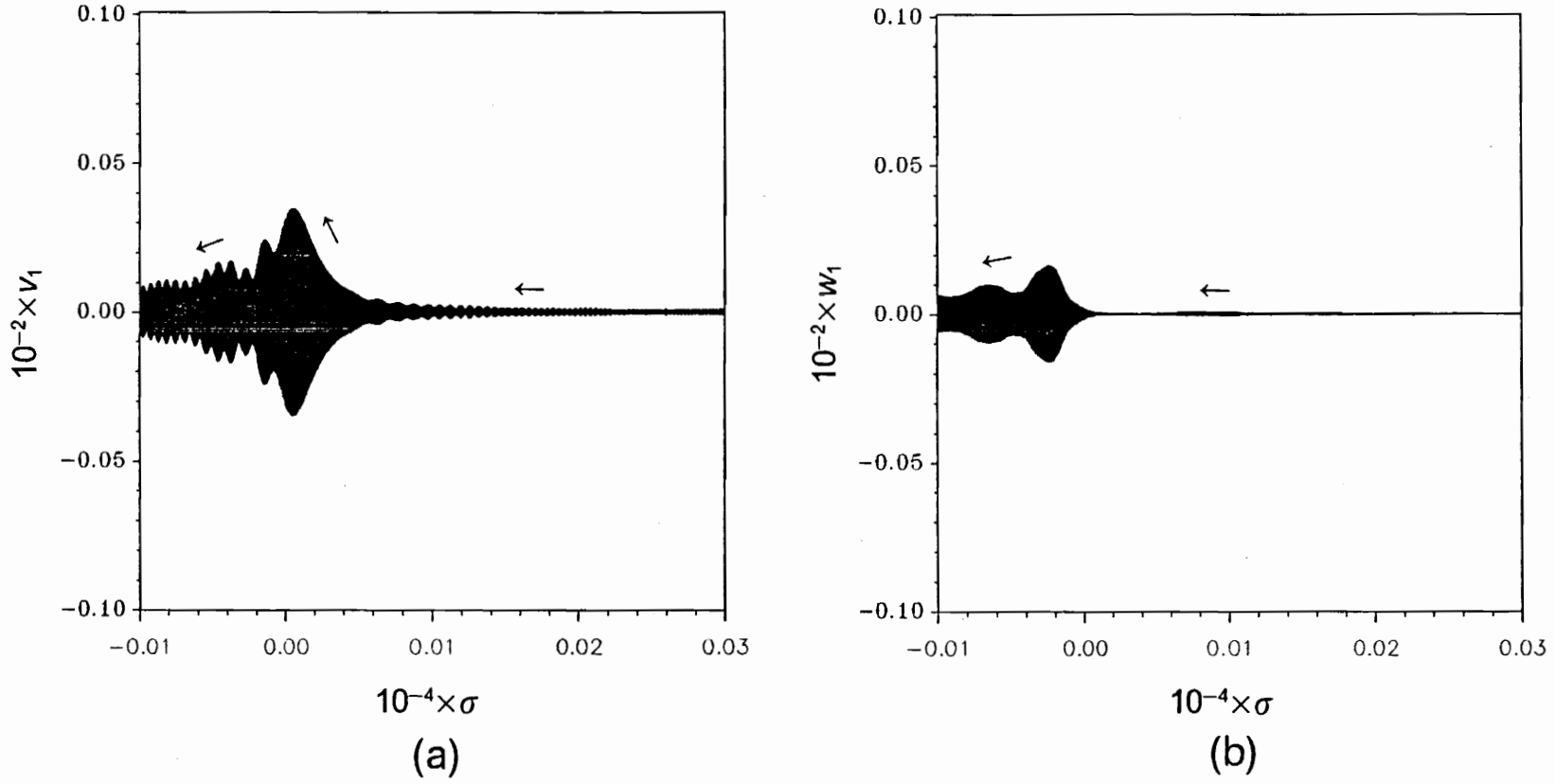

Figure 5.106 amplitudes from the integration of the original differential equations. First mode, primary resonance, f = 0.0005W, $\delta = 0.0002$, $\hat{\varepsilon}a_0 = 0.0001$, $\hat{\varepsilon}b_0 = \gamma_0 = \psi_0 = 0$, $\lambda = -1\times10^{-6}$, bound of the persistent random disturbance = 0.0001; (a) in-plane component, (b) out-of-plane component.

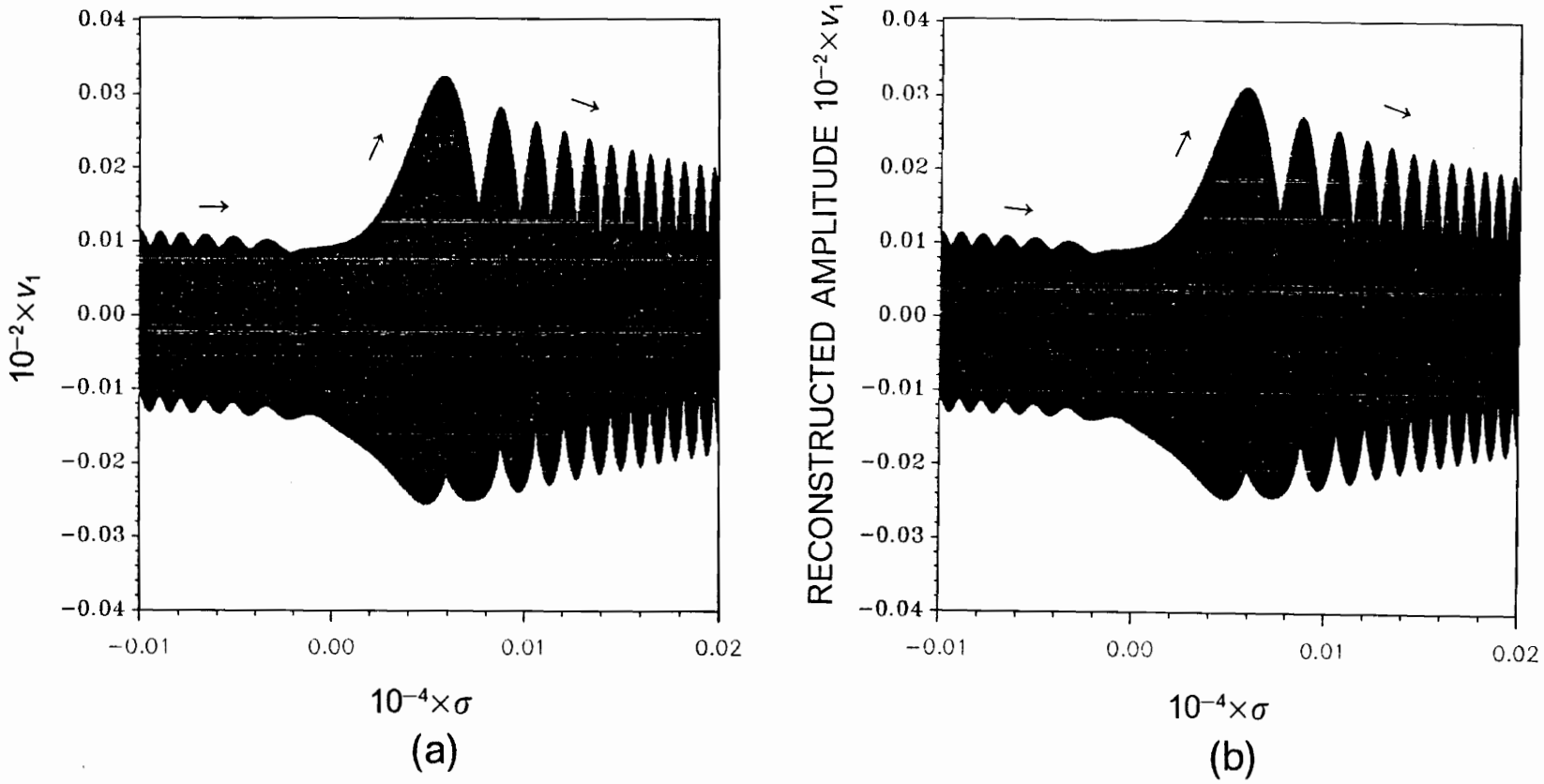

Figure 5.107 Comparison of the amplitudes from the integration of the original differential equations and the MMS. First mode, superharmonic resonance of order two, f = 0.5W, $\delta = 0.0002$, $\hat{\varepsilon}a_0 = 0.0001$, $\hat{\varepsilon}b_0 = \gamma_0 = \psi_0 = 0$, $\lambda = 1\times10^{-6}$; (a) amplitude from the integration of the original differential equations, (b) reconstructed amplitude from the result of MMS.

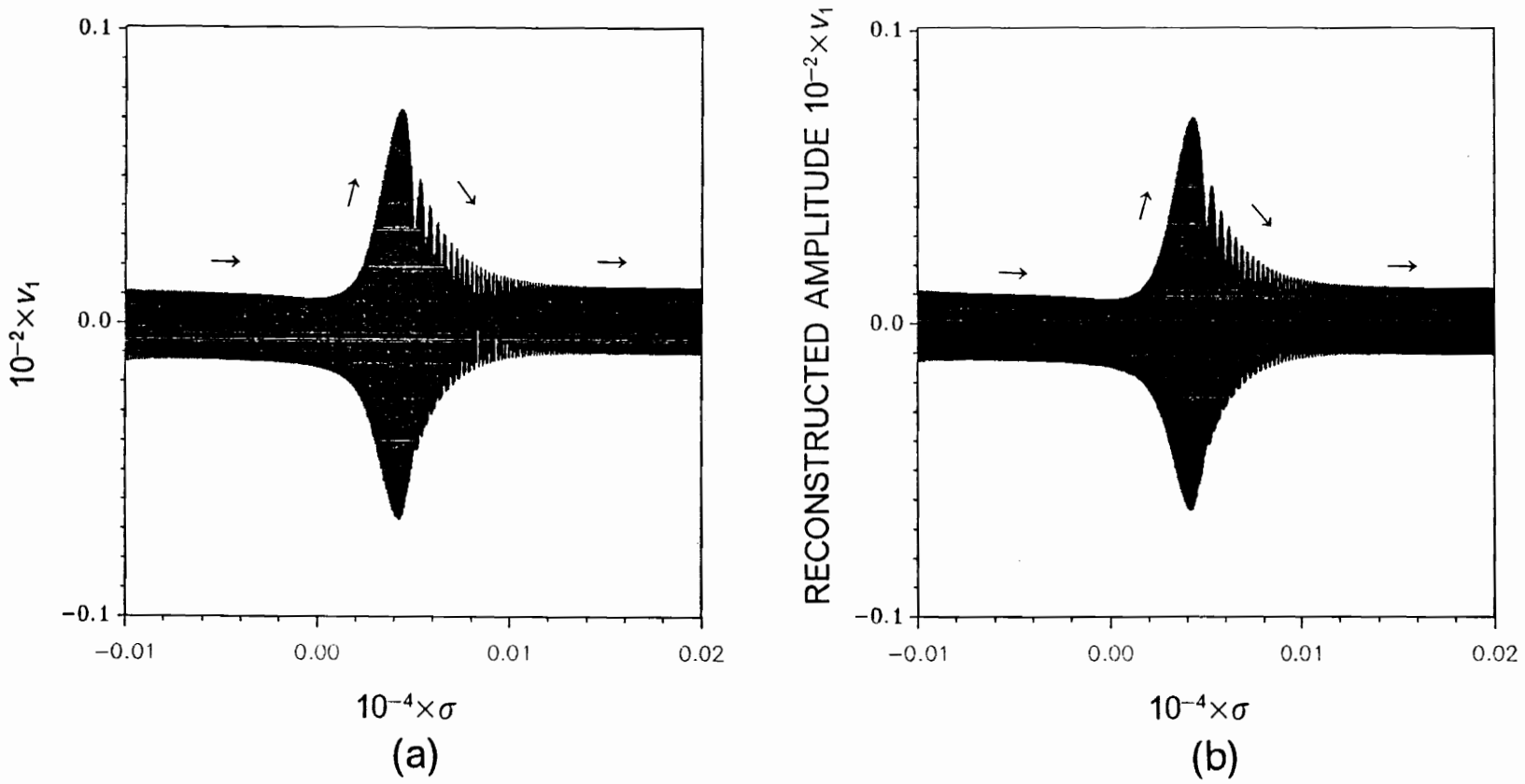

Figure 5.108 Comparison of the amplitudes from the integration of the original differential equations and the MMS. First mode, superharmonic resonance of order two, f = 0.5W, $\delta = 0.0002$, $\hat{\varepsilon}a_0 = 0.0001$, $\hat{\varepsilon}b_0 = \gamma_0 = \psi_0 = 0$, $\lambda = 1\times10^{-7}$; (a) amplitude from the integration of the original differential equations, (b) reconstructed amplitude from the result of MMS.

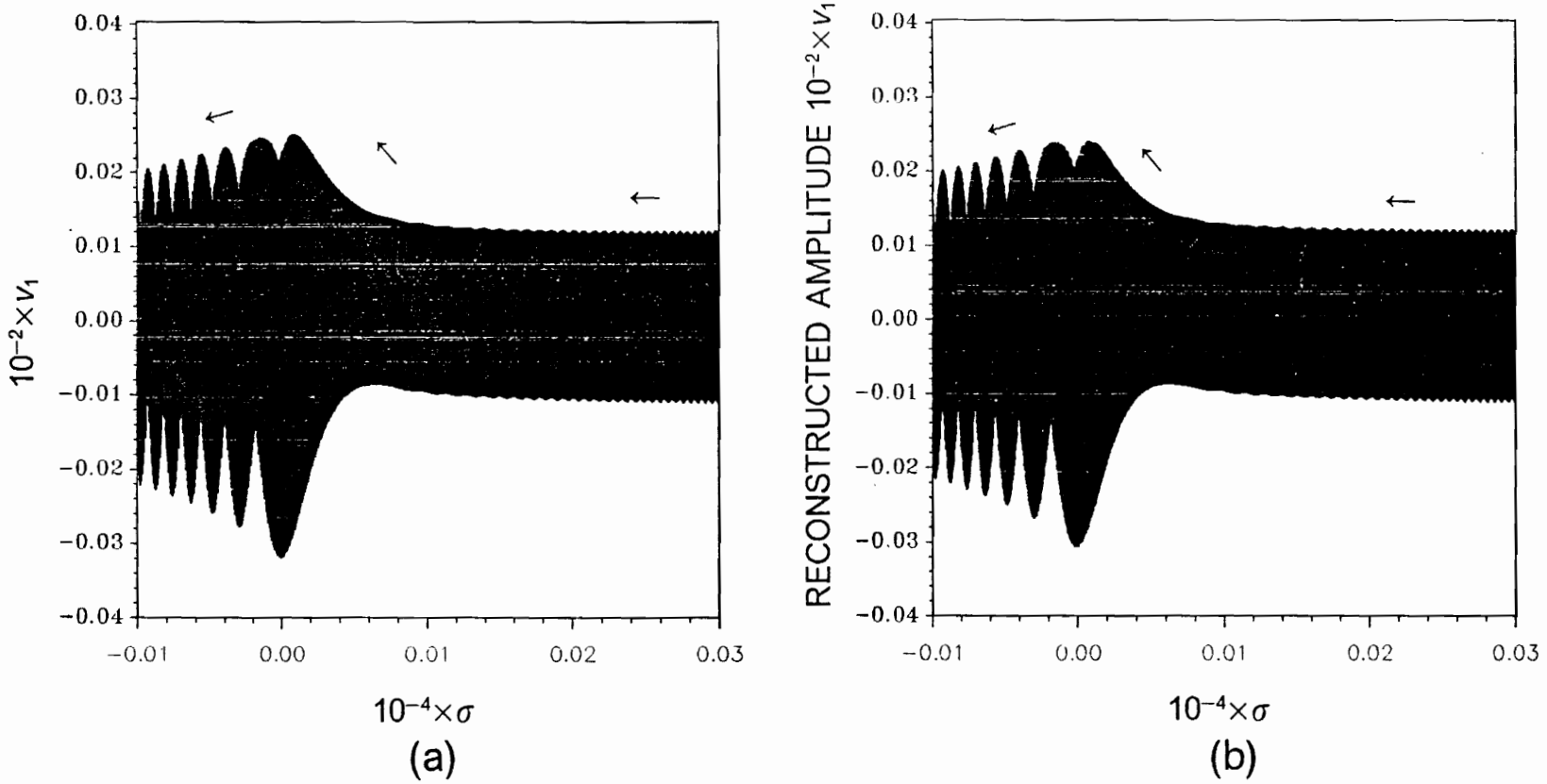

Figure 5.109 Comparison of the amplitudes from the integration of the original differential equations and the MMS. First mode, superharmonic resonance of order two, f = 0.5W, $\delta = 0.0002, \hat{\varepsilon}a_0 = 0.0001, \hat{\varepsilon}b_0 = \gamma_0 = \psi_0 = 0, \lambda = -1\times10^{-6}$; (a) amplitude from the integration of the original differential equations, (b) reconstructed amplitude from the result of MMS.

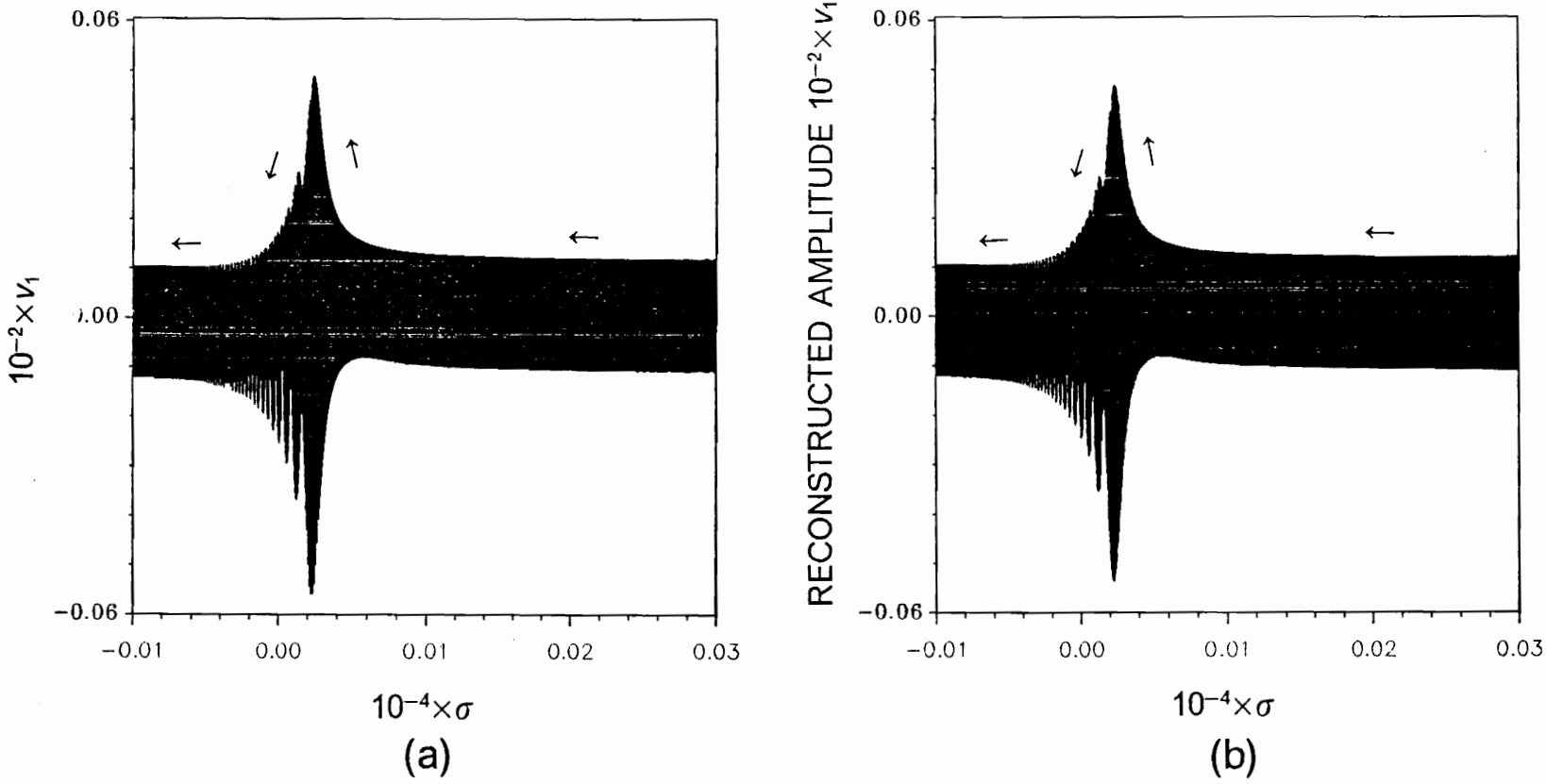

Figure 5.110 Comparison of the amplitudes from the integration of the original differential equations and the MMS. First mode, superharmonic resonance of order two, f = 0.5W, $\delta = 0.0002$, $\hat{\varepsilon}a_0 = 0.0001$, $\hat{\varepsilon}b_0 = \gamma_0 = \psi_0 = 0$, $\lambda = -1\times10^{-7}$; (a) amplitude from the integration of the original differential equations, (b) reconstructed amplitude from the result of MMS.

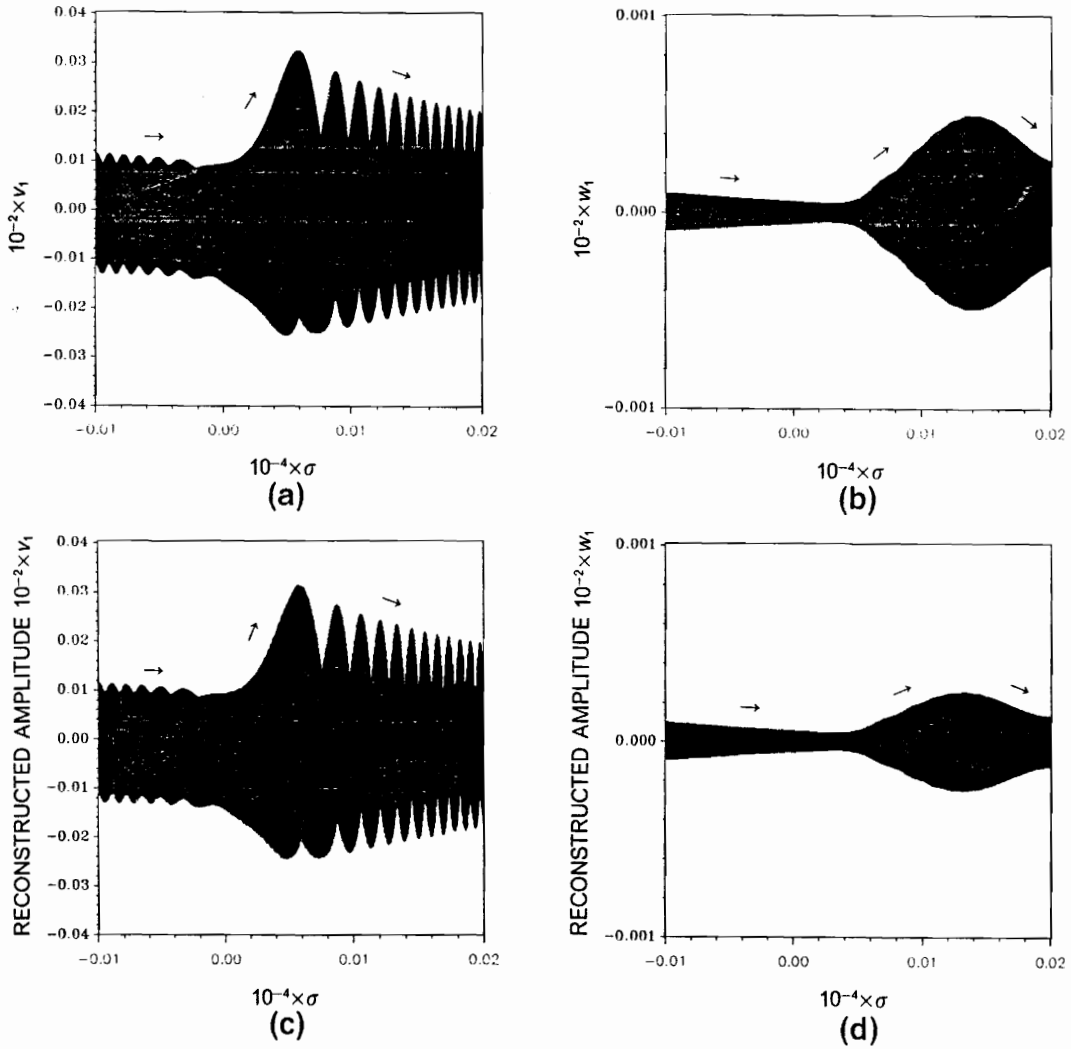

Figure 5.111 Comparison of the amplitudes from the integration of the original differential equations and the MMS. First mode, superharmonic resonance of order two, f = 0.5W, $\delta = 0.0002$, $\hat{\varepsilon}a_0 = \hat{\varepsilon}b_0 = 0.0001$, $\gamma_0 = \psi_0 = 0$, $\lambda = 1\times10^{-6}$; (a) in-plane component, (b) out-of-plane component of the amplitude from the integration of the original differential equations; (c) in-plane component, (d) out-of-plane component of the reconstructed amplitude from the result of MMS.

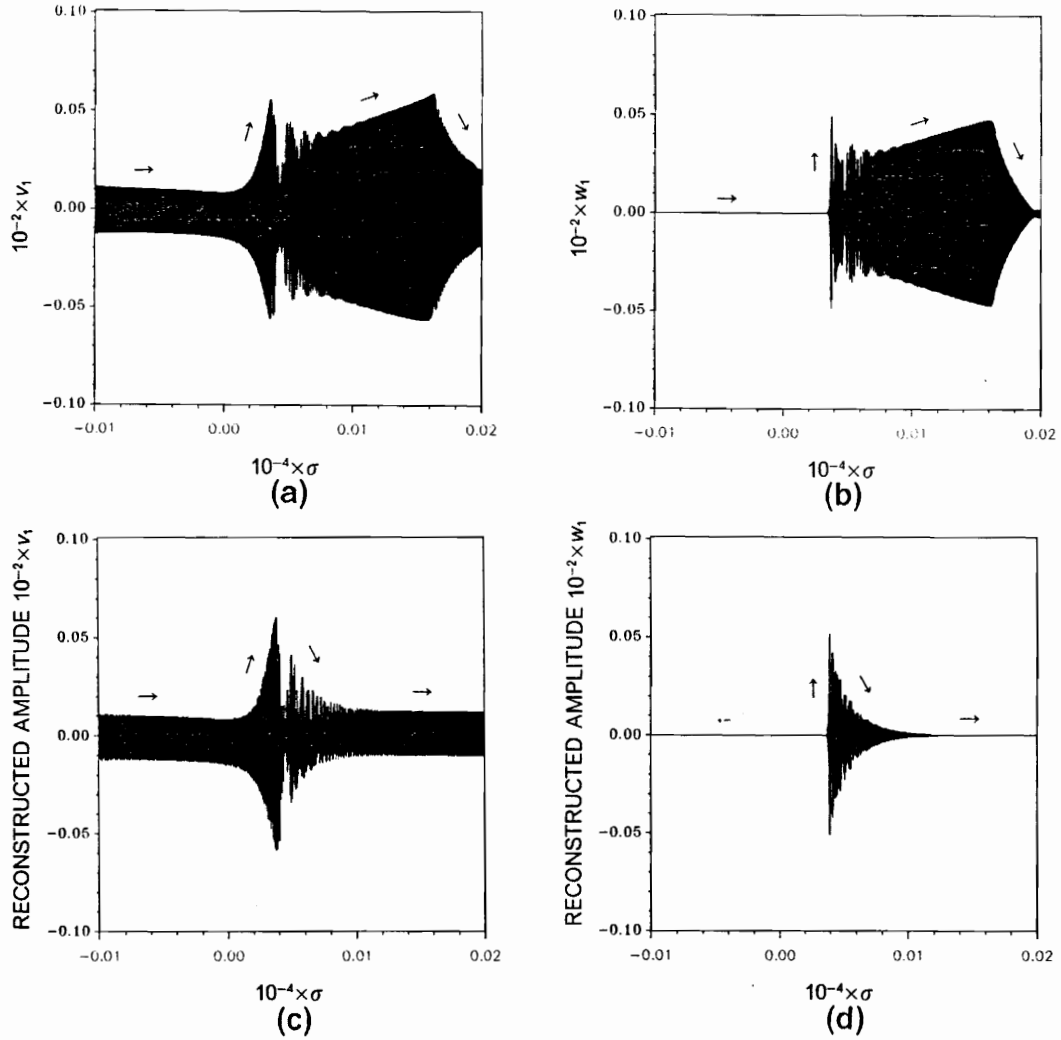

Figure 5.112 Comparison of the amplitudes from the integration of the original differential equations and the MMS. First mode, superharmonic resonance of order two, f = 0.5W, $\delta = 0.0002$, $\hat{\varepsilon}a_0 = \hat{\varepsilon}b_0 = 0.0001$, $\gamma_0 = \psi_0 = 0$, $\lambda = 1\times10^{-7}$; (a) in-plane component, (b) out-of-plane component of the amplitude from the integration of the original differential equations; (c) in-plane component, (d) out-of-plane component of the reconstructed amplitude from the result of MMS.

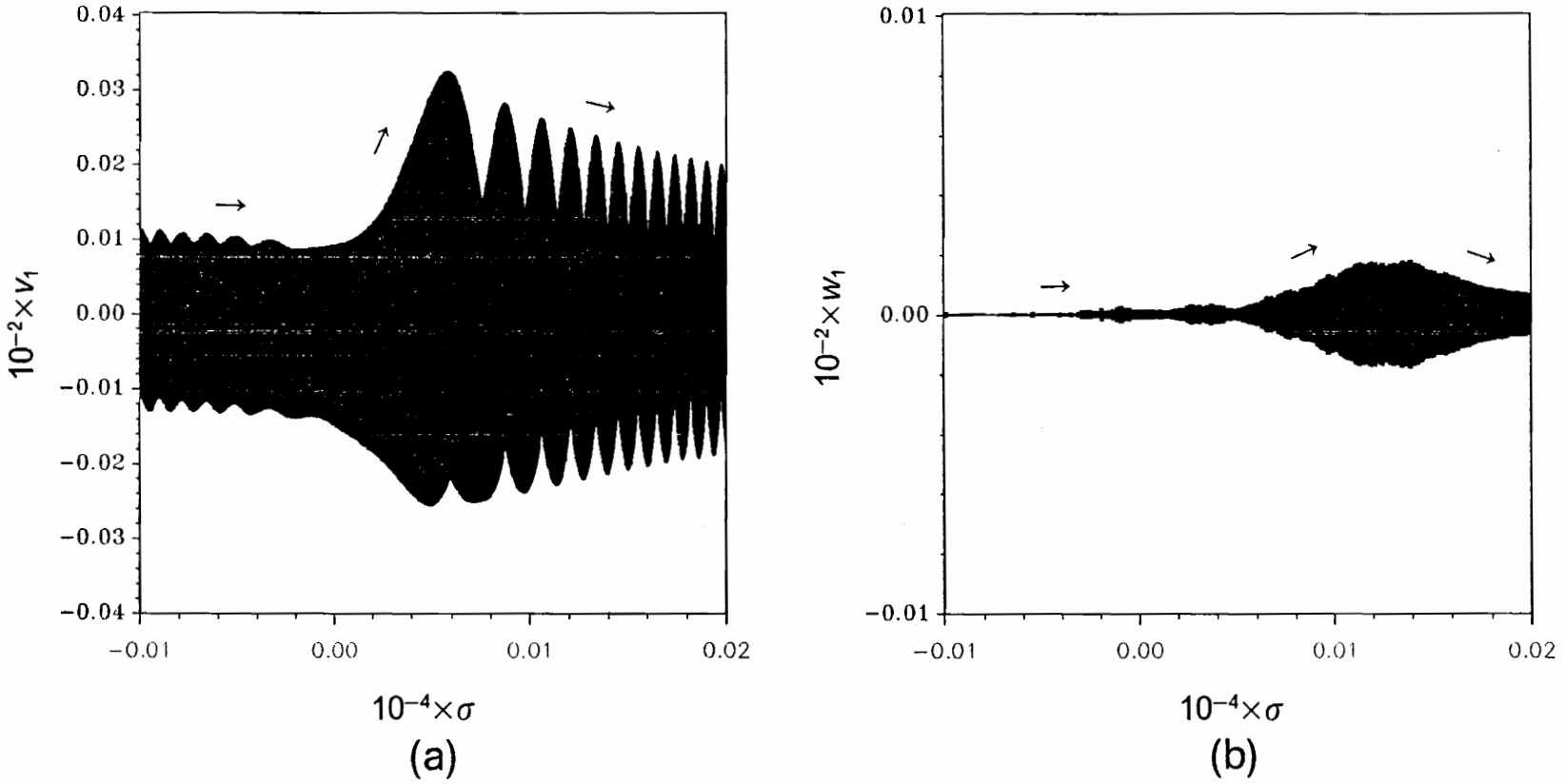

Figure 5.113 Amplitudes from the integration of the original differential equations. First mode, superharmonic resonance of order two, f = 0.5W, $\delta = 0.0002$, $\hat{\varepsilon}a_0 = 0.0001$, $\hat{\varepsilon}b_0 = \gamma_0 = \psi_0 = 0$, $\lambda = 1\times10^{-6}$, bound of the persistent random disturbance = 0.0001; (a) in-plane component, (b) out-of-plane component.

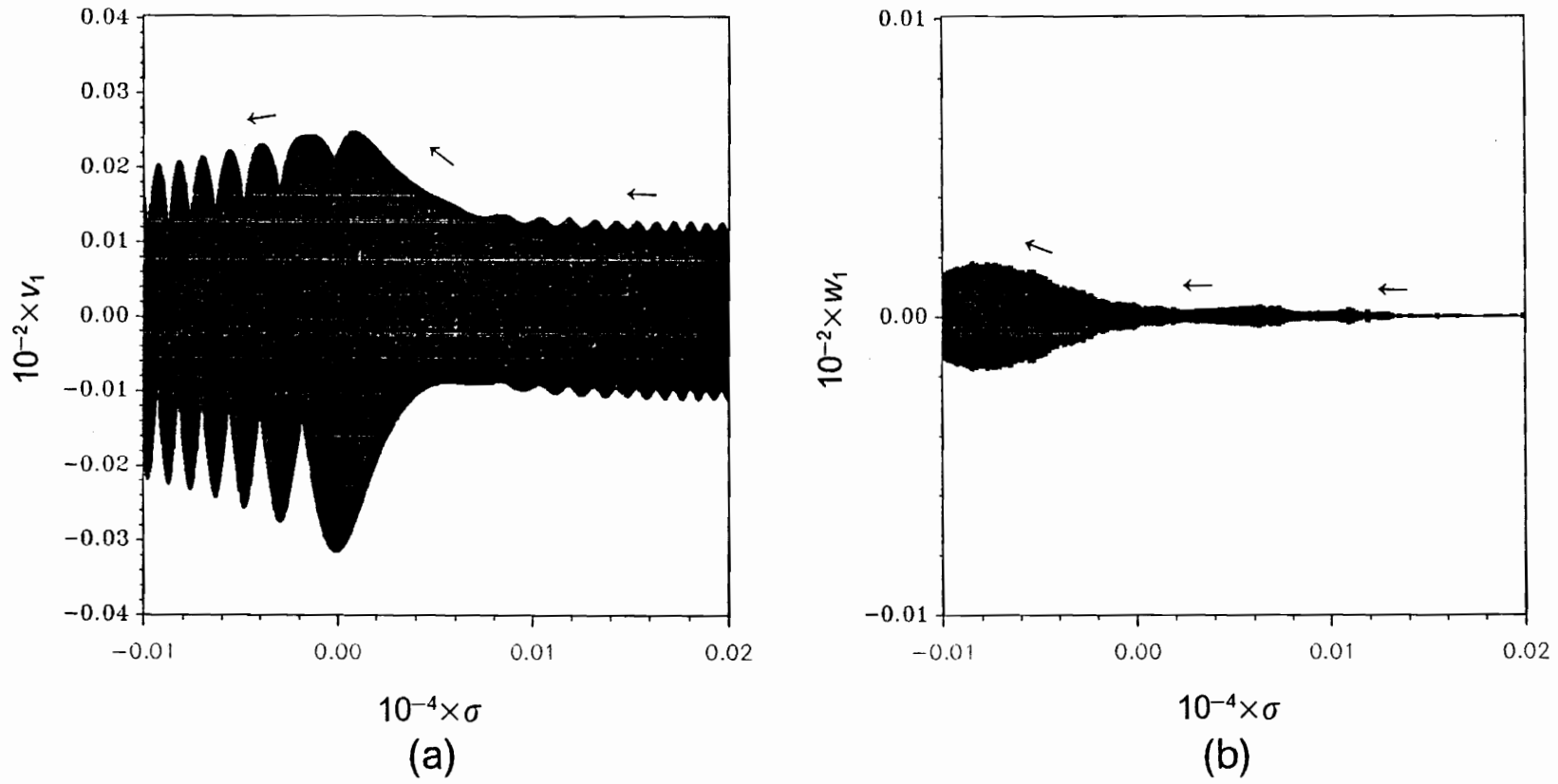

Figure 5.114 Amplitudes from the integration of the original differential equations. First mode, superharmonic resonance of order two, f = 0.5W, $\delta = 0.0002$, $\hat{\varepsilon}a_0 = 0.0001$, $\hat{\varepsilon}b_0 = \gamma_0 = \psi_0 = 0$, $\lambda = -1\times10^{-6}$, bound of the persistent random disturbance = 0.0001; (a) in-plane component, (b) out-of-plane component.

6 Conclusions

In this dissertation, stationary and non-stationary responses of a slender, elastic, cantilevered beam to a simple harmonic excitation are investigated. The effects of nonlinear curvature, nonlinear inertia, viscous damping and static deflection are included. The static deflection, new by developed in this dissertation, produces quadratic terms in the governing equations, and it introduces the possibility of a superharmonic resonance of order two and a subharmonic resonance of order two.

The nonlinear governing equations of the beam are derived by the Lagrangian approach. Galerkin's method is used to eliminate the spatial dependence from the governing equations, using the linear free-vibration modes. The method of multiple scales is applied to find the approximate solutions of the temporal equations. The modulation equations, obtained by eliminating the secular terms, are used to find both stationary and non-stationary solutions. Numerical integration of the original differential equations (the temporal equations) is carried out to verify the solutions from the method of multiple scales.

The study reveals that out-of-plane motion is possible in every resonance when the principal moments of inertia of the beam cross-section are approximately equal. Whirling motion occurs when the planar motion, subjected to out-of-plane disturbance, becomes unstable. The parameter studies for the stationary solutions show that this unstable region can be enlarged by increasing the force level or decreasing the damping coefficient. Hence, the larger the force is, and the smaller the

damping coefficient is, the more prominent the whirling motion becomes. Both stable and unstable nonplanar motions are found in every resonance. For some cases, limit cycles or chaotic motions might exist.

The study of passage through the resonance region shows that nonplanar motion can be caused by either an out-of-plane initial disturbance or a persistent random disturbance. The non-stationary amplitude will follow the stationary amplitude when the sweep rate is small. The larger the sweep rate is, the earlier the non-stationary amplitude deviates from the stationary amplitude and the greater the deviation. The maximum amplitude of the passage through resonance depends on the sweep rate, initial conditions, size of the disturbance, damping coefficient and force level. In general, the smaller the sweep is, the larger the maximum amplitude is when no out-of-plane disturbance is applied. But this is not always true when an out-of-plane disturbance is applied. The persistent random disturbance is beneficial to decrease the maximum amplitude only when it destroys the tendency of the non-stationary amplitude to follow the stationary amplitude to a large value. Otherwise, the persistent random disturbance can increase the maximum amplitude. Similarly, a large size of the disturbance is not always beneficial to decrease the maximum amplitude, depending on the sweep rate, the direction of sweep (acceleration or deceleration) and the excited mode number.

The non-stationary results show very good agreement with those from the numerical integration of the original differential equations in most cases. The computer process time consumed by the method of multiple scales is far less, at least by a factor 10, than that by the integration of the original differential equations. For those cases with very good agreement, it is suggested that the method of multiple scales can be used to save computing time.

Future work can include further investigation of the higher modes and the passage through the rest of the resonances, especially subharmonic resonance of order two. Subharmonic resonance of order two is not predicted when static deflection is not considered. The stationary solutions of this resonance indicates that the amplitude of the motion might be non-passable, which means the amplitude could grow extremely large, under some situations when the forcing frequency is passing through the resonance region. Subharmonic resonance of order two produces a large amplitude in

either the in-plane or out-of-plane direction when the non-passable phenomenon occurs. Furthermore, the integration of the original differential equations can be extended to investigate the responses of the higher modes, and the coupling between modes. After the characteristics of the passage through resonance region are known, control can be taken to suppress the undesired large amplitudes. The original differential equations can be used as a system model (may not be perfect) combined with measurements (such as position or velocity of the tip point of the beam) to apply an adaptive control on multiple modes and in multiple directions.

Appendix A Coefficients of the Original Differential Equations

$$T_{ij}{}^{v} = \sum_{k=1}^{m}\sum_{l=1}^{m}\beta_y(\beta_{8v,ijkl} + \beta_{9v,ijkl} + \beta_{8v,ikjl} + \beta_{9v,ikjl} + \beta_{8v,ilkj} + \beta_{9v,ilkj})v_{s_k}v_{s_l}$$

$$X_{ij}{}^{v} = \sum_{k=1}^{m}\sum_{l=1}^{m}\beta_{12v,ilkj}v_{s_k}v_{s_l}$$

$$\Lambda_{ijk}{}^{v1} = \sum_{l=1}^{m}[-(1-\beta_y)(\beta_{1v,ijlk} - \beta_{3v,ijlk} - \beta_x\beta_{5v,ijlk} - 2\beta_x\beta_{6v,ijlk}) - (1-\beta_y)(\beta_{2v,ilkj} - \beta_{4v,ilkj} - \beta_x\beta_{7v,ilkj}) + \beta_y\beta_{10v,ilkj} + \beta_y\beta_{11v,ilkj}]v_{s_l}$$

$$\Lambda_{ijk}{}^{v2} = \sum_{l=1}^{m}\beta_y(\beta_{8v,ijkl} + \beta_{9v,ijkl} + \beta_{8v,ijlk} + \beta_{9v,ijlk} + \beta_{8v,ilkj} + \beta_{9v,\,ilkj})v_{s_l}$$

$$Y_{ijk}{}^{v1} = \sum_{l=1}^{m}\beta_{12v,ilkj}v_{s_l}$$

$$Y_{ijk}{}^{v2} = \sum_{l=1}^{m}\beta_{13v,ilkj}v_{s_l}$$

$$Z_{ijk}{}^{v1} = \sum_{l=1}^{m}(\beta_{12v,iljk} + \beta_{12v,ijlk})v_{s_l}$$

$$Z_{ijk}{}^{v2} = \sum_{l=1}^{m}\beta_{13v,iljk}v_{s_l}$$

$$\Gamma_{ijkl}{}^{v1} = -(1-\beta_y)(\beta_{1v,ijkl} - \beta_{3v,ijkl} - \beta_x\beta_{5v,ijkl} - 2\beta_x\beta_{6v,ijkl})$$

$$\Gamma_{ijkl}{}^{v2} = -(1-\beta_y)(\beta_{2v,ijkl} - \beta_{4v,ijkl} - \beta_x\beta_{7v,ijkl}) + \beta_y\beta_{10v,ijkl} + \beta_y\beta_{11v,ijkl}$$

$$\Gamma_{ijkl}{}^{v3} = \beta_y(\beta_{8v,ijkl} + \beta_{9v,ijkl})$$

$$V_{ijkl}{}^{v1} = \beta_{12v,ijkl}$$

$$V_{ijkl}{}^{v2} = \beta_{13v,ijkl}$$

$$W_{ijkl}{}^{v1} = \beta_{12v,ijkl}$$

$$W_{ijkl}{}^{v2} = \beta_{13v,ijkl}$$

$$T_{ij}{}^{w} = \sum_{k=1}^{m}\sum_{l=1}^{m}[(1-\beta_y)(\beta_{1w,ilkj}+\beta_{2w,ilkj}-\beta_{3w,ilkj}-\beta_{4w,ilkj}+\beta_x\beta_{5w,ilkj}+2\beta_x\beta_{6w,ilkj}+\beta_x\beta_{7w,ilkj})$$
$$+\beta_{8w,ilkj}+\beta_{9w,ilkj}]v_{s_k}v_{s_l}$$

$$\Lambda_{ijk}{}^{w} = \sum_{l=1}^{m}[(1-\beta_y)(\beta_{1w,ijlk}+\beta_{2w,ijlk}-\beta_{3w,ijlk}-\beta_{4w,ijlk}+\beta_x\beta_{5w,ijlk}+2\beta_x\beta_{6w,ijlk}+\beta_x\beta_{7w,ijlk})$$
$$+\beta_{8w,ijlk}+\beta_{9w,ijlk}$$
$$+(1-\beta_y)(\beta_{1w,iljk}+\beta_{2w,iljk}-\beta_{3w,iljk}-\beta_{4w,iljk}+\beta_x\beta_{5w,iljk}+2\beta_x\beta_{6w,iljk}+\beta_x\beta_{7w,iljk})$$
$$+\beta_{8w,iljk}+\beta_{9w,iljk}]v_{s_l}$$

$$Z_{ijk}{}^{w} = \sum_{l=1}^{m}\beta_{12w,ijlk}v_{s_l}$$

$$\Gamma_{ijkl}{}^{w1} = (1-\beta_y)(\beta_{1w,ijkl}+\beta_{2w,ijkl}-\beta_{3w,ijkl}-\beta_{4w,ijkl}+\beta_x\beta_{5w,ijkl}+2\beta_x\beta_{6w,ijkl}+\beta_x\beta_{7w,ijkl})$$
$$+\beta_{8w,ijkl}+\beta_{9w,ijkl}$$

$$\Gamma_{ijkl}{}^{w2} = \beta_{10w,ijkl}+\beta_{11w,ijkl}$$

$$V_{ijkl}{}^{w1} = \beta_{12w,ijkl}$$

$$V_{ijkl}{}^{w2} = \beta_{13w,ijkl}$$

$$W_{ijkl}{}^{w1} = \beta_{12w,ijkl}$$

$$W_{ijkl}{}^{w2} = \beta_{13w,ijkl}$$

$$Q_{v_i} = \int_0^1 F_{v_i} Q_v ds$$

$$\beta_{1v,ijkl} = \int_0^1 F_{v_i}(F_{w_j}''' \int_1^s F_{v_k}'' F_{w_l}'' ds) ds$$

$$\beta_{2v,ijkl} = \int_0^1 F_{v_i}(F_{v_j}'' F_{w_k}'' F_{w_l}'') ds$$

$$\beta_{3v,ijkl} = \int_0^1 F_{v_i}(F_{w_j}'''' \int_0^s F_{v_k}'' F_{w_l}' ds) ds$$

$$\beta_{4v,ijkl} = \int_0^1 F_{v_i}(F_{v_j}'' F_{w_k}' F_{w_l}''') ds$$

$$\beta_{5v,ijkl} = \int_0^1 F_{v_i}(F_{w_j}'''' \int_0^s [\int_1^s F_{v_k}'' F_{w_l}'' ds] ds) ds$$

$$\beta_{6v,ijkl} = \beta_{1v,ijkl}$$

$$\beta_{7v,ijkl} = \beta_{2v,ijkl}$$

$$\beta_{8v,ijkl} = \int_0^1 F_{v_i}(F_{v_j}' F_{v_k}'' F_{v_l}'')' ds$$

$$\beta_{9v,ijkl} = \int_0^1 F_{v_i}(F_{v_j}' F_{v_k}' F_{v_l}''')' ds$$

$$\beta_{10v,ijkl} = \int_0^1 F_{v_i}(F_{v_j}' F_{w_k}'' F_{w_l}'')' ds$$

$$\beta_{11v,ijkl} = \int_0^1 F_{v_i}(F_{v_j}' F_{w_k}' F_{w_l}''')' ds$$

$$\beta_{12v,ijkl} = \int_0^1 F_{v_i}(F_{v_j}' \int_1^s [\int_0^s F_{v_k}' F_{v_l}' ds] ds)' ds$$

$$\beta_{13v,ijkl} = \int_0^1 F_{v_i}(F_{v_j}' \int_1^s [\int_0^s F_{w_k}' F_{w_l}' ds] ds)' ds$$

$$\bar{Q}_{w_i} = \int_0^1 F_{w_i} Q_w ds$$

$$\beta_{1w,ijkl} = \int_0^1 F_{w_i}(F_{v_j}''' \int_1^s F_{v_k}'' F_{w_l}'' ds) ds$$

$$\beta_{2w,ijkl} = \int_0^1 F_{w_i}(F_{v_j}'' F_{v_k}'' F_{w_l}'') ds$$

$$\beta_{3w,ijkl} = \int_0^1 F_{w_i}(F_{v_j}'''' \int_0^s F_{v_k}' F_{w_l}'' ds) ds$$

$$\beta_{4w,ijkl} = \int_0^1 F_{w_i}(F_{v_j}' F_{v_k}''' F_{w_l}'') ds$$

$$\beta_{5w,ijkl} = \int_0^1 F_{w_i}(F_{v_j}'''' \int_0^s [\int_1^s F_{v_k}'' F_{w_l}'' ds] ds) ds$$

$$\beta_{6w,ijkl} = \beta_{1w,ijkl}$$

$$\beta_{7w,ijkl} = \beta_{2w,ijkl}$$

$$\beta_{8w,ijkl} = \int_0^1 F_{w_i}(F_{v_j}'' F_{v_k}'' F_{w_l}')' ds$$

$$\beta_{9w,ijkl} = \int_0^1 F_{w_i}(F_{v_j}' F_{v_k}''' F_{w_l}')' ds$$

$$\beta_{10w,ijkl} = \int_0^1 F_{w_i}(F_{w_j}' F_{w_k}'' F_{w_l}'')' ds$$

$$\beta_{11w,ijkl} = \int_0^1 F_{w_i}(F_{w_j}' F_{w_k}' F_{w_l}''')' ds$$

$$\beta_{12w,ijkl} = \int_0^1 F_{w_i}(F_{w_j}' \int_1^s [\int_0^s F_{v_k}' F_{v_l}' ds] ds)' ds$$

$$\beta_{13w,ijkl} = \int_0^1 F_{w_i}(F_{w_j}' \int_1^s [\int_0^s F_{w_k}' F_{w_l}' ds] ds)' ds$$

Appendix B Coefficients of the Secular Terms for Secondary Resonances

$$\Lambda_{jkl}^{\nu 2^{\cdot}} = \Lambda_{jkl}^{\nu 2} + \Lambda_{kjl}^{\nu 2}$$

$$Y_{jkl}^{\nu 1^{\cdot}} = Y_{jkl}^{\nu 1} + Y_{kjl}^{\nu 1}$$

$$Z_{jkl}^{\nu 1^{\cdot}} = \omega_{\nu_k}^2 Z_{jkl}^{\nu 1} + \Omega^2 Z_{kjl}^{\nu 1}$$

$$\Gamma_{jkln}^{\nu 3^{\cdot}} = \Gamma_{jkln}^{\nu 3} + \Gamma_{kjln}^{\nu 3} + \Gamma_{jlkn}^{\nu 3} + \Gamma_{kljn}^{\nu 3} + \Gamma_{ljkn}^{\nu 3} + \Gamma_{lkjn}^{\nu 3}$$

$$\Gamma_{jkln}^{w 1^{\cdot}} = \Gamma_{jkln}^{w 1} + \Gamma_{kjln}^{w 1}$$

$$\Gamma_{jkln}^{w 2^{\cdot}} = \Gamma_{jkln}^{w 2} + \Gamma_{kjln}^{w 2} + \Gamma_{jlkn}^{w 2} + \Gamma_{kljn}^{w 2} + \Gamma_{ljkn}^{w 2} + \Gamma_{lkjn}^{w 2}$$

$$V_{jkln}^{\nu 1^{\cdot}} = \omega_{\nu_k}\omega_{\nu_l} V_{jkln}^{\nu 1} + \Omega\omega_{\nu_l} V_{kjln}^{\nu 1} + \omega_{\nu_l}\omega_{\nu_k} V_{jlkn}^{\nu 1} + \Omega\omega_{\nu_l} V_{kljn}^{\nu 1} + \Omega\omega_{\nu_k} V_{ljkn}^{\nu 1} + \Omega\omega_{\nu_k} V_{lkjn}^{\nu 1}$$

$$V_{jkln}^{w 1^{\cdot}} = \Omega\omega_{\nu_j} V_{jkln}^{w 1} + \Omega\omega_{\nu_j} V_{jlkn}^{w 1}$$

$$W_{jkln}^{\nu 1^{\cdot}} = \omega_{\nu_l}^2 W_{jkln}^{\nu 1} + \omega_{\nu_l}^2 W_{kjln}^{\nu 1} + \omega_{\nu_k}^2 W_{jlkn}^{\nu 1} + \omega_{\nu_j}^2 W_{kljn}^{\nu 1} + \omega_{\nu_k}^2 W_{ljkn}^{\nu 1} + \omega_{\nu_j}^2 W_{lkjn}^{\nu 1}$$

$$W_{jkln}^{\nu 1^{\cdot\cdot}} = \omega_{\nu_l}^2 W_{jkln}^{\nu 1} + \omega_{\nu_l}^2 W_{kjln}^{\nu 1} + \Omega^2 W_{jlkn}^{\nu 1} + \Omega^2 W_{kljn}^{\nu 1} + \Omega^2 W_{ljkn}^{\nu 1} + \Omega^2 W_{lkjn}^{\nu 1}$$

$$W_{jkln}^{\nu 1^{\cdot\cdot\cdot}} = \omega_{\nu_l}^2 W_{jkln}^{\nu 1} + \omega_{\nu_l}^2 W_{kjln}^{\nu 1} + \omega_{\nu_k}^2 W_{jlkn}^{\nu 1} + \Omega^2 W_{kljn}^{\nu 1} + \omega_{\nu_k}^2 W_{ljkn}^{\nu 1} + \Omega^2 W_{lkjn}^{\nu 1}$$

$$W_{jkln}^{w 1^{\cdot}} = \omega_{\nu_j}^2 W_{jkln}^{w 1} + \Omega^2 W_{jlkn}^{w 1}$$

$$W_{jkln}^{w 2^{\cdot}} = \omega_{\nu_l}^2 W_{jkln}^{w 2} + \omega_{\nu_l}^2 W_{kjln}^{w 2} + \omega_{\nu_k}^2 W_{jlkn}^{w 2} + \omega_{\nu_j}^2 W_{kljn}^{w 2} + \omega_{\nu_k}^2 W_{ljkn}^{w 2} + \omega_{\nu_j}^2 W_{lkjn}^{w 2}$$

Appendix C The Second-Order Equations for Hard Excitation

$$
\begin{aligned}
D_0{}^2 v_{n1} + \omega_{\nu_n}^2 v_{n1} = & -2i\Omega\mu_{\nu_n} E_n e^{i\Omega T_0} - 2i\omega_{\nu_n}(D_1 A_n + \mu_{\nu_n} A_n) e^{i\omega_{\nu_n} T_0} \\
& - \sum_{j=1}^{m} T_{jn}{}^{\nu}(A_j e^{i\omega_{\nu_j} T_0} + E_j e^{i\Omega T_0}) \\
& - \sum_{j=1}^{m} X_{jn}{}^{\nu}(-\omega_{\nu_j}^2 A_j e^{i\omega_{\nu_j} T_0} - \Omega^2 E_j e^{i\Omega T_0}) \\
& - \sum_{j=1}^{m}\sum_{k=1}^{m} \Lambda_{jkn}{}^{\nu 1}[B_j B_k e^{i(\omega_{w_j} + \omega_{w_k})T_0} + B_j \bar{B}_k e^{i(\omega_{w_j} - \omega_{w_k})T_0} \\
& \qquad + B_j \tilde{E}_k e^{i(\omega_{w_j} + \tilde{\Omega})T_0} + B_j \tilde{E}_k e^{i(\omega_{w_j} - \tilde{\Omega})T_0} \\
& \qquad + \tilde{E}_j B_k e^{i(\omega_{w_k} + \tilde{\Omega})T_0} + \tilde{E}_j \bar{B}_k e^{i(-\omega_{w_k} + \tilde{\Omega})T_0} \\
& \qquad + \tilde{E}_j \tilde{E}_k e^{i2\tilde{\Omega}T_0} + \tilde{E}_j \tilde{E}_k] \\
& - \sum_{j=1}^{m}\sum_{k=1}^{m} \Lambda_{jkn}{}^{\nu 2}[A_j A_k e^{i(\omega_{\nu_j} + \omega_{\nu_k})T_0} + A_j \bar{A}_k e^{i(\omega_{\nu_j} - \omega_{\nu_k})T_0} \\
& \qquad + A_j E_k e^{i(\omega_{w_j} + \Omega)T_0} + A_j E_k e^{i(\omega_{w_j} - \Omega)T_0} \\
& \qquad + E_j A_k e^{i(\omega_{\nu_k} + \Omega)T_0} + E_j \bar{A}_k e^{i(-\omega_{\nu_k} + \Omega)T_0} \\
& \qquad + E_j E_k e^{i2\Omega T_0} + E_j E_k] \\
& - \sum_{j=1}^{m}\sum_{k=1}^{m} Y_{jkn}{}^{\nu 1}[-\omega_{\nu_j}\omega_{\nu_k} A_j A_k e^{i(\omega_{\nu_j} + \omega_{\nu_k})T_0} + \omega_{\nu_j}\omega_{\nu_k} A_j \bar{A}_k e^{i(\omega_{\nu_j} - \omega_{\nu_k})T_0} \\
& \qquad - \Omega\omega_{\nu_j} A_j E_k e^{i(\omega_{\nu_j} + \Omega)T_0} + \Omega\omega_{\nu_j} A_j E_k e^{i(\omega_{\nu_j} - \Omega)T_0} \\
& \qquad - \Omega\omega_{\nu_k} E_j A_k e^{i(\Omega + \omega_{\nu_k})T_0} + \Omega\omega_{\nu_k} E_j \bar{A}_k e^{i(\Omega - \omega_{\nu_k})T_0} \\
& \qquad - \Omega^2 E_j E_k e^{i2\Omega T_0} + \Omega^2 E_j E_k]
\end{aligned}
$$

$$
\begin{aligned}
&-\sum_{j=1}^{m}\sum_{k=1}^{m} Y_{jkn}{}^{v2}[-\omega_{w_j}\omega_{w_k}B_jB_k e^{i(\omega_{w_j}+\omega_{w_k})T_0}+\omega_{w_j}\omega_{w_k}B_j\overline{B}_k e^{i(\omega_{w_j}-\omega_{w_k})T_0}\\
&\qquad -\tilde{\Omega}\omega_{w_j}B_j\tilde{E}_k e^{i(\omega_{w_j}+\tilde{\Omega})T_0}+\tilde{\Omega}\omega_{w_j}B_j\tilde{E}_k e^{i(\omega_{w_j}-\tilde{\Omega})T_0}\\
&\qquad -\tilde{\Omega}\omega_{w_k}\tilde{E}_jB_k e^{i(\tilde{\Omega}+\omega_{w_k})T_0}+\tilde{\Omega}\omega_{w_k}\tilde{E}_j\overline{B}_k e^{i(\tilde{\Omega}-\omega_{w_k})T_0}\\
&\qquad -\tilde{\Omega}^2\tilde{E}_j\tilde{E}_k e^{i2\tilde{\Omega}T_0}+\tilde{\Omega}^2\tilde{E}_j\tilde{E}_k]\\
&-\sum_{j=1}^{m}\sum_{k=1}^{m} Z_{jkn}{}^{v1}[-\omega_{v_k}^2A_jA_k e^{i(\omega_{v_j}+\omega_{v_k})T_0}-\omega_{v_k}^2A_j\overline{A}_k e^{i(\omega_{v_j}-\omega_{v_k})T_0}\\
&\qquad -\Omega^2A_jE_k e^{i(\omega_{v_j}+\Omega)T_0}-\Omega^2A_jE_k e^{i(\omega_{v_j}-\Omega)T_0}\\
&\qquad -\omega_{v_k}^2E_jA_k e^{i(\Omega+\omega_{v_k})T_0}-\omega_{v_k}^2E_j\overline{A}_k e^{i(\Omega-\omega_{v_k})T_0}\\
&\qquad -\Omega^2E_jE_k e^{i2\Omega T_0}-\Omega^2E_jE_k]\\
&-\sum_{j=1}^{m}\sum_{k=1}^{m} Z_{jkn}{}^{v2}[-\omega_{w_k}^2B_jB_k e^{i(\omega_{w_j}+\omega_{w_k})T_0}-\omega_{w_k}^2B_j\overline{B}_k e^{i(\omega_{w_j}-\omega_{w_k})T_0}\\
&\qquad -\tilde{\Omega}^2B_j\tilde{E}_k e^{i(\omega_{w_j}+\tilde{\Omega})T_0}-\tilde{\Omega}^2B_j\tilde{E}_k e^{i(\omega_{w_j}-\tilde{\Omega})T_0}\\
&\qquad -\omega_{w_k}^2\tilde{E}_jB_k e^{i(\tilde{\Omega}+\omega_{w_k})T_0}+\omega_{w_k}^2\tilde{E}_j\overline{B}_k e^{i(\tilde{\Omega}-\omega_{w_k})T_0}\\
&\qquad -\tilde{\Omega}^2\tilde{E}_j\tilde{E}_k e^{i2\tilde{\Omega}T_0}-\tilde{\Omega}^2\tilde{E}_j\tilde{E}_k]
\end{aligned}
$$

$$
\begin{aligned}
-\sum_{j=1}^{m}\sum_{k=1}^{m}\sum_{l=1}^{m}\Gamma_{jkln}{}^{v1}[&B_jA_kB_le^{i(\omega_{w_j}+\omega_{v_k}+\omega_{w_l})T_0}+B_jA_k\overline{B}_le^{i(\omega_{w_j}+\omega_{v_k}-\omega_{w_l})T_0}\\
&+B_j\overline{A}_kB_le^{i(\omega_{w_j}-\omega_{v_k}+\omega_{w_l})T_0}+B_j\overline{A}_k\overline{B}_le^{i(\omega_{w_j}-\omega_{v_k}-\omega_{w_l})T_0}\\
&+B_jA_k\widetilde{E}_le^{i(\omega_{w_j}+\omega_{v_k}+\tilde{\Omega})T_0}+B_jA_k\widetilde{E}_le^{i(\omega_{w_j}+\omega_{v_k}-\tilde{\Omega})T_0}\\
&+B_j\overline{A}_k\widetilde{E}_le^{i(\omega_{w_j}-\omega_{v_k}+\tilde{\Omega})T_0}+B_j\overline{A}_k\widetilde{E}_le^{i(\omega_{w_j}-\omega_{v_k}-\tilde{\Omega})T_0}\\
&+B_jE_kB_le^{i(\omega_{w_j}+\Omega+\omega_{w_l})T_0}+B_jE_k\overline{B}_le^{i(\omega_{w_j}+\Omega-\omega_{w_l})T_0}\\
&+B_jE_kB_le^{i(\omega_{w_j}-\Omega+\omega_{w_l})T_0}+B_jE_k\overline{B}_le^{i(\omega_{w_j}-\Omega-\omega_{w_l})T_0}\\
&+B_jE_k\widetilde{E}_le^{i(\omega_{w_j}+\Omega+\tilde{\Omega})T_0}+B_jE_k\widetilde{E}_le^{i(\omega_{w_j}+\Omega-\tilde{\Omega})T_0}\\
&+B_jE_k\widetilde{E}_le^{i(\omega_{w_j}-\Omega+\tilde{\Omega})T_0}+B_jE_k\widetilde{E}_le^{i(\omega_{w_j}-\Omega-\tilde{\Omega})T_0}\\
&+\widetilde{E}_jA_kB_le^{i(\tilde{\Omega}+\omega_{v_k}+\omega_{w_l})T_0}+\widetilde{E}_jA_k\overline{B}_le^{i(\tilde{\Omega}+\omega_{v_k}-\omega_{w_l})T_0}\\
&+\widetilde{E}_j\overline{A}_kB_le^{i(\tilde{\Omega}-\omega_{v_k}+\omega_{w_l})T_0}+\widetilde{E}_j\overline{A}_k\overline{B}_le^{i(\tilde{\Omega}-\omega_{v_k}-\omega_{w_l})T_0}\\
&+\widetilde{E}_jA_k\widetilde{E}_le^{i(2\tilde{\Omega}+\omega_{v_k})T_0}+\widetilde{E}_jA_k\widetilde{E}_le^{i\omega_{v_j}T_0}\\
&+\widetilde{E}_j\overline{A}_k\widetilde{E}_le^{i(2\tilde{\Omega}-\omega_{v_k})T_0}+\widetilde{E}_j\overline{A}_k\widetilde{E}_le^{-i\omega_{v_j}T_0}\\
&+\widetilde{E}_jE_kB_le^{i(\tilde{\Omega}+\Omega+\omega_{w_l})T_0}+\widetilde{E}_jE_k\overline{B}_le^{i(\tilde{\Omega}+\Omega-\omega_{w_l})T_0}\\
&+\widetilde{E}_jE_kB_le^{i(\tilde{\Omega}-\Omega+\omega_{w_l})T_0}+\widetilde{E}_jE_k\overline{B}_le^{i(\tilde{\Omega}-\Omega-\omega_{w_l})T_0}\\
&+\widetilde{E}_jE_k\widetilde{E}_le^{i(2\tilde{\Omega}+\Omega)T_0}+\widetilde{E}_jE_k\widetilde{E}_le^{i\Omega T_0}\\
&+\widetilde{E}_jE_k\widetilde{E}_le^{i(2\tilde{\Omega}-\Omega)T_0}+\widetilde{E}_jE_k\widetilde{E}_le^{-i\Omega T_0}]
\end{aligned}
$$

$$
\begin{aligned}
-\sum_{j=1}^{m}\sum_{k=1}^{m}\sum_{l=1}^{m}\Gamma_{jkln}^{v2}[&A_jB_kB_le^{i(\omega_{v_j}+\omega_{w_k}+\omega_{w_l})T_0}+A_jB_k\bar{B}_le^{i(\omega_{v_j}+\omega_{w_k}-\omega_{w_l})T_0}\\
&+A_j\bar{B}_kB_le^{i(\omega_{v_j}-\omega_{w_k}+\omega_{w_l})T_0}+A_j\bar{B}_k\bar{B}_le^{i(\omega_{v_j}-\omega_{w_k}-\omega_{w_l})T_0}\\
&+A_jB_k\tilde{E}_le^{i(\omega_{v_j}+\omega_{w_k}+\tilde{\Omega})T_0}+A_jB_k\tilde{E}_le^{i(\omega_{v_j}+\omega_{w_k}-\tilde{\Omega})T_0}\\
&+A_j\bar{B}_k\tilde{E}_le^{i(\omega_{v_j}-\omega_{w_k}+\tilde{\Omega})T_0}+A_j\bar{B}_k\tilde{E}_le^{i(\omega_{v_j}-\omega_{w_k}-\tilde{\Omega})T_0}\\
&+A_j\tilde{E}_kB_le^{i(\omega_{v_j}+\tilde{\Omega}+\omega_{w_l})T_0}+A_j\tilde{E}_k\bar{B}_le^{i(\omega_{v_j}+\tilde{\Omega}-\omega_{w_l})T_0}\\
&+A_j\tilde{E}_kB_le^{i(\omega_{v_j}-\tilde{\Omega}+\omega_{w_l})T_0}+A_j\tilde{E}_k\bar{B}_le^{i(\omega_{v_j}-\tilde{\Omega}-\omega_{w_l})T_0}\\
&+A_j\tilde{E}_k\tilde{E}_le^{i(\omega_{v_j}+2\tilde{\Omega})T_0}+A_j\tilde{E}_k\tilde{E}_le^{i\omega_{v_j}T_0}\\
&+A_j\tilde{E}_k\tilde{E}_le^{i\omega_{v_j}T_0}+A_j\tilde{E}_k\tilde{E}_le^{i(\omega_{v_j}-2\tilde{\Omega})T_0}\\
&+E_jB_kB_le^{i(\Omega+\omega_{w_k}+\omega_{w_l})T_0}+E_jB_k\bar{B}_le^{i(\Omega+\omega_{w_k}-\omega_{w_l})T_0}\\
&+E_j\bar{B}_kB_le^{i(\Omega-\omega_{w_k}+\omega_{w_l})T_0}+E_j\bar{B}_k\bar{B}_le^{i(\Omega-\omega_{w_k}-\omega_{w_l})T_0}\\
&+E_jB_k\tilde{E}_le^{i(\Omega+\omega_{w_k}+\tilde{\Omega})T_0}+E_jB_k\tilde{E}_le^{i(\Omega+\omega_{w_k}-\tilde{\Omega})T_0}\\
&+E_j\bar{B}_k\tilde{E}_le^{i(\Omega-\omega_{w_k}+\tilde{\Omega})T_0}+E_j\bar{B}_k\tilde{E}_le^{i(\Omega-\omega_{w_k}-\tilde{\Omega})T_0}\\
&+E_j\tilde{E}_kB_le^{i(\Omega+\tilde{\Omega}+\omega_{w_l})T_0}+E_j\tilde{E}_k\bar{B}_le^{i(\Omega+\tilde{\Omega}-\omega_{w_l})T_0}\\
&+E_j\tilde{E}_kB_le^{i(\Omega-\tilde{\Omega}+\omega_{w_l})T_0}+E_j\tilde{E}_k\bar{B}_le^{i(\Omega-\tilde{\Omega}-\omega_{w_l})T_0}\\
&+E_j\tilde{E}_k\tilde{E}_le^{i(\Omega+2\tilde{\Omega})T_0}+E_j\tilde{E}_k\tilde{E}_le^{i\Omega T_0}\\
&+E_j\tilde{E}_k\tilde{E}_le^{i\Omega T_0}+E_j\tilde{E}_k\tilde{E}_le^{i(\Omega-2\tilde{\Omega})T_0}]
\end{aligned}
$$

$$
\begin{aligned}
-\sum_{j=1}^{m}\sum_{k=1}^{m}\sum_{l=1}^{m}\Gamma_{jkln}^{v3}\{&A_jA_kA_le^{i(\omega_{v_j}+\omega_{v_k}+\omega_{v_l})T_0}+A_jA_k\overline{A}_le^{i(\omega_{v_j}+\omega_{v_k}-\omega_{v_l})T_0}\\
&+A_j\overline{A}_kA_le^{i(\omega_{v_j}-\omega_{v_k}+\omega_{v_l})T_0}+A_j\overline{A}_k\overline{A}_le^{i(\omega_{v_j}-\omega_{v_k}-\omega_{v_l})T_0}\\
&+A_jA_kE_le^{i(\omega_{v_j}+\omega_{v_k}+\Omega)T_0}+A_jA_kE_le^{i(\omega_{v_j}+\omega_{v_k}-\Omega)T_0}\\
&+A_j\overline{A}_kE_le^{i(\omega_{v_j}-\omega_{v_k}+\Omega)T_0}+A_j\overline{A}_kE_le^{i(\omega_{v_j}-\omega_{v_k}-\Omega)T_0}\\
&+A_jE_kA_le^{i(\omega_{v_j}+\Omega+\omega_{v_l})T_0}+A_jE_k\overline{A}_le^{i(\omega_{v_j}+\Omega-\omega_{v_l})T_0}\\
&+A_jE_kA_le^{i(\omega_{v_j}-\Omega+\omega_{v_l})T_0}+A_jE_k\overline{A}_le^{i(\omega_{v_j}-\Omega-\omega_{v_l})T_0}\\
&+A_jE_kE_le^{i(\omega_{v_j}+2\Omega)T_0}+A_jE_kE_le^{i\omega_{v_j}T_0}\\
&+A_jE_kE_le^{i\omega_{v_j}T_0}+A_jE_kE_le^{i(\omega_{v_j}-2\Omega)T_0}\\
&+E_jA_kA_le^{i(\Omega+\omega_{v_k}+\omega_{v_l})T_0}+E_jA_k\overline{A}_le^{i(\Omega+\omega_{v_k}-\omega_{v_l})T_0}\\
&+E_j\overline{A}_kA_le^{i(\Omega-\omega_{v_k}+\omega_{v_l})T_0}+E_j\overline{A}_k\overline{A}_le^{i(\Omega-\omega_{v_k}-\omega_{v_l})T_0}\\
&+E_jA_kE_le^{i(2\Omega+\omega_{v_k})T_0}+E_jA_kE_le^{i\omega_{v_k}T_0}\\
&+E_j\overline{A}_kE_le^{i(2\Omega-\omega_{v_k})T_0}+E_j\overline{A}_kE_le^{-i\omega_{v_k}T_0}\\
&+E_jE_kA_le^{i(2\Omega+\omega_{v_l})T_0}+E_jE_k\overline{A}_le^{i(2\Omega-\omega_{v_l})T_0}\\
&+E_jE_kA_le^{i\omega_{v_l}T_0}+E_jE_k\overline{A}_le^{-i\omega_{v_l}T_0}\\
&+E_jE_kE_le^{i3\Omega T_0}+E_jE_kE_le^{i\Omega T_0}\\
&+E_jE_kE_le^{i\Omega T_0}+E_jE_kE_le^{-i\Omega T_0}\}
\end{aligned}
$$

$$
\begin{aligned}
-\sum_{j=1}^{m}\sum_{k=1}^{m}\sum_{l=1}^{m} V_{jkln}{}^{v1}[& -\omega_{v_k}\omega_{v_l}A_jA_kA_le^{i(\omega_{v_j}+\omega_{v_k}+\omega_{v_l})T_0}+\omega_{v_k}\omega_{v_l}A_jA_k\bar{A}_le^{i(\omega_{v_j}+\omega_{v_k}-\omega_{v_l})T_0}\\
& +\omega_{v_k}\omega_{v_l}A_j\bar{A}_kA_le^{i(\omega_{v_j}-\omega_{v_k}+\omega_{v_l})T_0}-\omega_{v_k}\omega_{v_l}A_j\bar{A}_k\bar{A}_le^{i(\omega_{v_j}-\omega_{v_k}-\omega_{v_l})T_0}\\
& -\Omega\omega_{v_k}A_jA_kE_le^{i(\omega_{v_j}+\omega_{v_k}+\Omega)T_0}+\Omega\omega_{v_k}A_jA_kE_le^{i(\omega_{v_j}+\omega_{v_k}-\Omega)T_0}\\
& +\Omega\omega_{v_k}A_j\bar{A}_kE_le^{i(\omega_{v_j}-\omega_{v_k}+\Omega)T_0}-\Omega\omega_{v_k}A_j\bar{A}_kE_le^{i(\omega_{v_j}-\omega_{v_k}-\Omega)T_0}\\
& -\Omega\omega_{v_l}A_jE_kA_le^{i(\omega_{v_j}+\Omega+\omega_{v_l})T_0}+\Omega\omega_{v_l}A_jE_k\bar{A}_le^{i(\omega_{v_j}+\Omega-\omega_{v_l})T_0}\\
& +\Omega\omega_{v_l}A_jE_kA_le^{i(\omega_{v_j}-\Omega+\omega_{v_l})T_0}-\Omega\omega_{v_l}A_jE_k\bar{A}_le^{i(\omega_{v_j}-\Omega-\omega_{v_l})T_0}\\
& -\Omega^2A_jE_kE_le^{i(\omega_{v_j}+2\Omega)T_0}+\Omega^2A_jE_kE_le^{i\omega_{v_j}T_0}\\
& +\Omega^2A_jE_kE_le^{i\omega_{v_j}T_0}-\Omega^2A_jE_kE_le^{i(\omega_{v_j}-2\Omega)T_0}\\
& -\omega_{v_k}\omega_{v_l}E_jA_kA_le^{i(\Omega+\omega_{v_k}+\omega_{v_l})T_0}+\omega_{v_k}\omega_{v_l}E_jA_k\bar{A}_le^{i(\Omega+\omega_{v_k}-\omega_{v_l})T_0}\\
& +\omega_{v_k}\omega_{v_l}E_j\bar{A}_kA_le^{i(\Omega-\omega_{v_k}+\omega_{v_l})T_0}-\omega_{v_k}\omega_{v_l}E_j\bar{A}_k\bar{A}_le^{i(\Omega-\omega_{v_k}-\omega_{v_l})T_0}\\
& -\Omega\omega_{v_k}E_jA_kE_le^{i(2\Omega+\omega_{v_k})T_0}+\Omega\omega_{v_k}E_jA_kE_le^{i\omega_{v_k}T_0}\\
& +\Omega\omega_{v_k}E_j\bar{A}_kE_le^{i(2\Omega-\omega_{v_k})T_0}-\Omega\omega_{v_k}E_j\bar{A}_kE_le^{-i\omega_{v_k}T_0}\\
& -\Omega\omega_{v_l}E_jE_kA_le^{i(2\Omega+\omega_{v_l})T_0}+\Omega\omega_{v_l}E_jE_k\bar{A}_le^{i(2\Omega-\omega_{v_l})T_0}\\
& +\Omega\omega_{v_l}E_jE_kA_le^{i\omega_{v_l}T_0}-\Omega\omega_{v_l}E_jE_k\bar{A}_le^{-i\omega_{v_l}T_0}\\
& -\Omega^2E_jE_kE_le^{i3\Omega T_0}+\Omega^2E_jE_kE_le^{i\Omega T_0}\\
& +\Omega^2E_jE_kE_le^{i\Omega T_0}-\Omega^2E_jE_kE_le^{-i\Omega T_0}]
\end{aligned}
$$

$$
-\sum_{j=1}^{m}\sum_{k=1}^{m}\sum_{l=1}^{m} V_{jkln}{}^{v2}\Big[-\omega_{w_k}\omega_{w_l}A_jB_kB_le^{i(\omega_{v_j}+\omega_{w_k}+\omega_{w_l})T_0}+\omega_{w_k}\omega_{w_l}A_jB_k\bar{B}_le^{i(\omega_{v_j}+\omega_{w_k}-\omega_{w_l})T_0}
$$

$$
+\omega_{w_k}\omega_{w_l}A_j\bar{B}_kB_le^{i(\omega_{v_j}-\omega_{w_k}+\omega_{w_l})T_0}-\omega_{w_k}\omega_{w_l}A_j\bar{B}_k\bar{B}_le^{i(\omega_{v_j}-\omega_{w_k}-\omega_{w_l})T_0}
$$

$$
-\tilde{\Omega}\omega_{w_k}A_jB_k\tilde{E}_le^{i(\omega_{v_j}+\omega_{w_k}+\tilde{\Omega})T_0}+\tilde{\Omega}\omega_{w_k}A_jB_k\tilde{E}_le^{i(\omega_{v_j}+\omega_{w_k}-\tilde{\Omega})T_0}
$$

$$
+\tilde{\Omega}\omega_{w_k}A_j\bar{B}_k\tilde{E}_le^{i(\omega_{v_j}-\omega_{w_k}+\tilde{\Omega})T_0}-\tilde{\Omega}\omega_{w_k}A_j\bar{B}_k\tilde{E}_le^{i(\omega_{v_j}-\omega_{w_k}-\tilde{\Omega})T_0}
$$

$$
-\tilde{\Omega}\omega_{w_l}A_j\tilde{E}_kB_le^{i(\omega_{v_j}+\tilde{\Omega}+\omega_{w_l})T_0}+\tilde{\Omega}\omega_{w_l}A_j\tilde{E}_k\bar{B}_le^{i(\omega_{v_j}+\tilde{\Omega}-\omega_{w_l})T_0}
$$

$$
+\tilde{\Omega}\omega_{w_l}A_j\tilde{E}_kB_le^{i(\omega_{v_j}-\tilde{\Omega}+\omega_{w_l})T_0}-\tilde{\Omega}\omega_{w_l}A_j\tilde{E}_k\bar{B}_le^{i(\omega_{v_j}-\tilde{\Omega}-\omega_{w_l})T_0}
$$

$$
-\tilde{\Omega}^2A_j\tilde{E}_k\tilde{E}_le^{i(\omega_{v_j}+2\tilde{\Omega})T_0}+\tilde{\Omega}^2A_j\tilde{E}_k\tilde{E}_le^{i\omega_{v_j}T_0}
$$

$$
+\tilde{\Omega}^2A_j\tilde{E}_k\tilde{E}_le^{i\omega_{v_j}T_0}-\tilde{\Omega}^2A_j\tilde{E}_k\tilde{E}_le^{i(\omega_{v_j}-2\tilde{\Omega})T_0}
$$

$$
-\omega_{w_k}\omega_{w_l}E_jB_kB_le^{i(\Omega+\omega_{w_k}+\omega_{w_l})T_0}+\omega_{w_k}\omega_{w_l}E_jB_k\bar{B}_le^{i(\Omega+\omega_{w_k}-\omega_{w_l})T_0}
$$

$$
+\omega_{w_k}\omega_{w_l}E_j\bar{B}_kB_le^{i(\Omega-\omega_{w_k}+\omega_{w_l})T_0}-\omega_{w_k}\omega_{w_l}E_j\bar{B}_k\bar{B}_le^{i(\Omega-\omega_{w_k}-\omega_{w_l})T_0}
$$

$$
-\tilde{\Omega}\omega_{w_k}E_jB_k\tilde{E}_le^{i(\Omega+\omega_{w_k}+\tilde{\Omega})T_0}+\tilde{\Omega}\omega_{w_k}E_jB_k\tilde{E}_le^{i(\Omega+\omega_{w_k}-\tilde{\Omega})T_0}
$$

$$
+\tilde{\Omega}\omega_{w_k}E_j\bar{B}_k\tilde{E}_le^{i(\Omega-\omega_{w_k}+\tilde{\Omega})T_0}-\tilde{\Omega}\omega_{w_k}E_j\bar{B}_k\tilde{E}_le^{i(\Omega-\omega_{w_k}-\tilde{\Omega})T_0}
$$

$$
-\tilde{\Omega}\omega_{w_l}E_j\tilde{E}_kB_le^{i(\Omega+\tilde{\Omega}+\omega_{w_l})T_0}+\tilde{\Omega}\omega_{w_l}E_j\tilde{E}_k\bar{B}_le^{i(\Omega+\tilde{\Omega}-\omega_{w_l})T_0}
$$

$$
+\tilde{\Omega}\omega_{w_l}E_j\tilde{E}_kB_le^{i(\Omega-\tilde{\Omega}+\omega_{w_l})T_0}-\tilde{\Omega}\omega_{w_l}E_j\tilde{E}_k\bar{B}_le^{i(\Omega-\tilde{\Omega}-\omega_{w_l})T_0}
$$

$$
-\tilde{\Omega}^2E_j\tilde{E}_k\tilde{E}_le^{i(\Omega+2\tilde{\Omega})T_0}+\tilde{\Omega}^2E_j\tilde{E}_k\tilde{E}_le^{i\Omega T_0}
$$

$$
+\tilde{\Omega}^2E_j\tilde{E}_k\tilde{E}_le^{i\Omega T_0}-\tilde{\Omega}^2E_j\tilde{E}_k\tilde{E}_le^{i(\Omega-2\tilde{\Omega})T_0}\Big]
$$

$$
\begin{aligned}
-\sum_{j=1}^{m}\sum_{k=1}^{m}\sum_{l=1}^{m} W_{jkln}{}^{\nu 1}[& -\omega_{\nu_l}^2 A_j A_k A_l e^{i(\omega_{\nu_j}+\omega_{\nu_k}+\omega_{\nu_l})T_0} - \omega_{\nu_l}^2 A_j A_k \overline{A}_l e^{i(\omega_{\nu_j}+\omega_{\nu_k}-\omega_{\nu_l})T_0} \\
& - \omega_{\nu_l}^2 A_j \overline{A}_k A_l e^{i(\omega_{\nu_j}-\omega_{\nu_k}+\omega_{\nu_l})T_0} - \omega_{\nu_l}^2 A_j \overline{A}_k \overline{A}_l e^{i(\omega_{\nu_j}-\omega_{\nu_k}-\omega_{\nu_l})T_0} \\
& - \Omega^2 A_j A_k E_l e^{i(\omega_{\nu_j}+\omega_{\nu_k}+\Omega)T_0} - \Omega^2 A_j A_k E_l e^{i(\omega_{\nu_j}+\omega_{\nu_k}-\Omega)T_0} \\
& - \Omega^2 A_j \overline{A}_k E_l e^{i(\omega_{\nu_j}-\omega_{\nu_k}+\Omega)T_0} - \Omega^2 A_j \overline{A}_k E_l e^{i(\omega_{\nu_j}-\omega_{\nu_k}-\Omega)T_0} \\
& - \omega_{\nu_l}^2 A_j E_k A_l e^{i(\omega_{\nu_j}+\Omega+\omega_{\nu_l})T_0} - \omega_{\nu_l}^2 A_j E_k \overline{A}_l e^{i(\omega_{\nu_j}+\Omega-\omega_{\nu_l})T_0} \\
& - \omega_{\nu_l}^2 A_j E_k A_l e^{i(\omega_{\nu_j}-\Omega+\omega_{\nu_l})T_0} - \omega_{\nu_l}^2 A_j E_k \overline{A}_l e^{i(\omega_{\nu_j}-\Omega-\omega_{\nu_l})T_0} \\
& - \Omega^2 A_j E_k E_l e^{i(\omega_{\nu_j}+2\Omega)T_0} - \Omega^2 A_j E_k E_l e^{i\omega_{\nu_j}T_0} \\
& - \Omega^2 A_j E_k E_l e^{i\omega_{\nu_j}T_0} - \Omega^2 A_j E_k E_l e^{i(\omega_{\nu_j}-2\Omega)T_0} \\
& - \omega_{\nu_l}^2 E_j A_k A_l e^{i(\Omega+\omega_{\nu_k}+\omega_{\nu_l})T_0} - \omega_{\nu_l}^2 E_j A_k \overline{A}_l e^{i(\Omega+\omega_{\nu_k}-\omega_{\nu_l})T_0} \\
& - \omega_{\nu_l}^2 E_j \overline{A}_k A_l e^{i(\Omega-\omega_{\nu_k}+\omega_{\nu_l})T_0} - \omega_{\nu_l}^2 E_j \overline{A}_k \overline{A}_l e^{i(\Omega-\omega_{\nu_k}-\omega_{\nu_l})T_0} \\
& - \Omega^2 E_j A_k E_l e^{i(2\Omega+\omega_{\nu_k})T_0} - \Omega^2 E_j A_k E_l e^{i\omega_{\nu_k}T_0} \\
& - \Omega^2 E_j \overline{A}_k E_l e^{i(2\Omega-\omega_{\nu_k})T_0} - \Omega^2 E_j \overline{A}_k E_l e^{-i\omega_{\nu_k}T_0} \\
& - \omega_{\nu_l}^2 E_j E_k A_l e^{i(2\Omega+\omega_{\nu_l})T_0} - \omega_{\nu_l}^2 E_j E_k \overline{A}_l e^{i(2\Omega-\omega_{\nu_l})T_0} \\
& - \omega_{\nu_l}^2 E_j E_k A_l e^{i\omega_{\nu_l}T_0} - \omega_{\nu_l}^2 E_j E_k \overline{A}_l e^{-i\omega_{\nu_l}T_0} \\
& - \Omega^2 E_j E_k E_l e^{i3\Omega T_0} - \Omega^2 E_j E_k E_l e^{i\Omega T_0} \\
& - \Omega^2 E_j E_k E_l e^{i\Omega T_0} - \Omega^2 E_j E_k E_l e^{-i\Omega T_0}]
\end{aligned}
$$

$$
\begin{aligned}
-\sum_{j=1}^{m}\sum_{k=1}^{m}\sum_{l=1}^{m} W_{jkln}{}^{v2}[& -\omega_{w_l}^2 A_j B_k B_l e^{i(\omega_{v_j}+\omega_{w_k}+\omega_{w_l})T_0} - \omega_{w_l}^2 A_j B_k \bar{B}_l e^{i(\omega_{v_j}+\omega_{w_k}-\omega_{w_l})T_0} \\
& - \omega_{w_l}^2 A_j \bar{B}_k B_l e^{i(\omega_{v_j}-\omega_{w_k}+\omega_{w_l})T_0} - \omega_{w_l}^2 A_j \bar{B}_k \bar{B}_l e^{i(\omega_{v_j}-\omega_{w_k}-\omega_{w_l})T_0} \\
& - \tilde{\Omega}^2 A_j B_k \tilde{E}_l e^{i(\omega_{v_j}+\omega_{w_k}+\tilde{\Omega})T_0} - \tilde{\Omega}^2 A_j B_k \tilde{E}_l e^{i(\omega_{v_j}+\omega_{w_k}-\tilde{\Omega})T_0} \\
& - \tilde{\Omega}^2 A_j \bar{B}_k \tilde{E}_l e^{i(\omega_{v_j}-\omega_{w_k}+\tilde{\Omega})T_0} - \tilde{\Omega}^2 A_j \bar{B}_k \tilde{E}_l e^{i(\omega_{v_j}-\omega_{w_k}-\tilde{\Omega})T_0} \\
& - \omega_{w_l}^2 A_j \tilde{E}_k B_l e^{i(\omega_{v_j}+\tilde{\Omega}+\omega_{w_l})T_0} - \omega_{w_l}^2 A_j \tilde{E}_k \bar{B}_l e^{i(\omega_{v_j}+\tilde{\Omega}-\omega_{w_l})T_0} \\
& - \omega_{w_l}^2 A_j \tilde{E}_k B_l e^{i(\omega_{v_j}-\tilde{\Omega}+\omega_{w_l})T_0} - \omega_{w_l}^2 A_j \tilde{E}_k \bar{B}_l e^{i(\omega_{v_j}-\tilde{\Omega}-\omega_{w_l})T_0} \\
& - \tilde{\Omega}^2 A_j \tilde{E}_k \tilde{E}_l e^{i(\omega_{v_j}+2\tilde{\Omega})T_0} - \tilde{\Omega}^2 A_j \tilde{E}_k \tilde{E}_l e^{i\omega_{v_j}T_0} \\
& - \tilde{\Omega}^2 A_j \tilde{E}_k \tilde{E}_l e^{i\omega_{v_j}T_0} - \tilde{\Omega}^2 A_j \tilde{E}_k \tilde{E}_l e^{i(\omega_{v_j}-2\tilde{\Omega})T_0} \\
& - \omega_{w_l}^2 E_j B_k B_l e^{i(\Omega+\omega_{w_k}+\omega_{w_l})T_0} - \omega_{w_l}^2 E_j B_k \bar{B}_l e^{i(\Omega+\omega_{w_k}-\omega_{w_l})T_0} \\
& - \omega_{w_l}^2 E_j \bar{B}_k B_l e^{i(\Omega-\omega_{w_k}+\omega_{w_l})T_0} - \omega_{w_l}^2 E_j \bar{B}_k \bar{B}_l e^{i(\Omega-\omega_{w_k}-\omega_{w_l})T_0} \\
& - \tilde{\Omega}^2 E_j B_k \tilde{E}_l e^{i(\Omega+\omega_{w_k}+\tilde{\Omega})T_0} - \tilde{\Omega}^2 E_j B_k \tilde{E}_l e^{i(\Omega+\omega_{w_k}-\tilde{\Omega})T_0} \\
& - \tilde{\Omega}^2 E_j \bar{B}_k \tilde{E}_l e^{i(\Omega-\omega_{w_k}+\tilde{\Omega})T_0} - \tilde{\Omega}^2 E_j \bar{B}_k \tilde{E}_l e^{i(\Omega-\omega_{w_k}-\tilde{\Omega})T_0} \\
& - \omega_{w_l}^2 E_j \tilde{E}_k B_l e^{i(\Omega+\tilde{\Omega}+\omega_{w_l})T_0} - \omega_{w_l}^2 E_j \tilde{E}_k \bar{B}_l e^{i(\Omega+\tilde{\Omega}-\omega_{w_l})T_0} \\
& - \omega_{w_l}^2 E_j \tilde{E}_k B_l e^{i(\Omega-\tilde{\Omega}+\omega_{w_l})T_0} - \omega_{w_l}^2 E_j \tilde{E}_k \bar{B}_l e^{i(\Omega-\tilde{\Omega}-\omega_{w_l})T_0} \\
& - \tilde{\Omega}^2 E_j \tilde{E}_k \tilde{E}_l e^{i(\Omega+2\tilde{\Omega})T_0} - \tilde{\Omega}^2 E_j \tilde{E}_k \tilde{E}_l e^{i\Omega T_0} \\
& - \tilde{\Omega}^2 E_j \tilde{E}_k \tilde{E}_l e^{i\Omega T_0} - \tilde{\Omega}^2 E_j \tilde{E}_k \tilde{E}_l e^{i(\Omega-2\tilde{\Omega})T_0}]
\end{aligned}
$$

$$
+ cc \qquad (C.1)
$$

$$
\begin{aligned}
D_0^2 w_{n1} + \omega_{w_n}^2 w_{n1} = & -2i\tilde{\Omega}\mu_{w_n}\tilde{E}_n e^{i\tilde{\Omega}T_0} - 2i\omega_{w_n}(D_1 B_n + \mu_{w_n} B_n)e^{i\omega_{w_n}T_0} \\
& - \sum_{j=1}^{m} T_{jn}{}^{w}(B_j e^{i\omega_{w_j}T_0} + \tilde{E}_j e^{i\tilde{\Omega}T_0}) \\
& - \sum_{j=1}^{m}\sum_{k=1}^{m} \Lambda_{jkn}{}^{w}[A_j B_k e^{i(\omega_{v_j}+\omega_{w_k})T_0} + A_j \bar{B}_k e^{i(\omega_{v_j}-\omega_{w_k})T_0} \\
& \qquad + A_j \tilde{E}_k e^{i(\omega_{v_j}+\tilde{\Omega})T_0} + A_j \tilde{E}_k e^{i(\omega_{v_j}-\tilde{\Omega})T_0} \\
& \qquad + E_j B_k e^{i(\omega_{w_k}+\Omega)T_0} + E_j \bar{B}_k e^{i(-\omega_{w_k}+\Omega)T_0} \\
& \qquad + E_j \tilde{E}_k e^{i(\Omega+\tilde{\Omega})T_0} + E_j \tilde{E}_k e^{i(\Omega-\tilde{\Omega})T_0}] \\
& - \sum_{j=1}^{m}\sum_{k=1}^{m} Z_{jkn}{}^{w}[-\omega_{v_k}^2 B_j A_k e^{i(\omega_{w_j}+\omega_{v_k})T_0} - \omega_{v_k}^2 B_j \bar{A}_k e^{i(\omega_{w_j}-\omega_{v_k})T_0} \\
& \qquad - \Omega^2 B_j E_k e^{i(\omega_{w_j}+\Omega)T_0} - \Omega^2 B_j E_k e^{i(\omega_{w_j}-\Omega)T_0} \\
& \qquad - \omega_{v_k}^2 \tilde{E}_j A_k e^{i(\tilde{\Omega}+\omega_{v_k})T_0} - \omega_{v_k}^2 \tilde{E}_j \bar{A}_k e^{i(\tilde{\Omega}-\omega_{v_k})T_0} \\
& \qquad - \Omega^2 \tilde{E}_j E_k e^{i(\tilde{\Omega}+\Omega)T_0} - \Omega^2 \tilde{E}_j E_k e^{i(\tilde{\Omega}-\Omega)T_0}]
\end{aligned}
$$

$$
\begin{aligned}
-\sum_{j=1}^{m}\sum_{k=1}^{m}\sum_{l=1}^{m}\Gamma_{jkln}^{w1}[&A_jA_kB_le^{i(\omega_{v_j}+\omega_{v_k}+\omega_{w_l})T_0}+A_jA_k\overline{B}_le^{i(\omega_{v_j}+\omega_{v_k}-\omega_{w_l})T_0}\\
&+A_j\overline{A}_kB_le^{i(\omega_{v_j}-\omega_{v_k}+\omega_{w_l})T_0}+A_j\overline{A}_k\overline{B}_le^{i(\omega_{v_j}-\omega_{v_k}-\omega_{w_l})T_0}\\
&+A_jA_k\widetilde{E}_le^{i(\omega_{v_j}+\omega_{v_k}+\tilde{\Omega})T_0}+A_jA_k\widetilde{E}_le^{i(\omega_{v_j}+\omega_{v_k}-\tilde{\Omega})T_0}\\
&+A_j\overline{A}_k\widetilde{E}_le^{i(\omega_{v_j}-\omega_{v_k}+\tilde{\Omega})T_0}+A_j\overline{A}_k\widetilde{E}_le^{i(\omega_{v_j}-\omega_{v_k}-\tilde{\Omega})T_0}\\
&+A_jE_kB_le^{i(\omega_{v_j}+\Omega+\omega_{w_l})T_0}+A_jE_k\overline{B}_le^{i(\omega_{v_j}+\Omega-\omega_{w_l})T_0}\\
&+A_jE_kB_le^{i(\omega_{v_j}-\Omega+\omega_{w_l})T_0}+A_jE_k\overline{B}_le^{i(\omega_{v_j}-\Omega-\omega_{w_l})T_0}\\
&+A_jE_k\widetilde{E}_le^{i(\omega_{v_j}+\Omega+\tilde{\Omega})T_0}+A_jF_k\widetilde{E}_le^{i(\omega_{v_j}+\Omega-\tilde{\Omega})T_0}\\
&+A_jE_k\widetilde{E}_le^{i(\omega_{v_j}-\Omega+\tilde{\Omega})T_0}+A_jE_k\widetilde{E}_le^{i(\omega_{v_j}-\Omega-\tilde{\Omega})T_0}\\
&+E_jA_kB_le^{i(\Omega+\omega_{v_k}+\omega_{w_l})T_0}+E_jA_k\overline{B}_le^{i(\Omega+\omega_{v_k}-\omega_{w_l})T_0}\\
&+E_j\overline{A}_kB_le^{i(\Omega-\omega_{v_k}+\omega_{w_l})T_0}+E_j\overline{A}_k\overline{B}_le^{i(\Omega-\omega_{v_k}-\omega_{w_l})T_0}\\
&+E_jA_k\widetilde{E}_le^{i(\Omega+\omega_{v_k}+\tilde{\Omega})T_0}+E_jA_k\widetilde{E}_le^{i(\Omega+\omega_{v_j}-\tilde{\Omega})T_0}\\
&+E_j\overline{A}_k\widetilde{E}_le^{i(\Omega-\omega_{v_k}+\tilde{\Omega})T_0}+E_j\overline{A}_k\widetilde{E}_le^{i(\Omega-\omega_{v_k}-\tilde{\Omega})T_0}\\
&+E_jE_kB_le^{i(2\Omega+\omega_{w_l})T_0}+E_jE_k\overline{B}_le^{i(2\Omega-\omega_{w_l})T_0}\\
&+E_jE_kB_le^{i\omega_{w_l}T_0}+E_jE_k\overline{B}_le^{-i\omega_{w_l}T_0}\\
&+E_jE_k\widetilde{E}_le^{i(2\Omega+\tilde{\Omega})T_0}+E_jE_k\widetilde{E}_le^{i(2\Omega-\tilde{\Omega})T_0}\\
&+E_jE_k\widetilde{E}_le^{i\tilde{\Omega}T_0}+E_jE_k\widetilde{E}_le^{-i\tilde{\Omega}T_0}]
\end{aligned}
$$

$$
\begin{aligned}
-\sum_{j=1}^{m}\sum_{k=1}^{m}\sum_{l=1}^{m}\Gamma_{jkln}{}^{w2}[&B_jB_kB_le^{i(\omega_{w_j}+\omega_{w_k}+\omega_{w_l})T_0}+B_jB_k\bar{B}_le^{i(\omega_{w_j}+\omega_{w_k}-\omega_{w_l})T_0}\\
&+B_j\bar{B}_kB_le^{i(\omega_{w_j}-\omega_{w_k}+\omega_{w_l})T_0}+B_j\bar{B}_k\bar{B}_le^{i(\omega_{w_j}-\omega_{w_k}-\omega_{w_l})T_0}\\
&+B_jB_k\tilde{E}_le^{i(\omega_{w_j}+\omega_{w_k}+\tilde{\Omega})T_0}+B_jB_k\tilde{E}_le^{i(\omega_{w_j}+\omega_{w_k}-\tilde{\Omega})T_0}\\
&+B_j\bar{B}_k\tilde{E}_le^{i(\omega_{w_j}-\omega_{w_k}+\tilde{\Omega})T_0}+B_j\bar{B}_k\tilde{E}_le^{i(\omega_{w_j}-\omega_{w_k}-\tilde{\Omega})T_0}\\
&+B_j\tilde{E}_kB_le^{i(\omega_{w_j}+\tilde{\Omega}+\omega_{w_l})T_0}+B_j\tilde{E}_k\bar{B}_le^{i(\omega_{w_j}+\tilde{\Omega}-\omega_{w_l})T_0}\\
&+B_j\tilde{E}_kB_le^{i(\omega_{w_j}-\tilde{\Omega}+\omega_{w_l})T_0}+B_j\tilde{E}_k\bar{B}_le^{i(\omega_{w_j}-\tilde{\Omega}-\omega_{w_l})T_0}\\
&+B_j\tilde{E}_k\tilde{E}_le^{i(\omega_{w_j}+2\tilde{\Omega})T_0}+B_j\tilde{E}_k\tilde{E}_le^{i\omega_{w_j}T_0}\\
&+B_j\tilde{E}_k\tilde{E}_le^{i\omega_{w_j}T_0}+B_j\tilde{E}_k\tilde{E}_le^{i(\omega_{w_j}-2\tilde{\Omega})T_0}\\
&+\tilde{E}_jB_kB_le^{i(\tilde{\Omega}+\omega_{w_k}+\omega_{w_l})T_0}+\tilde{E}_jB_k\bar{B}_le^{i(\tilde{\Omega}+\omega_{w_k}-\omega_{w_l})T_0}\\
&+\tilde{E}_j\bar{B}_kB_le^{i(\tilde{\Omega}-\omega_{w_k}+\omega_{w_l})T_0}+\tilde{E}_j\bar{B}_k\bar{B}_le^{i(\tilde{\Omega}-\omega_{w_k}-\omega_{w_l})T_0}\\
&+\tilde{E}_jB_k\tilde{E}_le^{i(2\tilde{\Omega}+\omega_{w_k})T_0}+\tilde{E}_jB_k\tilde{E}_le^{i\omega_{w_k}T_0}\\
&+\tilde{E}_j\bar{B}_k\tilde{E}_le^{i(2\tilde{\Omega}-\omega_{w_k})T_0}+\tilde{E}_j\bar{B}_k\tilde{E}_le^{-i\omega_{w_k}T_0}\\
&+\tilde{E}_j\tilde{E}_kB_le^{i(2\tilde{\Omega}+\omega_{w_l})T_0}+\tilde{E}_j\tilde{E}_k\bar{B}_le^{i(2\tilde{\Omega}-\omega_{w_l})T_0}\\
&+\tilde{E}_j\tilde{E}_kB_le^{i\omega_{w_l}T_0}+\tilde{E}_j\tilde{E}_k\bar{B}_le^{-i\omega_{w_l}T_0}\\
&+\tilde{E}_j\tilde{E}_k\tilde{E}_le^{i3\tilde{\Omega}T_0}+\tilde{E}_j\tilde{E}_k\tilde{E}_le^{i\tilde{\Omega}T_0}\\
&+\tilde{E}_j\tilde{E}_k\tilde{E}_le^{i\tilde{\Omega}T_0}+\tilde{E}_j\tilde{E}_k\tilde{E}_le^{-i\tilde{\Omega}T_0}]
\end{aligned}
$$

$$
\begin{aligned}
-\sum_{j=1}^{m}\sum_{k=1}^{m}\sum_{l=1}^{m} V_{jkln}^{w1}[& -\omega_{\nu_k}\omega_{\nu_l}B_jA_kA_le^{i(\omega_{w_j}+\omega_{\nu_k}+\omega_{\nu_l})T_0}+\omega_{\nu_k}\omega_{\nu_l}B_jA_k\bar{A}_le^{i(\omega_{w_j}+\omega_{\nu_k}-\omega_{\nu_l})T_0}\\
&+\omega_{\nu_k}\omega_{\nu_l}B_j\bar{A}_kA_le^{i(\omega_{w_j}-\omega_{\nu_k}+\omega_{\nu_l})T_0}-\omega_{\nu_k}\omega_{\nu_l}B_j\bar{A}_k\bar{A}_le^{i(\omega_{w_j}-\omega_{\nu_k}-\omega_{\nu_l})T_0}\\
&-\Omega\omega_{\nu_k}B_jA_kE_le^{i(\omega_{w_j}+\omega_{\nu_k}+\Omega)T_0}+\Omega\omega_{\nu_k}B_jA_kE_le^{i(\omega_{w_j}+\omega_{\nu_k}-\Omega)T_0}\\
&+\Omega\omega_{\nu_k}B_j\bar{A}_kE_le^{i(\omega_{w_j}-\omega_{\nu_k}+\Omega)T_0}-\Omega\omega_{\nu_k}B_j\bar{A}_kE_le^{i(\omega_{w_j}-\omega_{\nu_k}-\Omega)T_0}\\
&-\Omega\omega_{\nu_l}B_jE_kA_le^{i(\omega_{w_j}+\Omega+\omega_{\nu_l})T_0}+\Omega\omega_{\nu_l}B_jE_k\bar{A}_le^{i(\omega_{w_j}+\Omega-\omega_{\nu_l})T_0}\\
&+\Omega\omega_{\nu_l}B_jE_kA_le^{i(\omega_{w_j}-\Omega+\omega_{\nu_l})T_0}-\Omega\omega_{\nu_l}B_jE_k\bar{A}_le^{i(\omega_{w_j}-\Omega-\omega_{\nu_l})T_0}\\
&-\Omega^2B_jE_kE_le^{i(\omega_{w_j}+2\Omega)T_0}+\Omega^2B_jE_kE_le^{i\omega_{w_j}T_0}\\
&+\Omega^2B_jE_kE_le^{i\omega_{w_j}T_0}-\Omega^2B_jE_kE_le^{i(\omega_{w_j}-2\Omega)T_0}\\
&-\omega_{\nu_k}\omega_{\nu_l}\tilde{E}_jA_kA_le^{i(\tilde{\Omega}+\omega_{\nu_k}+\omega_{\nu_l})T_0}+\omega_{\nu_k}\omega_{\nu_l}\tilde{E}_jA_k\bar{A}_le^{i(\tilde{\Omega}+\omega_{\nu_k}-\omega_{\nu_l})T_0}\\
&+\omega_{\nu_k}\omega_{\nu_l}\tilde{E}_j\bar{A}_kA_le^{i(\tilde{\Omega}-\omega_{\nu_k}+\omega_{\nu_l})T_0}-\omega_{\nu_k}\omega_{\nu_l}\tilde{E}_j\bar{A}_k\bar{A}_le^{i(\tilde{\Omega}-\omega_{\nu_k}-\omega_{\nu_l})T_0}\\
&-\Omega\omega_{\nu_k}\tilde{E}_jA_kE_le^{i(\tilde{\Omega}+\omega_{\nu_k}+\Omega)T_0}+\Omega\omega_{\nu_k}\tilde{E}_jA_kE_le^{i(\tilde{\Omega}+\omega_{\nu_k}-\Omega)T_0}\\
&+\Omega\omega_{\nu_k}\tilde{E}_j\bar{A}_kE_le^{i(\tilde{\Omega}-\omega_{\nu_k}+\Omega)T_0}-\Omega\omega_{\nu_k}\tilde{E}_j\bar{A}_kE_le^{i(\tilde{\Omega}-\omega_{\nu_k}-\Omega)T_0}\\
&-\Omega\omega_{\nu_l}\tilde{E}_jE_kA_le^{i(\tilde{\Omega}+\Omega+\omega_{\nu_l})T_0}+\Omega\omega_{\nu_l}\tilde{E}_jE_k\bar{A}_le^{i(\tilde{\Omega}+\Omega-\omega_{\nu_l})T_0}\\
&+\Omega\omega_{\nu_l}\tilde{E}_jE_kA_le^{i(\tilde{\Omega}-\Omega+\omega_{\nu_l})T_0}-\Omega\omega_{\nu_l}\tilde{E}_jE_k\bar{A}_le^{i(\tilde{\Omega}-\Omega-\omega_{\nu_l})T_0}\\
&-\Omega^2\tilde{E}_jE_kE_le^{i(\tilde{\Omega}+2\Omega)T_0}+\Omega^2\tilde{E}_jE_kE_le^{i\tilde{\Omega}T_0}\\
&+\Omega^2\tilde{E}_jE_kE_le^{i\tilde{\Omega}T_0}-\Omega^2\tilde{E}_jE_kE_le^{i(\tilde{\Omega}-2\Omega)T_0}]
\end{aligned}
$$

$$
\begin{aligned}
-\sum_{j=1}^{m}\sum_{k=1}^{m}\sum_{l=1}^{m} V_{jkln}^{w2}[& -\omega_{w_k}\omega_{w_l}B_jB_kB_le^{i(\omega_{w_j}+\omega_{w_k}+\omega_{w_l})T_0}+\omega_{w_k}\omega_{w_l}B_jB_k\bar{B}_le^{i(\omega_{w_j}+\omega_{w_k}-\omega_{w_l})T_0}\\
&+\omega_{w_k}\omega_{w_l}B_j\bar{B}_kB_le^{i(\omega_{w_j}-\omega_{w_k}+\omega_{w_l})T_0}-\omega_{w_k}\omega_{w_l}B_j\bar{B}_k\bar{B}_le^{i(\omega_{w_j}-\omega_{w_k}-\omega_{w_l})T_0}\\
&-\tilde{\Omega}\omega_{w_k}B_jB_k\tilde{E}_le^{i(\omega_{w_j}+\omega_{w_k}+\tilde{\Omega})T_0}+\tilde{\Omega}\omega_{w_k}B_jB_k\tilde{E}_le^{i(\omega_{w_j}+\omega_{w_k}-\tilde{\Omega})T_0}\\
&+\tilde{\Omega}\omega_{w_k}B_j\bar{B}_k\tilde{E}_le^{i(\omega_{w_j}-\omega_{w_k}+\tilde{\Omega})T_0}-\tilde{\Omega}\omega_{w_k}B_j\bar{B}_k\tilde{E}_le^{i(\omega_{w_j}-\omega_{w_k}-\tilde{\Omega})T_0}\\
&-\tilde{\Omega}\omega_{w_l}B_j\tilde{E}_kB_le^{i(\omega_{w_j}+\tilde{\Omega}+\omega_{w_l})T_0}+\tilde{\Omega}\omega_{w_l}B_j\tilde{E}_k\bar{B}_le^{i(\omega_{w_j}+\tilde{\Omega}-\omega_{w_l})T_0}\\
&+\tilde{\Omega}\omega_{w_l}B_j\tilde{E}_kB_le^{i(\omega_{w_j}-\tilde{\Omega}+\omega_{w_l})T_0}-\tilde{\Omega}\omega_{w_l}B_j\tilde{E}_k\bar{B}_le^{i(\omega_{w_j}-\tilde{\Omega}-\omega_{w_l})T_0}\\
&-\tilde{\Omega}^2B_j\tilde{E}_k\tilde{E}_le^{i(\omega_{w_j}+2\tilde{\Omega})T_0}+\tilde{\Omega}^2B_j\tilde{E}_k\tilde{E}_le^{i\omega_{w_j}T_0}\\
&+\tilde{\Omega}^2B_j\tilde{E}_k\tilde{E}_le^{i\omega_{w_j}T_0}-\tilde{\Omega}^2B_j\tilde{E}_k\tilde{E}_le^{i(\omega_{w_j}-2\tilde{\Omega})T_0}\\
&-\omega_{w_k}\omega_{w_l}\tilde{E}_jB_kB_le^{i(\tilde{\Omega}+\omega_{w_k}+\omega_{w_l})T_0}+\omega_{w_k}\omega_{w_l}\tilde{E}_jB_k\bar{B}_le^{i(\tilde{\Omega}+\omega_{w_k}-\omega_{w_l})T_0}\\
&+\omega_{w_k}\omega_{w_l}\tilde{E}_j\bar{B}_kB_le^{i(\tilde{\Omega}-\omega_{w_k}+\omega_{w_l})T_0}-\omega_{w_k}\omega_{w_l}\tilde{E}_j\bar{B}_k\bar{B}_le^{i(\tilde{\Omega}-\omega_{w_k}-\omega_{w_l})T_0}\\
&-\tilde{\Omega}\omega_{w_k}\tilde{E}_jB_k\tilde{E}_le^{i(2\tilde{\Omega}+\omega_{w_k})T_0}+\tilde{\Omega}\omega_{w_k}\tilde{E}_jB_k\tilde{E}_le^{i\omega_{w_k}T_0}\\
&+\tilde{\Omega}\omega_{w_k}\tilde{E}_j\bar{B}_k\tilde{E}_le^{i(2\tilde{\Omega}-\omega_{w_k})T_0}-\tilde{\Omega}\omega_{w_k}\tilde{E}_j\bar{B}_k\tilde{E}_le^{-i\omega_{w_k}T_0}\\
&-\tilde{\Omega}\omega_{w_l}\tilde{E}_j\tilde{E}_kB_le^{i(2\tilde{\Omega}+\omega_{w_l})T_0}+\tilde{\Omega}\omega_{w_l}\tilde{E}_j\tilde{E}_k\bar{B}_le^{i(2\tilde{\Omega}-\omega_{w_l})T_0}\\
&+\tilde{\Omega}\omega_{w_l}\tilde{E}_j\tilde{E}_kB_le^{i\omega_{w_l}T_0}-\tilde{\Omega}\omega_{w_l}\tilde{E}_j\tilde{E}_k\bar{B}_le^{-i\omega_{w_l}T_0}\\
&-\tilde{\Omega}^2\tilde{E}_j\tilde{E}_k\tilde{E}_le^{i3\tilde{\Omega}T_0}+\tilde{\Omega}^2\tilde{E}_j\tilde{E}_k\tilde{E}_le^{i\tilde{\Omega}T_0}\\
&+\tilde{\Omega}^2\tilde{E}_j\tilde{E}_k\tilde{E}_le^{i\tilde{\Omega}T_0}-\tilde{\Omega}^2\tilde{E}_j\tilde{E}_k\tilde{E}_le^{-i\tilde{\Omega}T_0}]
\end{aligned}
$$

$$
\begin{aligned}
-\sum_{j=1}^{m}\sum_{k=1}^{m}\sum_{l=1}^{m} W_{jkln}{}^{w1}[& -\omega_{v_l}^2 B_j A_k A_l e^{i(\omega_{w_j}+\omega_{v_k}+\omega_{v_l})T_0} - \omega_{v_l}^2 B_j A_k \overline{A}_l e^{i(\omega_{w_j}+\omega_{v_k}-\omega_{v_l})T_0} \\
& - \omega_{v_l}^2 B_j \overline{A}_k A_l e^{i(\omega_{w_j}-\omega_{v_k}+\omega_{v_l})T_0} - \omega_{v_l}^2 B_j \overline{A}_k \overline{A}_l e^{i(\omega_{w_j}-\omega_{v_k}-\omega_{v_l})T_0} \\
& - \Omega^2 B_j A_k E_l e^{i(\omega_{w_j}+\omega_{v_k}+\Omega)T_0} - \Omega^2 B_j A_k E_l e^{i(\omega_{w_j}+\omega_{v_k}-\Omega)T_0} \\
& - \Omega^2 B_j \overline{A}_k E_l e^{i(\omega_{w_j}-\omega_{v_k}+\Omega)T_0} - \Omega^2 B_j \overline{A}_k E_l e^{i(\omega_{w_j}-\omega_{v_k}-\Omega)T_0} \\
& - \omega_{v_l}^2 B_j E_k A_l e^{i(\omega_{w_j}+\Omega+\omega_{v_l})T_0} - \omega_{v_l}^2 B_j E_k \overline{A}_l e^{i(\omega_{w_j}+\Omega-\omega_{v_l})T_0} \\
& - \omega_{v_l}^2 B_j E_k A_l e^{i(\omega_{w_j}-\Omega+\omega_{v_l})T_0} - \omega_{v_l}^2 B_j E_k \overline{A}_l e^{i(\omega_{w_j}-\Omega-\omega_{v_l})T_0} \\
& - \Omega^2 B_j E_k E_l e^{i(\omega_{w_j}+2\Omega)T_0} - \Omega^2 B_j E_k E_l e^{i\omega_{w_j}T_0} \\
& - \Omega^2 B_j E_k E_l e^{i\omega_{w_j}T_0} - \Omega^2 B_j E_k E_l e^{i(\omega_{w_j}-2\Omega)T_0} \\
& - \omega_{v_l}^2 \tilde{E}_j A_k A_l e^{i(\tilde{\Omega}+\omega_{v_k}+\omega_{v_l})T_0} - \omega_{v_l}^2 \tilde{E}_j A_k \overline{A}_l e^{i(\tilde{\Omega}+\omega_{v_k}-\omega_{v_l})T_0} \\
& - \omega_{v_l}^2 \tilde{E}_j \overline{A}_k A_l e^{i(\tilde{\Omega}-\omega_{v_k}+\omega_{v_l})T_0} - \omega_{v_l}^2 \tilde{E}_j \overline{A}_k \overline{A}_l e^{i(\tilde{\Omega}-\omega_{v_k}-\omega_{v_l})T_0} \\
& - \Omega^2 \tilde{E}_j A_k E_l e^{i(\tilde{\Omega}+\omega_{v_k}+\Omega)T_0} - \Omega^2 \tilde{E}_j A_k E_l e^{i(\tilde{\Omega}+\omega_{v_k}-\Omega)T_0} \\
& - \Omega^2 \tilde{E}_j \overline{A}_k E_l e^{i(\tilde{\Omega}-\omega_{v_k}+\Omega)T_0} - \Omega^2 \tilde{E}_j \overline{A}_k E_l e^{i(\tilde{\Omega}-\omega_{v_k}-\Omega)T_0} \\
& - \omega_{v_l}^2 \tilde{E}_j E_k A_l e^{i(\tilde{\Omega}+\Omega+\omega_{v_l})T_0} - \omega_{v_l}^2 \tilde{E}_j E_k \overline{A}_l e^{i(\tilde{\Omega}+\Omega-\omega_{v_l})T_0} \\
& - \omega_{v_l}^2 \tilde{E}_j E_k A_l e^{i(\tilde{\Omega}-\Omega+\omega_{v_l})T_0} - \omega_{v_l}^2 \tilde{E}_j E_k \overline{A}_l e^{i(\tilde{\Omega}-\Omega-\omega_{v_l})T_0} \\
& - \Omega^2 \tilde{E}_j E_k E_l e^{i(\tilde{\Omega}+2\Omega)T_0} - \Omega^2 \tilde{E}_j E_k E_l e^{i\tilde{\Omega}T_0} \\
& - \Omega^2 \tilde{E}_j E_k E_l e^{i\tilde{\Omega}T_0} - \Omega^2 \tilde{E}_j E_k E_l e^{i(\tilde{\Omega}-2\Omega)T_0}]
\end{aligned}
$$

$$
\begin{aligned}
-\sum_{j=1}^{m}\sum_{k=1}^{m}\sum_{l=1}^{m} W_{jkln}^{w2}[& -\omega_{w_l}^2 B_j B_k B_l e^{i(\omega_{w_j}+\omega_{w_k}+\omega_{w_l})T_0} - \omega_{w_l}^2 B_j B_k \bar{B}_l e^{i(\omega_{w_j}+\omega_{w_k}-\omega_{w_l})T_0} \\
& - \omega_{w_l}^2 B_j \bar{B}_k B_l e^{i(\omega_{w_j}-\omega_{w_k}+\omega_{w_l})T_0} - \omega_{w_l}^2 B_j \bar{B}_k \bar{B}_l e^{i(\omega_{w_j}-\omega_{w_k}-\omega_{w_l})T_0} \\
& - \tilde{\Omega}^2 B_j B_k \tilde{E}_l e^{i(\omega_{w_j}+\omega_{w_k}+\tilde{\Omega})T_0} - \tilde{\Omega}^2 B_j B_k \tilde{E}_l e^{i(\omega_{w_j}+\omega_{w_k}-\tilde{\Omega})T_0} \\
& - \tilde{\Omega}^2 B_j \bar{B}_k \tilde{E}_l e^{i(\omega_{w_j}-\omega_{w_k}+\tilde{\Omega})T_0} - \tilde{\Omega}^2 B_j \bar{B}_k \tilde{E}_l e^{i(\omega_{w_j}-\omega_{w_k}-\tilde{\Omega})T_0} \\
& - \omega_{w_l}^2 B_j \tilde{E}_k B_l e^{i(\omega_{w_j}+\tilde{\Omega}+\omega_{w_l})T_0} - \omega_{w_l}^2 B_j \tilde{E}_k \bar{B}_l e^{i(\omega_{w_j}+\tilde{\Omega}-\omega_{w_l})T_0} \\
& - \omega_{w_l}^2 B_j \tilde{E}_k B_l e^{i(\omega_{w_j}-\tilde{\Omega}+\omega_{w_l})T_0} - \omega_{w_l}^2 B_j \tilde{E}_k \bar{B}_l e^{i(\omega_{w_j}-\tilde{\Omega}-\omega_{w_l})T_0} \\
& - \tilde{\Omega}^2 B_j \tilde{E}_k \tilde{E}_l e^{i(\omega_{w_j}+2\tilde{\Omega})T_0} - \tilde{\Omega}^2 B_j \tilde{E}_k \tilde{E}_l e^{i\omega_{w_j}T_0} \\
& - \tilde{\Omega}^2 B_j \tilde{E}_k \tilde{E}_l e^{i\omega_{w_j}T_0} - \tilde{\Omega}^2 B_j \tilde{E}_k \tilde{E}_l e^{i(\omega_{w_j}-2\tilde{\Omega})T_0} \\
& - \omega_{w_l}^2 \tilde{E}_j B_k B_l e^{i(\tilde{\Omega}+\omega_{w_k}+\omega_{w_l})T_0} - \omega_{w_l}^2 \tilde{E}_j B_k \bar{B}_l e^{i(\tilde{\Omega}+\omega_{w_k}-\omega_{w_l})T_0} \\
& - \omega_{w_l}^2 \tilde{E}_j \bar{B}_k B_l e^{i(\tilde{\Omega}-\omega_{w_k}+\omega_{w_l})T_0} - \omega_{w_l}^2 \tilde{E}_j \bar{B}_k \bar{B}_l e^{i(\tilde{\Omega}-\omega_{w_k}-\omega_{w_l})T_0} \\
& - \tilde{\Omega}^2 \tilde{E}_j B_k \tilde{E}_l e^{i(\omega_{w_k}+2\tilde{\Omega})T_0} - \tilde{\Omega}^2 \tilde{E}_j B_k \tilde{E}_l e^{i\omega_{w_k}T_0} \\
& - \tilde{\Omega}^2 \tilde{E}_j \bar{B}_k \tilde{E}_l e^{i(2\tilde{\Omega}-\omega_{w_k})T_0} - \tilde{\Omega}^2 \tilde{E}_j \bar{B}_k \tilde{E}_l e^{-i\omega_{w_k}T_0} \\
& - \omega_{w_l}^2 \tilde{E}_j \tilde{E}_k B_l e^{i(2\tilde{\Omega}+\omega_{w_l})T_0} - \omega_{w_l}^2 \tilde{E}_j \tilde{E}_k \bar{B}_l e^{i(2\tilde{\Omega}-\omega_{w_l})T_0} \\
& - \omega_{w_l}^2 \tilde{E}_j \tilde{E}_k B_l e^{i\omega_{w_l}T_0} - \omega_{w_l}^2 \tilde{E}_j \tilde{E}_k \bar{B}_l e^{-i\omega_{w_l}T_0} \\
& - \tilde{\Omega}^2 \tilde{E}_j \tilde{E}_k \tilde{E}_l e^{i3\tilde{\Omega}T_0} - \tilde{\Omega}^2 \tilde{E}_j \tilde{E}_k \tilde{E}_l e^{i\tilde{\Omega}T_0} \\
& - \tilde{\Omega}^2 \tilde{E}_j \tilde{E}_k \tilde{E}_l e^{i\tilde{\Omega}T_0} - \tilde{\Omega}^2 \tilde{E}_j \tilde{E}_k \tilde{E}_l e^{-i\tilde{\Omega}T_0}]
\end{aligned}
$$

$$
+ cc \qquad (C.2)
$$

Appendix D Procedures to Solve for the Steady-State Solutions of Primary and Superharmonic Resonances

The object is to find the steady-state solutions, a, b, γ, and ψ, of primary resonance and superharmonic resonances of order two and three as functions of σ from the modulation equations, eqs (4.4.12)-(4.4.15). One way to achieve this is to reduce the number of variables and obtain a one-to-one relationship, e.g., a versus σ, by manipulating the modulation equations and making use of the trigonometric identities, eqs (4.4.16a) and (4.4.16b).

First, eq (4.4.14) is used to express $\sin(2\psi)$ as a function of a (assuming $b \neq 0$):

$$\sin 2\psi = \frac{-\mu}{\beta_w a^2} \tag{D.1}$$

Then eq (D.1) is substituted into eq (4.4.12) to find $\sin\gamma$ (note: $\beta_w = \beta_v$ can be proved by substituting the parameters listed in Appendixes A and B into eqs (4.2.16f) and (4.2.17d)):

$$\sin\gamma = \frac{\omega\mu}{Ka}(a^2 + b^2) \tag{D.2}$$

Next, eqs (4.4.13) and (4.4.15) are used to eliminate $\cos(2\psi)$ and obtain $\cos\gamma$ with σ involved:

$$\cos\gamma = (\sigma + X_1 - \frac{\beta_v^* b^2 Y_1}{Y_2})/[\frac{K}{\omega a}(-1 + \frac{\beta_v^* b^2}{Y_2})] \tag{D.3}$$

where X_1, Y_1 and Y_2 are defined in eqs (4.4.18a) -- (4.4.18c). By substituting eqs (D.2) and (D.3) into eq (4.4.16a), we can obtain one equation involving a, b and σ only:

$$\sigma = -X_1 + \frac{\beta_v^* b^2 Y_1}{Y_2} \pm (-1 + \frac{\beta_v^* b^2}{Y_2}) \frac{1}{\omega a^2} \sqrt{K^2 a^2 - \omega^2 \mu^2 (a^2 + b^2)^2} \tag{D.4}$$

If we can find the expression for b in terms of a only, then we can vary a to find the corresponding value of b. The corresponding value of σ can be found from eq (D.4) once a and b are known. Eqs (D.1) and (D.2) are used to find $\cos(2\psi)$ and $\cos\gamma$ in terms of a and b through trigonometric identities, eqs (4.4.16a) and (4.4.16b) (note: there is no σ involved):

$$\cos 2\psi = \pm \frac{\sqrt{\beta_w^2 a^4 - \mu^2}}{\beta_w a^2} \tag{D.5}$$

$$\cos\gamma = \pm \frac{\sqrt{K^2 a^2 - \omega^2 \mu^2 (a^2 + b^2)^2}}{Ka} \tag{D.6}$$

Substituting eqs (D.5) and (D.6) into eq (4.4.15) and rearranging it into a polynomial in b with coefficients depending on a only, one can obtain:

$$AY^2 + 2BY + C = 0 \tag{D.7}$$

where

$$Y = b^2$$

$$A = {c_1}^2 + \frac{\mu^2}{a^4}$$

$$B = c_1 c_2 + \frac{\mu^2}{a^2}$$

$$C = {c_2}^2 - \frac{K^2}{\omega^2 a^2} + \mu^2$$

$$c_1 = \alpha_v^* - \alpha_w + \beta_v \pm \frac{\sqrt{{\beta_w}^2 a^4 - \mu^2}}{a^2}$$

$$c_2 = f_w - f_v + (\alpha_v - \alpha_w^* - \beta_w^*)a^2 \mp \sqrt{{\beta_w}^2 a^4 - \mu^2}$$

The solutions for b (or b^2) are:

$$Y = b^2 = \frac{-B \pm \sqrt{B^2 - AC}}{A} \qquad (D.8)$$

Once a is specified, b can be found from eq (D.8), and σ can be found from eq (D.4). Two phase angles can be found via eqs (D.1) and (D.2). The procedure is not unique. Instead of varying a to find the rest of the variables, we can vary b to find the rest by choosing different equations. But the steady-state solution is unique, no matter what procedure is used. Because the above calculations involve some squaring, not all of the solutions are true. Only a few of them are valid, depending on whether eqs (4.4.12) -- (4.4.16) are satisfied.

Appendix E Procedures to Solve for the Steady-State Solutions of Subharmonic Resonances of Order Two and Three

The object is to find the steady-state solutions, a, b, γ, and ψ, of subharmonic resonance of order two as functions of σ from the modulation equations, eqs (4.4.26)-(4.4.29). The strategy is to reduce the number of variables to a one-to-one relationship, e.g., a versus σ or b versus ψ, by arranging the modulation equations and the trigonometric identity in eq (4.4.31). It is assumed that $a \neq 0$ and $b \neq 0$.

First, eqs (4.4.26) and (4.4.28) can be used to express $\sin\gamma$ and $\cos\gamma$ as functions of a, b and ψ:

$$\sin\gamma = [\mu(a^2 + b^2) - \frac{g_w b^2}{2\omega}\sin\psi]\frac{2\omega}{g_v a^2} \tag{E.1}$$

$$\cos\gamma = (\mu - \frac{g_w}{2\omega}\sin\psi)\frac{1}{\beta_w a^2 \sin\psi} + [\mu(a^2 + b^2) - \frac{g_w b^2}{2\omega}\sin\psi]\frac{2\omega\cos\psi}{g_v a^2 \sin\psi} \tag{E.2}$$

Next, eqs (4.4.27) and (4.4.29) are used to obtain one equation without σ involved:

$$2f_v - 2f_w + 2(\alpha_v^* + \beta_v - \alpha_v)(a^2 - b^2) + 2\beta_w(a^2 - b^2)\cos(\psi - \gamma) + \frac{g_w}{\omega}\cos\psi - \frac{g_v}{\omega}\cos\gamma = 0 \quad (E.3)$$

Substituting eqs (E.1) and (E.2) into eq (E.3) to eliminate γ, we can obtain an equation involving only a, b and ψ. After a proper arrangement, a can be expressed as a function of b and ψ from the following equation:

$$AX^2 + BX + C = 0 \quad (E.4)$$

where

$$A = 2(\alpha_v^* + \beta_v - \alpha_v) + \frac{4\mu\beta_w\omega}{g_v \sin\psi}$$

$$B = 2f_v - 2f_w + [-2(\alpha_v^* + \beta_v - \alpha_v) - \frac{2\beta_w g_w}{g_v}]Y$$

$$C = -\frac{g_v\mu}{\beta_w\omega\sin\psi} + \frac{g_v g_w}{2\beta_w\omega^2} + (-\frac{4\mu\cos\psi}{\sin\psi} + \frac{2g_w\cos\psi}{\omega})Y + (-\frac{4\mu\beta_w\omega}{g_v\sin\psi} + \frac{2\beta_w g_w}{g_v})Y^2$$

$$X = a^2,\ Y = b^2$$

The solutions for a (or a^2) are:

$$X = a^2 = \frac{-B \pm \sqrt{B^2 - 4AC}}{2A} \quad (E.5)$$

Now, if we can find b as a function of ψ, then the rest of the variables can also be obtained. Because the equations involve transcendental functions, trigonometric identities can give another equation which expresses the relationship between b and ψ. We use

$$\sin^2(\psi - \gamma) + \cos^2(\psi - \gamma) = 1 \quad (E.6)$$

to find b as a function of ψ by substituting eqs (E.1), (E.2) and (E.5) into eq (E.6). After carrying out a few calculations, we end up with an eighth-order polynomial in Y (or b^2) with coefficients depending on ψ only., i.e.,

$$C_8(\psi)Y^8 + C_7(\psi)Y^7 + C_6(\psi)Y^6 + C_5(\psi)Y^5 + C_4(\psi)Y^4 + C_3(\psi)Y^3 + C_2(\psi)Y^2 + C_1(\psi)Y + C_0(\psi) = 0 \tag{E.7}$$

Due to the complication of the calculations, the coefficients were obtained by using MACSYMA (project MAC's SYmbolic MAnipulation system). Because these coefficients are lengthy, they are not shown in this dissertation. Once a value of ψ is specified, the corresponding solutions for b can be obtained from the above eighth-order polynomial. The IMSL subroutine DNEQNF is used to find the solutions. For every real solution of b obtained from the above polynomial, the solution for a is obtained by substituting b and ψ into eq (E.5). The solution for γ can be obtained by substituting a, b and ψ into either eq (E.1) or eq (E.2). The solution for σ can also be obtained from either eq (4.4.39) or eq (4.4.41). Because the above calculations involve some squaring, not all of the eight solutions are valid. Only a few of them are true, depending on whether eqs (4.4.26) - (4.4.29) are satisfied.

The procedure is not unique. Instead of varying ψ to find the rest of the variables, we can vary γ to find the rest by choosing different equations. But the steady-state solution is unique, no matter what procedure is used.

For subharmonic resonance of order three, the same procedure can be used to find the steady-state solutions. But due to the fact that the equations cannot be put in terms of the squares $X = a^2$ and $Y = b^2$, a twenty-fourth order polynomial is obtained. The calculations are not shown here.

Appendix F Damping Coefficient and the Logarithmic Decrement

Usually, a damping coefficient is defined approximately by a linear free-vibration system (for example, Meirovitch [1975]):

$$m\ddot{x} + c\dot{x} + kx = 0 \tag{F.1}$$

Damping is written as:

$$c = \zeta 2\sqrt{km} = \zeta c_{cr} \tag{F.2}$$

where ζ is known as the damping parameter (or viscous damping factor), which characterizes the damping, and c_{cr} is defined as the critical damping. The value of critical damping is $2\sqrt{km}$. It is noted that $\zeta = 1$ corresponds to critical damping. The magnitude of ζ is measured through the decrement of the amplitude of free vibration. The response of a linear free-vibration system, eq (F.1), is found as:

$$x = x_0 e^{-\zeta\omega_n t}\cos(\omega_d t - \phi) \tag{F.3}$$

where x_0 is the initial amplitude; $\omega_n = \sqrt{k/m}$ is the undamped natural frequency; ω_d is the damped natural frequency which is equal to $\sqrt{k/m - (c^2/4m^2)}$; ϕ is the phase angle; and t is the time. If we choose two peaks, x_1 and x_2, with the corresponding time difference $t_2 - t_1 = 2\pi/\omega_d = T =$ period, the ratio of these two amplitudes is:

$$\frac{x_1}{x_2} = \frac{x_0 e^{-\zeta\omega_n t_1}\cos(\omega_d t_1 - \phi)}{x_0 e^{-\zeta\omega_n t_2}\cos(\omega_d t_2 - \phi)} = e^{\zeta\omega_n T} \tag{F.4}$$

The logarithmic decrement δ is then defined as:

$$\delta = \ln\frac{x_1}{x_2} = \zeta\omega_n T = \frac{2\pi\zeta}{\sqrt{1-\zeta^2}} \tag{F.5}$$

After rearranging the above equation, eq (F.5), one can obtain the damping parameter ζ in terms of the logarithmic decrement δ:

$$\zeta = \frac{\delta}{\sqrt{4\pi^2 + \delta^2}} \simeq \frac{\delta}{2\pi} \tag{F.6}$$

For example, the damping coefficient of a beam is obtained from the linearized system:

$$m\ddot{v} + c\dot{v} + D_\zeta v'''' = 0 \tag{F.7}$$

where the parameters are defined in Chapter 2. After Galerkin's procedure is applied, one can obtain the following equation:

$$m\ddot{v}_i + c\dot{v}_i + D_\zeta \tilde{\lambda}^2 v_i = 0 \tag{F.8}$$

Then the damping c is found to be:

$$c = \zeta c_{cr} = \zeta 2\sqrt{D_\zeta \tilde{\lambda}^2 m} \tag{F.9}$$

The dimensionless form of damping c^* can be found as (for details see Section 2.4):

$$c^* = \zeta c_{cr} \frac{L^2}{\sqrt{mD_\eta}} = \zeta 2\lambda \sqrt{\frac{D_\zeta}{D_\eta}} \qquad (F.10)$$

If the cross section of the beam is circular or square, i.e., $D_\zeta = D_\eta$, then $c^* = \zeta 2\lambda$. For example, if the logarithmic decrement δ is 0.0002 (for example, Augus [1976], Walton [1971] and Walton [1981]), the dimensionless damping will be $0.00003183 \times 2\lambda$. The first eigenvalue $\lambda_1 = 3.516$ is used to approximate the damping coefficients for all modes in this dissertation.

Appendix G Bifurcation Points

The bifurcation points of primary and superharmonic resonances of order two and three can be found analytically from the steady-state out-of-plane equation, eq (D.8):

$$b^2 = \frac{-B \pm \sqrt{B^2 - AC}}{A} \tag{G.1}$$

Bifurcation points occur when the amplitude b obtained from the above equation is zero. This implies that the term AC inside the square root must be zero. In other words, either A or C is zero. But A also appears in the denominator, so only $C = 0$ is considered:

$$C = \left[f_w - f_v + (\alpha_v - \alpha_w^* - \beta_w^*) a^2 \mp \sqrt{\beta_w^2 a^4 - \mu^2} \right]^2 - \frac{K^2}{\omega^2 a^2} + \mu^2 = 0 \tag{G.2}$$

The value of a which satisfies $C = 0$ can be found as follows. First, eq (G.2) is expanded. Then, terms with the square root involved are collected and put on the right-hand-side. The rest are put on the left-hand-side. The equation is then squared to eliminate the square root. After moving every term to the left-hand-side and rearranging terms according to the power of a, the following polynomial in a is obtained:

$$D_6 X^6 + D_5 X^5 + D_4 X^4 + D_3 X^3 + D_2 X^2 + D_1 X + D_0 = 0 \tag{G.3}$$

where

$$X = a^2$$
$$p = f_w - f_v$$
$$q = \alpha_v - \alpha_w^* - \beta_w^*$$
$$D_6 = (q^2 - \beta_w^2)^2$$
$$D_5 = 4pq(q^2 - \beta_w^2)$$
$$D_4 = 6p^2q^2 - 2p^2\beta_w^2 + 4q^2\mu^2$$
$$D_3 = 4p^3q - \frac{2K^2}{\omega^2}(q^2 + \beta_w^2) + 8pq\mu^2$$
$$D_2 = p^4 - \frac{4K^2pq}{\omega^2} + 4p^2\mu^2$$
$$D_1 = \frac{-2K^2p^2}{\omega^2}$$
$$D_0 = \frac{K^4}{\omega^4}$$

The real and positive solutions $X(= a^2)$ of this polynomial give the bifurcation points.

References

Atluri, S., 1973, "Nonlinear Vibrations of a Hinged Beam Including Nonlinear Inertia Effects," *Journal of Applied Mechanics,* Vol. 40, pp. 121-126.

Augus, H. T., 1976, *Cast Iron : Physical and Engineering Properties,* second edition, Butterworths, London, Boston.

Collinge, I. R. and Ockendon, J. R., 1979, "Transition Through Resonance of a Duffing Oscillator," *SIAM Journal of Applied Mathematics,* Vol. 37, No. 2, pp. 350-357.

Crespo da Silva, M. R. M., 1978a, "Flexural-Flexural Oscillations of Beck's Column Subjected to a Planar Harmonic Excitation," *Journal of Sound and Vibration,* Vol. 60, pp. 133-144.

Crespo da Silva, M. R. M., 1978b, "Harmonic Non-Linear Response of Beck's Column to a Lateral Excitation," *International Journal of Solids and Structures,* Vol. 14, pp. 987-997.

Crespo da Silva, M. R. M., 1980, "Nonlinear Resonances in a Column Subjected to a Constant End Force," *Journal of Applied Mechanics,* Vol. 47, pp. 409-414.

Crespo da Silva, M. R. M., 1988a, "Non-Linear Flexural-Flexural-Torsional-Extensional Dynamics of Beam I. Formulation," *International Journal of Solids and Structures,* Vol. 24, No. 12, pp. 1225-1234.

Crespo da Silva, M. R. M., 1988b, "Non-Linear Flexural-Flexural-Torsional-Extensional Dynamics of Beam II. Response Analysis," *International Journal of Solids and Structures,* Vol. 24, No. 12, pp. 1235-1242.

Crespo da Silva, M. R. M. and Glynn, C. C., 1978a, "Nonlinear Flexural-Flexural-Torsional Dynamics of Inextensional Beams I. Equations of Motion," *Journal of Structural Mechanics,* Vol. 6, pp. 437-448.

Crespo da Silva, M. R. M. and Glynn, C. C., 1978b, "Nonlinear Flexural-Flexural-Torsional Dynamics of Inextensional Beams II. Forced Motions," *Journal of Structural Mechanics,* Vol. 6, pp. 449-461.

Crespo da Silva, M. R. M. and Glynn, C. C., 1979a, "Non-Linear Non-Planar Resonant Oscillations in Fixed-Free Beams with Support Asymmetry," *International Journal of Solids Structures,* Vol. 15, pp. 209-219.

Crespo da Silva, M. R. M. and Glynn, C. C., 1979b, "Out-of-Plane Vibrations of a Beam Including Non-Linear Inertia and Non-Linear Curvature Effects," *Vertica,* Vol. 3, pp. 261-271.

Crespo da Silva, M. R. M. and Zaretzky, C. L., 1990, "Non-Linear Modal Coupling in Planar and Non-Planar Responses of Inextensional Beams," *International Journal of Non-Linear Mechanics,* Vol. 25, No. 2/3, pp. 227-239.

Crespo da Silva, M. R. M. and Zaretzky, C. L., 1991, "Effects of Approximations on the Static and Dynamic Responses of a Cantilever with a Tip Mass," *International Journal of Solids and Structures,* Vol. 27, No. 5, pp. 565-583.

Dowell, E. H. and Traybar, J., 1977, "An Experimental-Theoretical Correlation Study of Non-Linear Bending and Torsion Deformations of a Cantilever Beam, " *Journal of Sound and Vibration,* Vol. 50(4), pp. 533-544.

Evan-Iwanowski, R. M., 1976, *Resonance Oscillations in Mechanical Systems,* Elsevier Scientific Publishing Company, Amsterdam-Oxford-New York.

Haight, E. C. and King, W. W., 1972, "Stability of Nonlinear Oscillations of an Elastic Rod," *The Journal of the Acoustical Society of America,* Vol. 52, pp. 899-911.

Ho, C.-H., Scott, R. A. and Eisley, J. G., 1975, "Non-Planar, Non-Linear Oscillations of a Beam-I. Forced Motions," *International Journal of Non-Linear Mechanics,* Vol. 10, pp. 113-127.

Ho, C.-H., Scott, R. A. and Eisley, J. G., 1976, "Non-Planar, Non-Linear Oscillations of a Beam-II. Free Motions," *Journal of Sound and Vibration,* Vol. 47, pp. 333-339.

Hughes, G. C. and Bert, C. W., 1990, "Effect of Gravity on Nonlinear Oscillations of a Horizontal, Immovable-End," Abstracts, Third Conference on Nonlinear Vibrations, Stability, and Dynamics of Structures and Mechanics, Virginia Polytechnic Institute and State University, Blacksburg, Virginia.

Hyer, M. W., 1978a, "Whirling of a Base-Excited Cantilever Beam," *The Journal of the Acoustical Society of America,* Vol. 65, pp. 931-939.

Hyer, M. W., 1978b, "Preliminary Investigations into the Active Control of Large Space Structures--Whirling Motion of a Viscously Damped, Base-Excited Cantilever Beam," NACA Report, Research Grant NSG 1279.

Hyer, M. W., 1978c, "The Effect of Nonlinear Curvature and Inertia on the Predictions for the Planar Response and Stability of an Inextensible Base-Excited Cantilever," Virginia Polytechnic Institute and State University, Report No. VPI-E-78-28.

Hyer, M. W., 1980a, "Stability of a Base-Excited Cantilever to Out-of-Plane Pertubations," in Developments in Theoretical and Applied Mechanics, Vol. 10 (Proceedings of the 10th Southeastern Conference on Theoretical and Applied Mechanics) ed. J. E. Stoneking, Univ. of Tennessee Press, Knoxville, pp. 505-521.

Hyer, M. W., 1980b, "Nonplanar Motions of a Base-Excited Cantilever," in Recent Advances in Structural Dynamics, Vol. 2, ed. M. Petyt, published by Institute of Sound and Vibration Research, Univ. of Southampton, Southampton, England, pp. 621-630.

Ishida, Y., Ikeda, T. and Yamamoto, T., 1987, "Transient Vibration of a Rotating Shaft with Nonlinear Spring Characteristics During Acceleration Through a Critical Speed, " *JSME International Journal,* Series III, Vol. 30, No. 261, pp. 458-466.

Ishida, Y., Ikeda, T., Yamamoto, T. and Murakami, S., 1989, "Nonstationary Vibration of a Rotating Shaft with Nonlinear Spring Characteristics During Acceleration Through a Critical Speed

(A Critical Speed of a 1/2-Order Subharmonic Oscillation)," *JSME International Journal,* Series III, Vol. 32, No. 4, pp. 575-584.

Ishida, Y., Yamamoto, T., Ikeda, T. and Murakami, S., 1990, "Nonstationary Vibration of a Rotating Shaft with Nonlinear Spring Characteristics During Acceleration Through a Critical Speed (A Critical Speed of a Summed-and-Differential Harmonic Oscillation)," *Nonlinear Dynamics,* Vol. 1, No. 5, pp. 341-358.

Kim, T. and Dugundji, J., 1991 "Nonlinear Large Amplitude Vibration of Composite Helicopter Blade at Large Static Deflection," Proceedings of the 32nd AIAA/ASME/ASCE/AHS/ASC Structures, Structural Dynamics and Materials Conference, Baltimore, April 8-10, 1991, part 3, pp. 2071-2081.

Kevorkian, J., 1971 "Passage Through Resonance for a One-Dimensional Oscillator with Slowly Varying Frequency," *SIAM Journal on Applied Mathematics,* Vol. 20, No. 3, pp. 364-372.

Love, A. E. H., 1944, *The Mathematical Theory of Elasticity,* Dover Publications, New York, 4th edition, Chapter 18.

Lewis, F. M., 1932, "Vibration During Acceleration Through a Critical Speed, " *Transactions of the American Society of Mechanical Engineers,* Vol. 54, pp. 253-261.

Meirovitch, L., 1975, *Elements of Vibration Analysis,* McGraw-Hill, New York.

Minguet, P. J. A., 1989, "Static and Dynamic Behavior of Composite Helicopter Rotor Blades Under Large Deflection," Ph.D. Dissertation, Department of Aeronautics and Astronautics, Massachusetts Institute of Technology, Boston, Massachusetts.

Nayfeh, A. H., 1980, *Introduction to Perturbation Techniques,* Wiley, New York.

Nayfeh, A. H. and Asfar, K. R., 1988, "Non-Stationary Parametric Oscillations," *Journal of Sound and Vibration,* Vol. 124, No. 3, pp. 529-537.

Nayfeh, A. H. and Mook, D. T., 1979, *Nonlinear Oscillations,* Wiley, New York.

Nayfeh, A. H. and Pai, P.-J. F., 1989, "Non-Linear Non-Planar Parametric Responses of an Inextensional Beam," *International Journal of Non-Linear Mechanics,* Vol. 24, No. 2, pp. 139-158.

Neal, H. L. and Nayfeh, A. H., 1990, "Response of a Single-Degree-of-Freedom System to a Non-Stationary Principal Parametric Excitation," *International Journal of Non-Linear Mechanics,* Vol. 25, No. 2/3, pp. 275-284.

Pai, P.-J. F., 1990, "Nonlinear Flexural-Flexural-Torsional Dynamics of Metallic and Composite Beam," Ph.D. Dissertation, Department of Engineering Science and Mechanics, Virginia Polytechnic Institute and State University, Blacksburg, Virginia.

Pai, P.-J. F. and Nayfeh, A. H., 1990, "Non-Linear Non-Planar Oscillations of a Cantilever Beam Under Lateral Base Excitations," *International Journal of Non-Linear Mechanics,* Vol. 25, No. 5, pp. 455-474.

Rosen, A. and Friedmann, P., 1979, "The Nonlinear Behavior of Elastic Slender Straight Beams Undergoing Small Strains and Moderate Rotations," *Journal of Applied Mechanics,* Vol. 46, pp. 161-168.

Rosen, A., Loewy, R. G. and Mathew, M. B., 1987a, "Nonlinear Analysis of Pretwisted Rods Using "Principal Curvature Transformation" Part I: Theoretical Derivation," *AIAA Journal,* Vol. 25, pp. 470-478.

Rosen, A., Loewy, R. G. and Mathew, M. B., 1987b, "Nonlinear Analysis of Pretwisted Rods Using "Principal Curvature Transformation" Part II: Numerical Results," *AIAA Journal,* Vol. 25, pp. 598-604.

Rosen, A., Loewy, R. G. and Mathew, M. B., 1987c, "Nonlinear Dynamics of Slender Rods," *AIAA Journal,* Vol. 25, pp. 611-619.

Satio, H., Sato, K. and Yutani, T., 1976, "Non-Linear Forced Vibrations of a Beam Carrying Concentrated Mass Under Gravity," *Journal of Sound and Vibration,* Vol. 46, pp. 515-525.

Sato, K., Saito, H. and Otomi, K., 1978, "The Parametric Response of a Horizontal Beam Carrying a Concentrated Mass Under Gravity," *Journal of Applied Mechanics,* Vol. 45, pp. 643-648.

Schumacher, I. B., 1970, "Das Verhalten eines elastischen Tragers mit nichtlinearen Randbedingungen bei Durchgang durch die Resonanz " *Ingenieur-Archiv,* Band 39, Heft 2, pp. 115-123.

Shih, C.-F., Chen, J. C. and Garba, J., 1986, "Vibration of a Large Space Beam Under Gravity Effect," *AIAA Journal,* Vol. 24, pp.1213-1216.

Tseng, W. Y. and Dugundji, J., 1970, "Nonlinear Vibrations of a Beam Under Harmonic Excitation," *Journal of Applied Mechanics,* Vol. 37, pp. 292-297.

Tseng, W. Y. and Dugundji, J., 1971, "Nonlinear Vibrations of a Buckled Beam Under Harmonic Excitation," *Journal of Applied Mechanics,* Vol. 38, pp. 467-476.

Wagner, H., 1965, "Large-Amplitude Free Vibrations of a Beam," *Journal of Applied Mechanics,* Vol. 32, pp. 887-892.

Walton, C. F., 1971, *Gray and Ductile Iron Castings Handbook,* Gray and Ductile Iron Founder's Society, Cleveland, Ohio.

Walton, C. F. and Timothy, J. O., 1981, *Iron Castings Handbook,* Iron Castings Society, Rocky River, Ohio.

Vita

The author, In-Ming Kevin Shyu, was born on May 6, 1961 in Taipei, Taiwan, R.O.C. He entered National Tsing-Hua University at Hsin-Chu, Ta'wan in August, 1979, and graduated with a Bachelor of Science degree in May, 1983 from the Department of Nuclear Engineering. After graduation, he served two years of compulsory military service in the army. After his military service, he was employed as an assistant in the Department of Nuclear Engineering, National Tsing-Hua University from June, 1985 to July, 1986. Then, he entered the Mechanical and Aerospace Engineering Department at State University of New York at Buffalo in August, 1986. He obtained a Master of Science degree in July, 1988. In August, 1988, he entered the Aerospace and Ocean Engineering Department at Virginia Polytechnic Institute and State University. In November, 1988, he transferred to the Department of Engineering Science and Mechanics at the same university and has worked toward the Ph.D. degree since then.